Immunogenic peptide identification in H1N1 virus as target for vaccine design

A thesis

Submitted in the partial fulfilment of the requirements

for the degree of

DOCTOR OF PHILOSOPHY

IN

BIOTECHNOLOGY

NEHA LOHIA

(Registration No. 901000006)

Department of Biotechnology

Thapar University,

Patiala, Punjab

March, 2017

CERTIFICATE

Certified that the thesis "**Immunogenic peptide identification in H1N1 virus as target for vaccine design**" submitted by Ms. Neha Lohia, in the fulfilment of the requirement for the award of the Degree of **Doctor of Philosophy** in the department of Biotechnology, Thapar University Patiala, is a record of candidate's own independent and original research work carried out by herself in my supervision and guidance. The material embodied in this thesis has not been submitted in parts or full in any other university or institute for the award of any degree.

Supervisor

Dr. Manoj Baranwal
Assistant Professor
Department of Biotechnology
Thapar University, Patiala
(147004), Punjab, India

DECLARATION

I hereby declare that the work presented in the thesis entitled "**Immunogenic peptide identification in H1N1 virus as target for vaccine design**" in the fulfilment of the requirement for the award of the Degree of **Doctor of Philosophy** in the department of Biotechnology, Thapar University Patiala, is an authentic record of my own work during the period January 2011 to June 2016, under the supervision of Dr. Manoj Baranwal Assistant Professor, Department of Biotechnology Thapar University, Patiala. The material embodied in this thesis has not been submitted in parts or full in any other university or institute for the award of any degree in India or Abroad.

Place: Patiala
Date: 10/3/2017

Neha Lohia

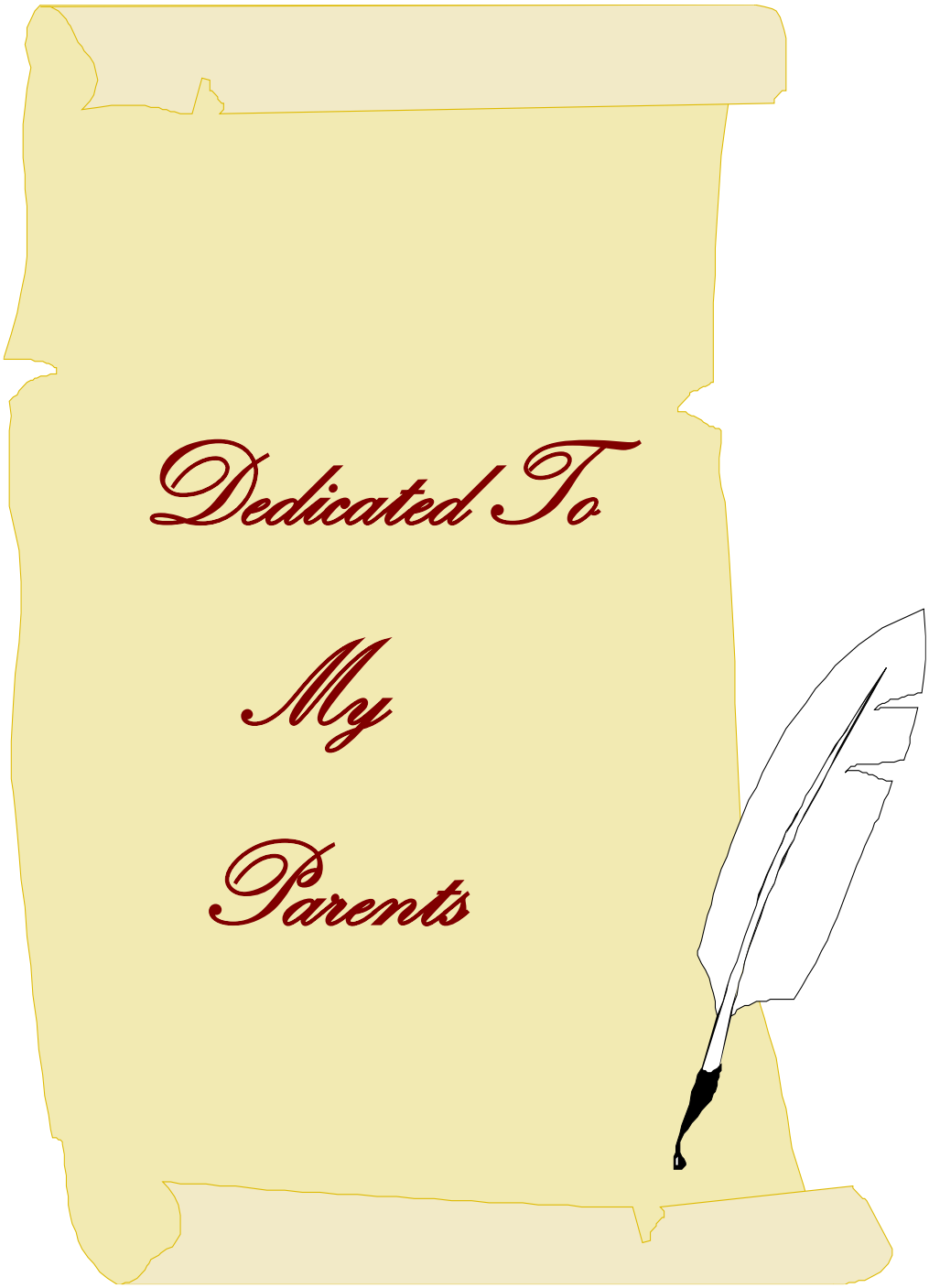
Dedicated To
My
Parents

ACKNOWLEDGEMENT

In pursuit of this academic endeavor, I feel that I have been singularly fortunate because inspiration, guidance, direction, cooperation, love and care - all came my way in abundance. I feel nostalgic when i look back at the last five years of my PhD and it seems almost impossible to acknowledge everyone involved in adequate terms. One of the joys of completion is to look over the past and remember all the people who supported me throughout this long but fulfilling journey. Without them, I may not have accomplished my goals, at least not sanely.

First and foremost I will forever be thankful to the person who made the biggest difference in my life, my supervisor, ***Dr. Manoj Baranwal****, Assistant Professor, Department of Biotechnology, Thapar University, Patiala. He has always been there to help me at every single step of this journey, motivating, guiding and encouraging me to take up new challenges every day and tackle them with determination and an optimistic attitude. It was his support which made me thrive for excellence and nothing less. His intelligent ideas, thought provoking discussions and pertinent guidance helped me sail through this tedious journey. Besides being a supportive advisor throughout, he gave me full freedom to pursue independent work which inculcated great confidence in me. Not only has he been a great scientist, but a very kind and helpful human being. His association with this endeavor will remain a beacon light to me throughout my life.*

I wish to express my thanks to ***Prof. Prakash Gopalan****,* ***Director,*** *Thapar University, Patiala, for providing infrastructure and helping me towards the smooth and timely completion of my research work. I extend my sincere word of thanks to* ***Prof. O.P. Pandey****, Dean (Research and Sponsored Projects), Thapar University, Patiala, for his encouragement and support during my research work in the Institute.*

I take this opportunity to thank ***Prof. Moushumi Ghosh*** *(Head, Biotechnology Department)****, Prof. Dinesh Goyal*** *and* ***Prof. M. Sudhakara Reddy****, Ex-Head, Biotechnology Department, Thapar University, for their constant support during the course of my study. My special word of thanks should also go to members of my doctoral committee,* ***Dr. Vikas Handa****,* ***Dr. Sidhharth Sharma****, BTD, TU and* ***Prof. N. Tejo Prakash****, School of Energy and*

environment for their invaluable suggestion, constant support and encouragement during the course of my study.

A sincere token of gratitude to ***Prof. N Das,*** *BTD, TU for his encouragement, constructive suggestions and support during the course of my academics in Thapar University. I wish to place on record my thanks to all the faculty members of DBT, TU, Patiala, for their constant motivation and invaluable suggestions during my research work.*

This research was possible due to the support of the ***Department of Science and technology, Government of India*** *for proving me financial support to accomplish my work.*

I take the opportunity to acknowledge all the volunteers who consented to participate in this research project. I am enormously grateful to ***Dr. Akshey Jain*** *(Nitin Hospital, Patiala) and* ***Dr. Rimpreet Singh Walia*** *(Lifeline blood bank, Patiala) for providing the blood samples of these volunteers, as and when required.*

Most of the work would have been incomplete without the sincere support of Lab technicians. So, I owe a word of thanks to ***Mr. Ram Newal, Ms. Lalita*** *and* ***Mr. Chandan.*** *I am very thankful to* ***Mr. Lallan Yadav, Mr. Surinder, Mr. Mohinder*** *and* ***Mr. Phul Chand*** *for their timely help and cooperation. I am grateful to* ***Mr. Anirudh Handa*** *for his generous and ungrudging assistance. I am also thankful to* ***Mr. Vijay Verma*** *for his help and suggestion in financial matters which enabled smooth running of this research project.*

Some friends are never too busy to give us a hand whenever it is needed. I want to make a special mention for a friend who showed faith in me and my intellect even when I felt like digging a hole and crawling into one because I didn't have faith in myself. I could not have asked for more than what I got from you. I express my sincere love and gratitude towards a benevolent soul and true friend ***Dr. Neha Singh.*** *I owe my deepest gratitude to my dearest friend* ***Dr. Jaspreet Kaur*** *for her continuous support and inspiration. She made her support available in infinite number of ways every time and anytime.*

Words fail me to express my appreciation for my loving friends ***Vivek, Gourav, Prerna, Sahil, Parul, Pawandeep, Methoxy, Dr. Nadeem*** *and* ***Charu*** *for their constant support and motivation. My friends, thanks for being with me through thick and thin. I wish you all, best of luck in all life has to offer you.*

*I warmly thank my lovely friends **Mehendi**, **Sapna** and **Tavleen** for their immense help, especially at the time of thesis correction and defending.*

*I find it difficult to pen down my deepest sense of indebtedness towards my parents who soulfully provided me their constant support and right impetus to undertake the challenge of this proportion like all other spheres of life, for what I cannot measure but treasure. They believed in me before I believed in myself. When my words ebbed and enthusiasm waned, it was my **Mother** and **Father** who helped me in getting out of it, a feat that can never be paid back in feelings or words. To them, I owe my wonderful today and dream filled future.*

*I would also like to extend my deep gratitude to my **Massi**, **Mausji** and **Chachaji** for their unconditional love and faith. I feel lacunae of words to acknowledge **Chachiji** who left us untimely. You will always be missed and loved. I consider myself the luckiest in the world to have such a supportive family, standing behind me with their love and support.*

*I highly appreciate unsolicited cooperation and cheery assistance of my brothers **Nitish** and **Chirag**, my sister **Reetu** and my dearest nephew **Aditya**. Their abundant affection and unflagging love were the constant source of inspiration for me.*

*I would like to recompense my veneration to the **Almighty** for giving me strength and patience to work through all these years so that today I can stand proud with my head held high.*

*It has been a great privilege to spend several years in the **Department of Biotechnology, Thapar University, Patiala** and its members will always remain dear to me.*

Last but not the least, I wish to acknowledge all those, whose names have not figured here, but who helped me in any form during the period of my research work.

Date: March 10, 2017

Place: Patiala

(Neha Lohia)

List of Publication

Accepted

1. Lohia, N. & Baranwal, M. (2014) Conserved peptides containing overlapping $CD4^+$ and $CD8^+$ T-cell epitopes in the H1N1 influenza virus: an immunoinformatics approach. *Viral immunology*, 27: 225-34. (SCI, IF=1.51).
2. Lohia, N. & Baranwal, M. (2015) Identification of conserved peptides comprising multiple T cell epitopes of Matrix 1 protein in H1N1 influenza virus. *Viral immunology,* 28: 570-79. (SCI, IF=1.51)
3. Dhiman, G., Lohia, N., Jain, S. & Baranwal, M. (2016) Metadherin peptides containing $CD4^+$ and $CD8^+$ T cell epitopes as vaccine candidate against cancer. *Microbiology and immunology*. (Accepted). (SCI, IF= 1.43).

Communicated

1. Lohia N, & Baranwal M. Immune response of highly conserved influenza A virus matrix 1 peptides. Microbiology and Immunology (Manuscript MAI-2017-027; under review).
2. Lohia N, & Baranwal M. Highly conserved hemagglutinin peptides of H1N1 influenza virus elicit immune response. Comp Immunol Microbiol Infect Dis (under review).
3. Sharma V & Lohia N, Handa V and Baranwal M. Amomum subulatum exhibit Antioxidant, Cytotoxic and Immunosuppressive effect. Indian J Exp Biol, (revision submitted).

Manuscript under preparation

1. Lohia, N. & Baranwal, M. *In vitro* studies to assess immune response of highly conserved peptides of neuraminidase and matrix 1 proteins of H1N1 influenza virus.

Participation in Conferences and Symposia

International

1. **Lohia N**, Baranwal M (2015). Prediction of conserved immunogenic peptides containing overlapping $CD4^+$ and $CD8^+$ T cell epitopes in H1N1 Matrix 1 Protein: An immunoinformatics approach. "4th European Congress of Immunology" Vienna, Austria, (September 6 –9, 2015).
2. **Lohia N**, Baranwal M (2015). In silico and in vitro to identify conserved immunogenic peptides containing overlapping $CD4^+$ and $CD8^+$ T cell epitopes of H1N1 proteins. INDO UK workshop on sustainable Polymer Applications (IUWSPA), Thapar University, Patiala, India (December 8-9, 2015).

National

1. **Lohia N**, Baranwal M (2014). *In silico* Prediction of con served immunogenic peptides containing overlapping $CD4^+$ and $CD8^+$ T cell epitopes in influenza-A H1N1 neuraminidase. "Accelerating Biology 2014 - Computing Life" organized by C-DAC, Pune, India (February 18-20, 2014).
2. Baranwal M, **Lohia N**. An immunoinformatics approach to identify immunogenic peptide of hemagglutinin protein in H1N1 virus, IMMUNOCON-13 40th Annual conference of Indian Immunological society, University college of Medical Science, Delhi University, Delhi, India (November 15-17, 2013).
3. Attended "Workshop on Flow cytometry experimental designing and data analysis" conducted by Institute of Liver and Biliary Sciences, New Delhi, India (August 19-20, 2014).
4. Attended one month training in "Bioinformatics" organized by Jaypee University of Information technology, Solan, India in June-July, 2013.

Abstract

Last 100 years have witnessed two pandemic outbreaks of H1N1 influenza viz. Spanish flu in 1918 and swine flu in 2009. It has been the most prevalent subtype of influenza virus in humans responsible for significant morbidity and mortality worldwide. In case of unforeseen outbreaks of influenza, antiviral prophylaxis is chosen to put an immediate check on its spread, However, the efficacy of antiviral drugs in treating influenza seems uncertain due to the rise of drug resistant strains. Further, influenza vaccines presently available are strain specific and require periodic reformulation to include combination of circulating influenza A and B virus strains. The problem associated with such vaccines is the induction of humoral immune response directed against the highly mutable hemagglutinin protein. Further, their timely and adequate availability is difficult in case of a sudden outbreak. Thus, there is a pressing need to develop a refined vaccine approach which can offer universal or at least broad protection against the ever mutating influenza virus strains in the population distributed worldwide. Highly conserved T cell epitopes of influenza A protein are known to be cross protective. Such T cell epitopes which have the capacity to bind to an array of HLA molecules are anticipated to serve as candidates for universal or broadly reactive influenza vaccine. In light of the above facts, the present study focused on identifying highly conserved promiscuous peptides containing multiple overlapping $CD8^+$ and $CD4^+$ T cell epitopes from hemagglutinin (HA), neuraminidase (NA) and matrix 1 (M1) protein of H1N1 influenza virus using different epitope prediction tools and molecular docking. Further, peripheral blood mononuclear cells from healthy volunteers were subjected to repetitive stimulation by these chemically synthesized peptides and their proliferation and IFN-γ level was measured by MTT and ELISA assay respectively to assess immunogenic response. Epitope prediction tools identified 24 $CD8^+$ and 11 $CD4^+$ T cell epitopes of HA, 13 $CD8^+$ and nine $CD4^+$ T cell epitopes of NA and ten $CD8^+$ and nine $CD4^+$ T cell epitopes of the M1 protein. Overlapping epitopes were merged to generate 14 peptides containing multiple $CD8^+$ and $CD4^+$ T cell epitopes from the HA, NA and M1 protein (five HA, six NA and three M1 peptides) belonging to H1N1 subtype of influenza virus. Four peptides (two each from NA and HA) were excluded from current study as these peptides were reported to induce immunogenic response in previous

studies. Ten peptides (P_H1, P_H3 and P_H4 of HA, P_N2, P_N4, P_N5 and P_N6 of NA and P_M1, P_M2 and P_M3 of M1 protein) were selected for further evaluation. Population coverage analysis of the selected peptides revealed that five peptides viz. P_H1, P_N2, P_N6, P_M1 and P_M2 showed excellent coverage in Asia, Europe, Africa, North America, South America and Oceania countries. In order to confirm the unrestrained binding capacity of selected peptides with multiple HLA molecules, docking was carried out by AutoDock vina. The binding energy obtained after docking of most of the $CD8^+$ T cell epitopes and peptides containing multiple $CD4^+$ T cell epitopes with various HLA class I and II molecules was comparable to that of the native peptides except for three $CD8^+$ T cell epitopes (two of HA and one of M1 protein). Interestingly, binding energy obtained for some of epitopes/peptides was higher than the native peptides of corresponding HLA. *In vitro* peptide stimulation assays revealed that HA and M1 peptides elicited better immunogenic response in terms of proliferation and IFN-γ secretion among various PBMC samples as compared to NA peptides. Higher number of positive responders were observed in case of HA and M1 peptides. Peptides P_H1, P_H4, P_N5, P_N6, P_M1 and P_M2 induced proliferative response in most of the healthy samples (≥5). Similarly, significantly higher secretion of IFN-γ level was observed in P_H1, P_H4, P_M2 and P_M3 peptide stimulated cells in most of the healthy samples (≥5). The results suggested that the *in silico* approach applied in combination with *in vitro* experimentation successfully identified peptides of hemagglutinin, neuraminidase and matrix 1 protein which were capable of eliciting immune response, thus making them potential candidates for universal influenza vaccine development.

TABLE OF CONTENT

LIST OF FIGURES

LIST OF TABLES

LIST OF ABBREVATIONS

ABTS	2,2'-Azinobis[3-ethylbenzothiazoline-6-sulfonicacid]-diammonium salt
ADCC	Antibody dependent cell mediated cytotoxicity
ADT	AutoDock tools
ANN	Artificial neural network
ANOVA	Analysis of variance
APC	Antigen presenting cells
ATF-2	Activating transcription factor 2
ATP	Adenosine triphosphate
AuNP	Gold nanoparticles
AVANA	Antigen variability analyser
BALB/c	Bagg Albino (inbred research mouse strain)
BCR	B cell receptor
BIMAS	Bioinformatics and molecular analysis section
BLASTp	Basic local alignment search tool for protein sequences
BrDU	5-Bromo-2'-deoxyuridine
BSA	Bovine serum albumin
C57BL/6	C57 black 6 (inbred strain of laboratory mouse)
CARD	Caspase activation and recruitment domains
CASP	Cytohesin-associated scaffolding protein
CBC	Cap binding complex
CC	Chemokines
CCT	Chaperonin containing TCP-1 (T-complex protein 1)
CD	Cluster of differentiation
CDC	Centers for disease control and prevention (USA)
CFSE	Carboxyfluorescein succinimidyl ester
Cgmp	Cyclic guanosine monophosphat

ClustalW	Clustal weighted
CO_2	Carbon dioxide
ConA	Concanavalin A
CpG	Cytosine-guanine rich oligonucleotide
CPSF4	Cleavage and polyadenylation specificity factor 4
CRM1	Chromosomal region maintenance 1
cRNA	Complementary ribonucleic acid
cRNP	Complementary ribonucleoprotein complex
CTA1-DD	Cholera toxin fused to dimer of D fragment (*Staphylococcus aureus* protein A)
CTL	Cytotoxic T lymphocytes
DC	Dendritic cells
DMSO	Dimethyl sulfoxide
DNA	Deoxyribonucleic acid
dsRNA	Double stranded ribonucleic acid
EBV	Epstein–Barr virus
EDTA	Ethylenediaminetetraacetic acid
eIF4E	Eukaryotic translation initiation factor 4E
ELISA	Enzyme-linked immunosorbent assay
ELISPOT	Enzyme-linked immunospot assay
Fab	Fragment antigen-binding (antibody)
Fc	Fragment crystallizable
FDA	Food and drug administration
Gal	Galactose
GDP	Guanosine diphosphate
GISAID	Global initiative on sharing all influenza data
GTP	Guanosine triphosphate
GUI	Guest user interphase
HA	Hemagglutinin

HBC	Hepatitis B virus core
HBx	Hepatitis B viral protein
HEPES	4-(2-hydroxyethyl)-1-piperazineethanesulfonic acid
His	Histidine
HLA	Human leucocyte antigen
HMM	Hidden Markov model
HRP	Horseradish peronodxidase
Hsp90	Heat shock protein 90
IAV	Influenza A virus
iBALT	Inducible bronchus-associated lymphoid tissue
IC_{50}	Half maximal inhibitory concentration
ICOS	Inducible costimulator
ICS	Intracellular cytokine staining
ICTV	International committee on taxonomy of viruses
IEDB	Immune epitope database
IFN	Interferon gamma
Ig	Immunoglobulin
IIV	Inactivated influenza vaccine
IL	Interleukin
IMGT	International immunogenetics information system
IPD	Immuno polymorphism database
IRD	Influenza research database
IRF	Interferon regulatory factor 3
ISAV	Infectious salmon anemia virus
ISED	Influenza sequence and epitope database
ISG	Interferon-stimulated genes
ISS	Immuno stimulating sequence
IVBD	Influenza virus database

JAK	Janus kinase
KCl	Potassium Chloride
KH_2PO_4	Potassium phosphate monobasic
LAIV	Live attenuated influenza vaccine
LDH	Lactate dehydrogenase
M1	Matrix 1 protein
M2	Matrix 2 proton channel
M2e	M2 protein extracellular domain
MAFFT	Multiple Alignment using Fast Fourier Transform
MDSC	Myeloid derived suppressor cells
MHC	Major histocompatibility antigen
ML	Machine learning
mRNA	Messenger ribonucleic acid
MTS	(3-(4,5-dimethylthiazol-2-yl)-5-(3-carboxymethoxyphenyl)-2-(4-sulfophenyl)-2H-tetrazolium)
MTT	3-(4,5-Dimethylthiazol-2-yl)-2,5-diphenyltetrazolium bromide
MUSCLE	Multiple sequence comparison by log-expectation
MVAS	Mitochondrial antiviral signaling protein
Mx	Myxovirus
MxA	Myxovirus resistance protein 1
NA	Neuraminidase
Na_2HPO_4	Sodium phosphate dibasic
NaCl	Sodium Chloride
$NaHCO_3$	Sodium Bicarbonate
NCBI	National centre for biotechnology information
NEP	Nuclear export protein
NF-κB	Nuclear factor kappa-light-chain-enhancer of activated B cells
NIAID	National institute of allergy and infectious diseases

NIH	National institute of health
NK	Natural killer cells
NKp44	Natural killer cell p44-related protein
NKT	Natural killer T cell
NLRP3	Nucleotide-binding oligomerization domain, leucine-rich repeat and pyrin domain containing protein 3
NLS	Nuclear localization signal
NOD	Nucleotide-binding oligomerization domain
NOS2	Nitric oxide synthase-2
NP	Nucleoprotein
NS1	Non-structural protein 1
NS2	Non-structural protein 2
NS3	Non-structural protein 3
NS5A	Non-structural 5A protein of hepatitis C virus
NXF1	Nuclear RNA Export Factor 1 (also known as tip associating protein)
OMPC	Outer membrane protein complex
OPEP	Optimized Potential for Efficient protein structure Prediction
P-value	Probability value
PA	Polymerase acid
PAMP	Pathogen associated molecular patterns
PB1	Polymerase basic 1
PB2	Polymerase basic 2
PBMC	Peripheral blood mononuclear cell
PBS	Phosphate buffer saline
PDB	Protein data bank
PR8	Puerto Rico/8/1934 strain (influenza A H1N1)
PRR	Pattern recognition receptors
PSSM	Position specific scoring matrix

QIV	Quadrivalent inactivated vaccine
qRT-PCR	Quantitative real time-polymerase chain reaction
Ran	RAS-related Nuclear protein
RIG-I	Retinoic acid inducible gene-1
RNA	Ribonucleic acid
RNP	Ribonucleoprotein
RPMI-1640	Rosewell Park Memorial Institute -1640 medium
SA	Sialic acid/ N-acetylneuraminic acid
SI	Stimulation index
SFC	Spot forming cells
SMM	Stabilized matrix method
ssRNA	Single stranded ribonucleic acid
STAT	Signal transducer and activator of transcription
STF	Salmonella typhimurium flagellin
SVM	Support vector machine
svRNAs	Small viral RNAs
SYBR	Synergy Brands, Inc.
SYFPEITHI	Peptide (Serine-Tyrosine-Phenylalanine-Proline- Glutamic Acid- Isoleucine-Threonine-Histidine- Isoleucine)
TAP	Tip associating protein
TAP	Transporter associated with antigen processing
Tat-SF1	Tat-specific factor 1
T-Coffee	Tree-based Consistency Objective Function for alignment Evaluation
TCR	T cell receptor
Tfh	T follicular helper cells
Th	T helper cells
TIV	Trivalent inactivated vaccine
TLR	Toll-like receptor

TNF-α	Tumor necrosis Factor alpha
TRAIL	Tumor necrosis factor related apoptosis-inducing ligand
Tregs	Regulatory T cells
TREX	Transcription/export complex
Trp	Tryptophan
Trp	Tryptophan
VLP	Virus like particle
vRNA	Viral ribonucleic acid
WHO	World Health Organization
WST-1	2-(4-Iodophenyl)-3-(4-nitrophenyl)-5-(2,4-disulfophenyl)-2H-tetrazolium

LIST OF SYMBOLS

$	dollar
%	Percentage
~	similar
<	Less than
>	Greater than
±	plus - minus
≤	Less than or equal to
≥	Greater than or equal to
®	Registered
°C	Degree Celsius
µ	Micron
µg/mL	Microgram per milliliter
^{51}Cr	Chromium isotope
Å	Angstrom
H	Hydrogen
h	Hours
IU	International Unit
L	Litre
mM	Millimolar
mL	milliliter
pg/mL	picogram per milliliter
™	Trademark
α	Alpha
β	Beta
γ	Gamma
δ	Delta

Chapter 1: Introduction

Influenza is a contagious respiratory viral infection that causes both seasonal endemics and periodic but unpredictable pandemics. The infection caused by influenza can be mild to severe and sometimes lethal. Influenza is one of the major public health concerns worldwide. Prophylaxis of influenza is still a subject to debate in spite of the collaborative efforts being made by researchers and medical professionals around the world towards its control. Global annual occurrence rate of influenza is estimated to be 5%–10% in adults and 20%–30% in children. According to World health organization, these annual epidemics result in about 3 to 5 million cases of severe illness and about 0.25 to 0.50 million deaths worldwide (WHO, 2014). Seasonal outbreaks are confined to winters in temperate regions whereas in tropical regions influenza outbreaks are known to occur throughout the year (WHO, 2014a). Influenza virus is transmitted among humans through direct contact with infected individual or exposure to virus containing fomite or aerosol (Morens et al., 2010).

Influenza virus evolves rapidly due to positive selection pressure imposed by immune surveillance of the host. Illness in humans is caused by three types of influenza virus i.e. influenza A, B and C virus. The three virus differ in their genome organization, mutability, host range and pathogenicity. Among these, influenza A virus is capable of causing pandemics and thus considered deadlier than influenza B and C. Influenza A virus is further classified into various subtypes; subtype H1N1 and H3N2 are capable of human transmission and are responsible for majority of influenza cases reported. Influenza A virus undergoes gene re-assortment and results in pandemics across the world. The last pandemic outbreak of H1N1 (swine flu) in 2009 affected 214 countries worldwide claiming 18449 lives (WHO, 2010). In India alone, Swine flu pandemic of 2009 affected 20604 people and 1763 deaths were reported (Mishra, 2015). Furthermore, reemergence of influenza A (H1N1) 09 virus in India caused 405 deaths out of 5044 reported cases in 2012 and 692 deaths out of 5250 cases in 2013. However, this count was quite high in the year 2014-15 when over 30,000 cases of influenza A (H1N1) 09 were reported countrywide claiming 2000 lives (till 28th March, 2015) (Mishra, 2015).

Influenza outbreak can be prevented and controlled by two ways viz. vaccines and antiviral prophylaxis. In case of sudden outbreaks of influenza, chemoprophylaxis (antiviral drug therapy) is chosen to prevent its spread**.** Two classes of antiviral drugs are used for the treatment of influenza; M2-channel inhibitors and neuraminidase inhibitors (Krol et al., 2014). Currently, the use of M2-channel inhibitors has been suspended due to high prevalence of resistant strains of influenza A virus across the world, the side effects reported and their specificity against influenza A virus. Lately, resistant strains of influenza virus have also been reported against neuraminidase inhibitor oseltamivir which is used for the treatment of influenza A and B infections (Samson et al., 2013). Hence, efficacy of antiviral drugs in treating influenza seems uncertain. Vaccines which are considered to be the safest mode of protection against infectious diseases appear to be the next viable option.

Vaccination is considered to be one of the most successful interventions ever introduced in the field of public health. For instance, smallpox was declared eradicated globally, in 1979 as a result of the vaccine which was introduced in the 19th and 20th centuries (WHO, 2016a). In 2011, rinderpest virus which is an infectious agent among cattle was declared eradicated by vaccine (Mariner et al., 2012). Another pathogenic virus on the verge of eradication is the Polio virus because of effective vaccination (WHO, 2016c). Various vaccination strategies are available to protect against influenza. Currently available influenza vaccine are traditional formulations like trivalent inactivated vaccine (TIV), quadrivalent inactivated vaccine (QIV) and live attenuated vaccines (Soema et al., 2015). These vaccines are composed of the combination of strains of circulating influenza A and B virus in inactivated or attenuated form. Apart from these, various other vaccines which have been licensed in the recent past include recombinant hemagglutinin (HA) vaccine, adjuvanted inactivated influenza vaccine (IIV), cell-culture derived IIV (Krammer & Palese, 2015). These strain specific vaccines require annual reformulation and their efficacy varies among individuals belonging to different age groups. Vaccine strains are selected as a result of continuous surveillance of influenza outbreaks and the causative strains. In case of unexpected outbreak, their prompt and sufficient supply is difficult due to long time frame required for their production. Moreover, in case of mismatch between the vaccine strain and the circulating strain, vaccine may not impart desired immunity.

Recurrent mutations enable influenza virus to escape host's immune surveillance and cause disease. The current vaccine strategies primarily induce antibody mediated humoral immune response targeted against the surface glycoprotein, mainly hemagglutinin (HA). HA undergoes frequent mutation to change the host specificity of influenza virus. Such vaccines are effective only against their matched influenza virus strains; they don't neutralize the unmatched strain of influenza virus. This is a major limitation of antibody mediated immune response against influenza. Lot of work was done to develop cross-protective mucosal IgA based vaccine which may be effective against closely related influenza A virus. But the cross-protectivity offered by this approach was found to be modest against distantly related strains of influenza A virus (Soema et al., 2015). In light of the above mentioned facts, vaccine approach based on highly conserved regions of influenza virus proteins is of appreciable importance.

The other arm of immunity called the cell mediated immunity is induced after the humoral response during natural influenza infection. T cells have a conspicuous role in controlling influenza virus infection and its eventual clearance (Sun & Braciale, 2013). Cell mediated immunity targets surface (structural) as well internal (non-structural) influenza proteins. Also, it is substantially cross reactive as it is directed against the epitopes which are likely to be shared among various strains and subtypes of influenza A virus unlike humoral immune response (La Gruta & Turner, 2014). T cells recognize small antigenic peptides bond to specialized molecules called human leucocyte antigen (Coughlan & Lambe, 2015) on the surface of cells. Upon activation, $CD8^+$ cells exhibit cytotoxic activity and restrain virus infection. $CD4^+$ T cell provide secondary signal for optimum humoral response and produce pro-inflammatory and antiviral cytokines which in turn enhance the $CD8^+$ T cell activation and proliferation. These facts calls upon the need to identify potential immunogenic peptides capable of inducing T cell based immunity for inclusion in future vaccine strategy (La Gruta & Turner, 2014).

In general, the concept of peptide based vaccines is more convenient and practical as compared to conventional vaccine approaches. Culturing of virus and many other pathogens for vaccine production is a difficult task. Also, many deleterious sequences of an antigenic protein or pathogen which are known to be oncogenic or generate autoimmunity. In contrast to that, peptides easy to synthesize with desired purity level and can be tailored easily to remove deleterious sequences. Peptides can be easily modified chemically by introducing lipids, phosphates or polysaccharides to enhance

immunogenicity and stability. They are devoid of any risk of reversion, genetic recombination or integration. Large scale production, modification, storage and transportation (in freeze dried form) of peptides is relatively easy as compared to the traditional vaccines (Purcell et al., 2007).

The extensive mutability of influenza virus significantly enhances its propensity to escape immune recognition, thus causing inadequate immune response of the host against all the circulating variants. Besides this, HLA gene polymorphism causes differential induction of immune responses directed against a specific epitopes from one individual to other. Various influenza peptides have been reported to elicit immunogenic response but majority of those of peptides are either strain specific or binding to limited HLA molecules (Vita et al., 2015). Therefore, a peptide candidate for universal influenza vaccine should be highly conserved, recognized in the context of various HLA alleles and elicit T cell mediated immune. Such peptides capable of binding to multiple HLA alleles are generally referred to as promiscuous peptide (Brusic et al., 2002). Such peptides can serve as prime targets for vaccine projected to impart immunity to higher proportions of the human population.

Immunoinformatics is a branch of immunology which aims to investigate genomic and proteomic data related to immunology by means of various statistical models and machine learning algorithms to obtain immunologically relevant results. Epitope prediction tools have now enabled us to screen the whole proteome of a pathogen and focus finely on the resultant sets of predicted peptides containing epitopes. It has dramatically reduced the time and efforts required to identify the potential epitopes based on their capability to bind HLA in contrast to the traditional approach which involves the synthesis and assessment of all possible overlapping epitopes. Therefore, it offers a promising alternative method which is less expensive as compared to the experimental determination. Further, molecular docking has been recognized as a valuable technique in computer aided drug and vaccine design (Patronov & Doytchinova, 2013; Singh et al., 2014). The epitope enriched peptides identified by immunoinformatics and docking approach is a screening step and not a stand-alone technology to identify immunogenic peptides. These peptides are required to be validated for eliciting T cell mediated immune response in *in vitro* and *in vivo* systems. T cell activation can be analysed by various techniques including cytokine secretion (IFN-γ) and proliferation.

Considering these facts, the present study was planned to identify highly conserved promiscuous peptides containing multiple overlapping $CD8^+$ and $CD4^+$ T cell epitopes from hemagglutinin, neuraminidase and matrix 1 protein of H1N1 influenza virus using different epitope prediction tools and molecular docking followed by *in vitro* experimentations to analyse the immunogenicity of these chemically synthesised peptides. This may help to formulate future vaccine strategy based on highly conserved and promiscuous T cell peptides for the control of Influenza A virus.

Therefore objectives of the present investigations are:

1. Prediction of peptides containing overlapping T cell epitopes using immunoinformatics tools from the conserved peptide regions of different proteins in H1N1 virus which can act as vaccine targets
2. Structure analysis and molecular modeling approach to assess the binding affinity of peptide to the HLA complex
3. Assessment of potential of peptide to stimulate T cell proliferation in peripheral blood mononuclear cells (PBMC) culture
4. Determination of immune response of these predicted peptides based on cytokines production/expression in PBMC culture

Review of Literature

2.1 Influenza

Influenza is a highly contagious viral infection of respiratory tract which causes both endemic seasonal infections and periodic but unpredictable pandemics. The infection caused by influenza virus can vary from mild to severe and sometimes might be lethal. Individuals suffering from influenza show symptoms like cough, rhinitis, sore throat, high fever, muscle ache, headache, fatigue etc. Usually these symptoms last for 1-2 weeks, however, in some cases it can result in pneumonia, bronchitis, sinusitis, myocarditis, pericarditis, ear infections and even death. Although influenza can affect anyone, but some high risk groups have been identified which are prone to develop influenza related complications. These groups include infants (<5 years), elderly people (>65 years), pregnant women, individuals working in health care facilities and people of American Indians and Alaskan native origin (CDC USA, 2015). Global annual occurrence rate of influenza is estimated to be 5%–10% in adults and 20%–30% in children. According to a study conducted in US, the annual economic costs for treatment of seasonal influenza varies from $13.9 thousand to $957.5 million across US counties, based on 2010 census (Mao et al., 2012).

2.2. Influenza virus

Influenza is caused by influenza virus which belongs to a family of single stranded segmented RNA (negative sense) virus called Orthomyxovirdae.

2.2.1 Classification and nomenclature

According to the classification system designed by International Committee on Taxonomy of Viruses (ICTV), Orthomyxoviridae family of virus is classified into six genera viz. influenza virus A, B, and C; Thogotovirus; Isavirus and Quaranjavirus (ICTV, 2014). The genus Thogotovirus contains two different species viz. Dhori virus and Thogoto virus, both isolated from ticks and thus, differ from influenza virus with respect to their host range. The genus Isavirus includes infectious salmon anemia virus (ISAV) which is very distinct from influenza virus A, B, and C; although various genetic, morphologic, and biochemical studies have identified these isolates as the members of

the Orthomyxoviridae family. The genus Quaranjavirus contains two species viz. Johnston Atoll virus and Quaranfil virus.

All influenza A and B virus possess eight single stranded RNA segments (negative sense) which encode for 11 proteins, whereas influenza C virus only have seven RNA segments which encode for nine proteins (Palese & Shaw, 2007). Influenza virus are categorized as A, B and C types depending upon their internal proteins viz. matrix proteins and nucleoprotein (Palese & Young, 1982). Influenza virus emerges from zoonotic reservoir of wild aquatic birds and cause acute respiratory illness in mammals (including humans) and domestic poultry.

Influenza A virus are (IAV) are classified depending upon the serologic reactivity of two surface glycoproteins viz. hemagglutinin (HA) and neuraminidase (NA) proteins. Eighteen serotypes of HA (H1-H18) and 11 serotypes of NA (N1 to N11) have been identified to circulate in birds, humans, swine and bats (Tong et al., 2013). Identification of H17N10 and H18N11 in bat samples, averted the notion of birds being the exclusive influenza A virus reservoir (Tong et al., 2013). Twentieth century witnessed the spread of various influenza subtypes in humans via person to person transmission or zoonosis. These include H1N1, H3N2 and H2N2. Fortunately, influenza virus of H5N1, H6N1, H7N9, H7N7, H7N2, H7N3 and H10N7 subtypes, have not acquired the potential for human to human transmission so far (Liu et al., 2013). Although, few confirmed cases have been reported among humans (Schrauwen & Fouchier, 2014). In their natural reservoirs, influenza A virus show insignificant evolution and infection pattern is asymptomatic. After acquiring transmission in other species, it mutates rapidly causing pandemics and epidemics in poultry and mammals.

Influenza B virus are classified into two categories viz. Yamagata-like and Victoria-like. Host range of influenza B and C virus is narrow. Other than humans, these virus also infect seals and pigs. Difference between the three types of influenza virus exists at the level of genomic organization, structure and severity of illness caused. Influenza A virus is associated with severe illness, influenza B with moderate illness and influenza C with mild symptoms. However, the complications associated with influenza infection may vary among individuals depending upon their age and special medical conditions.

Nomenclature system of influenza virus strains includes the virus type (A, B or C based on the antigenic specificity of nucleoprotein), the host of origin (except for humans), the

geographical origin, the strain number followed by the year of isolation and antigenic description in case of influenza A virus (H and N subtypes in parenthesis) (WHO, 1980).

2.2.2 Structure of influenza A virus

The structure of influenza A virus is shown in figure 2.1 (page 9). The segmented influenza A virus genome comprises of eight single-strands of negative-sense RNA associated with proteins viz. nucleoprotein (NP) and polymerase complex to form a ribonucleoprotein (RNP) complex. RNP complex forms fundamental unit for viral transcription and replication. The lipid bilayer encapsulating the RNP is embedded with 400-500 spikes of the glycoproteins HA and NA proteins in the ratio of 4:1 along with matrix 2 proton channel (M2) (Bouvier & Palese, 2008). The matrix protein (M1) lies beneath the lipid envelop and encompasses the inner ribonucleoprotein complex, providing structural integrity to the viral particle. Three high molecular weight proteins viz. PA polymerase acid (PA), polymerase basic 1 (PB1) and polymerase basic 2 (PB2) form RNA dependent RNA polymerase complex, which carries out the synthesis of mRNA from genomic RNA template.

The genome size of Influenza A virus genome is 13.5 Kb with the size of each segment varying from 0.89 to 2.341 Kb. These segments code for 11 different proteins (Figure 2.2, page 9). Influenza A virus (IAV) adopts various approaches like alternative mRNA splicing, alternative translational initiation and ribosomal frameshift to optimize its coding potential (Dubois et al., 2014). By exploiting these mechanisms, IAV has been reported to encode seven new proteins in recent past (Table 2.1, page 10). For instance, segment 2 mRNA undergoes alternative translation initiation to encode for PB1-F2, and PB1-N40. Also, PA-X is formed as a result of ribosomal frameshift in segment 3. Some other forms of PA i.e. PA-N155 and PA-N182 have also been reported to exist due to alternative translation initiation. These two proteins are truncated at the N-terminus. Well known mechanism of alternative mRNA splicing causes segment 7 to encode for the matrix protein M1, proton channel M2 and M42 protein and segment 8 to code nonstructural protein NS1, nuclear export protein (NEP/NS2), and NS3.

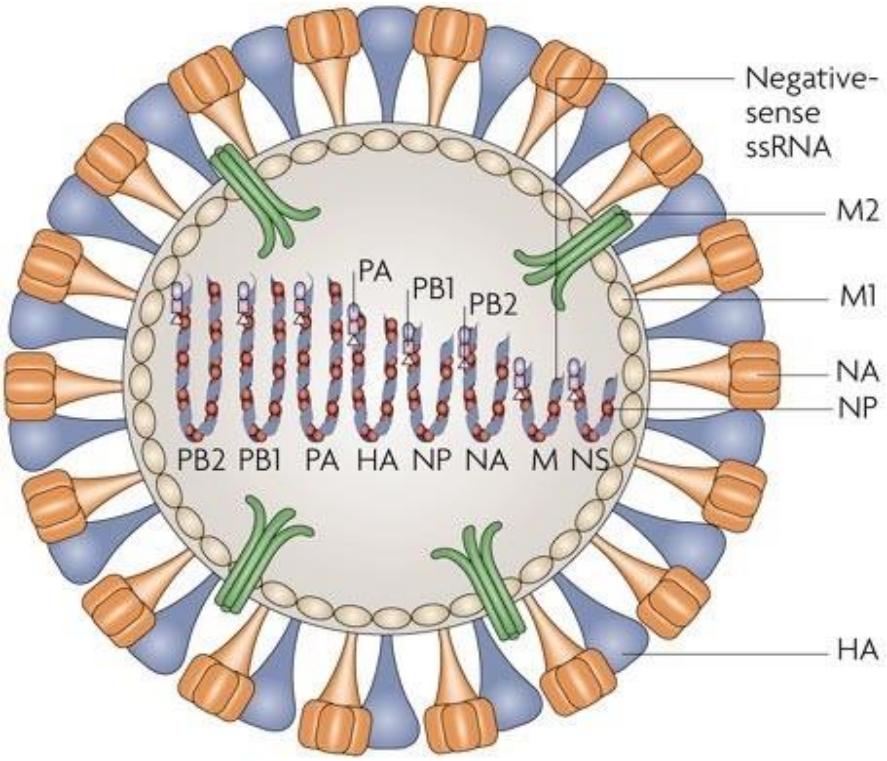

Figure 2.1: Structure of influenza A virus (Nelson & Holmes, 2007)

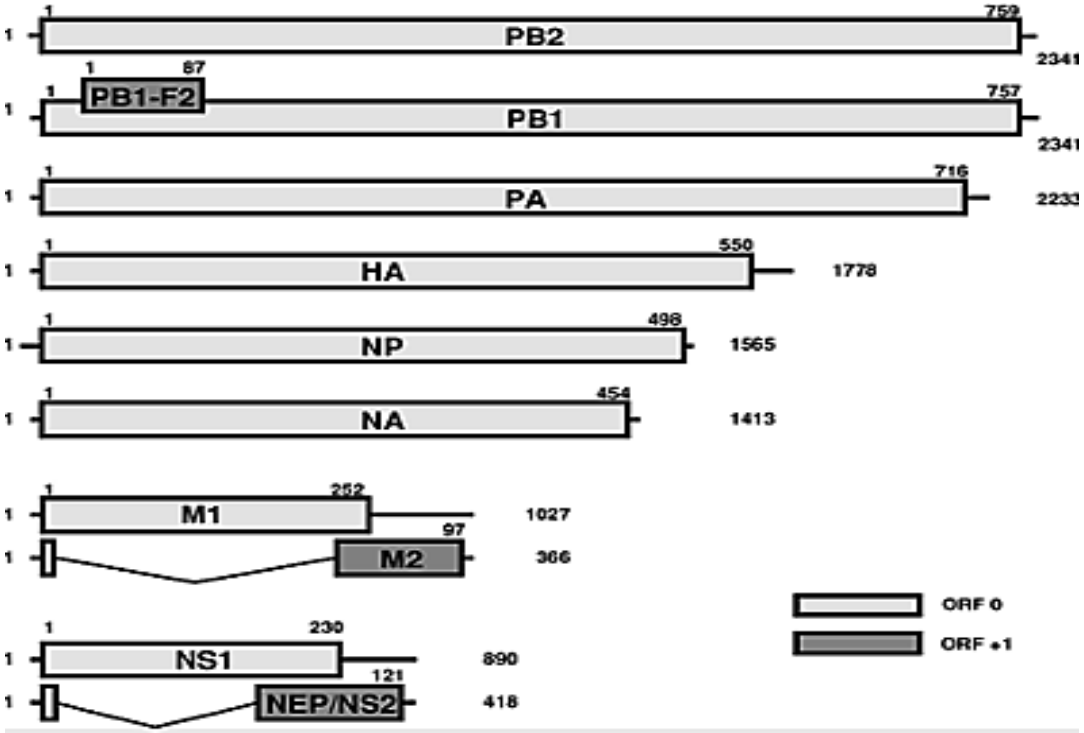

Figure 2.2: Genome organization of influenza A virus (Palese & Shaw, 2007)

Table 2.1: Newly discovered proteins of Influenza A virus genome

Segment	Size of gene (kb)	Gene	Viral Protein	Size of protein	Reference
2	2341	PB1	PB1 -F2	87	Chen et al., 2001
2	2341	PB1	PB1 -N40	718	Wise et al., 2009
3	2233	PA	PA-X	252	Jagger et al., 2012
3	2233	PA	PA-N155	154	Muramoto et al., 2013
3	2233	PA	PA-N182	181	Muramoto et al., 2013
7	1027	M	M42	99	Wise et al., 2012
8	890	NS	NS3	194	Selman et al., 2012

2.2.2.1 Hemagglutinin (HA)

It is an integral membrane protein which forms spikes that project outwardly. It constitutes about 40% of the total mass of viral particle. Cylindrical HA molecule is approximately 135Å long and 35–70Å radius (Isin et al., 2002). HA is a 565 amino acid long protein. It is a homotrimeric assembly wherein each monomer is composed of HA1 (18 – 343 amino acid) and HA2 (344 – 565 amino acid) subunits which are linked by a disulfide bridge and is anchored to the host derived virion membrane via a 27 amino acid long C-terminal of the HA2 subunit (transmembrane segment). Three monomers are organized into a central α-helical coiled coil which forms stem-like domain (HA1 and HA2) and three globular heads (HA1) which accommodate the sialic acid-binding sites (Weis et al., 1990). HA is cardinal to the adherence and penetration of the virus particle into the host cell. HA binds to sialic acid moiety of host's cell surface proteins and causes the fusion of the viral envelope with the host endosomal membrane via N-terminal fusion peptide of the HA2 subunit (Bullough et al., 1994; Skehel et al., 1982). Full functionality of this molecule requires post translation modifications (i.e. glycosylation and palmitoylation) of precursor, removal of signal peptide in endoplasmic reticulum and cleavage into HA1 and HA2 (Palese & Shaw, 2007).

2.2.2.2 Neuraminidase (NA)

It is a homotetrameric enzymatic protein (exosialidase; EC 3.2.1.18) present on the surface of the influenza virus, which catalyzes the cleavage of terminal sialic acid residue linked α-ketosidically to an array of surface biomolecule-like glycoproteins and

glycolipids on the surface of host cell. NA is a 453 amino acid long protein distributed in intravirion region (1 – 6), transmembrane region (7 – 35) and virion surface (36 – 453). Mushroom-shaped NA molecule has a head region (80x80x40 Å) on the stem (15x60-100 Å). Active site of NA along with calcium binding site, which is essential to stabilize the molecule at low pH, resides in the head region (Shtyrya et al., 2009). The removal of sialic acid moiety from the surface protein of the host cell as well as newly formed virions is essential for the release of viral progeny. One of the findings suggested that removal of sialic acid from the cilia for respiratory tract, mucine and glycocalyx by NA limits the access of virus to the other target cells (Matrosovich et al., 2004).

2.2.2.3 Matrix 2 protein (M2)

It is a small homotetrameric protein which serves as a pH gated proton channel on the membrane of influenza virus. 97 amino acid long M2 protein is a single pass membrane protein. Viral membrane is sparsely covered with M2 molecules as compared to HA (1:10-100) (Bouvier & Palese, 2008). After the endosome mediated entry of virus particle inside host cell, M2 proton channels open up in response to low pH. Sudden flux of proton in virus triggers the fusion of endosomal membrane with viral membrane and segregation of viral RNP from matrix 1 protein. As a result, viral RNA is released in the cytoplasm of host cell. M2 is also responsible for counter balancing the acidity of trans-golgi network and thus conserving the structural integrity of the acid-sensitive HA protein during transportation (Sugrue et al., 1990). Four transmembrane helices pack tightly to form a channel in which His^{37} acts as the pH sensor and Trp^{41} as gate (Schnell & Chou, 2008). High pH favors closure of channel whereas low pH opens (activates) the channel.

2.2.2.4 Matrix 1 protein (M1)

It is a 60 Å long monomeric protein which carries two globular domains. The N-terminal domain binds to the viral membrane (1 to 164 amino acid) and the C-terminal domain binds to ribonucleoprotein (165 to 252 amino acid) both these domains are linked by a loop like structure which is protease-sensitive (Ruigrok et al., 2000). N terminal globular domain is composed of nine α-helices (H1-H9) (Sha & Luo, 1997). These α-helices are organized into two bundles, each having 4-helices H1-H4 and H6-H9 connected via another H5 helix linker. M1 exists as a homodimer or a homomultimer.

M1 lies below the viral envelop and plays diverse roles in the life cycles of influenza A virus. It binds to viral envelop as well as the RNA at the same time. M1 shells the RNP complex in the membrane envelop and stabilizes the virion architecture. M1 also forms the crosslink between with the cytoplasmic tails of HA and NA and initiates viral budding from the host cell. Low pH inside endosomal compartment induces a structural change in M1 leading to the formation of unstable M1 monomers during the virus entry (Fontana et al., 2012). This dislodging of M1 protein shell facilitates the release of vRNP into the cytoplasm. vRNPs thus enter the nucleus and initiate the transcription and replication of viral genome (Bui et al., 1996). M1 and NEP (Nuclear export protein) together promote the nucleocytoplasmic transport of newly formed vRNPs. Influenza virus exists in 2 different morphological forms: spherical (~100-nm diameter) and filamentous (~100 nm × 2 to 20 μm) virions (Fujiyoshi et al., 1994). The filamentous trait of influenza virus has been traced to Helix six domain of M1 protein (Burleigh et al., 2005). The helix 6 (H6) domain (91 to 105 amino acid) of M1 has been recognized as multifunctional domain, serving as nuclear localization signal (NLS) for the translocation of M1 in nucleus as well as transcription inhibition motifs. Positively charged sequence 101-RKLKR-105 of H6 domain is the NLS and NEP binding motif.

2.2.2.5 Nucleoprotein (NP)

It encapsulates the negative stranded viral RNA and protects it from nucleases. The crescent shaped NP monomer is mostly α-helical. It has a head domain and a body formed by discontinuous polypeptide regions i.e. segments 150–272 and 438–452 form the head domain whereas the body domain consists of the 21–149, 273–396 and 453–489 segments (Ye et al., 2006). It is a positively charged protein at neutral pH, rich in arginine, serine and glycine amino acids. It forms a protein scaffold to support viral RNA fragment by homomultimerizing. It interacts with various other molecules of viral origin (ssRNA, PB1, PB2, PA, M1) as well as cellular origin (Importin α, F-actin, CRM1/exportin-1 and helicase BAT1/UAP56). It binds to ssRNA with high affinity but no sequence specificity is reported. The stoichiometry of their interaction is approximately 1 NP molecule per 24 nucleotides of RNA. Nucleoprotein interacts with the viral polymerase and promotes viral RNA replication.

2.2.2.6 Viral RNA polymerase

RNA dependent RNA polymerase is an assembly of three protein subunits i.e. PA polymerase acid (PA), polymerase basic 1 (PB1) and polymerase basic 2 (PB2) subunit which together transcribe and replicate viral RNA segments. The three proteins exist in tight association as PA-PB1 -PB2 (linear arrangement from N- to C-terminal). Hence, PB1 binds to PA as well as PB2. PA and PB1 complex is transported from cytoplasm to nucleus via RanBP5 protein, whereas PB2 is imported separately to the nucleus. Assembly and nuclear export of vRNA polymerase is mediated by cellular chaperons like Hsp90 (Naito et al., 2007) and CCT (Fislová et al., 2010). Cryo-electron microscopy affirmed a double helical arrangement of vRNP in which RNA polymerase is located at a corner (Arranz et al., 2012).

The viral polymerase interacts with the hyperphosphorylated C-terminal domain of large subunit of cellular RNA pol II (Engelhardt et al., 2005). It also binds to both the terminal ends of vRNA and cRNA. PB2 initiates transcription by binding to 5' cap of pre-mRNA. PA by means of its endonuclease activity cleaves the 5' methylated cap of cellular mRNA, 10 to 13 nucleotides downstream of the cap structure, thus generating primer for viral mRNA synthesis (Bier et al., 2011). These short capped RNAs are used as primers by PB1 for transcription of viral mRNAs which catalyse the sequential extension of nucleotide chain. Motif S-D-D at positions 444 to 446 is the anticipated active site for polymerization.

2.2.2.7 Non-structural protein 1 (NS1)

It is a non-structural protein encoded along with its splice variants NEP/NS2. It is synthesized in inflected cells but not incorporated in influenza virion. NS1 plays multiple roles in the virus infected cells. The most studied role of NS1 is the suppression of type I interferon (IFN-α/β) mediated innate immune response. NS1 inhibits activation of IRF-3, NFκB and ATF-2/c-Jun transcription factors (Gack et al., 2009). It binds and inhibits the cleavage and polyadenylation specificity factor (CPSF4) and the poly (A)-binding protein involved in the processing of 3'end of cellular mRNA and thus blocks the post transcriptional modifications of host pre-mRNA. Consequently, 3' end of pre-mRNA remains unprocessed and results in accumulation of host pre-mRNA in the nucleus and cessation cellular protein synthesis (Zürcher et al., 2000). NS1 has also

been reported to be associated with the regulation of apoptosis of host cell in case of H5N1 and H11N1 (Mukherjee et al., 2012).

2.2.2.8 Non-structural protein 2 (NS2)

It is a 121 amino acid long protein encoded by alternatively spliced mRNA of NS1. This protein was renamed as nuclear export protein (NEP) because its presence was detected in purified virion. NEP along with M1 protein is considered to be necessary for the nucleocytoplasmic export of vRNP (O'Neill et al., 1998). Although NEP lacks intrinsic RNA binding ability, it acts as an adaptor between vRNPs and nuclear export machinery of the host cell. N-terminal of NS2/NEP interacts with cellular protein CRM1 (chromosome region maintenance 1) whereas its C-terminus extending from residues 81–100, is associated with the viral M1 protein (Shimizu et al., 2011). CRM1, which belongs to importin-β superfamily of nuclear transport receptors, binds to nuclear export signal of NEP. It is also reported to regulate the replication and transcription of vRNA (Robb et al., 2009). It reduces the accumulation of transcription product (viral mRNA) and simultaneously promotes the accumulation of replication product.

2.2.3 Life cycle of influenza A virus

Life cycle of influenza is divided into various phases (Figure 2.3, page14).

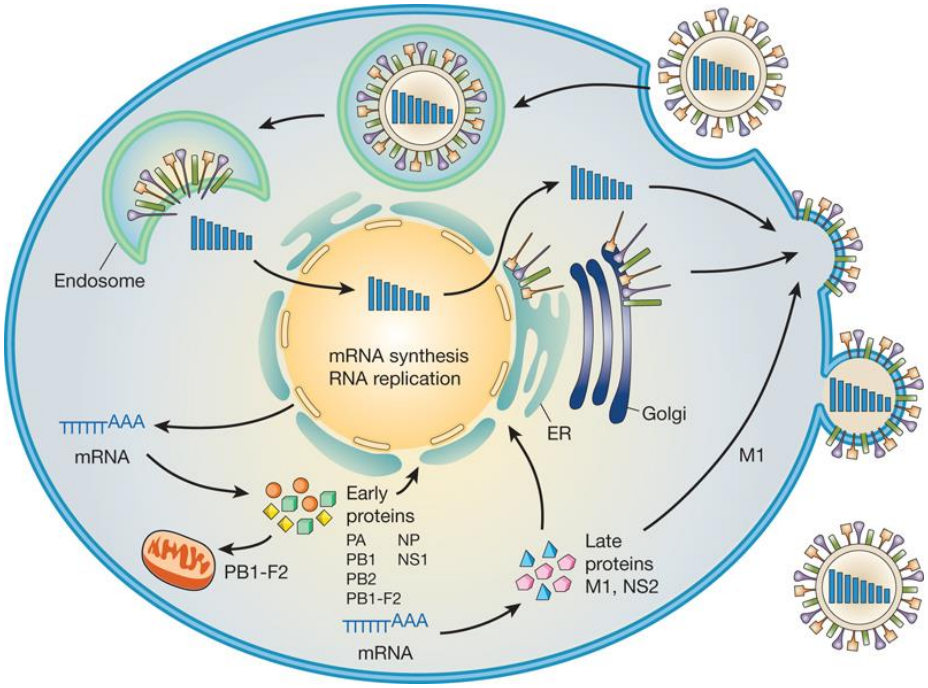

Figure 2.3: Life cycle of influenza A Virus (Neumann et al., 2009)

2.2.3.1 Attachment, entry, fusion and uncoating

Influenza virus attaches via surface glycoprotein HA to sialic acid residue on the host cell membrane. Human influenza virus prefers to bind to sialic acid (also called N-acetylneuraminic acid) attached to the penultimate galactose sugar by an α (2,6) linkage (SAα2,6Gal) whereas those from avian origin mostly bind to sialic acid with an α(2,3) linkage (SAα2,3Gal) on the host cell surface. Swine host serves as a mixing vessel for influenza virus since influenza virus recognizes both the linkages viz. α (2,6) and α(2,3) (Skehel & Wiley, 2000). It is known that this receptor binding specificity is not absolute as both the sialic acid linkages are found in human as well as avian cells. Further, virus passaged in a particular host mutates its receptor binding sites thus, adapting itself to that host. Single amino acid mutation is capable of altering the receptor binding specificity of influenza virus (Glaser et al., 2005). It was demonstrated that mutation of single amino acid in HA (D190E) changed the binding preference of influenza A/New York/1/18 HA from α (2,6) to α (2,3). HA_0 is cleaved by arginine-specific endoprotease secreted by the bronchial epithelial cells, resulting in the formation of HA1 and HA2, which are joined by a disulfide bond with the elimination of an arginine residue. Upon binding to the host cell, influenza virus undergoes receptor mediated endocytosis (primarily clathrin mediated) (Lakadamyali et al., 2004). Along the endocytic pathway, virus are trafficked into late endosomes (pH 5). Low pH inside the endosome triggers an irreversible change in conformation of HA2 subunit, thereby exposing the hydrophobic fusion peptide at the N-terminus of HA2. Fusion peptide inserts itself in the endosomal membrane and thus, leads to the fusion of the viral envelop with endosomal membrane. Further, acidic environment of endosome causes the influx of H^+ ions via viral M2 proton channel into the virus particle, which disrupts the interactions between viral proteins. Consequently, RNP devoid of M1 matrix protein is released in cell cytoplasm.

2.2.3.2 Nuclear import of ribonucleoproteins

Viral RNA is coated with nucleoprotein along the length whereas three polymerase proteins are bound to the partially complementary ends of the viral RNA. This whole assembly, termed as ribonucleoprotein complex doesn't pass via passive diffusion into the nucleus because of its large size. NP which carries three nuclear localization signals (NLSs), mediate the interaction of RNP with the nuclear import machinery. NLSs are

recognized by karyopherins α and β (importins). NP carrying NLS recruit karyopherin α1 which further binds to karyopherin β forming a trimeric complex which enters into the nucleus in a RanGDP-dependent manner along with P_{10} (O'Neill et al., 1995).

2.2.3.3 Influenza virus RNA synthesis: transcription and replication

vRNA is associated with multiple copies of NP along its length (1 NP for every 24 nucleotides). 5′ and 3′ termini of vRNA are highly conserved and base pairs to form partial double stranded structure which binds to trimeric RNA polymerase complex (PB1, PB2 and PA). In nucleus, vRNA polymerase transcribes vRNA into viral mRNA which is capped at 5' end and polyadenylated at 3' end. mRNA is exported to cytoplasm of host cells where it gets translated by cellular machinery into viral proteins. vRNA polymerase also copies vRNA to cRNA (complementary RNA), which in turn serves as a template for the synthesis of vRNA.

Thirteen nucleotides at the 5' end and 12 nucleotides at 3'end of vRNA segments are conserved in all the eight segments of influenza A virus. These conserved stretches of vRNA have partial inverse complementarity which forms secondary structure. The secondary structures are proposed as the vRNA promoters and thus bind to cis-acting vRNA polymerase. Viral mRNA synthesis relies on cellular RNA polymerase II activity. The 5' capped primer required for viral mRNA synthesis is abducted from host pre-mRNA synthesized by RNA polymerase II. This phenomenon is called cap snatching. Transcription commences with the binding of PB1 to 5'-end of vRNA. Allosteric changes promote the binding of PB2 to 5' cap of host mRNA. Following this, PA cleaves the host mRNA and 5' capped primer is generated for transcription. G residue at the 3' end of capped primer positions itself just opposite to penultimate C residues of the 3' end of template vRNA, in the active site of PB1. PB1 subunit catalyzes the addition of nucleotide to the caped primer, complementary to vRNA. Transcription proceeds until the encounter of a sequence of 5-7 uracil residue located 16 nucleotides upstream from 5'end of vRNA, which serves as the polyadenylation sequence. Steric hindrance posed by polymerase bound 5-'end doesn't allow the elongation to proceed to the last nucleotide of vRNA. Thus, after addition of polyA tail transcription terminates. PolyA tail is essential for the nuclear transport of viral mRNAs.

Replication of vRNA genome is a two-step process, involving replication of vRNA to form cRNA and this cRNA serves as a template for vRNA synthesis which lacks 5' cap

and 3’ poly (A) tail. vRNA gets encapsulated by associating itself to polymerase and NP. Studies indicate that domains of PB1 responsible for vRNA replication and transcription are different (Binh et al., 2013). Replication of viral genomic fragments is a primer independent process. Binding of GTP to polymerase marks the initiation of this replication. GTP is directed opposite to the penultimate cytosine residue at 3’-terminal vRNA. Phosphodiester bond formation occurs with ATP at position 1, thus forming pppApG dinucleotide, which is further elongated by *trans*-acting polymerases. The copied 3’-end of vRNA rejoins virus polymerase. 5’-end of freshly synthesized cRNA binds to *trans*-acting polymerase and NP to form cRNP complex. Binding of NP to nascent RNA is reported to be facilitated by cellular UAP56 and Tat-SF1 chaperones (Momose et al., 2001; Naito et al., 2007). It has been suggested that in early phase of viral life cycle, in the absence of NP and vRNA polymerase cRNA is quickly degraded. It has been proposed that replication of cRNA to vRNA follows similar mechanism.

Regulation of viral RNA synthesis is proposed to be mediated by NEP. A study concluded that the expression of the viral NEP alters viral RNA levels by down regulating the accumulation of viral mRNA and simultaneously up regulating the accumulation of cRNA and vRNA (Robb et al., 2009). Also, it has been suggested that NEP regulates the vRNA synthesis via 22-27 nucleotide long small viral RNAs (svRNAs). Their expression has been found to be correlated to the accumulation of vRNA. It has also been suggested that svRNAs cause a shift from transcription to replication by interacting with PA subunit of vRNA polymerase (Perez et al., 2012).

2.2.3.4 Nuclear export of ribonucleoproteins

5’ cap of nascent viral mRNA releases itself from PB2 subunit and binds to nuclear cap binding complex (CBC) and further TREX (Transcription-export) complex and NXF1/TAP, which ensures its nuclear export. CBC is assumed to be replaced by host eIF4E (Bier et al., 2011). Viral mRNA Segments 7 and 8 undergo alternate mRNA splicing to code for various viral proteins. For this, host splicing machinery plays a vital role. Viral NS1 protein also regulates the ratio of spliced and unspliced mRNA product of segment 7 of vRNA (Robb & Fodor, 2012).

Replication products of viral genome i.e. vRNPs are exported out of cytoplasm via Crm1 dependent pathway. NEP interacts with cellular nuclear export protein Crm1 (Chromosomal Maintenance 1, also called Exportin 1) and the viral M1 bound to vRNPs

to promote nuclear export (Paterson & Fodor, 2012). Also, it is evident that the vRNPs are selectively transported out of nucleus to be packed in viral progeny, although the molecular mechanism behind this selectivity is still under investigation. Currently, chromatin targeting of vRNPs is the proposed mechanism of their selective cellular export machinery (Chase et al., 2011).

2.2.3.5 Virus assembly and release

Viral assembly and budding of influenza virus is a complex multistep process (Rossman & Lamb, 2011). Soon after the synthesis of the three viral surface proteins viz. HA, NA and M2 by membrane bound ribosomes, HA and NA (not M1) are glycosylated and folded inside the endoplasmic reticulum. Further, they are directed via golgi network to the site of viral budding which is apical side of polarized host cell. Lipid raft domain on the host cell plasma membrane is the site of influenza virus assembly and budding. Viral HA and NA protein are directed to lipid raft domains, thus causing its enlargement and deformation. Also, association of HA with lipid raft is considered to be essential for efficient replication of vRNA. Some workers suggest that HA is not essential for viral budding. Its mutation or deletion doesn't affect the virion count budding from the virus-infected cell, although the viral entry in impaired. In such cases, NA compensates the lack of HA and initiates the viral budding. M1 binds to the glycoproteins HA and NA (cytoplasmic domain) and to the RNP-NEP complex, thus acting as a bridge between the inner core components and the membrane proteins. The binding of M1 to RNP-NEP complex is likely to be mediated by F-actin. M2 binds to cholesterol, thus remains confined to the raft periphery. Within the cytoplasmic tail of M2 protein lies a highly conserved 17 amino acid amphipathic helix which alters the curvature of membrane near the neck of budding virus, thus mediating the excision and release of viral particle (Rossman et al., 2010). After the membrane scission, virion remains attached to the host cell membrane, because of viral HA- membrane bound sialic acid moiety. NA comes to play the role of sialidase, disrupting the HA-sialic acid interaction by cleaving off sialic acid moiety from the cell surface, thus releasing the viral progeny. HA, NA, M1 and M2 function in harmony with each other at a precisely defined time and space to carryout budding of influenza A virus.

Fully infectious virion must contain full complement of RNA genome segments, assembled and packed correctly. Various models have been given to explain the packing

of vRNA fragments into virion. According to selective incorporation model, unique signals present in the 5' and 3' regions of viral segments dictate the packing of viral genome, thus ensuring the presence of each of the eight viral segments in a viral particle. Packing signal sequences have been reported for NS, NA, PA, PB1 and PB2 vRNA segments of influenza (Fujii et al., 2005; Fujii et al., 2003; Liang et al., 2005; Watanabe et al., 2003).

2.3 Epidemiology of Influenza

Although single infection is sufficient to produce lifelong immunity against the invading virus strain (Kim et al., 2009); nevertheless, the novel strain/subtypes result in frequent seasonal outbreaks and occasional pandemics. Constant antigenic variations enable the influenza virus to escape host immune response. The influenza virus undergoes antigenic variation by the mechanism of antigenic drift and shift occurring frequently (Zambon, 1999). Antigenic drift occurs every 2-8 years on an average, in response to selection pressure to evade human immunity (Plotkin et al., 2002). Antigenic drift involves subtle point mutation within the binding sites of HA, NA or both, probably each time the virus replicates, leading to gradual rise of a new influenza strain against which limited immunity exists in the host. Host antibodies raised against the previously circulated strains fails to neutralize the new virus, leading to the rapid spread of new viral strain among the population (Webby & Webster, 2001). Antigenic shift is the process of inception of novel influenza virus subtype in humans which has not circulated earlier in humans (Neumann et al., 2009). It can occur via direct zoonotic transmission from animal reservoir or via the process of genetic reassortment i.e. exchange of gene segments among two or more influenza A virus during their co-circulation in a host (Potter, 2001; Schrauwen & Fouchier, 2014). Antigenic shift is observed only in case of influenza A virus, whereas antigenic shift occurs in all strains of influenza A and B virus. Antigenic shifts result in pandemic which are estimated to occur thrice in every 100 years (Potter, 2001). The new subtype is susceptible to antigenic drift like any other influenza virus. Thus, antigenic shift is responsible for worldwide pandemics against which the population has no immunity and antigenic drifts give rise to epidemics since partial immunity exists in people due to existence of cross- reacting antibodies induced by former infection.

Pandemics (worldwide outbreak) are rather rare events. Four pandemic outbreaks have been recorded in the past 100 years (Table 2.2, page 21), out of which Spanish flu (1918-19) has been cited as the most disastrous pandemic in world medical history (Morens et al., 2010). After the Spanish flu outbreak, influenza returned in a pandemic form in 1957-1958 (Asian flu) were replaced when descendants of H1N1 circulating in humans by new H2N2 pandemic strain and, again, in 1968-1969 (Hong Kong flu) due to appearance of H3N2. But, these pandemics were much less severe than the 1918-1919 pandemic. April, 2009 witnessed the outbreak of another pandemic in California (USA) and Mexico which disseminated worldwide through human to human transmission in the following three months, resulting in the first influenza pandemic outbreak of the 21st century (Galiano et al., 2011). As of 1 August 2010, around 214 countries and overseas territories reported laboratory confirmed cases of pandemic influenza H1N1 2009 (WHO, 2010). Currently, H1N1 and H3N2 subtypes of influenza virus are circulating in humans (WHO, 2014).

Most of influenza virus circulating in animals (avian or swine) do not infect humans however, they can be zoonotic. Best known examples of influenza virus subtypes at the human-animal interphase are H5N1, H5N6, H7N9, H7N3, H7N7, H9N2, H10N8 etc. (Table 2.3, page 22). Human transmission of these virus has not been reported clearly, however, speculations are rife regarding the increased risk of emergence of pandemic virus strains that are easily transmissible among humans.

Table 2.2. History of Influenza A pandemics

Pandemic	Year	Influenza A subtype	Origin of virus	First outbreak	Age group most affected	Deaths caused worldwide	Reference
Spanish flu	1918-19	H1N1	H1N1 swine virus	-	Young adults (15-44 years)	≈ 50 million	Morens et al., 2010; WHO, 2005
Asian flu	1957-58	H2N2	Reassortment between human and avian influenza virus (HA, NA and PB1 from avian H2N2 and rest of the gene segments from H1N1)	East Asia (China)	Very young and very old	≈ 2 million	Schrauwen & Fouchier, 2014; WHO, 2005
Hong Kong flu	1968-69	H3N2	Reassortment between human and avian influenza virus (HA, and PB1 from avian H3 virus)	Hong Kong		≈ 1 million	Schrauwen & Fouchier, 2014
Swine flu	2009-10	H1N1	Reassortant virus (NA and M gene segments from 'Eurasian swine' influenza lineage, other genes from triple reassortant influenza virus of swine, human and avian influenza virus)	Mexico	>65 years	18449	Dawood et al.; 2012; Galiano et al., 2011; WHO, 2010

Table 2.3. Influenza at the human-animal interface

Subtype	Year	Location	Confirmed cases	Deaths	Reference
H5N1	2003-15	Southeast and East Asia	844	449	WHO, 2015
H7N9	2013-15	China	707	280	WHO, 2016; WHO, 2015
H7N7	2003,2009	Netherlands	92	1	Fouchier et al., 2004; Puzelli et al., 2014; WHO, 2003
H7N3	2004-13	Mexico, Italy, UK	5	-	Nguyen-Van-Tam et al., 2006; Puzelli et al., 2014; Tweed et al., 2004
H5N6	2015	China	4	-	WHO, 2015
H3N2v	2005-16	USA	354	1	CDC USA, 2016
H1N1v	2005-16	USA	20		CDC USA, 2016
H1N2v	2005-16	USA	5		CDC USA, 2016
H9N2	2014-15	China	28	0	WHO, 2016b
H10N8	2013	Taiwan, China	3	2	Liu et al., 2015; WHO, 2013

2.4. Immune response to influenza

2.4.1 Innate immune response

Innate defence mechanisms are crucial barriers to check influenza virus infection (Figure 2.4, page 25). Virus invades human body by inhalation of aerosol containing virus particles. After its entry, virus encounters mucous (covering the respiratory epithelia). Viral RNA in infected cells is recognized as extraneous entity by various pattern recognition receptors (PRRs). This results in release of various cytokines. Type I interferons are secreted by macrophages, dendritic cells, pneumocytes. They upregulate the expression of IFN stimulated genes (ISGs) through JAK/STAT signalling pathway and induce antiviral state in neighbouring cells. Mx gene is an ISG which encodes a GTPase called the MxA protein which elicits strong anti-influenza activity by inhibiting replication (Kreijtz et al., 2011). Chemokines recruit natural killer (NK) cells and other immune cells at the site of infection. Eicosanoids and pro-inflammatory cytokines act by evoking local and systemic response against the viral infection such as inflammation, fever etc. (Iwasaki & Pillai, 2014).

Innate immune system of the host uses patterns recognition receptors (PRR) to recognize influenza virus infection via pathogen associated molecular patterns (PAMP). PRR such as Toll-like receptor 3 (TLR3) recognizes ds-RNA in endosome, which induces the NF-*k*B dependent pro inflammatory cytokine expression. However, studies carried out on $TLR3^{-/-}$ mice reveal that TLR3 is dispensable for generating normal humoral and cell mediated immunity (Heer et al., 2007; Iwasaki & Pillai, 2014). TLR7 recognizes ssRNA of influenza virus in endosome, resulting in activation of IFN-regulatory factor 7 (IRF7) or NF-*k*B. These transcription factors stimulate expression of type I IFNs and pro-inflammatory cytokine to arrest influenza viral replication and boosts antiviral response (Diebold et al., 2004; Iwasaki & Pillai, 2014).

Inside the infected cell, viral ssRNA (having 5' triphosphate) in cytosol is recognized by repressor domain of retinoic acid inducible gene (RIG-I). RIG-I undergoes a conformational change exposing the caspase activation and recruitment domains (CARDs) which undergoes ubiquitination. RIG-I then binds to mitochondrial antiviral signalling protein (MVAS) leading to activation of IRF3 and NF-κB transcription factors. RIG-I mediated recognition is considered to be the key determinant of innate antiviral response in infected host. Influenza protein NS1 is capable of blocking RIG-I signaling.

Another class of PRRs, NOD-like receptor family member NLRP3 (NOD-, LRR- and pyrin domain containing protein 3) forms multiprotein complexes called inflammasomes. It results in the activation of caspase 1 and proteolytic maturation of IL-1β and IL-18. Accumulation of PB1-F2 fibrils in the phagosomes also results in activation of NLRP3, IL1β and IL-18.

Other than intracellular innate sensing, innate immune system deploys various cells such as dendritic cells (DC), alveolar macrophages, and natural killer (NK) cells to fight influenza infection. Activated alveolar macrophages act by phagocytosing influenza infected cells and produce nitric oxide synthase-2 (NOS2) and TNF-α thus, limiting the spread of influenza (Kreijtz et al., 2011). DC are designated as professional APCs of influenza virus infection. They detect and neutralize the virions and apoptotic bodies. $CD11c^+$ conventional DC and $CD21^+$ follicular DC contribute towards the formation and persistence of iBALT (inducible bronchus-associated lymphoid tissue) (Foo & Phipps, 2010). DC degrade the viral proteins and present these influenza virus derived immune-peptides (epitopes) to T cells via MHCs and activate the adaptive immune response. NK cells are the effector cells which recognize the antibody bound influenza infected cells via NKp44 and NKp46 cytotoxicity receptors. NK cells upon their binding to the influenza virus HA protein results in lysis of infected cells (Kreijtz et al., 2011).

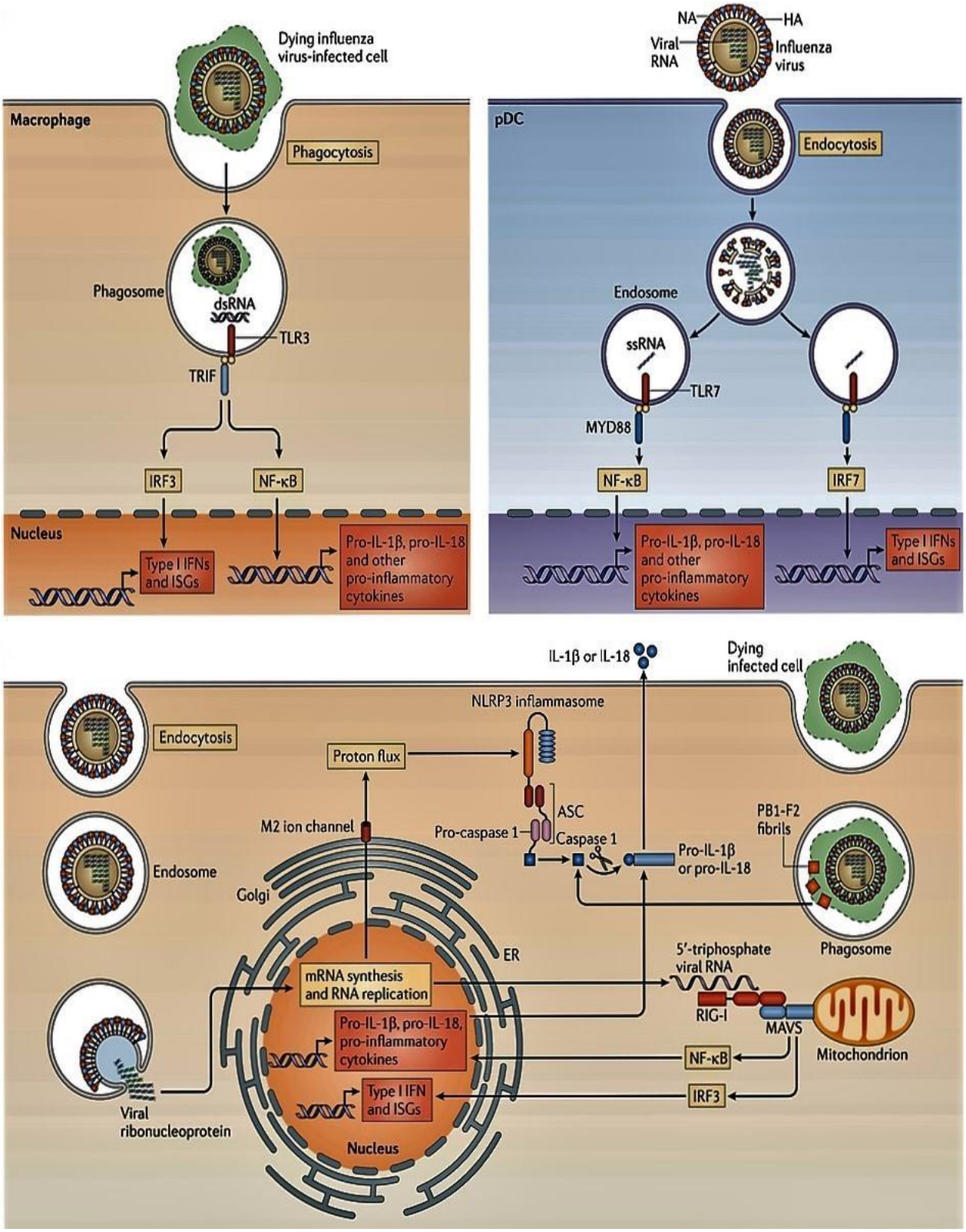

Figure 2.4. Innate immunity against influenza virus (Iwasaki & Pillai, 2014)

2.4.2 Adaptive immune response

Adaptive or acquired immunity is a more comprehensive line of defence, capable of recognizing subtle molecular differences among different pathogens, thus acting against pathogen specifically. It relies on B and T lymphocytes and is relativity slow upon first encounter with the antigen (primary response). A distinguished attribute of adaptive immune response is immunologic memory which is the capability to respond promptly and efficiently at the time of second exposure to the same pathogen (secondary or anamnestic response).

Influenza specific antibodies correspond mainly to IgA, IgM and IgG isotype. IgM plays major role in primary infection and assists in complement mediated neutralization of influenza virus (Jayasekera et al., 2007). Secretory IgA in the mucous serves to protect respiratory epithelium from viral infection. Dimeric IgA neutralizes the newly formed viral influenza proteins intracellularly and thus, interrupts viral assembly (Mazanec et al., 1995). Further, high level of serum IgA is a prognostic feature of acute influenza (Rothbarth et al., 1999). IgG in the respiratory tract imparts long-lived immunity against influenza. Plasma IgG acts as a substitute for secretory IgA-mediated protection in the nasal compartment (Renegar et al., 2004).

Virus-specific antibodies produced by B cells, particularly directed against HA (trimeric globular head) and NA, imparts protective immunity against influenza infection. Antibodies bind to the globular head region of HA, neutralize the virus and prevents the attachment of virus to host cells. It further expedites the process of its phagocytosis of virus by cells carrying Fc receptor on their surface. Anti-HA antibodies induce its ADCC mediated killing of the infected cells. These anti-HA antibodies are strain-specific and thus fails to neutralize the variants of influenza virus subtypes formed due to antigenic drift. Therefore, humoral immunity does not provide long-lasting protection. However, in the recent past, an antibody named Fab28 capable of recognizing 16 different subtypes and neutralizing group 1 and group 2 influenza virus has been identified (Corti et al., 2011).

Antibodies have also been reported against various influenza proteins such as neuraminidase (NA), matrix protein 2 (M2) and nucleoprotein (Ungchusak et al.). NA specific antibodies have been reported to control influenza via ADCC in macaques (Jegaskanda et al., 2013). NA, M2 and NP specific non neutralizing antibodies reduce the

pulmonary titer of virus and morbidity (Carragher et al., 2008; Mozdzanowska et al., 1999).

Cell mediated immune response, on the other hand, is directed against viral epitopes which are probably shared between different virus strains and subtypes, thus offering large dimensions to the immunity imparted against different influenza virus.

Upon infection, influenza virus activates cytotoxic ($CD8^+$) T cells and helper T cell ($CD4^+$) and regulatory T cell response. During influenza inflection viral antigen is presented by migratory dendritic cells ($CD103^+$ and $CD11b^+$ DC) to naive $CD8^+$ and $CD4^+$ T cells in lymph nodes (Kim & Braciale, 2009). $CD8^+$ T cells undergo activation, proliferation and differentiation. Effector T cells thus formed are transported to lungs from these secondary lymphoid organs to eliminate virus infected cells. However, a study suggested that after initial activation of $CD8^+$ cells in lymph nodes, they require additional antigen dependent interaction with lung DC (McGill et al., 2010). Lung DC provide IL15 and CD28 costimulatory signal for survival and proliferation of effector T cells during influenza infection (Dolfi et al., 2011). IL-27 produced by lung APCs along with IL2 (produced by Th-cells) promotes the release of IL-10 by effector $CD8^+$ T cells, which is essential to reduce the respiratory inflammation caused by antiviral immune response (Sun et al., 2009).

Viral peptide bound to MHC class I is recognized by T cell receptor of $CD8^+$ T cell. These cells employ perforin/granzyme or Fas/Fas-Ligand mediated mechanism to clear viral infection. Sometimes TRAIL (TNF related apoptosis-inducing ligand) facilitated mechanism is also involved in the clearance of viral infection. Further, effector $CD8^+$ T cells secrete cytokines (IFN-γ, TNF α, IL-2, IL-4, IL-5, IL-9, IL-10, IL-17, IL-21, IL-22,) as well as chemokines (CCL3, CCL4, CCL5, CXCL9, and CXCL10) to recruit NK cells, macrophages, eosinophils, B and T cells to lungs (Hamada et al., 2013).

T helper cells ($CD4^+$ T cells) are classified depending upon the type of cytokines they produce. Th1 cells (produce IL-2 and IFN-γ) and Th2 cells (IL-13 and IL-4). Th1 cells are primarily responsible for cellular immune response whereas, Th2 cells promote B cell response. $CD4^+$ T cells contribute towards antiviral immunity mainly by assisting $CD8^+$ cells and B cells. Although, a study has revealed the presence of cytolytic $CD4^+$ T cells in response to influenza viral infections (Soghoian & Streeck, 2010). Direct cytotoxicity of lung $CD4^+$ T cells expressing granzyme B and perforin was observed against influenza infected cells along with IFNγ secretion (Brown et al., 2012).

Studies conducted in the recent past have described follicular helper $CD4^+$ T cells (Tfh) as B cell helpers (Crotty, 2011). Tfh cells are critical for the formation of germinal centre, its maintenance and regulation of differentiation of B cell into plasma and memory B cells in germinal centre (Crotty, 2011). Formation of germinal centre by activated $CD4^+$ T cells results in affinity maturation and isotype switching mediated by T cell co-stimulatory (ICOS) and IL-21 (Knowlden & Sant, 2016; La Gruta & Turner, 2014). "Innate" like T cell called natural killer T cells ($CD1^+$, $CD4^+$, TCRs) have also been reported to protect against influenza infection in murine model (Sun & Braciale, 2013). NKT cells exhibit their effect by the suppressing the function of myeloid derived suppressor cells (MDSCs), thus stimulating antiviral T cell response (Kok et al., 2012). NKT cells also eliminate inflammatory monocytes to prevent lung injury by influenza inflection (Kok et al., 2012). NKT cells produce IL-22 which prevents the disintegration of lung epithelium during influenza infection (Paget et al., 2012).

Cell mediated immune response is regulated by regulatory T cells (Tregs) and Th17. Post-infection, Tregs limits the response of $CD4^+$ and $CD8^+$ T cells, whereas after vaccination they abate $CD4^+$ response while not affecting the B cell response. On the contrary, Th17 cells inhibits the functioning of Treg by producing IL-16, thus boosting the T helper function (Kreijtz et al., 2011). Ag-specific memory Tregs are thus anticipated to shape the cellular immune response against secondary influenza virus challenges and thus pose as an additional constraint in determining the efficacy of vaccinations (Woodland, 2004).

2.5. Prevention and control of Influenza

The unexpected mutations or re-assortments can give rise to a new highly virulent influenza strains which can cause new epidemics or pandemics. Nowadays, two main strategies are applied to restrain the spread of influenza infections: vaccination and antiviral treatment.

2.5.1 Antiviral drugs

Post-exposure prophylaxis by means of antiviral drugs are an important adjunct to vaccine in fighting influenza. In case of sudden outbreaks, antiviral drugs play a crucial role in checking the immediate spread of infection, since vaccine development against the new strain of Influenza virus requires a certain time period for development and

manufacturing. Besides this, antiviral drugs arrest the development of serious flu-related complications in case of immunocompromised patients and people with high risk health conditions where vaccine may not impart desired immunity. Two types of antiviral drugs are used for the treatment of influenza: M2 channel inhibitors and neuraminidase inhibitors (Krol et al., 2014). Two well-known M2 channel inhibitor viz. amantadine and rimantadine are derivatives of adamantine which are assumed to intercalate into the interior of proton channel and prevent the influx of H^+, thus preventing the uncoating and release of viral RNP. The usefulness of M2 channel inhibitor is limited these days due to widespread resistance reported among influenza A virus. Resistance arises due to single amino acid substitutions at various positions in M2 protein, most commonly S31M. Consequently, M2 channel inhibitors have been replaced by neuraminidase inhibitors. Neuraminidase inhibitors impair the release of viral progeny from the host cells, thus checks the spread of influenza at later stages of infections. Neuraminidase has sialidase activity which cleaves the terminal sialic acid moiety from the host receptor. Thus it prevents the self-aggregation of viral particles inside infected cells and also prevents the re-infection. NA inhibitors limit the transmission of virus by causing the aggregation of viral particles inside host cells. Neuraminidase inhibitors are effective against influenza A and B virus, whereas M2 channel inhibitors works only against influenza A virus. Currently, three neuraminidase inhibitors viz. Relenza (zanamivir), Tamiflu (oseltamivir phosphate) and Rapivab (peramivir) are FDA approved influenza antiviral drugs (FDA, 2015). Anti-viral drugs are effective only if they are taken early after onset (within 48 hours) of influenza. Although, anti-viral drugs may be the immediate means of preventing influenza infection but do not treat illness. So, they are regarded as the second line of defence.

2.5.2 Vaccine

Vaccine is the most efficient way to prevent influenza infection (Woodland, 2016). Virus infections are important public health concern and cause substantial morbidity and mortality throughout the world. Existing influenza virus vaccines are effective against infection but require periodic reformulation owing to frequent mutations (antigenic drift). Progress have been made in the recent past to enhance the immunity elicited by seasonal and pandemic vaccines, and to accelerate the process of vaccine production in case of sudden pandemic outbreak.

2.5.2.1 Licensed influenza vaccines

Trivalent inactivated vaccine (TIV) is extensively used against seasonal influenza. It comprises of two influenza A subtypes i.e. H1N1 and H3N2, currently existing in human circulation and one influenza B virus. TIV protects against influenza primarily by eliciting anti-HA antibody production. Influenza PR8 strain (A/Puerto Rico/8/34) or reassortant virus which has been adapted to grow in embryonated chicken eggs with high growth capacity is used for inactivated influenza vaccine production. PR8 strain is modified to contain NA and HA genes of the circulating influenza virus and internal protein coding gene segments of PR8 strain. This vaccine comes as three different formulations: inactivated whole virus, split and subunit. An inactivated whole virus vaccine is a preparation of purified virus, which is chemically inactivated by formalin or β-propiolactone treatment. It was first approved for use in United States in 1975. Split preparation is prepared by nonionic detergent mediated disruption of influenza virus to remove the lipid envelope. Subunit preparation requires additional purification of HA. Split and subunit formulation of TIV is preferred over whole virus vaccines because of their less reactogenicity in primed population. Quadrivalent inactivated vaccine (QIV) against influenza incorporates circulating strains of H1N1 and H3N2 subtypes of influenza A virus and two strains of influenza B virus (Victoria and Yamagata). It was designed mainly to avoid the mismatch occurring to influenza B strains. FDA has approved the manufacturing of a quadrivalent split vaccine named Fluarix (GlaxoSmithKline Biologics) (Bekkat-Berkani et al., 2016).

Live attenuated influenza virus (LAIV) vaccines against influenza are available as intranasal spray (FluMist). Strains (master donor virus) of LAIV are cold adapted, temperature sensitive and attenuated to prevent illness by means of series of mutations in the internal protein coding gene segments. LAIV is a reassortant virus vaccine composed of wild type surface glycoproteins and internal proteins of master strain. This vaccine induces serum IgG, mucosal IgA, $CD4^+$, $CD8^+$ and γδT cells in children below 3 years (Hoft et al., 2011). Use of this vaccine has not been approved for adults (>50 years)

Major bottlenecks of conventional inactivated influenza vaccines include variable efficacy among different age group of individuals and the antigenic variability of the circulating virus due to which it requires annual reformulation. Furthermore, long production time frame restricts their timely and adequate supply of vaccine. Also, their

manufacturing is an elaborate process and production is limited to availability of chicken eggs (Lee et al., 2014).

2.5.2.2. Whole virus vaccine

GammaFlu™ is a whole virus broad spectrum vaccine developed by Gamma vaccine (Australia). It is a preparation of gamma irradiated whole influenza virus, in whole the genetic material of the virus is destroyed (non-replicating), leaving all the surface and internal protein intact. This approach has been shown to generate robust immune response against homologous and heterosubtypic challenges in mice. This cross protective immunity was found to be mainly mediated by cytotoxic T cells in gene knockout mice (Furuya et al., 2010).

2.5.2.3. Influenza virosome

Virosome is a virus-like particle which lacks genetic material. It is an influenza virus envelope which conserves its cell binding and membrane fusion properties just like native virus. Repetitive arrangement of surface glycoprotein HA evokes B cell as well as T cell mediated immunity in addition to their interaction with APCs. Presently, H5N1 virosome adjuvanted with Matrix M™ is undergoing Phase I clinical trials. Vaccine has shown Th1/Th2 $CD4^+$ T cell responses in adults (Pedersen et al., 2014).

2.5.2.4. Universal influenza vaccine development

Vaccine constructs that induce universal or broad reactive immunity are presently in preclinical and clinical development. Such vaccination paradigm rely heavily on epitopes that are conserved across influenza virus subtypes.

2.5.2.4.1. M2e based universal vaccine

A stretch of 18–24 amino acid of the M2 proton channel which extends outwardly from the membrane surface of the influenza virus (M2e) is reported as a highly conserved sequence among human influenza virus, and has been a target for universal vaccine development (Neirynck et al., 1999). Although, small size and low density of M2 epitope on the surface causes a weak M2 specific immune response by seasonal vaccine or infections; considerable efforts have been made to improve its immunogenicity. Currently, safety and immunogenic ability of recombinant M2e-*Salmonella typhimurium*

flagellin (STF2.4xM2e) is being tested in phase II clinical trials by VaxInnate (USA) (Berlanda Scorza et al., 2016). This vaccine passed the phase I trials successfully (Turley et al., 2011). Another recombinant preparation of M2e-HBc (ACAM-FLU-A) was tested successfully in human using VLPs/CTA1-DD platform by Acambis Inc (De Filette et al., 2008).

In preclinical studies, M2e-based baculovirus-expressed virus-like particles induced immune response against pandemic H1N1, H3N2 and H5N1 virus, when administered as inactivated whole virus preparation in female BALB/c mice (Song et al., 2011). M2e based nanoparticle vaccine preparations have also shown broad range of protection against influenza in mice models. Protein nanoclusters from conformation-stabilized M2e tetramers when used to vaccinate mice, high levels of antigen-specific T cell, serum IgG and mucosal antibody responses were observed. Thus, it is capable of conferring complete protection against lethal challenge with various influenza subtypes (Wang et al., 2014). In another study, M2e conjugated to gold nanoparticles (AuNPs), used to immunize BALB/c mice with CpG (cytosine-guanine rich oligonucleotide) as an adjuvant offered complete protection against lethal A/PR8 (H1N1) (Tao et al., 2014). Other than these, VLP, microneedle, lipopeptide based platforms are being explored for the development of M2e based vaccines (Zhang et al., 2014).

Although, the potential of M2e as a vaccine candidate is now well known, but its application as a universal vaccine is only limited to influenza A virus. Small size of ectodomain of influenza B M2 protein (5-6 amino acids) renders it rather non immunogenic. Further, 21 variants have been identified for allegedly conserved M2e peptide, with mutations in the middle part of M2e domain (Gottlieb & Ben-Yedidia, 2014). Such findings raises doubts on the universality of M2e based influenza vaccine. Furthermore, two amino acids, threonine (position 5) and the glutamic acid (position 6), in conserved M2e domain were recognized to be associated with antibody-escaping, 2014 variants (Wang et al., 2009).

2.5.2.4.2. HA based universal vaccine

HA protein is an appealing target for a universal influenza virus because of its large size, abundance, surface accessibility and its crucial role in mediating in viral adhesion and entry in host cell. Cleavage site of HA_o is highly conserved among various subtypes of influenza A virus as well as both the lineages of B virus. This 19 amino acid peptide

linked to outer membrane protein of *Niesseria meningitides* when administered in BALB/c mice offered complete protection against lethal challenge of influenza B virus. This response was experimentally proven to be antibody mediated. Fcγ knock out revealed the involvement of ADCC and macrophage phagocytosis in viral clearance. Injecting H3 peptide linked to OMPC offered protection against influenza A and B virus in mice (Bianchi et al., 2005).

The stalk of HA (HA2) is less exposed and possess high degree of conservation. Various approaches have been applied to develop universal vaccine based on HA stalk. Various *Escherichia coli* expressed HA stalk (H1N1) domain immunogens impart complete protection to mice against homologous viral challenges as well as against different strains and subtypes (Bommakanti et al., 2010). Further, various "headless" constructs of HA were developed in attempt to broaden the vaccine response against HA stalk. An immunongen of HA in which the globular head was replaced by a glycine linker was designed. C57BL/6 mice was primed and boosted with DNA preparation encoding this headless HA and VLP expressing headless HA in combination with Freund's adjuvant. Mice when challenged with PR8/H1N1 were protected and generated immune sera with broad reactivity (Steel et al., 2010).

Chimeric hemagglutinin constructs (exotic head domain on the native stalk) have also been engineered and tested for their efficacy in generating stalk based broader immune response (Krammer et al., 2013). Besides this, a recombinant HA protein expressed as virus-like particle (VLP) in *Nicotiana benthamiana* was tested for its reactogenicity and protective immunogenicity in randomized, placebo-controlled phase I trials (Cummings et al., 2014). Currently, this concept is undergoing phase II trials.

2.5.2.4.3. Neuraminidase based universal vaccine

NA is the second most abundant glycoprotein on the surface of influenza virus. Its sialidase activity facilitating the release of new formed virus particles. Antibodies blocking this enzyme activity may restrict virus replication *in vitro*. Its candidature for universal influenza vaccine has not been investigated much, so far. Although, some reports suggest that antibodies directed against highly conserved regions of NA could be cross reactive against various influenza subtypes. Antibodies raised against two synthesized conserved peptides were shown to be capable of being cross reactive to nine subtypes of NAs (Gravel et al., 2011). Recombinant NA of different subtypes,

expressed in a baculovirus system were used to immunize mice before challenging them with lethal dose of homologous, heterologous, or heterosubtypic influenza virus (Wohlbold et al., 2015). This study demonstrated that NA was successful in eliciting protective response against lethal dose of homologous and heterologous influenza.

2.5.2.5. Peptide based vaccines

Conventional vaccines are prepared from an attenuated or inactivated version of the pathogen or its proteins. However, the immunogen to which the immune system actually responds are often smaller peptides. Therefore, the concept of peptide based vaccines is an appealing alternative strategy which involves usage of short synthetic peptides to engineer a highly targeted immune response.

Peptide based vaccines offer many advantages over traditional vaccine approach based on inactivated, subunit or recombinant DNA vaccines (Purcell et al., 2007; Slingluff, 2011). Peptide sequences having potential oncogenicity or autoreactivity can be selectively eliminated at developmental stage. Well known examples of oncogenic proteins include Epstein–Barr virus (EBV) nuclear antigens (EBV), E6/E7 oncoprotein (human papillomavirus), HBx antigen (Hepatitis A virus) and NS5A protein (hepatitis C virus) (Fae et al., 2005; Mesri et al., 2014; Purcell et al., 2007). Autoreactive antigen M protein of streptococci triggers heart lesions in rheumatic heart disease (Fae et al., 2005). Peptide preparations lack risk associated with attenuated vaccines and DNA vaccines such as reversion, gene recombination or integration. Peptide-based immunogens can be designed to incorporate multiple epitopes of a pathogen or epitopes from different pathogens.

Immunogenicity, solubility and stability of peptides can be augmented by introduction of carbohydrate, lipid, and phosphate groups. Peptides offer ease of chemical synthesis, characterization, analysis, quality control and scale up. Storage and distribution of peptide preparation in freeze-dried form eliminates the need of cold-chain' facility normally required for storage, transport and distribution of traditional vaccines. Thus the identified immunogenic peptides when targeted as vaccines can serve as excelling alternative to the whole organism (inactivated or live attenuated).

Numerous advances have been made in the development of peptide vaccines against cancer, influenza and many other diseases. One of the most promising and successful approach is an active cellular immunotherapy called Provenge (Sipuleucel-T), which is

the first FDA-approved cancer vaccine for the treatment of castration-resistant prostate cancer patients (Cheever & Higano, 2011). It contains autologous PBMC (including antigen-presenting cells) stimulated *ex vivo* with a recombinant fusion peptide PA2024 (prostatic acid phosphatase fused to granulocyte–macrophage colony-stimulating factor) (Kantoff et al., 2010). Vacc-4x is another peptide based HIV-1 therapeutic vaccine composed of four conserved peptides of p24 (Gag) has completed clinical phase II trials (Pollard et al., 2014). The vaccine was declared safe, well tolerable, immunogenic and evidently contributed towards a viral-load set point reduction.

Taking into account the development made in the field of peptide based vaccine against influenza, BiondVax Pharmaceuticals announced the acceptance of Investigational New Drug Application (IND) for its epitope based influenza vaccine Multimeric-001 by the US Food and Drug Administration in 2015 (Arnon et al., 2000; Biondvax, 2016). The design of this vaccine includes 9 conserved epitopes from the HA, NP and M1 proteins expressed as a single recombinant protein in *E. coli.* This vaccine induces both humoral and cellular immunity against type A and B influenza virus (Ben-Yedidia & Arnon, 2005). National Institute of Allergy and Infectious Diseases (NIAID/ NIH) decided to conduct a new phase II trial of Multimeric-001 in the United States in 2015-16. The trials were conducted to assess the ability of this vaccine in enhancing protective immunity against highly pathogenic H7N9. This vaccine has already been successfully tested for its protective efficacy against H1N1 swine pandemic virus. Further, clinical trials shall be conducted in European population against to test its efficacy in H5N1 avian pandemic virus.

Dynavax Technologies Corporation launched first human clinical trial of its universal influenza vaccine, termed as N8295, in 2010 (Dynavax, 2010). N8295 is a fusion protein comprising of M2e epitope with highly conserved nucleoprotein and TLR9 agonist ISS (Immuno stimulating sequence). Preclinical trials revealed that NP promotes cytotoxic T-cell activation, whereas cytotoxic antibodies are induced by M2e. Phase 1a and 1b trails confirmed cellular as well as humoral immune response in 54 subjects. Anti H1 response was observed in all N8295 dose groups when N8295 was given in combination with non-immunogenic dose of H5N1 vaccine.

VGX™-3400X is another prophylactic DNA vaccine containing conserved regions of NA, M2e-NP and influenza HA proteins (variable subtypes), has completed phase I Clinical trials (Inovio, 2010). Flu V vaccine (pepTcell), another conserved $CD8^{+}$T cell epitopes

based vaccine, has entered phase II clinical trials. Phase I trials have shown that vaccinated subjects show low symptom score and viral titer, in addition to cross reactivity against array of influenza A and B virus, as compared to the controls (Stoloff & Caparros-Wanderley, 2007).

Hence, it is evident that various approaches leading to formulation of peptide based influenza vaccines are under extensive research and development worldwide.

2.6 Immunoinformatics

Sequencing of complete genome and proteome of pathogenic microbes marked the beginning of new era of vaccine research called Immunoinformatics or computational immunology. It emerged as an intersection between the experimental and informatics approach to study host pathogen interaction, molecular interaction in reference to HLA-peptide-T cell receptor, predict epitopes as targets for vaccine, design and engineering of immune therapeutics and diagnostics. Applications of B and T cell epitope prediction include personalized immunotherapies as well as prophylactic and therapeutic vaccines (Backert & Kohlbacher, 2015).

Conventional methods of epitope identification involve the synthesis and experimental screening of all the overlapping epitopes of pathogenic proteins. Pathogens express copious proteins containing numerous potential epitopes, however only a small subset of peptide sequences actually capable of eliciting immunity. Indeed, accurate identification of such epitopes is equivalent to looking for “a needle in a haystack”. Immunoinformatics enables us to reduce the experimental screening by identifying the potential epitopes.

Such infirmities in the traditional techniques have drawn attention towards the use of advanced vaccine design algorithms, specifically epitope prediction/mapping tools in identifying putative epitope. Immunoinformatics tools enables us to screen entire proteome of a pathogen and facilitate the rapid spotting of putative T-cell epitopes. Such information is not only valuable for the vaccines development, but also in diagnostics.

Various studies have certainly demonstrated that epitope prediction tools expedite the search for viral sequences displaying good immunogenic response *in vitro* and *in vivo*. A study on vaccinia virus WR strain acknowledged the vast potential of immunoinformatics in accurately identifying epitopes. The response against these identified peptides/epitopes was tested in murine model by intracellular cytokine

staining and IFN-γ ELISpot assay, as well as MHC peptide binding assay (Moutaftsi et al., 2006). Since then, a lot of immunoinformatics based work has been done in the field of influenza vaccine research to identify promiscuous T cell epitopes of influenza virus which can projected for universal influenza vaccine development. FLU-v is a peptide based influenza vaccine which is currently in phase II clinical trials (Pleguezuelos et al., 2012; Stoloff & Caparros-Wanderley, 2007). It serves as a fine example to confirm the ability of immunoinformatics based epitope prediction tools in accurately identifying immunogenic peptides.

2.6.1. Various T cell epitope prediction tools

Availability of adequate experimental data is critical for the development of epitope prediction tools. Various databases have been established for collection of experimental immunological data. Next generation sequencing and high-throughput screening of HLA binding assays have taken the lead in identification of novel MHC alleles and understanding of their binding patterns. One of them is SYFPEITHI, which is a database of 7000 naturally processed MHC ligands and peptide motifs (Rammensee et al., 1999). Immune epitope database (IEDB) contains natural/synthetic epitope (Vita et al., 2015). Other databases of T cell and B cell epitopes, MHC, TCR and BCR are MHCBN 4.0, IMGT and AntiJen databases (Lata et al., 2009; Lefranc et al., 2015; Toseland et al., 2005). Immuno Polymorphism Database (IPD) comprises of International immunogenetic information system (IMGT/HLA) database which serves as a platform for curation, nomenclature and publication of HLA. As of October 2015, 14015 HLA and related alleles have been included in the IMGT/HLA Database (Robinson et al., 2015).

Expanding knowledge of HLAs will enable the training of the existing T cell epitope prediction tools on large data, thus improving the performance of the prediction tools. The computational tools are pattern recognition methods trained on large data obtained from *in vitro* experiments. Pattern recognition is an application of machine learning (ML) in computer sciences. ML is employed for the study and construction of algorithms that can recognise motifs/pattern from the training data (binding peptides) and make predictions. Various ML techniques are extensively used in immunoinformatics, which include support vector machines (SVMs), position specific scoring matrices (PSSMs), artificial neural networks (ANNs), hidden Markov models (HMMs). Various immunoinformatics tools based on these MLs have been developed so far to predict

epitopes, antigen processing steps and HLA typing. Few of them are listed in Table 2.4. (Page 40).

NetCTL 1.2 server (Centre of biological sequence analysis, Technical University of Denmark) integrates the MHC class I epitope binding prediction with antigen processing steps including C-terminal proteasomal cleavage and TAP (transporter associated with antigen processing) transport efficiency (Larsen et al., 2007). It predicts epitopes for 12 supertypes of MHC class I (A1, A2, A3, A24, A26, B7, B8, B27, B39, B44, B58, B62). Supertype is defined as the cluster of functionally related HLA alleles that share binding specificities towards the same panel of peptides owing to similar structural features of HLAs peptide binding groove (Lund et al., 2004). *In vitro* efficacy of this prediction tool was proved by a study carried out to identify epitopes of West Nile virus (WNV) (Larsen et al., 2010). NetCTL predicted peptides were synthesized and tested on WNV patient. Peptide immunogenicity was demonstrated by means of IFN-γ ELISPOT assay and Intracellular cytokine staining.

BIMAS (Bioninformatics and molecular analysis section, National Institute of Health USA) predicts epitopes *in silico* by analysing the refolding capabilities of HLA heavy chain exposed to the given peptide in the presence of β2 microglobulin or their dissociation rate ($t_{1/2}$). Binding of a peptide to particular MHC I molecule boosts the stability of the two MHC chains (heavy chain and β2 microglobulin) which bind non-covalently among themselves. BIMAS identifies epitopes that contain allele-specific binding motifs for 33 HLA class I alleles (9 HLA-A, 20 HLA-B, and 4 HLA-C)(Parker et al., 1994). Various *In vitro* studies carried on BIMAS predicted peptides have proven its productivity (Limberis et al., 2007; Sundar et al., 2007).

SYFPEITHI (Department of Immunology, University of Tubingen and BioMedical Informatics (BMI) - Heidelberg) was first publically available database of more than 7000 peptides reported in published literature to bind MHC molecules (Rammensee et al., 1999). This database adopted its name from the peptide SYFPEITHI derived from the JAK1 tyrosine kinase was the first natural MHC ligand to be sequenced directly (Harpur et al., 1993). Attributes like motif, ligand or epitope search with their respective references and T-cell epitope prediction makes it a unique database. T cell epitope prediction relies on published motifs. It considers the anchor, auxiliary anchor positions of amino acids and other frequent amino acids. Scores are calculated by assigning amino acids a specific value depending on whether they are anchor, auxiliary anchor or

preferred residue. Further, at each of these positions ideal anchors are assigned 10 points, unusual anchors 6-8 points, auxiliary anchors 4-6 and preferred residues 1-4 points. Amino acids that are accounted for adverse effect on the binding ability are allotted negative values (-1 and -3). SYFPEITHI predicts epitopes for 33 MHC class I Alleles (Coughlan & Lambe, 2015). Epitope predictions carried out with SYFPEITHI in combination with NetCTL and BIMAS have been validated for their immunogenicity in *in vitro* and *in vivo* studies (Chen et al., 2012; Hassainya et al., 2005).

The Immune Epitope database (IEDB) is a free resource since 2004, funded by a contract from the National Institute of Allergy and Infectious Diseases (NIAID, USA) (Vita et al., 2015). It provides easy search of experimental data characterizing antibody and T cell epitopes related to infectious diseases, allergies, autoimmunity, and transplants, reported in humans, and other species. It also hosts various tools for prediction and analysis of B cell and T cell epitopes. Prediction of MHC class II epitopes can be done by eight various methods. One of the methods of IEDB, SMM align attempts to recognize MHC class II binding motifs by generating a position-specific scoring matrix that ideally reproduces the IC50 affinity values for each peptide (Nielsen et al., 2007). Predictive performance of this algorithm has been demonstrated to be superior to other prediction tools.

ProPred (Institute of Microbial Technology, India) is a matrix-based prediction algorithm for 51 HLA-DR alleles (MHC class II) (Singh & Raghava, 2001). It employs amino acid /position coefficient table derived from pocket profile database described by Sturniolo and coworkers (Sturniolo et al., 1999). Promiscuous nature peptides of MPT83 lipoprotein of *Mycobacterium tuberculosis* having *in vitro* immunogenic properties was predicted using Propred (Mustafa, 2011).

NetMHC II v2.2 (Center of biological sequence analysis, Technical University of Denmark) predicts epitope binding to 14 HLA-DR, 6 HLA-DQ, and 6 HLA-DP alleles using artificial neural networks. Results are expressed in terms of IC50 and percentage rank to a set of 1,000,000 random natural peptides (Nielsen & Lund, 2009). It can predict epitopes for 14 HLA-DR, 6 HLA-DP, 6 HLA- DQ alleles. Predictions are categorized as strong (IC50 < 50 nM), weak (IC50 < 500 nM) and non-binders (IC > 5000 nM).

Table 2.4. T-cell epitope prediction tools

Prediction	Tool	Method	Reference
MHC class I epitope	SYFPEITHI	PSSM	Rammensee et al., 1999
	BIMAS	PSSM	Parker et al., 1994
	RANKPEP	PSSM	Reche et al., 2002
	netMHC	ANN	Andreatta & Nielsen, 2016
	CTLPred	SVM and ANN	Bhasin & Raghava, 2004
MHC class II epitope	ProPred	Quantitative matrix	Singh & Raghava, 2001
	netMHC II	ANN	Nielsen & Lund, 2009
	PickPocket	PSSM	Zhang et al., 2009
	KISS	SVM	Jacob & Vert, 2008
	SMM-Align	Quantitative matrix	Nielsen et al., 2007
Proteasomal cleavage	netChop 20S	ANN	Nielsen et al., 2005
	netCHop Cterm	ANN	Nielsen et al., 2005
	FragPredict	PSSM	Holzhutter et al., 1999
	Pcleavage	SVM	Bhasin & Raghava, 2005
TAP transport	PredTAP	HMM/ANN	Zhang et al., 2006
	SVMTAP	SVM	Donnes & Kohlbacher, 2005
T cell reactivity	POPI	SVM	Tung & Ho, 2007
	POPISK	SVM	Tung et al., 2011
HLA typing	ATHLATES	Contig assembly	Liu et al., 2013
	Polysolver	Bayesian classification	Shukla et al., 2015

Other than these sequence based approaches, molecular docking is also being used as a tool for epitope identification. The ready availability of three dimensional structural data i.e. the X-ray structure of the peptide—MHC protein complex has enabled the researchers to analyse peptide-HLA binding. This structure-based method doesn't require extensive clinical or experimental data. Various research group have used docking for the accurate identification of putative T cell epitopes (Agallou et al., 2014; Akiyama et al., 2012; Antunes et al., 2010; Oliveira et al., 2016; Patronov et al., 2011; Srivastava et al., 2016; Yasmin et al., 2016; Zhang, 2013). Autodock Vina, AutoDock 4.2, ClusPro program and PatchDock docking programs have been used in these studies to generate reliable predictions. Docking requires the generation of the structures of interacting partners. Structure of small peptides can be generated by softwares like

PepFOLD, PepBUILD and PEPstrMOD (Shen et al., 2014; Singh, 2004; Singh et al., 2015) Immunoinformatics as well as molecular docking has been used in various studies to identify putative T cell epitopes of influenza virus.

2.6.2. Influenza databases

Genomic sequencing projects involving high throughput experimental techniques have led to the accumulation and submission of enormous data to publicly available databases. This includes immunologically relevant data of clinical, epidemiological and experimental studies. With the collaborative efforts of various research institutes, sequencing data of influenza virus is being stored, organized, updated and maintained in specialized databases. Also, these databases make available analytical resources, bioinformatics tools, workspaces and services for data analysis.

One such database is influenza Virus Resource, created in 2004. It is mainly a NCBI influenza virus sequence database combined with tools for flu sequence analysis (BLAST, alignment, phylogenetic tree), annotation and submission to GenBank (Bao et al., 2008). NIAID launched the Influenza Genome Sequencing Project. Viral sequences were obtained and annotated at J. Craig Venter Institute, and National Center for Biotechnology Information (NCBI). The sequences were submitted in GenBank resource.

Influenza research database (IRD) is also funded by the NIAID (NIH/DHHS) and is an association between Northrop Grumman Health IT, Vecna Technologies and J. Craig Venter Institute (Squires et al., 2012). In addition to the sequence data, this database also provides information about experimental epitopes, data from assays of virulence etc.

Various other influenza databases are the Global initiative on sharing avian influenza data (GISAID), EpiFlu Database (Bogner et al., 2006), Influenza sequence & epitope database (ISED) (Yang et al., 2009), the Influenza virus database (IVBD) (Yang et al., 2009), and the OpenFlu Database (Liechti et al., 2010).

Vast pool of regularly updated information provided by these influenza databases serve as a boon to researchers working worldwide in the field of influenza vaccine development and other therapeutics.

2.6.3. Role of Immunoinformatics in the development of influenza vaccine

As per the records available till August 16, 2016, 5,287 strain of H1N1 virus (including pandemic strains) exists in influenza research database for which whole genome sequences are available (Squires et al., 2012). Drawing inference of immunological importance to human from this huge data is imaginable only with the help of immunoinformatics and other bioinformatics based softwares. Number of immunoinformatics studies have identified epitopes of all the influenza proteins of specific influenza strains viz. HA, NA, M1. M2, NP, NS1, NS2, PB1 and PB2 (Assarsson et al., 2008; Duvvuri et al., 2014; Gustiananda, 2011; Parida et al., 2007; Stoloff & Caparros-Wanderley, 2007; Sun et al., 2010).

Some studies specifically focused on surface glycoproteins HA and NA to identify potential immunogenic epitopes using *in silico* immunoinformatics approach (De Groot et al., 2009; Duvvuri et al., 2013; Gupta et al., 2011; Huang et al., 2013; Somvanshi et al., 2008). With the aim of predicting and identifying cross conserved epitopes of HA and NA protein among S-OIV A/California/04/09 H1N1 and three strains included in seasonal conventional influenza vaccine of 2008-2009, De Groot and colleagues utilized EpiMatrix, a T-cell epitope mapping tool and Conservatrix (EpiVax) tools (De Groot et al., 2009). This study revealed a good cross reactivity between predicted MHC class II epitopes and HA epitopes of different virus strains. Authors also suggested that immunogenic consensus sequence generated by overlapping cross conserved 9-mer epitope shall improve the design of epitope based influenza vaccine. In another study conducted by Huang and colleagues, putative immunogenic epitopes of HA and NA were identified from the nine pandemic H1N1 isolates from Guangdong, China using two widely used prediction algorithms, BIMAS and SYFPEITHI (Huang et al., 2013). Twenty nine conserved epitopes of HA and eight conserved epitopes of NA proteins (conserved among seasonal H1N1 and pandemic H1N1) were identified. Similar study was conducted for HA and NA (H5N1) isolated from chicken, duck, goose and human (Somvanshi et al., 2008). This study listed various epitopes binding to MHC class I and II, based on ProPred and ProPred I predictions. An exclusive study on H1N1, neuraminidase conducted by Gupta and co-workers reported nine $CD8^+$ T-cell epitopes and eight $CD4^+$ T-cell epitopes as novel candidates for vaccine development (Gupta et al., 2011). One more study identified novel $CD4^+$ T cell epitopes of H1N1, HA using NetMHCIIpan were predicted. The same study established a $CD4^+$ T cell mediated recall

response of the predicted epitopes by means of IFN-γ ELISPOT assay and IgG ELISA (Duvvuri et al., 2013).

Internal influenza proteins are less mutable compared with surface proteins, therefore nucleoprotein and matrix protein are considered to be good targets for universal vaccine development (Wang et al., 2015). H5N1 nucleoprotein epitopes were identified by means of molecular docking which were validated *in vitro* in chickens by means of IFN-γ ELISA and flow cytometry analysis (Hou et al., 2012). Further, attempts have been made to identify epitopes of matrix protein with the help of epitope prediction algorithms as well as molecular docking (Zhang, 2013). Zhang identified HLA-A2/A0201 restricted epitope of H5N1 matrix protein using multiple prediction tools as well as peptide-MHC-TCR docking. It is quite evident that *in silico* approach to identification is taking a lead in accurate identification of epitopes and greatly reduce the number of peptides required for experimental assays.

2.7. Validation of the peptide immunogenicity by *in vitro* assays

In silico prediction can never be an autonomous technique in identifying immunogenic epitopes for vaccine development. It can serve as a sorting out technique for potentially immunogenic epitopes among the pool of peptides. Immunogenicity of the peptides can only be confirmed by *in vitro* or *in vivo* experimentation. Conventional assays which measures the outcomes of T-cell activation *in vitro* include cytokine secretion, T-cells phenotyping, determining antigen induced T-cell proliferation and determining antigen-specific cytotoxicity (Coughlan & Lambe, 2015; Jawa et al., 2013).

Cytokines (i.e. IFN-γ, IL-2, IL-4, and IL-10) secreted by T cells are measured by enzyme linked immunosorbent assays (ELISA)(Chakraborty et al., 2008; Jupelli et al., 2008; Pasricha et al., 2006; Pujari et al., 2015) and enzyme-linked immunosorbent spot-forming (ELISpot) assays (Li et al., 2013). ELISA measures the level of extracellularly secreted cytokines in culture supernatants of antigen stimulated T cells. Therefore, it can be employed to measure the magnitude of response and type of cytokines secreted into the supernatant. ELISpot assays measures the number of cytokine-producing cells (to the extent of 1 cell per million) within the population of antigen stimulated cells *in vitro.* ELISpot assay is established as more sensitive and qualitative technique for assessing cytokine response (Jawa et al., 2013). Immunofluorescent staining of intracellular cytokines is a flow cytometry based technique for measuring the

production and accumulation of cytokines within the endoplasmic reticulum and golgi apparatus after cell stimulation and simultaneously linking their expression to the phenotype of each cell based on the surface markers. Quantitative real-time PCR (qRT-PCR) employing SYBR green technology is also used to assess antigen-specific T cell activation. This technique relies on the up-regulation of IFN-γ mRNA transcription after *in vitro* peptide stimulation of PBMC (Chakraborty et al., 2008; Karrow et al., 2001; Lowe et al., 2014).

PBMC proliferation in response to the antigenic stimulation can used to measure the induction of cell mediated immune response *in vitro*. Proliferation can be assessed by measuring the incorporation of nucleosides into newly synthesized DNA strands of proliferating cells using radioactivity (^{3}H-thymidine) (Alizadeh et al., 2003; Pujari et al., 2010) or antibody [5-bromo-2'-deoxyuridine (BrdU)](Brincks et al., 2013). 3H-thymidine uptake assay is slow and cumbersome technique which involves the use of potentially hazardous radioactive material (Coughlan & Lambe, 2015). Flow cytometry based carboxyfluorescein succinimidyl ester (CFSE) assay is another alternative to measure cell proliferation (Alizadeh et al., 2003; Roy et al., 2013). CFSE binds to intracellular molecules. As the CFSE-labeled undergoes division, each cell of the progeny receives half the number of CFSE tagged molecules. Cell division is therefore assessed by determining the corresponding decrease in cell fluorescence (Quah & Parish, 2010). Tetrazolium salts serves as an alternative to radioactivity based assays in measuring cell proliferation (Owen et al., 2013). Mitochondrial dehydrogenase enzymes of metabolically active cells reduce water soluble tetrazolium salt into colored insoluble formazan products, which when solubilized, can be measured spectrophotometrically. One tetrazolium salt is MTT (3-[4,5-dimethylthiazol-2-yl]-2,5- diphenyltetrazolium bromide). Yellow colored water soluble MTT is reduced to purple colored formazan crystals, which when solubilized in DMSO or isopropanol yields maximum absorbance at 570nm as the measure of cell count (Mosmann, 1983). Therefore, MTT assay can measure cell proliferation as well as cell death (Chauhan et al., 2011). Another formazan based assay used to measure cell viability (proliferation as well as cytotoxicity) is MTS assay, in which MTS tetrazolium compound is reduced by viable cells to generate a colored formazan product that is soluble in cell culture media (Minu et al., 2016).

Radioactivity based chromium release assay (^{51}Cr) and fluorescence based calcein-acetoxymethyl (Calcein-AM) release assay can specifically measure the cytotoxic T cell

killing activity (Furuya et al., 2010; Matza et al., 2009). Certain enzymes which are released post-cytolysis antigen specific CTLs such as lactate dehydrogenase (LDH) and alkaline phosphatase also give the measure of antigen specific CTL activity (Coughlan & Lambe, 2015).

In light of these facts, present study was planned for computational identification of promiscuous peptides containing multiple T cell epitopes from conserved region of HA, NA and M1 proteins of H1N1 influenza virus by means of various epitope prediction tools and molecular docking. The predicted promiscuous peptides were further chemically synthesised and tested by *in vitro* experimentation to confirm the immunogenic response by lymphoproliferative assay and IFN-γ cytokine release assay.

Chapter 3: Materials and Methods

3.1 Prediction of peptides containing overlapping T cell epitopes

T cell recognize antigen in the form of peptide-HLA complex presented to them on the surface of antigen presenting cell (APC). In order to identify the peptides containing multiple epitopes, conserved regions were identified from the full length sequences of three influenza proteins viz. hemagglutinin (HA), neuraminidase (NA) and matrix 1 (M1) protein. Epitopes were predicted using six different *in silico* epitope prediction tools (three each for HLA class I and II). Epitopes predicted commonly by each of prediction tools were selected for further studies. Epitopes homologous to any of the human protein sequences were eliminated by BLASTp analysis. Overlapping epitopes were merged to generate peptides having single or multiple $CD8^+$ and $CD4^+$ T cell epitopes.

3.1.1 Sequence retrieval from influenza databases

Full-length sequences of HA, NA and M1 protein of H1N1, infecting humans all over the world were retrieved from the NCBI Influenza virus resource database and Influenza research database (IRD)(Bao et al., 2008; Squires et al., 2012).

3.1.2 Conserved peptide identification

The protein sequences were aligned using multiple sequence comparison by log-expectation (MUSCLE). MUSCLE is an iteration based alignment tool. It offers a wide range of options that provide improved speed and accuracy compared with currently available programs. Its accuracy is statistically equivalent to T-Coffee and MAFFT and has been rated as fastest among T-Coffee, MAFFT and CLUSTALW for large number sequences (Edgar, 2004).

Entropy is a measure of sequence variability. The antigenic variability analyser (AVANA) tool analyses multiple sequence alignments based on entropy and measures variability at a given position. AVANA creates a graphical presentation of entropy profile for multiple sequence alignments, thus enabling users to examine position specific variants and their frequencies (Miotto et al., 2008). AVANA tool was used to find the conserved peptide stretch (minimum length 9 amino acids) from the aligned

sequences that exhibited at least 80% (90% for M1 protein) conservation among the reported H1N1 HA, NA and M1 peptide sequences. “Conservation’’ in the current study is referred to identical peptide sequences that are present in at least 80% (90% in case of M1 protein) of total HA and NA protein sequences.

3.1.3 CD8$^+$ T-cell binding peptide prediction

Three different immunoinformatics tools—NetCTL v1.2, BIMAS and SYFPEITHI were employed to predict nonamers that have the ability to bind to class I HLA molecules (Larsen et al., 2007; Parker et al., 1994; Rammensee et al., 1999). NetCTL v1.2 predicts CD8$^+$ T-cell epitopes for 12 supertypes of class I HLA taking into account TAP transport efficiency, C terminal cleavage, and HLA class I binding peptide (Larsen et al., 2007). Each HLA supertypes represents a set of HLA alleles that share largely overlapping peptide binding specificity. BIMAS identifies epitopes that contain allele-specific binding motifs for 33 HLA class I alleles based on measurement of the dissociation half-life ($t_{1/2}$) of β2 microglobulin (Parker et al., 1994). The algorithm generates and scans all possible overlapping nonamers against each one of the 33 HLA alleles. The SYFPEITHI database is a collection of class I and II HLA ligands and peptide motifs of human and other species, which are continuously updated (Rammensee et al., 1999). The prediction is based on reported motifs and takes into account the amino acids at the anchor and auxiliary anchor locus, as well as other frequently appearing amino acids. The scoring system assesses every amino acid within a given peptide and allocates a score based on the frequency of the respective amino acids in natural ligands, T-cell epitopes, or binding peptides. All the HLA alleles/supertypes provided in each prediction tool were considered for epitope prediction in the current study (Table 3.1, page 48). Predicted epitopes from each tool were compared to find the common epitopes. Peptides were only defined as epitopes and selected for further analysis when they were commonly predicted by all three tools.

3.1.4 CD4$^+$ T cell binding peptide prediction

The HLA class II complex presents peptides to CD4$^+$ T cells that evoke cellular and antibody mediated immunity against the foreign antigen. Three different tools were used to predict class II HLA restricted epitopes: SMM align, NetMHC II and ProPred (Nielsen & Lund, 2009; Nielsen et al., 2007; Singh & Raghava, 2001). SMM align

attempts to recognize MHC class II binding motifs by generating a position-specific weight matrix that ideally reproduces the IC_{50} affinity values for each peptide (Nielsen et al., 2007). NetMHC II v2.2 predicts epitope binding to class II HLA using artificial neural networks. Results are expressed in terms of IC_{50} and percentage rank to a set of 1,000,000 random natural peptides (Nielsen & Lund, 2009). ProPred is a matrix-based prediction algorithm for class II HLA prediction, which employs a literature-based amino acid position coefficient table (Singh & Raghava, 2001). Epitope predictions were carried out for all HLA alleles provided in each prediction tool (Table 3.1, page 48). Peptides were considered as epitopes only when they were commonly predicted by each tool, as discussed for the prediction of $CD8^+$ epitopes.

Table 3.1. HLA alleles provided in different epitope prediction tools

$CD8^+$ T cell epitope		**$CD4^+$ T cell epitope**	
Prediction tools	HLA alleles/ Supertypes	Prediction tools	HLA alleles
NetCTL v1.2	5 HLA-A & 7 HLA-B	IEDB-SMM	5 HLA-DP, 6 HLA-DQ, & 15 HLA-DR
BIMAS	9 HLA-A, 20 HLA-B, & 4 HLA-C	NetMHC II v2.2	6 HLA-DP, 6 HLA-DQ & 14 HLA-DR
SYFPEITHI	7 HLA-A & 26 HLA-B	ProPred	51 HLA-DR

3.1.5 BLASTp screening

Immunogenic response is not mounted against self-peptides unless failure of clonal deletion leads to selection of autoreactive T cells. Further, similarity of the identified peptides with host self-protein may sometimes lead to an unwanted immunogenic response called autoimmunity. Hence, in order to obtain non-self-peptides, epitopes predicted for class I and II HLA molecules were analysed for their homology with annotated human proteome using BLASTp (Altschul et al., 1990). Nonamers sharing a minimum seven out of nine identical amino acids with the human peptides, without any gaps or mismatches, were eliminated from further consideration. The final conserved epitopes showing an overlap were merged into a single peptide fragment.

3.2 Structure analysis and molecular modelling approach to assess the binding affinity of peptide to the HLA complex

3.2.1 Mapping of peptide fragments

The Discovery Studio v3.5 visualizer tool was used to locate the predicted peptide fragments of HA, NA and M1 on the three-dimensional structure of the respective proteins. The protein structures for HA (A/California/04/2009 [H1N1]; PDB id 3LZG), NA (A/California/04/2009 [H1N1]; PDB id 3TI3) and M1 (A/Puerto Rico/8/34[H1N1]); PDB id 5CQE) available in the PDB database were used as the model structures to visualize the predicted peptide fragments of HA and NA proteins respectively.

3.2.2 Molecular docking of peptides comprising epitopes

The interaction of the predicted peptides containing epitopes with the various HLA class I and II molecules was further studied by means of molecular docking. High-resolution crystallographic structures of nine class I HLA and ten class II HLA molecules were retrieved from the protein data bank (Berman et al., 2000). The naturally bound peptides (native peptides) of the HLA molecule were separated using the Discovery studio visualizer (v4.1). The resultant HLA molecules were used as receptors to dock the *in silico* identified epitopes/peptides and separated naturally bound peptides (as positive controls) using the AutoDock Vina tool (Trott & Olson, 2010). The grid for each of the HLA molecules was defined based on native peptides. The structure of the peptides comprising epitopes was generated using the PEP-FOLD server (Shen et al., 2014). PEP-FOLD provides a fast and user friendly approach for the *de novo* design of small peptides (9 to 36 residues). It is based on OPEP coarse grained force field for molecular simulation. The top model structures predicted for the peptides were used for docking.

Docking with AutoDock vina involves a series of steps including ligand and receptor preparation, finding the search space (grid), preparing the configuration file and visualisation of the AutoDock vina results. AutoDockTools (ADT) is the graphical user Interphase (GUI) employed by AutoDock to set up the ligand, receptor, search space and to visualise the results. The input files for the receptor and the ligand as well as the

output obtained after docking are in PDBQT format, which stores the atomic coordinates, partial charges and AutoDock atom types.

3.2.2.1 Receptor preparation

HLA molecules (receptor) were obtained from PDB database in the form of a coordinate data file (PDB file format). PDB structure of HLA was opened in Discovery studios v3.5 visualizer tools. All the ligand and heteroatoms were selectively removed. Hydrogen atoms were added to the HLA peptide chains and the resultant file was saved as receptor.pdb. As the receptor.pdb file was opened in ADT using macromolecule option in Grid widget, ADT detected the charges on molecules. Inherent charge on the receptor molecule was preserved. In case of absence of any inherent charges Gasteiger charges was automatically added to each atom. ADT determined the type of atoms in the macromolecule. Output was saved as receptor.pdbqt file.

3.2.2.2. Ligand preparation

Structure of peptide ligands were generated from PEP-FOLD server in form of a coordinate data file (PDB file format). Naturally bound peptides were obtained from parent HLA by selectively removing the HLA chains and heteroatoms from the PDB structures in Discovery Studios v3.5 visualizer tool. Hydrogen atoms were added at polar and non-polar positions and the resultant file was saved as the ligand.pdb. As the ligand.pdb file was opened in ADT, it computed and added Gasteiger charges for the entire ligand (in case the charge is zero); else partial charge were used. ADT assigned an 'autodock type' to each atom in the ligand: atoms forming hydrogen bond and aromatic carbons. Output was saved as ligand.pdbqt file.

3.2.2.3 Setting the search space

In order to define the location and size of the 3D area to be searched during the AutoDock vina experiment, grid box option in grid widget of ADT was used. Using the thumbwheels in grid option panel, search space was defined by specifying a center, the number of points in each dimension (x, y, z) plus the spacing between points. The output grid dimension file was saved and the grid option was closed.

3.2.2.4 Preparing the configuration File

A text file called configuration file which contains the information regarding the name of inputs files i.e. ligand.pdbqt and receptor.pdbqt, name of the output file to be generated, search space parameters (center as well as the points in each dimension) and exhaustiveness (the time spent on the search) was prepared and saved as conf.text.

3.2.2.5 Starting AutoDock vina

AutoDock vina program runs in command line interphase. In a designated folder, copied ligand.pdbqt, receptor.pdbqt and conf.txt files. The command-line interface terminal was opened and cd command was used to change the current working directory in operating system. The docking program can be started by using configuration file (--config conf.txt --log log.txt) or by explicitly specifying all input parameters in command-line interface terminal. After the completion of docking (100%), the output was generated in the form of one multimodel out.pdbqt file containing all the predicted binding modes. This file was split into individual models using a separate program called "vina_split".

3.2.2.6 Visualising the output

Individual or multimodel outcomes were visualised by using analyze widget in ADT to locate the position of peptide in the HLA groove as well as to analyse molecular interaction.

3.2.3 HLA distribution analysis

There is a drastic difference in the frequencies of expression of various HLA types among individuals from different continents. Because of this, population coverage analysis of the HLA alleles corresponding to the predicted immunogenic peptides becomes important. The population coverage tool by IEDB calculates the proportion of individuals responding to a given set of epitopes with known HLA restriction taking into account HLA genotypic frequency (Bui et al., 2006). Population coverage analysis tool obtains the HLA allele frequencies for a different individual population from the Allele frequency net database (Gonzalez-Galarza et al., 2015). In population coverage analysis tool, the populations are organized in a pecking order based upon geographical area,

country and ethnicity. The data from the individual populations in each group was combined to evaluate the allele frequencies for each merged population. Analysis can be achieved for population distributed in different continents viz. Asia (East Asia, Northeast Asia, South Asia, Southeast Asia, Southwest Asia), Europe, Africa (East Africa, West Africa, Central Africa, North Africa, South Africa), North America (North America and Central America), South America and Oceanic countries. Population coverage analysis of the peptides was carried out for the population distributed across these continents. HLA peptide restriction data acquired from epitope prediction was used as input data for population coverage analysis.

3.3. Assessment of potential of peptide to stimulate T cell proliferation in peripheral blood mononuclear cells (PBMC) culture

3.3.1. Blood sampling from healthy volunteers

Healthy human volunteers of age greater than or equal to 18 years having no history of hepatitis B, C, and/or HIV infection were included in the study. Blood was drawn via venipuncture by the trained technicians of Lifeline blood bank, Patiala and Nitin Hospital, Patiala (India) in blood collection EDTA quoted tubes (BD Vacutainer® Tubes). All the volunteers gave their informed consent to donate blood for the experiments and the study was approved by institutional ethical committee.

3.3.2 Synthesis of peptides

In silico identified peptides of HA, NA and M1 each containing multiple $CD8^+$ and $CD4^+$ T cell epitopes were synthesised by GenScript (USA) and GL Biochem (Shanghai) Ltd (China) with purity ≥ 85%. Peptides were dissolved in suitable solvents (sterile MilliQ water or DMSO) at a concentration of 1 mg/mL and stored in small aliquotes at -20 °C.

3.3.3 Chemicals and reagents used

All the chemicals and reagents used this work were were of cell culture grade (Table 3.2, page 53).

Table 3.2. List of chemicals and reagents

S.No.	Reagents/ Chemical	Company
1	ABTS (2,2'-Azinobis[3-ethylbenzothiazoline-6-sulfonicacid]-diammonium salt) substrate	ThermoFisherScientific, USA
2	Amphotericin B	Sigma Aldrich, USA
3	Bovine serum albumin	Sigma Aldrich
4	Concanavalin A	Sigma Aldrich
5	Dimethyl Sulphoxide	Merck, Germany
6	Foetal bovine Serum	Gibco®Life Technologies, USA
7	Glutamine	Himedia, India
8	HEPES buffer	Sigma Aldrich
9	Histopaque® -1077	Sigma Aldrich
10	Human IFN-γ Mini ABTS ELISA Development Kit	PeproTech, USA
11	MTT(3-(4,5-Dimethylthiazol-2-yl)-2,5-Diphenyltetrazolium Bromide)	Sigma Aldrich
12	Penicillin Sodium	Himedia
13	Potassium Chloride (KCl)	Himedia
14	Potassium phosphate monobasic (KH_2PO_4)	Himedia
15	Recombinant human Interleukin-2	Sigma Aldrich
16	Rosewell Park Memorial Institute (RPMI)-1640 medium	Sigma Aldrich
17	Sodium Bicarbonate ($NaHCO_3$)	Himedia
18	Sodium Chloride (NaCl)	Himedia
19	Sodium phosphate dibasic (Na_2HPO_4)	Himedia
20	Streptomycin	Sigma Aldrich
21	Trehalose	Sigma Aldrich
22	Trypan blue	Himedia
23	Tween 20	Sigma Aldrich

3.3.4 Isolation of peripheral blood mononuclear cells (PBMC)

Peripheral Blood mononuclear cells (PBMC) were isolated by ficoll density gradient method (Kumar et al., 2006). Eight ml of whole blood was carefully layered onto equal volume of Histopaque®-1077 and centrifuged at 400xg for 30 min at room temperature in swinging bucket rotor (Thermo Scientific Biofuge Stratos). This density based centrifugation technique fractionates blood into plasma, red blood cells and peripheral blood mononuclear cells (PBMC). After centrifugation, the upper plasma layer was discarded with a micropipette and opaque interface (buffy coat) was containing PBMC in a sterile 15-mL conical centrifuge tube. The cells were washed twice in 10 mL of isotonic phosphate buffered saline solution and centrifuged at 250 x g for 10 min. Finally, the cell pellet was re-suspended in 1 mL of complete media (RPMI-1640 supplemented with 10% foetal bovine serum, 100 µg/mL streptomycin, 100 IU/mL penicillin and 10 mM HEPES).

3.3.5 Cell enumeration

Cells were counted on haemocytometer by trypan blue exclusion assay (Strober, 2001). Briefly, 10 µL of cell sample was diluted with 0.4% Trypan Blue solution in the ratio 1:5 or 1:10 in a vial and incubated for 1-2 min. The preparation was loaded on a haemocytometer and examined immediately under a microscope at 40X magnification (Nikon Eclipse E100-LED). The number of unstained viable cells (non-viable cells take up dye and appear blue) were counted in all the four corner squares. Number of viable cells in the original cell suspension was calculated from the following formula

$$\text{Number of viable cells/mL} = \frac{\text{Total no of unstained cells x dilution factor x } 10^4}{4}$$

3.3.6 Peptide stimulation assay

Freshly isolated healthy PBMC were cultured with individual peptides in order to test the immunogenic potential of peptides *in vitro* (Figure 3.1, page 55) (Wullner et al., 2010).

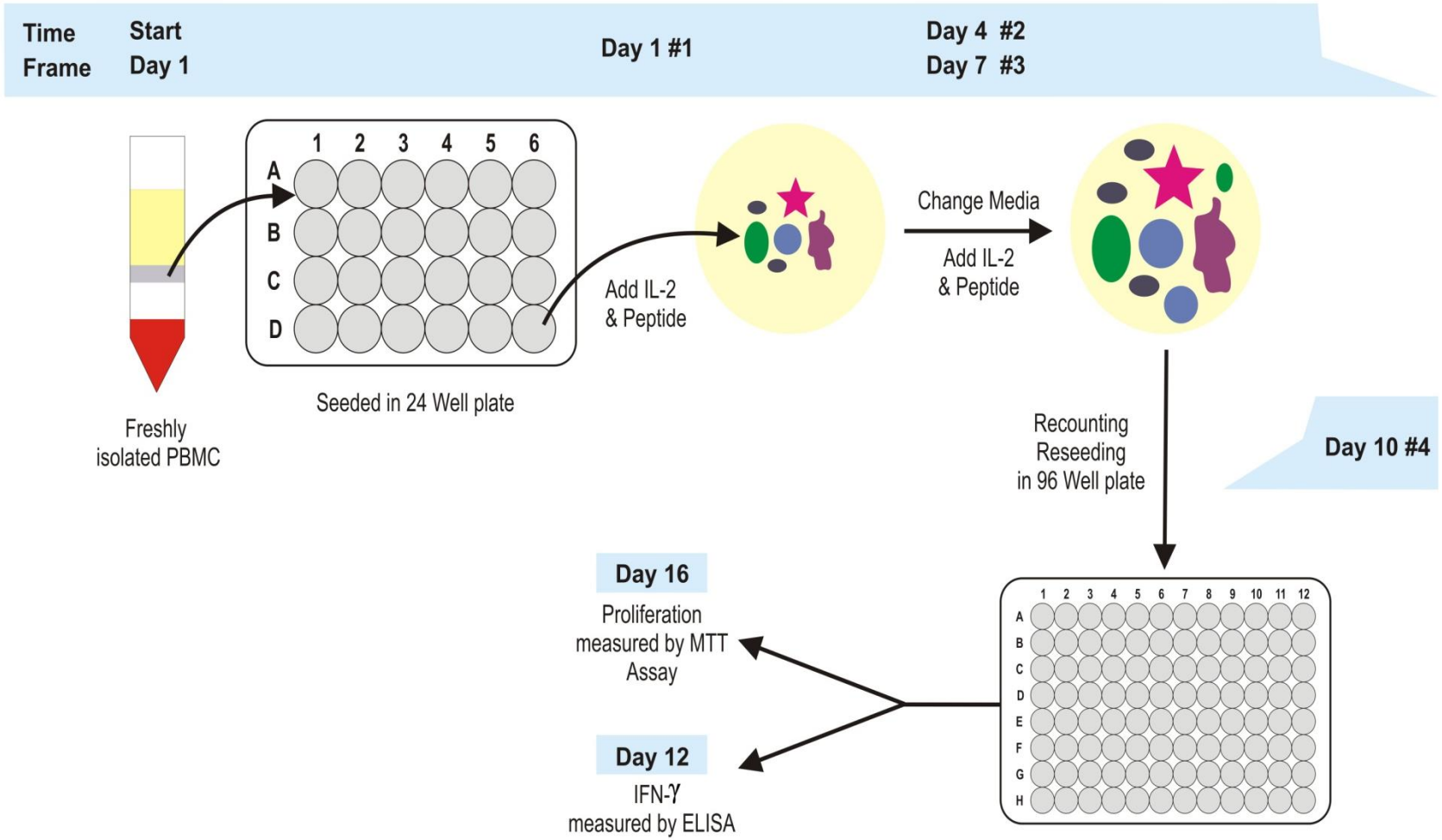

Figure 3.1. Schematic presentation of the peptide stimulation assay

In a 24-well flat bottom cell culture plate (Thermo Scientific™), 2×10^6 cells were stimulated with each individual peptide (25µg/ml) in the presence of recombinant IL-2 (20 ng/mL) and complete RPMI-1640 media in total volume of 2 mL (day 1). Unstimulated cells were supplemented with complete cell culture medium and IL-2. The plate was incubated at 37˚C in a humidified incubator maintained at 5% CO_2 (Eppendorf New Brunswick™ Galaxy). At days 4 and 7, the PBMC culture was re-stimulated by replacing 1 mL of cell culture media with fresh complete RPMI-1640 media containing the same concentration of peptide and IL-2 (Figure 3.1, page 55). On 10th day, peptide stimulated and unstimulated cells were harvested and recounted for further assessing the peptide induced interferon γ production and proliferative response (Figure 3.1, page 55).

3.3.7 PBMC proliferation assay

Peptide induced proliferation of PBMC was measured by MTT (3-(4, 5-dimethylthiazolyl-2)-2, 5-diphenyltetrazolium bromide) based colorimetric assay (do Livramento et al., 2013). MTT assay measures the cell viability based on reduction of the yellow colored tetrazolium salt MTT into purple formazan crystals by mitochondrial succinate dehydrogenase of metabolically active cells (Mosmann, 1983). To measure proliferation, cells harvested from unstimulated wells were distributed in two set of triplicates; one set stimulated with 10 µg/mL of concanavalin A (con A) served as positive control, whereas the other set having the unstimulated cells served as negative control. Peptide stimulated cells distributed in triplicates were given final stimulus with 25 µg/mL peptide in the presence of IL-2 (20 ng/ml). At the end of 6th day, MTT (0.5 mg/mL) was added to the cell culture and the plate was again incubated at 37 ˚C at 5% CO_2. After an incubation of 4 h, 170 µl of the media was removed from each well without disturbing the purple colored crystals. These formazan crystals were solubilized in 100 µL DMSO. Finally, absorbance of each well was recorded at 570 nm, taking 630 nm as the reference wavelength, using the microplate reader (Tecan Austria). Proliferation was calculated in terms of stimulation index (SI) as following:

SI= Average absorbance of the peptide stimulated cells/unstimulated cells

3.4 Determination of immune response of these predicted peptides based on cytokines production/expression in PBMC culture

In order to detect extracellular secretion of IFN-γ by peptide stimulated T cells, the cells harvested on 10th day were seeded again in triplicates as discussed in section 3.3.7. Culture supernatant was collected after 48 h incubation and stored at -80˚C. Extracellular IFN-γ secretion in the culture supernatant was measured by sandwich ELISA (Agallou et al., 2014; Ohkuri et al., 2009) in 96-well ELISA plate (Nunc MaxiSorp®) as per manufacturer's instruction.

Briefly 100 µl of capture antibody (1µg/ml in PBS) was added to each ELISA plate well and incubated overnight at room temperature. The wells were aspirated to remove liquid and the plate was washed four times with 300 µl wash buffer (0.05% Tween-20 in PBS) per well. After the last wash, the plate was tapped in inverted position to remove residual buffer on paper towel. 300 µl of blocking buffer (1% BSA in PBS) was added to each well and the plate was incubated for 1 h at room temperature. After washing the plate four times with wash buffer, 100µl of the test sample and the IFN-γ standard were added to each well in triplicate. IFN-γ standard was diluted to concentrations ranging from 3000 pg/mL to zero in sample diluent buffer (0.05% Tween-20, 0.1% BSA in PBS). The plate was incubated at room temperature for overnight. The plate was washed 4 times and 100 µl of detection antibody (1µg/ml in sample diluent buffer) was added to each ELISA plate well and incubated at room temperature for 2 h. Plate was washed four times and 100 µl of diluted avidin-HRP conjugate (1:2000) in sample diluent was added and incubated for 1h. Plate was again washed four times and 100 µl of ABTS substrate solution was added to each well. The plate was wrapped in a foil and incubated at room temperature for 15 min for color development. Absorbance was recorded at 405 nm with wavelength correction set at 650 nm in ELISA plate reader (Tecan, Austria). IFN-γ production was expressed as fold change in cytokine release as following:

Fold change = Average absorbance of the peptide stimulated cells/unstimulated cells

3.5. Statistical Analysis

All statistical analysis was performed using GraphPad Prism 6 statistical software. Molecular docking data was analysed by one way ANOVA with Tukey's multiple

comparisons test. PBMC proliferation and extracellular IFNγ secretion data was analysed by t-test for unpaired data. P-values < 0.05 were considered statistically significant.

Chapter 4: Results

4.1 Prediction of peptides containing overlapping T cell epitopes using immunoinformatics tools from the conserved peptide regions of different proteins in H1N1 virus which can act as vaccine targets

Full length protein sequences of hemagglutinin (HA), neuraminidase (NA) and matrix 1 (M1) protein were obtained from various influenza sequences databases. Aligned sequences of these proteins were used to identify conserved sequences by AVANA. From the conserved sequences, epitope prediction was carried out using six different epitope prediction tools (three for each class of HLA). Epitopes having similarity with the human self-peptides were eliminated using BLASTp. Overlapping epitopes were merged to generate peptides having multiple $CD8^+$ and $CD4^+$ T cell epitopes.

4.1.1 Conserved peptides of HA, NA and M1 protein of the H1N1 virus

Unique (non-redundant) sequences of HA, NA and M1 protein were obtained from influenza sequence databases (NCBI Influenza virus resource; IRD) in order to cover the majority of genetic variants of H1N1 isolates around the world (Table 4.1.1, page 60). Because of the frequent antigenic variations in H1N1, previously identified epitopes may lose their potency to generate an immune response against all the variants. Hence, it was important to find those peptides of HA, NA and M1 proteins that are conserved across the various strains of the H1N1 virus. The sequences were aligned by MUSCLE tool and then conservation of the aligned sequences was analysed using the AVANA tool. Surface glycoproteins HA and NA are regarded as the highly mutable proteins of influenza as compared to the internal proteins. Therefore, the criteria for conservation was relaxed by 10% for HA and NA as compared to M1 protein. Conservation was set to a minimum of 80% in case of HA and NA, whereas for M1 protein it was set to a minimum of 90%. In total, 37 conserved regions were identified in these three proteins of H1N1 influenza virus viz. 12 for HA (Table 4.1.2, page 60), 15 for NA (Table 4.1.3, page 61) and 10 for M1 (Table 4.1.4, page 61). These conserved were used as input for various epitope prediction tools.

Table 4.1.1. Description of H1N1 protein sequences considered for alignment and conservation estimation

Protein	Time interval for which sequences have been considered	Number of Sequences
Hemagglutinin	January 1918 to February 2013	3661
Neuraminidase	January 1918 to February 2013	2079
Matrix 1 protein	January 1918 to April 2015	458

Table 4.1.2. Conserved peptide fragments of H1N1 virus hemagglutinin protein

	Conserved peptide sequences	Length
CS_H1	CIGYHANNSTDTVDTVLEKNVTVTHSVNLLE	31
CS_H2	AGWILGNPECE	11
CS_H3	YEELREQLSSVSSFERFEIFPK	22
CS_H4	PSIQSRGLFGAIAGFIEGGWTGMVDGWYGYHHQNEQGSGYAAD	43
CS_H5	ITNKVNSVIEKMNTQFTAVGKEFN	24
CS_H6	ENLNKKVDDGF	11
CS_H7	DIWTYNAELLVLLENERTLD	20
CS_H8	HDSNVKNLYEKV	12
CS_H9	QLKNNAKEIGNGCFEFYHKC	20
CS_H10	CMESVKNGTYDYPKYSEE	18
CS_H11	YQILAIYSTVASSLVL	16
CS12	VSLGAISFWMCS	12

Table 4.1.3. Conserved peptide fragments of H1N1 virus neuraminidase protein

	Conserved peptide sequences	**Length**
CS_N1	MNPNQKIITIGS	12
CS_N2	LQIGNIISIW	10
CS_N3	KDNSIRIGSKGDVFVIREPFISCS	24
CS_N4	LECRTFFLTQGALLNDKHSNGT	22
CS_N5	FESVAWSASACHDG	14
CS_N6	WLTIGISGPDNGAVAVLKYNGIIT	24
CS_N7	ILRTQESEC	9
CS_N8	YEECSCYPD	9
CS_N9	CVCRDNWHGSNRPWVSFNQNL	21
CS_N10	YQIGYICSG	9
CS_N11	YGNGVWIGRTKS	12
CS_N12	GFEMIWDPNGWT	12
CS_N13	WSGYSGSFVQHPELTGLDCIRPCFWVEL	28
CS_N14	TIWTSGSSISFCGVNSDT	18
CS_N15	WSWPDGAELPFTIDK	15

Table 4.1.4. Conserved peptide fragments of H1N1 virus matrix 1 protein

	Conserved peptide sequences	**Length**
CS_M1	MSLLTEVETYVLSI	14
CS_M2	PSGPLKAEIAQRLE	14
CS_M3	VFAGKNTDLEALMEWLKTRPILSPLTKGILGFVFTLTVPSERGLQRRRF	49
CS_M4	QNALNGNGDPNNMDRAV	17
CS_M5	KLKREITFHGAKE	13
CS_M6	GALASCMGLIYNRMG	15
CS_M7	CATCEQIADSQH	12
CS_M8	TTTNPLIRHENRMVLASTTAKAMEQ	25
CS_M9	AGSSEQAAEAMEV	13
CS_M10	NLQAYQKRMGVQMQRFK	17

4.1.2 Prediction of peptides containing overlapping CD8+ and CD4+ T-cell epitopes

Different tools use different parameters to predict epitopes, therefore the idea of epitope prediction by consensus approach was captivating. Different immunoinformatics tools were used for CD8+ T-cell epitopes (NetCTL, BIMAS, and SYFPEITHI) and CD4+ T-cell epitopes (NetMHCII 2.2, ProPred and IEDB SMM align) prediction. The predicted epitopes were compared, and then a set of epitopes was obtained that was predicted by all the tools. All the predicted epitopes were analysed by BLASTp to exclude any potential auto-immunogenic epitopes. The overlapping CD8+ and CD4+ T cell epitopes obtained after BLASTp analysis were merged into a single peptide fragment.

4.1.2.1. Hemagglutinin peptides containing multiple T cell epitopes

HA is an antigenic glycoprotein that is present on the surface of the H1N1 virus and is associated with membrane fusion. Initially, 32 CD8+ T cell epitopes (HLA class I binding epitopes) in 11 conserved regions and 12 CD4+ T cell epitopes (HLA class II binding epitopes) in six conserved regions were identified. Homology with human proteome assessed by BLASTp analysis lead to elimination of eight CD8+ T cell epitopes and one CD4+ T cell epitope (Table 4.1.5, page 63). After BLASTp analysis, set of completely non self-epitopes comprising of 24 CD8+ and 11 CD4+ T cell epitopes were obtained (Table 4.1.6, page 64).

The epitopes that had overlapping amino acid sequences were merged to generate a single peptide fragment. Ten HLA class I binding peptides were obtained after merging the overlapping CD8+ T cell epitopes. Similarly, six HLA class II binding peptides were obtained after merging the overlapping CD4+ T cell epitopes. Each peptide and number of constituent epitopes are listed in table 4.1.7 (page 65) Further, these HLA class I and II peptides were merged among themselves to form five peptides, each composed of single or multiple CD8+ and CD4+ T cell epitopes (Table 4.1.7, page 65).

Table 4.1.5. Epitopes identical to human peptides which were eliminated by BLASTp

Conserved sequences	Epitopes*	Human Peptides	Human proteins
CS 3	$CD8^+$ T cell epitopes: ELREQLSSV EQLSSVSSF SSVSSFERF	LREQLSS	Protein CASP
	$CD4^+$ T cell epitope: LREQLSSVS	ELREQLS	cGMP-dependent protein kinase 2
CS 7	$CD8^+$ T cell epitopes: IWTYNAELL TYNAELLVL	AELLVLLE	titin isoform N2-B, novex-1, X5, novex-2
	VLLENERTL WTYNAELLV YNAELLVLL	ELLVLLE	angiopoietin-related protein 6 precursor, spatacsin isoform 1

* Each of these epitopes may not necessarily share identity of 7/9 with human peptide but peptide formed by overlapping these epitopes satisfy the criterion of 7/9 identity without any gap or mismatch.

Table 4.1.6. $CD8^+$ and $CD4^+$ T cell epitopes of H1N1 virus hemagglutinin protein

Conserved sequences	$CD8^+$ T cell epitopes	$CD4^+$ T cell epitopes
CS_H1	DTVDTVLEK	LEKNVTVTH
	STDTVDTVL	VTVTHSVNL
	TVLEKNVTV	
	TVTHSVNLL	
CS_H3	VSSFERFEI	LSSVSSFER
	SSFERFEIF	
CS_H4	GLFGAIAGF	FGAIAGFIE
	GMVDGWYGY	
	IAGFIEGGW	
	WTGMVDGWY	
	HQNEQGSGY	
CS_H5	KMNTQFTAV	IEKMNTQFT
	KVNSVIEKM	MNTQFTAVG
	QFTAVGKEF	
CS_H7		LVLLENERT
CS_H8	HDSNVKNLY	
CS_H9	EIGNGCFEF	
CS_H10	MESVKNGTY	
	SVKNGTYDY	
CS_H11	IYSTVASSL	ILAIYSTVA
	QILAIYSTV	IYSTVASSL
	STVASSLVL	LAIYSTVAS
	YQILAIYST	YQILAIYST
CS_H12	SLGAISFWM	
	VSLGAISFW	

Table 4.1.7. H1N1 hemagglutinin peptides containing overlapping $CD8^+$ and $CD4^+$ T cell epitopes

Conserved sequences	**Peptides enriched with $CD8^+$ T cell epitopes**	**No. of epitopes**	**Peptides enriched with $CD4^+$ T cell epitopes**	**No. of epitopes**	**Peptides containing multiple $CD8^+$ and $CD4^+$ T cell epitopes**
CSH1	STDTVDTVLEKNVTVTHSVNLL	4	LEKNVTVTHSVNL	2	STDTVDTVLEKNVTVTHSVNLL (P_H1)
CSH3	VSSFERFEIF	2	LSSVSSFER	1	LSSVSSFERFEIF (P_H2)
CSH4	GLFGAIAGFIEGGWTGMVDGWYGY HQNEQGSGY	4 1	FGAIAGFIE	1	GLFGAIAGFIEGGWTGMVDGWYGY (P_H3)
CSH5	KVNSVIEKMNTQFTAVGKEF	3	IEKMNTQFTAVG	2	KVNSVIEKMNTQFTAVGKEF (P_H4)
CSH7			LVLLENERT	1	
CSH8	HDSNVKNLY	1			
CSH9	EIGNGCFEF	1			
CSH10	MESVKNGTYDY	2			
CSH11	YQILAIYSTVASSLVL	4	YQILAIYSTVASSL	4	YQILAIYSTVASSLVL (P_H5)
CSH12	VSLGAISFWM	2			

4.1.2.2 Neuraminidase peptide containing multiple T cell epitopes

NA plays vital role in the release of viral progeny from the infected cells. In the present study, 13 $CD8^+$ T cell epitopes located in eight conserved regions and nine $CD4^+$ T cell epitopes in six conserved regions were identified based on the criteria that they should be predicted by each of the tools (Table 4.1.8, page 66). BLASTp analysis of NA epitopes revealed no homology of the predicted epitopes with any of the annotated human proteins. Nine peptides binding to HLA class I and six peptides binding to HLA class II binding were obtained after merging overlapping $CD8^+$ and $CD4^+$ T cell epitopes respectively (Table 4.1.9, page 67). Six conserved peptides sequences containing overlapping multiple $CD8^+$ and $CD4^+$ T-cell epitopes were generated (Table 4.1.9, page 67).

Table 4.1.8. $CD8^+$ and $CD4^+$ T cell epitopes of H1N1 virus neuraminidase protein

Conserved sequences	$CD8^+$ T cell epitopes	$CD4^+$ T cell epitopes
CS_N2	LQIGNIISI QIGNIISIW	LQIGNIISI
CS_N3	DVFVIREPF VFVIREPFI	FVIREPFIS IRIGSKGDV
CS_N4	FFLTQGALL	FFLTQGALL FLTQGALLN
CS_N6	GPDNGAVAV	
CS_N9	GSNRPWVSF	WHGSNRPWV
CS_N13	GSFVQHPEL IRPCFWVEL VQHPELTGL	FVQHPELTG
CS_N14	TIWTSGSSI WTSGSSISF	ISFCGVNSD WTSGSSISF
CS_N15	WPDGAELPF	

Table 4.1.9. H1N1 neuraminidase peptides containing overlapping $CD8^+$ and $CD4^+$ T cell epitopes

Conserved sequences	Peptides enriched with $CD8^+$ T cell epitopes	No. of epitopes	Peptides enriched with $CD4^+$ T cell epitopes	No. of epitopes	Peptides containing $CD8^+$ and $CD4^+$ T cell epitopes
CS_N2	LQIGNIISIW	2	LQIGNIISI	1	LQIGNIISIW(P_N1)
CS_N3	DVFVIREPFI	2	IRIGSKGDVFVIREPFIS	2	IRIGSKGDVFVIREPFIS (P_N2)
CS_N4	FFLTQGALL	1	FFLTQGALLN	2	FFLTQGALLN (P_N3)
CS_N6	GPDNGAVAV	1			
CS_N9	GSNRPWVSF	1	WHGSNRPWV	1	WHGSNRPWVSF (P_N4)
CS_N13	GSFVQHPELTGL IRPCFWVEL	2 1	FVQHPELTG	1	GSFVQHPELTGL (P_N5)
CS_N14	TIWTSGSSISF	2	WTSGSSISFCGVNSD	2	TIWTSGSSISFCGVNSD (P_N6)
CS_N15	WPDGAELPF	1			

4.1.2.3 Matrix 1 peptides containing multiple T cell epitopes

Matrix 1 protein binds to viral RNP as well as membrane protein and plays multiple roles in virus entry, uncoating, replication, assembly and budding of influenza virus. Following the same approach of epitope selection, epitopes were identified for M1 protein. Ten $CD8^+$ T cell epitopes (from five conserved sequences) and nine $CD4^+$ T cell epitopes (from three conserved sequences) of the M1 protein were obtained after BLASTp analysis (Table 4.1.10, page 68). BLASTp results revealed no specific homology of the human proteome with any of the predicted $CD4^+$ T cell epitopes, however among $CD8^+$ T cell epitopes of the M1 protein, one epitope GILGFVFTL was found to be homologous as per the set criterion, so it was eliminated from further studies. Epitopes having overlapping amino acid sequences in the respective conserved regions were merged to generate a peptide having multiple epitopes. Six peptides of $CD8^+$ T cell epitopes and three peptides containing $CD4^+$ T epitopes were obtained (Table 4.1.11, page 69). Further, these putative overlapping peptides were merged to generate a single peptide containing multiple $CD4^+$ and $CD8^+$ T cell epitopes, confined to a particular conserved region. Three peptides composed of overlapping $CD4^+$ and $CD8^+$ T cell epitopes were obtained (Table 4.1.11, page 69).

Table 4.1.10. $CD8^+$ and $CD4^+$ T cell epitopes of H1N1 virus matrix 1 protein

Conserved sequences	**$CD8^+$ T cell epitopes**	**$CD4^+$ T cell epitopes**
CS_M1	SLLTEVETY	
	LLTEVETYV	
CS_M2	LKAEIAQRL	
CS_M3	ERGLQRRRF	FVFTLTVPS
	KTRPILSPL	FTLTVPSER
	RPILSPLTK	ILGFVFTLT
CS_M8	IRHENRMVL	IRHENRMVL
	MVLASTTAK	MVLASTTAK
		VLASTTAKA
		LIRHENRMV
CS_M9	QAYQKRMGV	LQAYQKRMG
	KRMGVQMQR	YQKRMGVQM

Table 4.1.11. H1N1 matrix 1 peptides containing overlapping $CD8^+$ and $CD4^+$ T-cell epitopes

Conserved Sequences	Peptides enriched with $CD8^+$ T cell epitopes	No. of epitopes	Peptides enriched with $CD4^+$ T cell epitopes	No. of epitopes	Peptides containing $CD8^+$ and $CD4^+$ T cell epitopes
CS_M1	SLLTEVETYV	2			
CS_M2	LKAEIAQRL	1			
CS_M3	ERGLQRRRF	1	ILGFVFTLTVPSER	3	ILGFVFTLTVPSERGLQRRRF (P_M1)
CS_M3	KTRPILSPLTK	2			
CS_M8	IRHENRMVLASTTAK	2	LIRHENRMVLASTTAKA	4	LIRHENRMVLASTTAKA (P_M2)
CS_M9	QAYQKRMGVQMQR	2	LQAYQKRMGVQM	2	LQAYQKRMGVQMQR (P_M3)

4.1.2.4. Selected peptides containing CD8⁺ and CD4⁺ T cell epitopes of HA, NA and M1 protein

Peptides P_H1, P_H3, P_H4, P_N2, P_N4, P_N5, P_N6 and P_M1 have not been reported exactly in the earlier studies. Some peptides which share partial identity with these peptides have been reported to induce T cell proliferation and IFN-γ secretion, but the immunogenicity of the complete peptides has not been reported as such. The other two peptides P_M2 and P_M3 of M1 protein form a part of bigger peptides which have been reported immunogenic. Matrix 1 peptides are highly conserved and thus considered to be more promising candidates for universal T cell based influenza vaccine. Hence, all the three peptides of matrix 1 protein (P_M1, P_M2 and P_M3) were considered for further evaluation. Ten H1N1 peptides obtained from three proteins were selected for further studies.

These selected peptides of HA, NA and M1 protein containing multiple $CD8^+$ and $CD4^+$ T cell epitopes identified by consensus approach were found be conserved in more than 90% of the sequences obtained for the respective proteins except P_N6 which was conserved in 80% of the sequences obtained for NA (Table 4.1.12, page 70). Further, these peptides not only contain multiple T cell epitopes but were also predicted to bind to diverse array of HLA molecules (class I and II) (Table 4.1.12, page 70).

Table 4.1.12. Selected Peptides containing both $CD8^+$ and $CD4^+$ T cell epitopes of HA, NA and M1 protein

	Peptides	**T cell epitopes**	**HLA class I alleles**	**HLA class II alleles**	**Conservation (%)**
P_H1	STDTVDTVLEKNVTVTHSVNLL	6	26	12	90.4
P_H3	GLFGAIAGFIEGGWTGMVDGWYGY	5	17	7	91.5
P_H4	KVNSVIEKMNTQFTAVGKEF	5	13	15	95.5
P_N2	IRIGSKGDVFVIREPFIS	4	16	43	90.9
P_N4	WHGSNRPWVSF	2	9	4	97.3
P_N5	GSFVQHPELTGL	3	21	8	97.7
P_N6	TIWTSGSSISFCGVNSD	4	18	10	80.0
P_M1	ILGFVFTLTVPSERGLQRRRF	4	1	55	93.5
P_M2	LIRHENRMVLASTTAKA	6	9	49	94.6
P_M3	LQAYQKRMGVQMQR	4	5	22	94.3

4.2 Structure analysis and molecular modelling approach to assess the binding affinity of peptide to the HLA complex

The selected ten peptide fragments of hemagglutinin, neuraminidase and matrix 1 protein, identified in the previous section were studied for their location on the crystallised structures of the respective proteins. Further, the structures of the $CD8^+$ T cell epitopes and peptides containing multiple $CD4^+$ T cell epitopes which were part of the selected peptides, were generated using online web server PEP-FOLD. These peptides were analysed for their binding with various HLA molecules (HLA class I and II) using molecular docking (Autodock Vina tool). These peptides were further analysed by IEDB population coverage analysis tool to estimate the percentage of individuals around the world expected to show immunogenic response against these identified peptides based on the HLA-restriction obtained by virtue of various epitope predictions.

4.2.1 Structural analysis

The three-dimensional structures of HA (PDB id 3LZG), NA (PDB id 3TI3) and M1 protein (5CQE) were taken as the model structures to map the selected peptides. HA and NA have a multimeric structure (HA homotrimeric, NA homotetrameric) whereas M1 protein exists as monomer. The PDB structures of the respective proteins were edited to remove the multimeric structures leaving only monomers using Discovery Studio v4.1 visualizer. Selected peptides were mapped on the crystal structure of respective protein using the same software. Few of them could not be mapped on the respective crystal structures due to the absence of the transmembrane or cytoplasmic domains (HA and NA) and RNA binding domain (M1 protein) in the crystal structures.

HA is a 565 amino acid long protein having extracellular domain (18-528), transmembrane domain (529 – 549) and cytoplasmic domain (550 – 565) (Consortium, 2015). All the three selected peptides of HA viz. P_H1, P_H3 and P_H4 were found to be located in the extracellular domain of HA and thus mapped on the crystal structure (Figure 4.2.1a, page 72). NA is a 453 amino acid long protein having intravirion domain (1-6), transmembrane domain (7-35) and external head domain (36 – 453) (Consortium, 2015). Four selected peptides of NA viz. P_N2, P_N4, P_N5, P_N6 were found to be part of the external head domain of neuraminidase and thus mapped in that domain (Figure 4.2.1b, page 72). M1 protein is a small protein of 252 amino acids having membrane binding domain (1 –

164) and ribonucleoprotein binding domain (165 – 252) (Consortium, 2015). Only peptide of M1 protein i.e. P_M1 was found to be located in the membrane binding domain of M1 protein hence mapped on the crystal structure of M1 (Figure 4.2.1c, page 72). P_M2 and P_M3 were located in ribonucleoprotein binding domain of M1, hence could not be mapped.

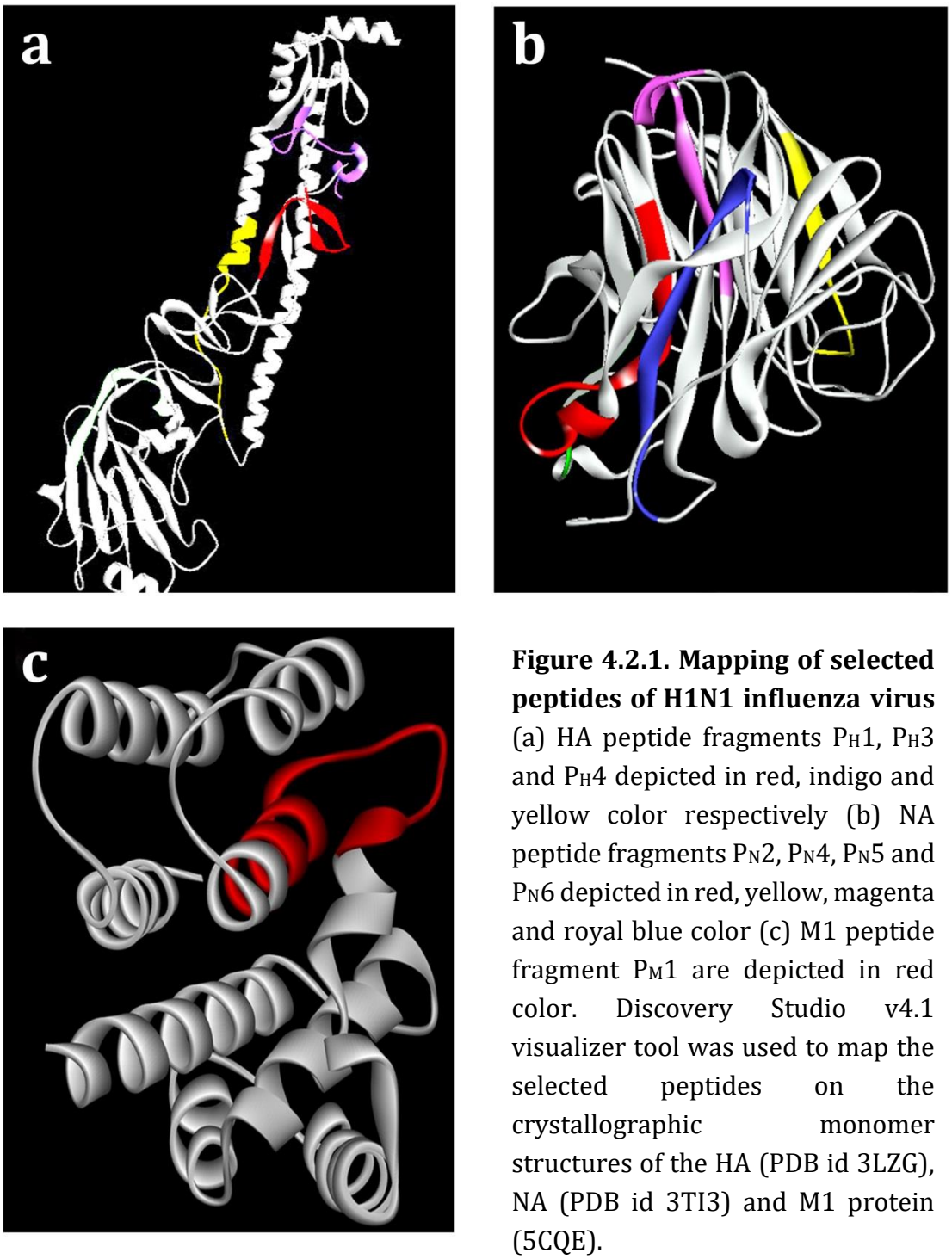

Figure 4.2.1. Mapping of selected peptides of H1N1 influenza virus (a) HA peptide fragments P_H1, P_H3 and P_H4 depicted in red, indigo and yellow color respectively (b) NA peptide fragments P_N2, P_N4, P_N5 and P_N6 depicted in red, yellow, magenta and royal blue color (c) M1 peptide fragment P_M1 are depicted in red color. Discovery Studio v4.1 visualizer tool was used to map the selected peptides on the crystallographic monomer structures of the HA (PDB id 3LZG), NA (PDB id 3TI3) and M1 protein (5CQE).

4.2.2 Molecular docking

The first and the foremost step towards the generation of an efficient adaptive immune response is the binding of immunogenic peptide to the peptide binding groove of HLA molecule inside the host cell. Autodock vina tool was employed to calculate the binding affinity of the selected peptide containing multiple epitopes with HLA class I and II molecules in terms of binding energy. High resolution crystallographic structures of peptide bound HLA molecules (nine and ten for HLA class I and II respectively typifying each supertype) were obtained from the PDB database for docking (Table 4.2.1, page 73). Binding energy obtained by docking the natural peptides separated from the parent HLA complex with the corresponding HLA molecules served as positive control group. HLA class II accommodates longer peptides (~18–20 amino acid) in contrast to HLA class I which binds to smaller peptides (8-10 amino acid)(O'Brien et al., 2008). Accordingly from the selected peptides of three proteins, PEP-FOLD generated structure of the $CD8^+$ T cell epitopes (nonamer peptide) and peptides containing multiple $CD4^+$ T cell epitopes were used for docking with the class I and II HLA molecules respectively. Some of the $CD8^+$ epitopes/peptides containing $CD4^+$ T cell epitopes which did not bind within the peptide binding groove of HLA were regarded as non-binders. Hence, the binding energy values were not assigned for non-binders.

Table 4.2.1. HLA molecules used for docking

HLA Class I			HLA Class II		
PDB id	**HLA molecules**	**Resolution**	**PDB id**	**HLA molecules**	**Resolution**
3BO8	HLA-A1	1.8 Å	4P5M	HLA-DP2	1.7 Å
3MRK	HLA-A2	1.4 Å	1UVQ	HLA-DQ0602	1.8 Å
3RL1	HLA-A3	2.0 Å	3PL6	HLA-DQ1	2.55 Å
3WL9	HLA-A24	1.66 Å	1S9V	HLA-DQ2	2.22 Å
3VCL	HLA-B7	1.7 Å	2NNA	HLA-DQ8	2.1 Å
3SPV	HLA-B8	1.3 Å	1KLU	HLA-DR1	1.93 Å
2A83	HLA-B27	1.4 Å	1FV1	HLA-DR2	1.9 Å
2HJL	HLA- B5703	1.5 Å	1A6A	HLA-DR3	2.75 Å
3C9N	HLA-B62	1.87 Å	1D5M	HLA-DR4	2.0 Å
			3C5J	HLA-DR52c	1.8 Å

4.2.2.1 Hemagglutinin

Eleven $CD8^+$ T cell epitopes viz. four of P_H1 (Figure 4.2.2 a, page 75), four of P_H3 (Figure 4.2.2 b, page 75) and three of P_H4 (Figure 4.2.2c, page 75) were docked to nine HLA class I molecules and three peptides containing $CD4^+$ T cell epitopes (each corresponding to P_H1, P_H2 and P_H3) were docked to ten HLA class II molecules (Figure 4.2.3a, page 76). The binding energy of most of these docked epitopes/peptides were comparable to native HLA peptides. However, some peptide-HLA docked complexes were found to have higher binding energy than native peptides. $CD8^+$ T cell epitopes IAGFIEGGW (HLA A2, A24 and B7), WTGMVDGWY (HLA A3) and GLFGAIAGF (HLA A2 and A3) (Figure 4.2.2b, page 75) and $CD4^+$ epitope enriched peptides FGAIAGFIE (HLA-DQ0602, DR1, DR2, DR3 and DR52C) of P_H3 peptides (Figure 4.2.3b, page 76) have shown higher binding energies than native peptide. $CD4^+$ T cell epitope enriched peptides IEKMNTQFTAVG (DR1, DQ8)) of P_H4 and LEKNVTVHSVNL (DQ1) of P_H1 were also found to have higher binding energy (Figure 4.2.3b, page 76). STDTVDTVL and TVTHSVNLL of P_H1 could not bind to HLA-A2, B27 and B5703, thus their binding energy is not shown in the figure 4.2.2a (page 75). Similarly, some other peptides/epitopes could not bind to binding groove of HLA molecules, hence their binding energy is not assigned in the respective figure. Based on the number of HLA molecules which showed binding with the constituent epitopes of the peptides and number of epitope-HLA combinations showing higher binding energy than the native peptides of respective HLA, P_H3 has shown good binding followed by P_H4 and P_H1. All the binding energies of all the $CD8^+$ T cell epitopes and peptides enriched $CD4^+$ T cell epitopes were identified within the range of native peptides for both the classes of HLA. Statistical analysis revealed no significant difference in binding energies of most of epitopes/peptides and the native peptides of both classes of HLA (Figure 4.2.2d, page 75and Figure 4.2.3b, page 76). $CD8^+$ T cell epitopes DTVDTVLEK (P_H1) and KVNSVIEKM (P_H4) were found to have significantly lower binding energy (Figure 4.2.2d, page 75). Although, all three peptides were found to have overall good binding affinity but P_H3 appears to be better than other two. Representative poses of HLA class I and II dockings with $CD8^+$ T cell epitope and $CD4^+$ epitope enriched peptide respectively, which resulted in highest binding energies are shown in Figure 4.2.4 (page 77).

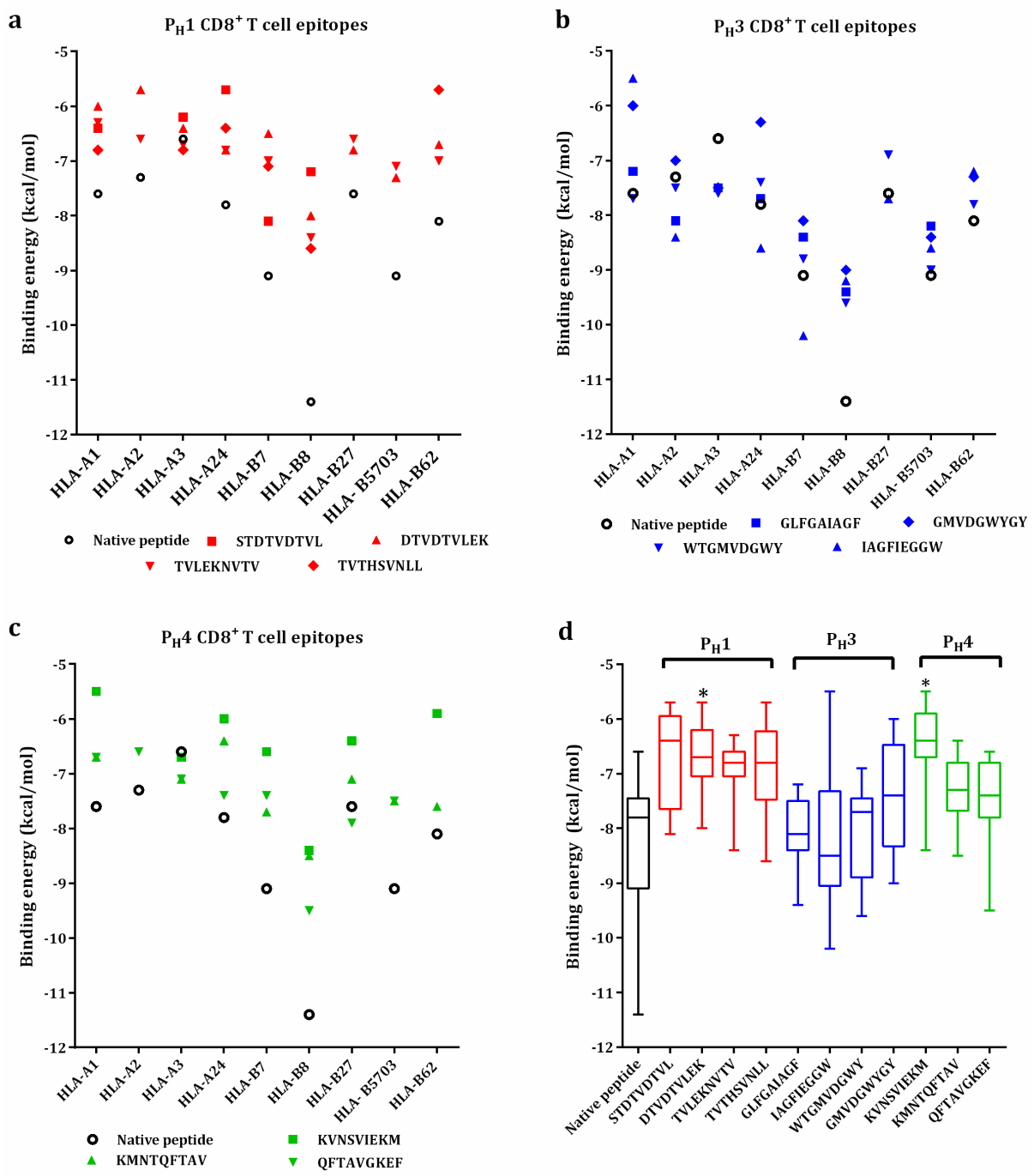

Figure 4.2.2. Docking of CD8+ T cell epitopes of HA with HLA class I molecules. The binding energy of each HLA-epitope complex (a) P_H1 epitopes in red (b) P_H3 epitopes in blue (c) P_H4 epitopes in green (d) Combined binding energy of each epitope and native peptides with nine HLA molecules. Native peptides were excised from the original PDB structures of HLA class I molecule using Discovery Studio v4. 1 visualizer tool. The structure of epitopes were build using the PEP-FOLD tool. The native peptide and the CD8+ T cell epitopes of HA were docked to HLA class I molecules using Autodock vina. The bars extend from the 25th percentile to the 75th percentile with a horizontal line at the median. Whiskers extend from the smallest value up to the largest. Statistical significant differences of the mean values between native and CD8+ T cell epitopes were assessed by Tukey's multiple comparison test. * ($P<0.05$) represents the peptides having binding energy significantly different to that of the native peptides.

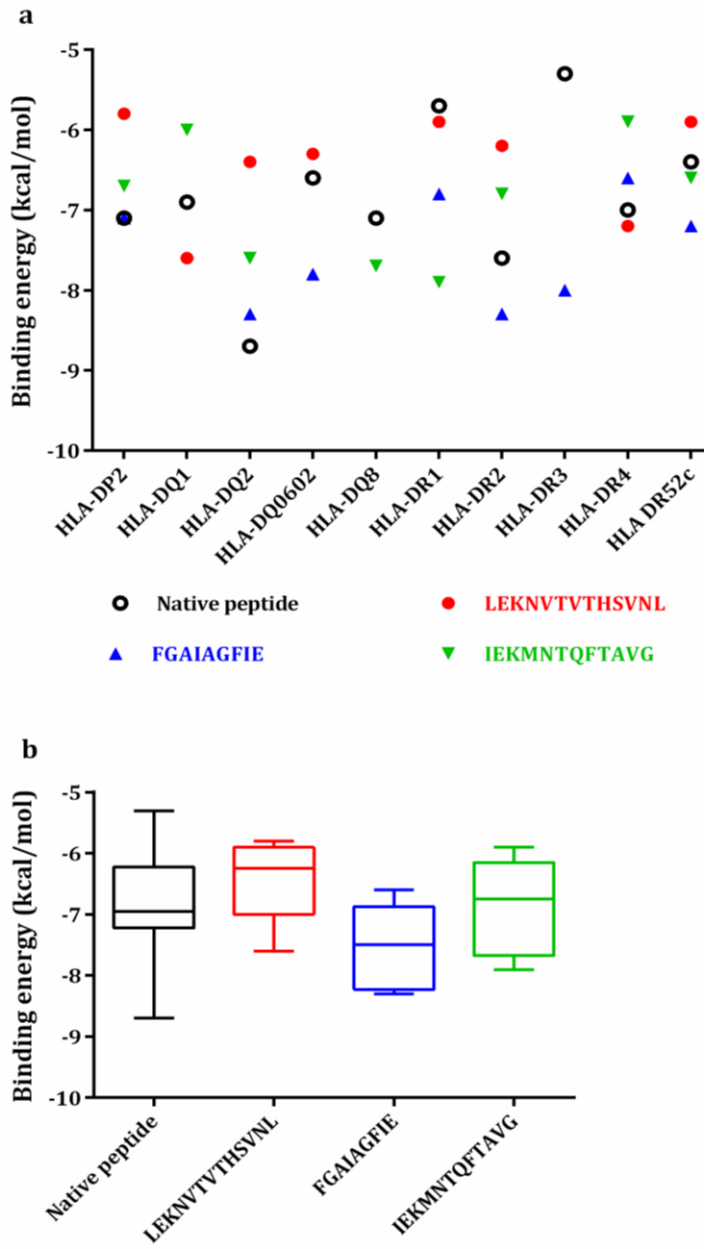

Figure 4.2.3. Docking of peptides containing CD4⁺ T cell epitopes of HA (P_H1 in red, P_H3 in blue and P_H4 in green) with HLA class II molecules. (a) Binding energy obtained for each peptide-HLA complex after docking (b) Combined binding energy of each epitope and native peptides with ten HLA molecules. Native peptides were excised from the original PDB structures of HLA class I molecule using Discovery Studio v4. 1 visualizer tool. The structure of epitopes were build using the PEP-FOLD tool. The native peptide and the peptides containing multiple CD4⁺ T cell epitopes of HA were docked to HLA class II molecules using Autodock vina. The bars extend from the 25th percentile to the 75th percentile with a horizontal line at the median. Whiskers extend from the smallest value up to the largest. Statistical significant differences of the mean values between native and CD8+ T cell epitopes were assessed by Tukey's multiple comparisons test. * ($P<0.05$) represents the peptides having binding energy significantly different to that of the native peptides.

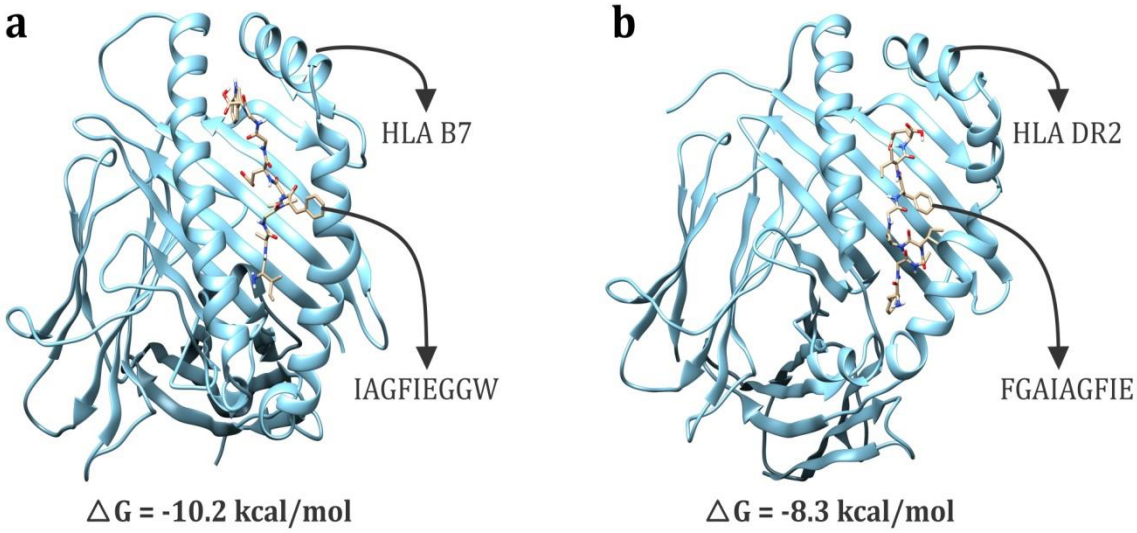

Figure 4.2.4. Poses of dockings showing highest binding energy obtained for (a) CD8⁺ T cell epitope of HA (b) CD4⁺ T cell peptide of HA

4.2.2.2 Neuraminidase

Seven CD8⁺ T cell epitopes belonging to four NA peptides viz. P_N2 (Figure 4.2.5a, page 78), P_N4 (Figure 4.2.5b, page 78), P_N5 (Figure 4.2.5c, page 78) and P_N6 (Figure 4.2.5d, page 78) and four peptides containing various CD4⁺ T cell epitopes (each for P_N2, P_N4, P_N5 and P_N6) were docked to respective HLA class molecules (Figure 4.2.6a, page 79). Comparable binding energy was observed among all the docked NA epitopes/peptides and the native peptides (Figure 4.2.5e, page 78 and Figure 4.2.6b, page 79). CD8⁺ T cell epitopes viz. DVFVIREPF (HLA B27and B62) and VFVIREPFI (HLA A3) of P_N2, GSNRPWVSF (HLA A3) of P_N4 and TIWTSGSSI (HLA A3 and B62) of P_N6 have shown higher binding energy than the corresponding native peptides of HLA molecules (Figure 4.2.5a, b, d, page 78). Similarly, CD4⁺ T cell peptides WHGSNRPWV (HLA DP2, DQ1, DQ2, DQ8, DR1, DR2, DR3 and DR4) of P_N4, FVQHPELTG (HLA DQ1, DQ0602, DR1, DR2, DR3, DR4 and DR52c) of P_N5 and WTSGSSISFCGVNSD (HLA DR1 and DR3) of P_N6 were found to have higher binding energy (Figure 4.2.6a, page 79). The results of CD8⁺ epitope/CD4⁺ peptide-HLA interactions indicated that P_N4 and P_N6 were better binders than other two. Even CD4⁺ peptides WHGSNRPWV of P_N4 were found to have significantly higher binding energy than native peptides. Statistical analysis revealed that binding energy of all other epitopes/peptides and the native peptides had no significant difference for both the classes of HLA (Figure 4.2.5e, page 78 and Figure 4.2.6b, page 79)

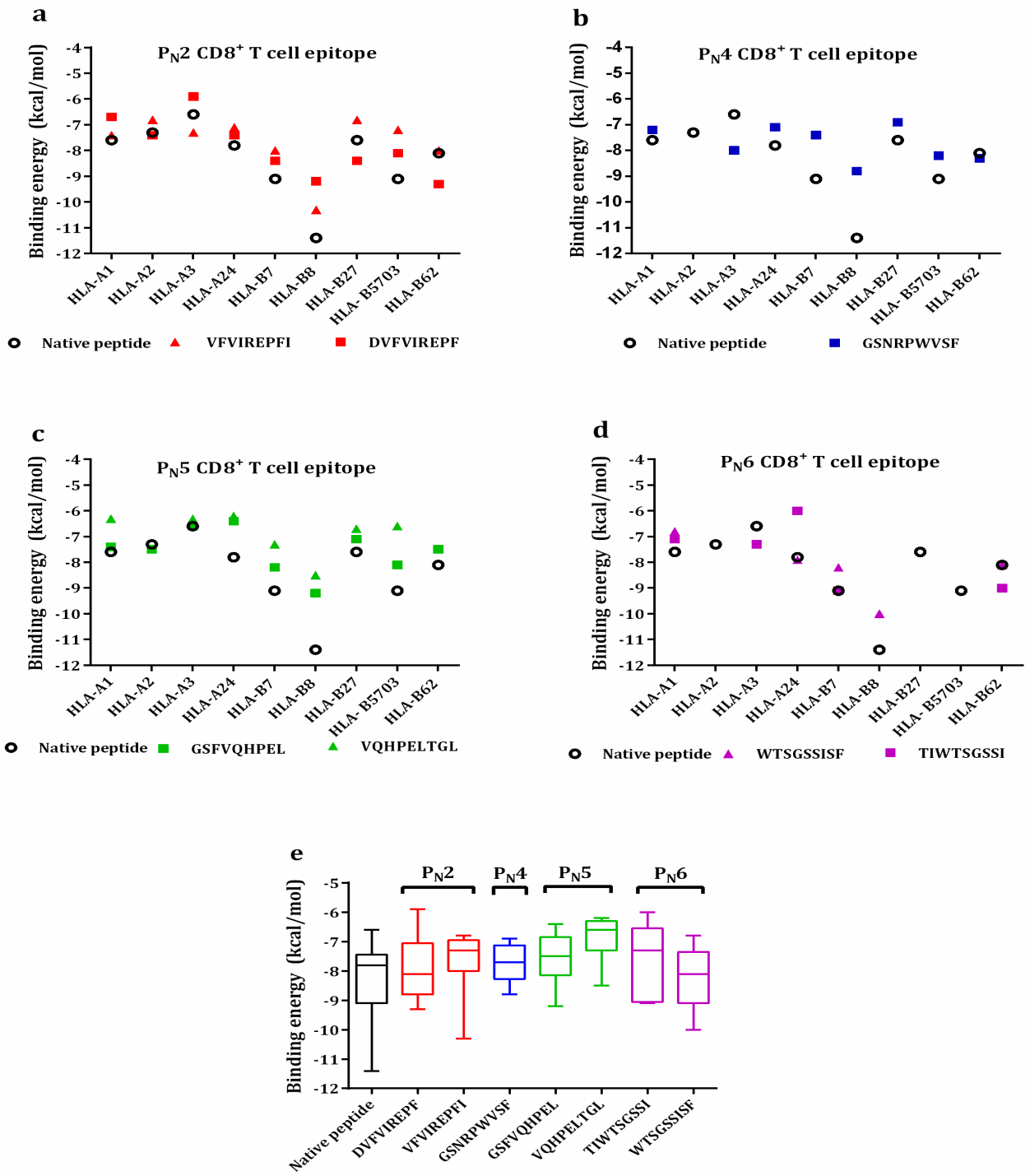

Figure 4.2.5. Docking of CD8⁺ T cell epitopes of NA with HLA class I molecules. Binding energy of each HLA-epitopes complex (a) P_N2 epitope in red (b) P_N4 epitopes in blue (c) P_N5 epitopes in green (d) P_N6 epitopes in purple (e) Combined binding energy of each epitope and native peptides with nine HLA molecules. Native peptides were excised from the original PDB structures of HLA class I molecule using Discovery Studio v4. 1 visualizer tool. The structure of epitopes were build using the PEP-FOLD tool. The native peptide and the CD8⁺ T cell epitopes of NA were docked to HLA class I molecules using Autodock vina. The bars extend from the 25th percentile to the 75th percentile with a horizontal line at the median. Whiskers extend from the smallest value up to the largest. Statistical significant differences of the mean values between native and CD8+ T cell epitopes were assessed by Tukey's multiple comparisons test.

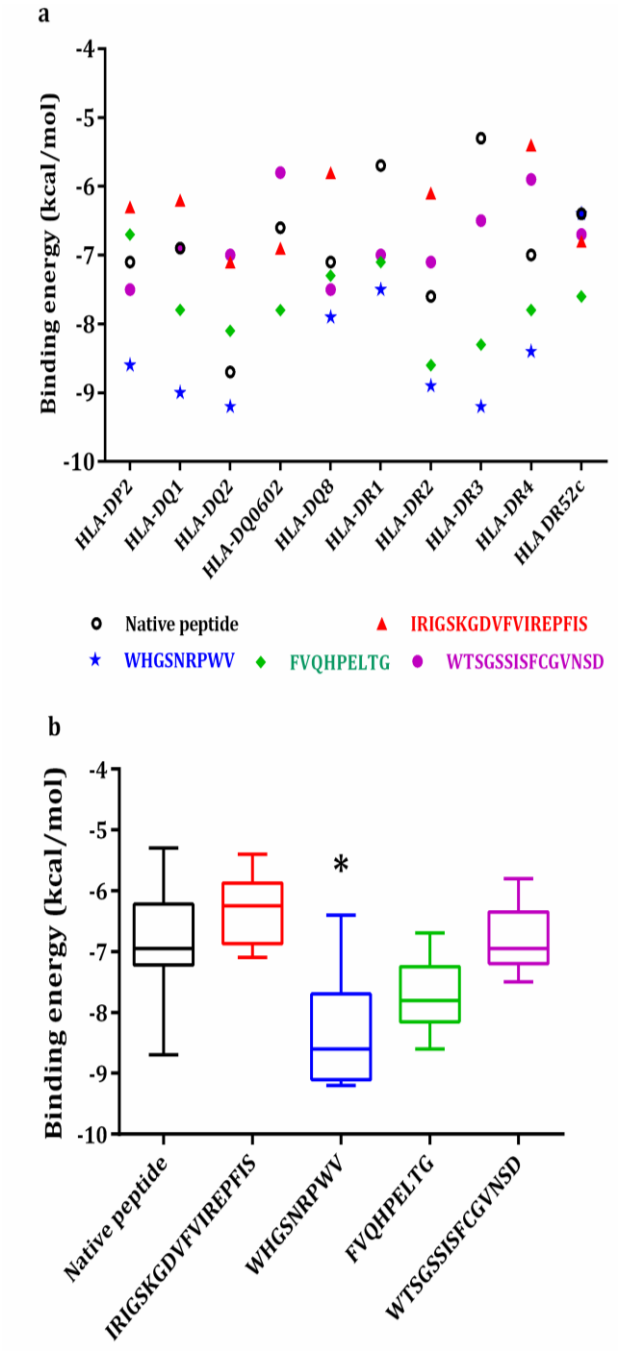

Figure 4.2.6. Docking of peptides containing CD4+ T cell epitopes of NA (P_N2 in red, P_N4 in blue, P_N5 in green and P_N6 in purple) with HLA class II molecules. (a) Binding energy obtained for each peptide-HLA complex after docking (b) Combined binding energy of each epitope and native peptides with ten HLA molecules. Native peptides were excised from the original PDB structures of HLA class I molecule using Discovery Studio v4. 1 visualizer tool. The structure of epitopes were build using the PEP-FOLD tool. The native peptide and the peptides containing multiple $CD4^+$ T cell epitopes of NA were docked to HLA class II molecules using Autodock vina. The bars extend from the 25^{th} percentile to the 75^{th} percentile with a horizontal line at the median. Whiskers extend from the smallest value up to the largest. Statistical significant differences of the mean values between native and CD8+ T cell epitopes were assessed by Tukey's multiple comparisons test. * ($P<0.05$) represents the peptides having binding energy significantly different to that of the native peptides.

4.2.2.3 Matrix 1 protein

Five $CD8^+$ T cell epitopes including one for P_M1 (Figure 4.2.7a, page 81), two for P_M2 (Figure 4.2.7b, page 81) and two for P_M3 (Figure 4.2.7c, page 81) and three peptides containing $CD4^+$ T cell epitopes (Figure 4.2.8a, page 82) were docked to respective HLA class molecules. Comparable binding energy was observed between all docked epitopes/peptides of matrix 1 protein and native peptides. Except MVLASTTAK, a $CD8^+$ T cell epitope of P_M2, the binding energy of all $CD8^+$ T cell epitope and $CD4^+$ T cell epitope containing peptide had no significant difference from native peptides of HLA class I and II molecules respectively (Figure 4.2.7d, page 81 and Figure 4.2.8b, page 82) which demonstrated that the binding energy of docked epitopes/peptides were in the range of native peptides. $CD8^+$ T cell epitopes ERGLQRRRF of P_M1 (HLA-A3) (Figure 4.2.7a, page 81) and $CD4^+$ T cell peptides ILGFVFTLTVPSER of P_M1 (HLA DR1 and DR3) (Figure 4.2.8a, page 82) had higher binding energy than native peptides. Similarly, $CD4^+$ T cell peptides LIRHENRMVLASTTAKA of P_M2 and LQAYQKRMGVQM of P_M3 have higher binding energy for HLA-DR3 (Figure 4.2.8a, page 82). Although all three peptides of matrix peptides were good binder but P_M1 was better than other two.

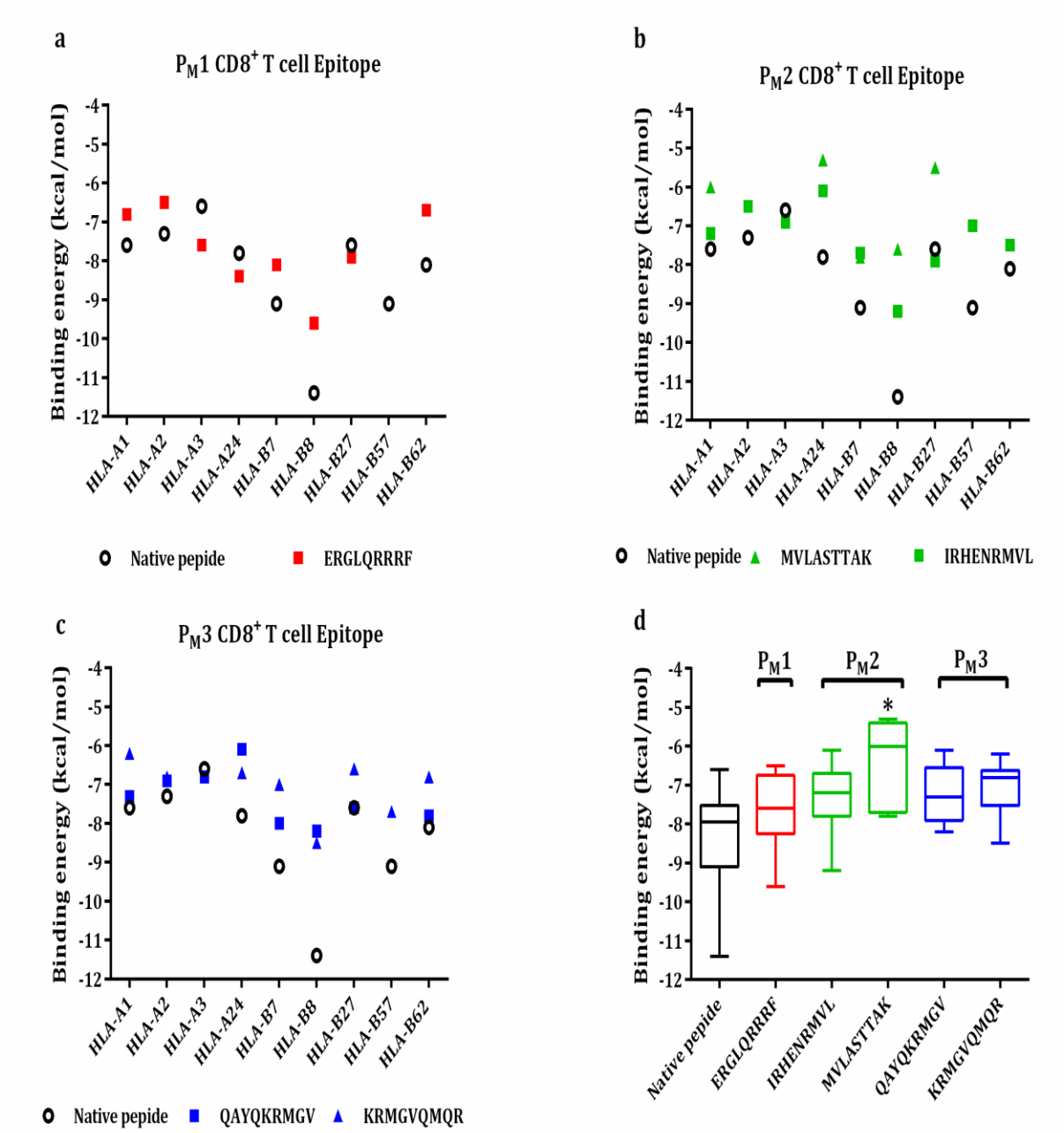

Figure 4.2.7. Docking of CD8+ T cell epitopes of M1 with HLA class I molecules. Binding energy of each HLA-epitopes complex a) P_M1 epitopes in red (b) P_M2 epitopes in green (c) P_M3 epitopes in blue (d) Combined binding energy of each epitope and native peptides with nine HLA molecules. Native peptides were excised from the original PDB structures of HLA class I molecule using Discovery Studio v4. 1 visualizer tool. The structure of epitopes were build using the PEP-FOLD tool. The native peptide and the $CD8^+$ T cell epitopes of M1 protein were docked to HLA class I molecules using Autodock vina. The bars extend from the 25th percentile to the 75th percentile with a horizontal line at the median. Whiskers extend from the smallest value up to the largest. Statistical significant differences of the mean values between native and CD8+ T cell epitopes were assessed by Tukey's multiple comparisons test. *($P<0.05$) represents the peptides having binding energy significantly different to that of the native peptides.

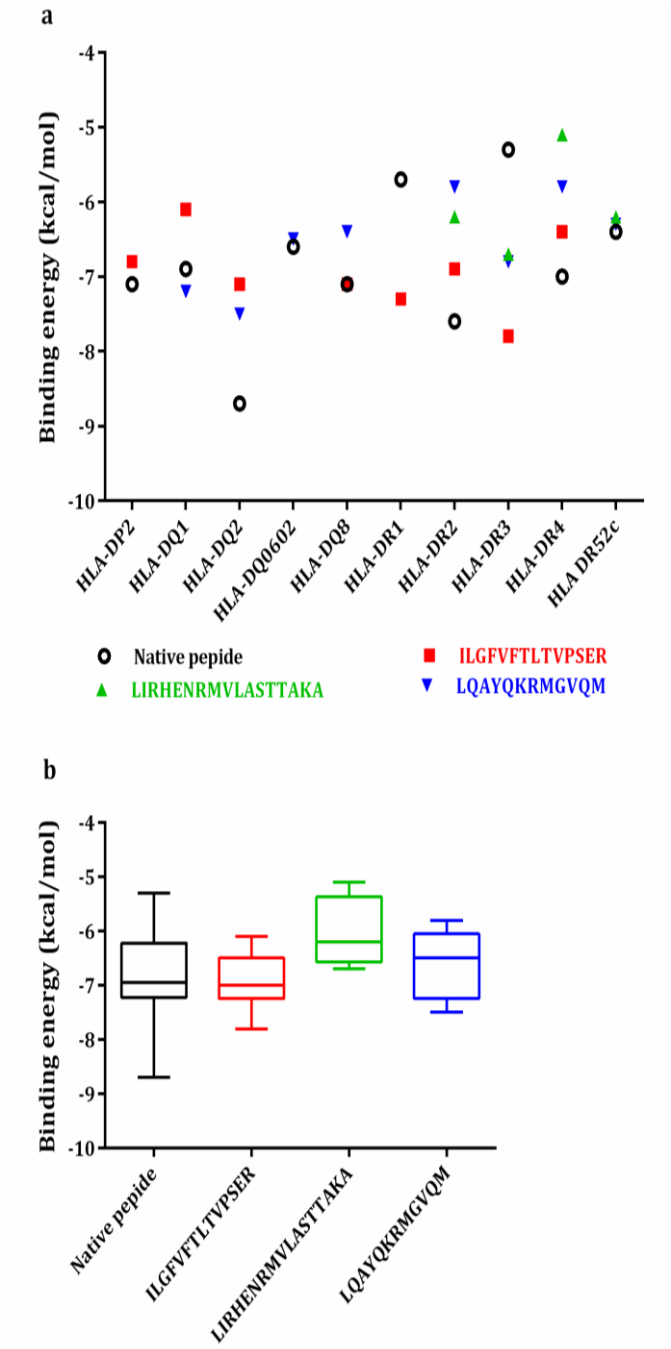

Figure 4.2.8. Docking of peptides containing CD4+ T cell epitopes of M1 (P_M1 in red, P_M2 in green and P_M3 in blue) with HLA class II molecules. (a) Binding energy obtained for each peptide-HLA complex after docking (b) Combined binding energy of each epitope and native peptides with ten HLA molecules. Native peptides were excised from the original PDB structures of HLA class I molecule using Discovery Studio v4. 1 visualizer tool. The structure of epitopes were build using the PEP-FOLD tool. The native peptide and the epitopes containing multiple CD4+ T cell epitopes of M1 protein were docked to HLA class II molecules using Autodock vina. The bars extend from the 25th percentile to the 75th percentile with a horizontal line at the median. Whiskers extend from the smallest value up to the largest. Statistical significant differences of the mean values between native and CD8+ T cell epitopes were assessed by Tukey's multiple comparisons test. *($P<0.05$) represents the peptides having binding energy significantly different to that of the native peptides.

4.2.3 Population coverage analysis

HLA polymorphism among populations distributed in different continents result in variation in peptide induced immunogenic response among humans. Therefore, population coverage analysis becomes necessary for calculating the expected response of predicted peptides in different populations of the world. Selected peptides containing $CD4^+$ and $CD8^+$ T-cell epitopes for HA (P_H1, P_H3, P_H4), NA (P_N2, P_N4, P_N5, P_N6) and M1 (P_M1, P_M2, P_M3) (Tables 4.1.12, page 70), were taken into consideration for population coverage analysis by IEDB. These peptides fragments along with the predicted HLA binding data (HLA class I and II) obtained by virtue of the epitope prediction servers were used as input for IEDB population coverage analysis. Based on the input data, the tool calculated the fraction of individuals from Asia, Europe, Africa, North America, South America and Oceania countries that were expected to respond to these peptide fragments. Population coverage was expressed as an average in case of Asia (East Asia, Northeast Asia, South Asia, Southeast Asia, and Southwest Asia), Africa (East Africa, West Africa, Central Africa, North Africa, South Africa) and North America (North America, Central America) (Figure 4.2.9, page 84, Figure 4.2.10, page 84 and Figure 4.2.11, page 85).

Expected response of populations residing in different continents against the H1N1 peptides was variable. P_H1, P_N2, P_N6, P_M1 and P_M2 peptides have shown excellent coverage in most of the populations studied (except the coverage of P_H1 in North American population) (Figure 4.2.9, page 84, Figure 4.2.10, page 84 and Figure 4.2.11, page 85). Peptides P_H3, P_H4, P_N4 and P_N5 are expected to give highly variable immunogenic response ranging from 50-90% in different populations (Figure 4.2.9, page 84 and Figure 4.2.10, page 84). The response of peptide P_M3 is expected to be average (50 to 75% approx.) in all the populations under consideration (Figure 4.2.11, page 85).

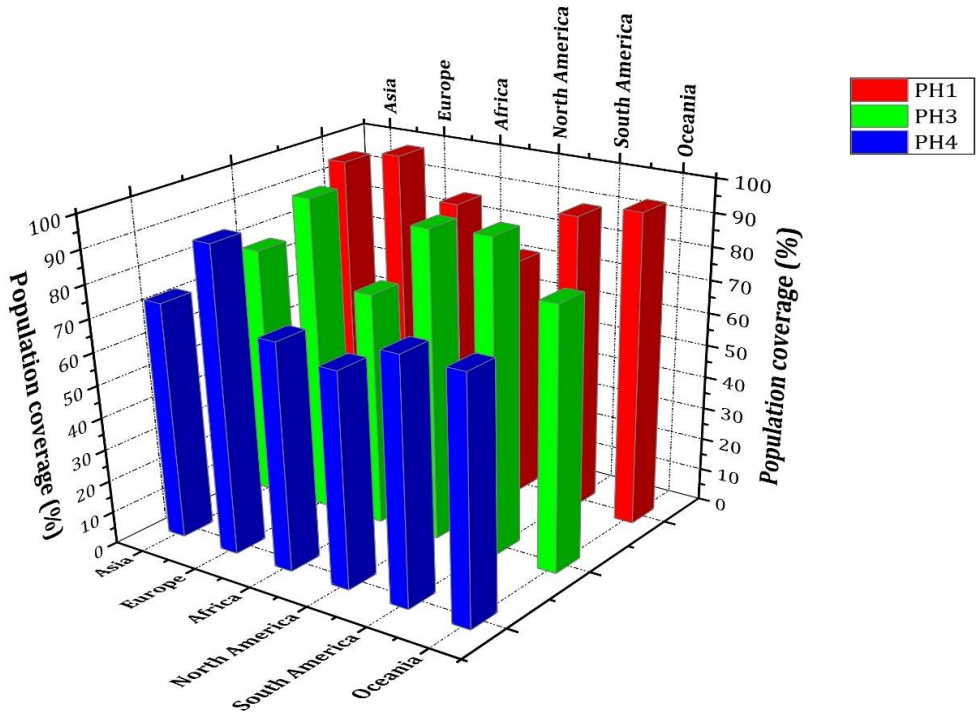

Figure 4.2.9. Population coverage analysis of HA peptides. Human populations residing in different continents were screened to assess the expected immunogenic response of predicted HA peptides by IEDB population coverage analysis tool using HLA-epitope restriction data generated by virtue of epitope prediction tools

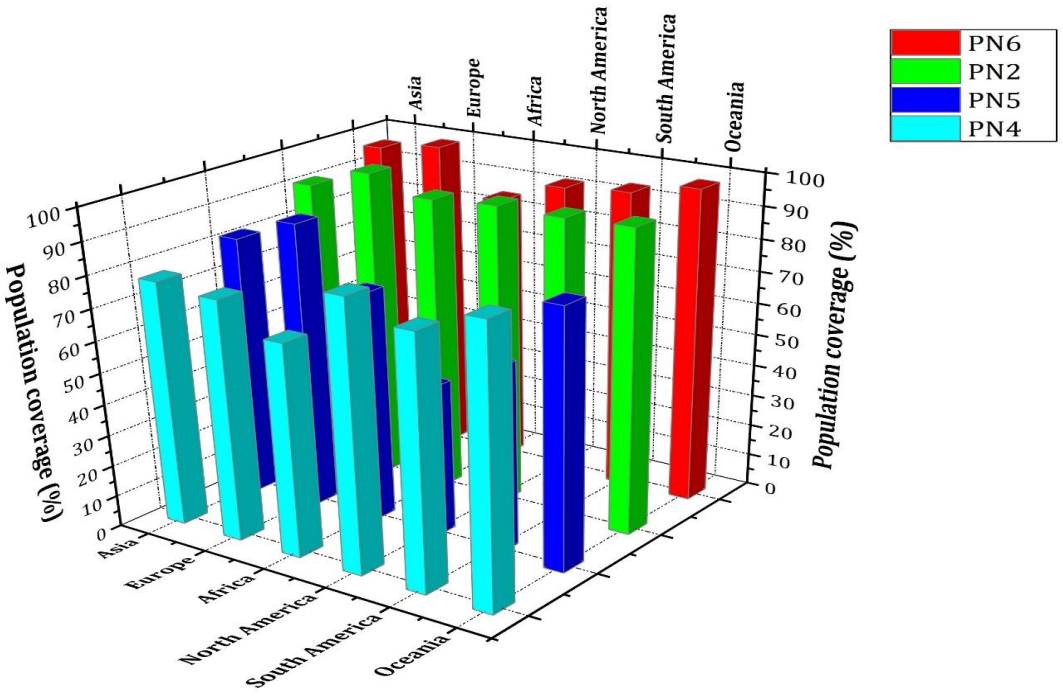

Figure 4.2.10. **Population coverage analysis of NA peptides**. Human populations residing in different continents were screened to assess the expected immunogenic response of predicted NA peptides by IEDB population coverage analysis tool using HLA-epitope restriction data generated by virtue of epitope prediction tools

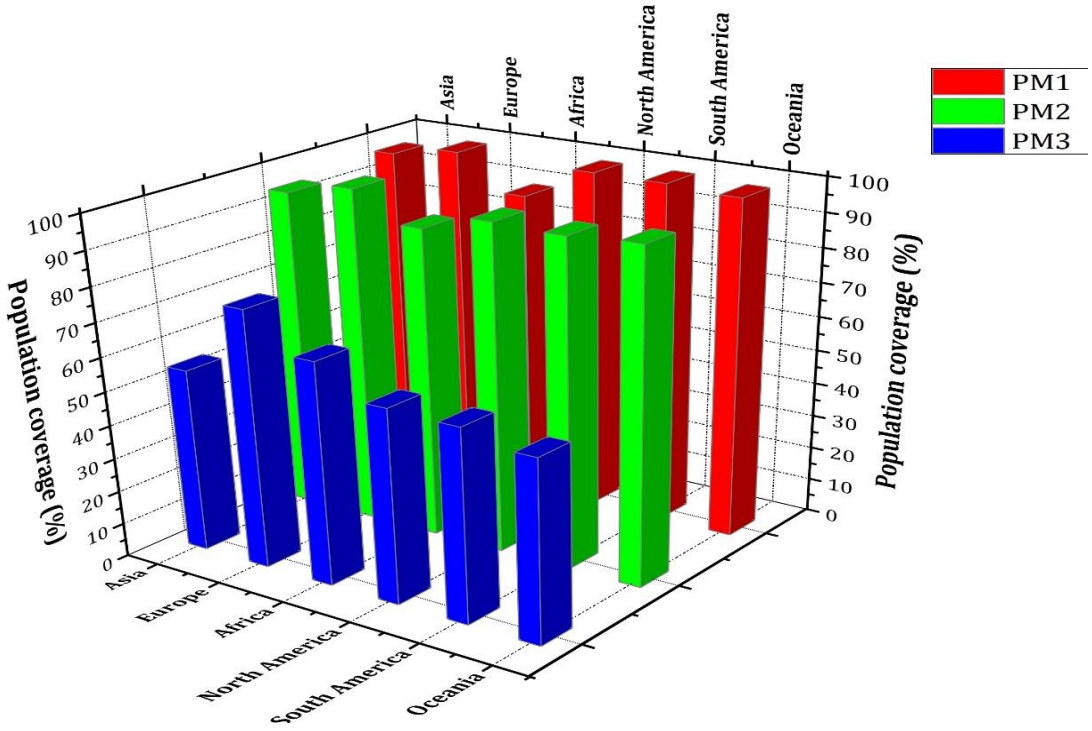

Figure 4.2.11. **Population coverage analysis of M1 peptide.** Human populations residing in different continents were screened to assess the expected immunogenic response of predicted M1 peptides by IEDB population coverage analysis tool using HLA-epitope restriction data generated by virtue of epitope prediction tools

4.3 Assessment of potential of peptide to stimulate T cell proliferation in peripheral blood mononuclear cells (PBMC) culture

Peptides containing multiple T cell epitopes identified by means of epitope prediction were commercially synthesised. Nine peptides were commercially synthesised out of the ten selected peptides. Peptide P_H3 could not be synthesised with desired purity level (in two different attempts), so was not be evaluated for immunogenic response.

In order to measure the peptide induced proliferation, peripheral blood mononuclear cells (PBMC) isolated from the blood samples of healthy volunteers were given repeated peptide stimulus and MTT assay was carried out to assess the proliferation of peptide stimulated PBMC. Concanavalin A (con A) was used as positive control, whereas unstimulated cells served as negative control.

4.3.1. Optimization of MTT assay to measure the PBMC proliferation

PBMC were stimulated with 5 µg/ml of con A in triplicates and proliferation was measured at day 2, 3 and 4. Proliferation was expressed as stimulation index (SI) which

is the ratio of absorbance of the con A stimulated cell and unstimulated cells. It was observed that SI increased with time (Figure 4.3.1a, page 86). After 4 days incubation SI recorded was quite low (SI=1.63). Hence, incubation time was increased upto 6 days. Cell proliferation showed a gradual increase and after 6 days pronounced proliferation was observed (SI=5.5) in Con A stimulated cells (Figure 4.3.1b, page 86). Hence, for further experiments on peptide induced proliferation, the minimum time of incubation was fixed to 6 days.

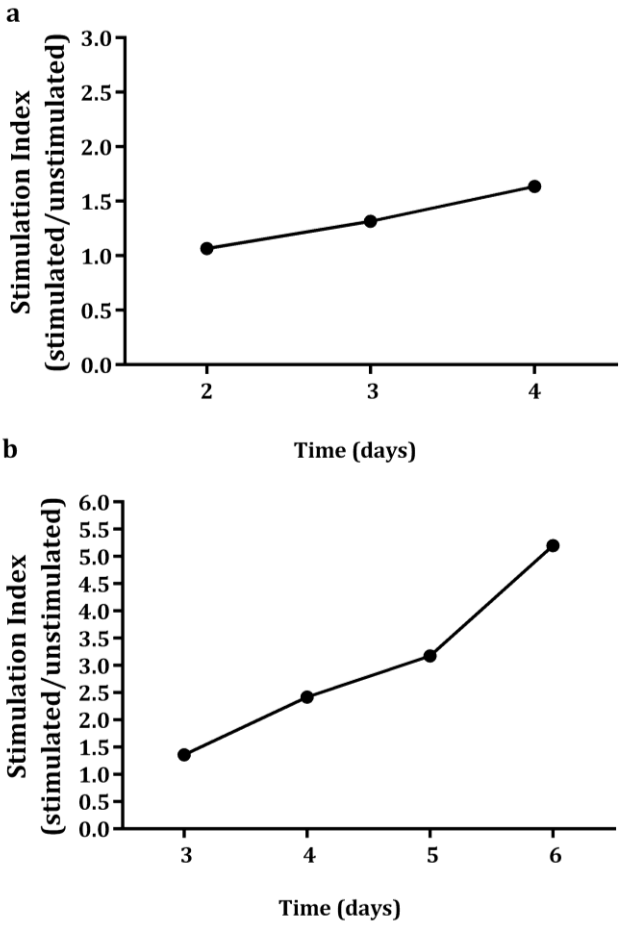

Figure 4.3.1. Concanavalin A induced PBMC proliferation. PBMC isolated from the healthy blood samples, and distributed in two set of triplicates in 96 well plate at $1x10^5$ cells per well. One set was stimulated with Concanavalin A (5 µg/ml) and other set of unstimulated cells served as negative control. Resultant proliferation was measured by MTT assay at (a) day 2, 3 and 4 (b) day 3, 4, 5 and 6. Stimulation index (SI) is the ratio of average absorbance of the peptide stimulated cells and unstimulated cells measured at 570/630 nm.

4.3.2. Peptide induced PBMC proliferation

Peptide stimulation assay was carried to measure the peptide induced proliferation in PBMC. Peptide stimulation assay is initiated in 24 well flat bottom cell culture plate with

$2x10^6$ cells per well (day 1). Since the viability of PBMC is low under *in vitro* conditions (they lack inherent capacity to divide on their own) thus large cell count of PBMC was taken initially in 24 well culture plate, so that considerable amount of viable and peptide activated cells can be obtained at the end of day 10, before they are transferred to 96 well cell culture plate for last stimulation. During this 10 days incubation in 24 well plate, cells were stimulated on day 1, 4 and 7. After 10 days, cells were recounted and seeded again in triplicates in 96 well plate at $1x10^5$ cells per well. Six days after the fourth and last peptide stimulation, proliferation was measured.

Detecting the presence of immunogen-reactive T lymphocytes *in vitro* is difficult by assaying antigen induced proliferation of cells. This difficulty could be attributed to number of facts viz. presence of very small number of reactive cells, state of anergy or the influence of regulatory T cells, in appropriate antigen presentation, sub-optimal culture conditions. IL-2 has the ability to interact with and augment division of those lymphocytes which are activated by antigen recognition. Activated cells express high affinity IL-2 receptors and proliferate in presence of IL-2 cytokine. Although other cytokines can also be used for this purpose, but IL-2 is readily available with the desired attributes (Kennell et al., 2014). Many studies have demonstrated the use of IL-2 in the establishment of peptide antigen specific T cells (Alizadeh et al., 2003; Choo et al., 2014; Smith et al., 2015; Wullner et al., 2010). Hence, the culture was supplemented with IL-2 along with peptide during each stimulation.

Experiments were carried with different peptides and con A in few healthy samples to seek consistency of the result. It was observed that the proliferation results are substantial as well as consistent with the different PBMC samples (Figure 4.3.2, page 87). Samples showing stimulation index >1 were considered to be positive responders.

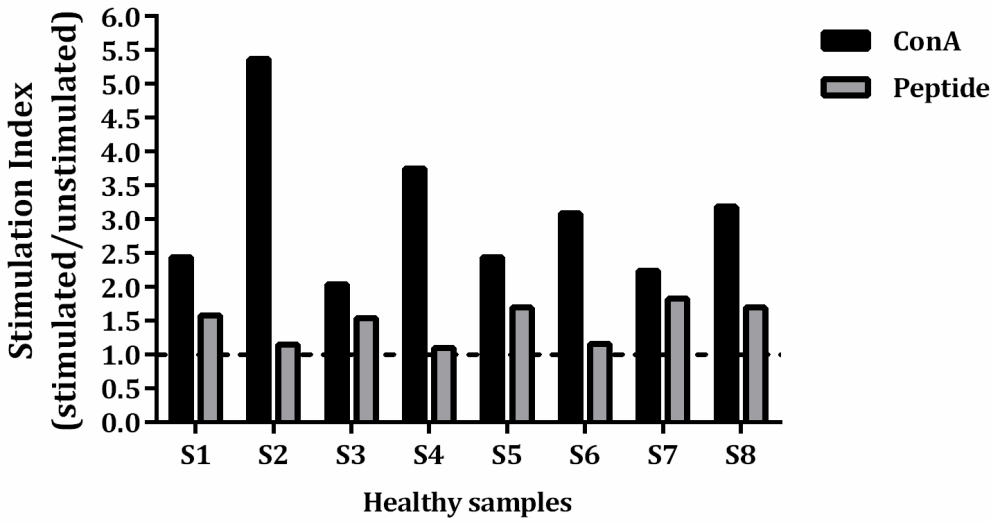

Figure 4.3.2. Con A and peptide induced proliferation of different PBMC samples. 2×10^6 cells/well were stimulated with peptide (25μg/ml) in the presence of rIL-2 (20 ng/mL) and complete RPMI-1640 in a 24 well cell culture plate, along with some wells containing unstimulated cells. The PBMC culture was re-stimulated with peptide and rIL-2 by replacing 1 ml of fresh media at days 4 and 7. On 10th day, peptide stimulated and unstimulated cells were harvested, recounted. Unstimulated cells were distributed in two set of triplicates; one set stimulated with 10 μg/mL of con A (positive control), whereas the other set having the unstimulated cells (negative control). Peptide stimulated cells distributed in triplicates were given final stimulus with 25 μg/mL peptide in the presence of rIL-2 (20 ng/ml). At the end of 16th day, proliferation was measured by MTT assay. Stimulation index (SI) is the ratio of average absorbance of the peptide stimulated cells and unstimulated cells measured at 570/630 nm.

4.3.2.1. Hemagglutinin peptide induced PBMC proliferation

Two hemagglutinin peptides P_H1 and P_H4 were assessed for peptide induced proliferation of PBMC obtained from seven different blood samples. Six out of seven samples responded positively on P_H1 stimulation, whereas five samples responded positively against P_H4 peptide (Figure 4.3.3a and b, page 88). Statistical analysis of the positive responders revealed that significant proliferation was observed in four samples each for P_H1 and P_H4 respectively as compared to the unstimulated cells. Except one or two PBMC samples, all the samples have shown good proliferative response to P_H1 and P_H4 stimulation indicating strong immunogenic potential of these peptides (Figure 4.3.3 a and b, page 88). An average stimulation index (SI) of positive responders equal to 1.50 ± 0.32 and 1.52 ± 0.45 for P_H1 and P_H4 respectively (Table 4.3.1, page 92).

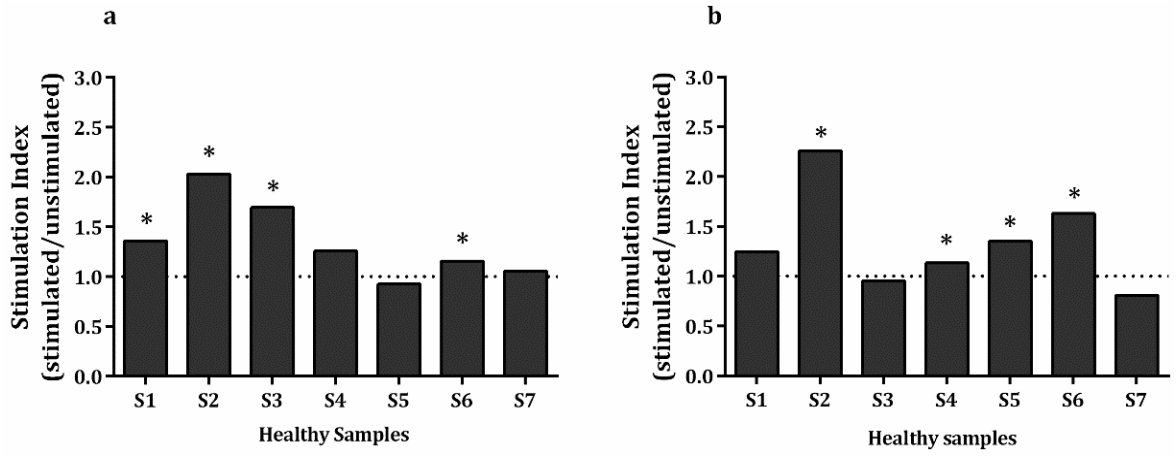

Figure 4.3.3. Hemagglutinin peptides induced PBMC proliferation. (a) P_H1 and (b) P_H4. 2×10^6 cells/well were stimulated with peptide (25µg/ml) in the presence of rIL-2 (20 ng/mL) and complete RPMI-1640 in a 24 well cell culture plate, along with some wells containing unstimulated cells. The culture was re-stimulated with peptide and rIL-2 at days 4 and 7. On 10th day, peptide stimulated and unstimulated cells were harvested, recounted. Unstimulated cells were distributed in two set of triplicates; one set stimulated with 10 µg/mL of con A (positive control), whereas the other set having the unstimulated cells (negative control). Peptide stimulated cells distributed in triplicates were given final stimulus with 25 µg/mL peptide in the presence of IL-2 (20 ng/ml). At the end of 16th day, proliferation was measured by MTT assay. Stimulation index (SI) is the ratio of average absorbance of the peptide stimulated cells and unstimulated cells measured at 570/630 nm. Statistical significant differences of the mean values between unstimulated vs. peptide stimulated cells were assessed by unpaired Student's t – test, as indicated by * ($P<0.05$).

4.3.2.2. Neuraminidase peptide induced PBMC proliferation

Four peptides of NA (P_N2, P_N4, P_N5 and P_N6) were tested for their immunogenic potential in different PBMC samples and stimulation index were calculated to analyse the response of these peptides. Proliferative response of P_N2 was assessed in six heathy samples while rest of the peptides were tested in seven samples. NA peptides induced variable response in different PBMC samples. P_N6 was found to be best among all the four peptides as all seven samples tested have shown proliferation, with six samples showing significant response (Figure 4.3.4d, page 89). P_N5 also demonstrated a good immunogenic potential in six samples out of which four significant responders (Figure 4.3.4c, page 89). Average SI of positive responders was 1.31 ± 01.8 and 1.28 ± 0.04 in P_N6 and P_N5 respectively (Table 4.3.1, page 92). Only two significant responders were observed among the three samples showing positive response in P_N4 (Figure 4.3.4b, page 89) with average of SI of responders equal to 1.14 ± 0.09 which indicated that P_N4 served as a weak immunogenic

stimulus. It was evident that the PBMC proliferation response induced against P_N2 was better as compared to P_N4. It has shown positive response in four samples with three showing significant proliferation (Figure 4.3.4a, page 89) with average SI of 1.65 ± 0.63 (Table 4.3.1, page 92).

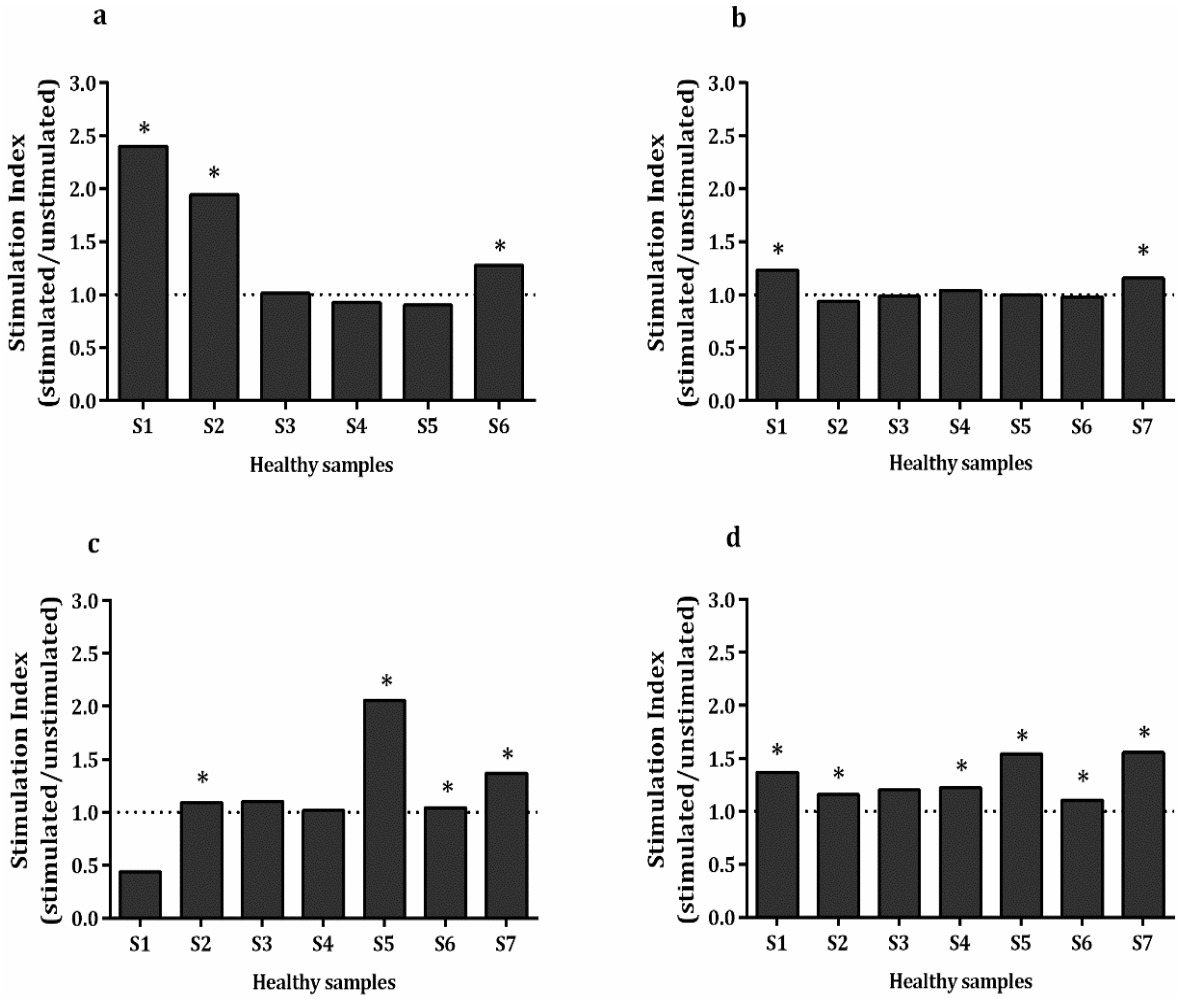

Figure 4.3.4. Neuraminidase peptides induced PBMC proliferation. (a) P_N2 (b) P_N4 (c) P_N5 and (d) P_N6. 2×10^6 cells/well were stimulated with peptide (25µg/ml) in the presence of rIL-2 (20 ng/mL) and complete RPMI-1640 in a 24 well cell culture plate, along with some wells containing unstimulated cells. The PBMC culture was re-stimulated with peptide and rIL-2 by replacing 1 ml of fresh media at days 4 and 7. On 10th day, peptide stimulated and unstimulated cells were harvested, recounted. Unstimulated cells were distributed in two set of triplicates; one set stimulated with 10 µg/mL of con A (positive control), whereas the other set having the unstimulated cells (negative control). Peptide stimulated cells distributed in triplicates were given final stimulus with 25 µg/mL peptide in the presence of IL-2 (20 ng/ml). At the end of 16th day, proliferation was measured by MTT assay. Stimulation index (SI) is the ratio of average absorbance of the peptide stimulated cells and unstimulated cells measured at 570/630 nm. Statistical significant differences of the mean values between unstimulated vs. peptide stimulated cells were assessed by unpaired Student's t – test, as indicated by * ($P<0.05$).

4.3.2.3. Matrix 1 peptide induced PBMC proliferation

Two peptides P_M1 and P_M2 of M1 protein were analysed in seven healthy PBMC samples while P_M3 in six samples. All the seven samples showed significant proliferative response on P_M1 stimulation with average SI of 2.17 ± 0.86 (Figure 4.3.5a, page 90). Similarly, the number of positive responders observed as a result of P_M2 stimulation were seven with six showing significant proliferation with average SI of 1.56 ± 0.60 (Figure 4.3.5 b, page 90). Thus it was evident that P_M1 and P_M2 peptides exhibited strongest immune response. All four positive responders against P_M3 peptide displayed significant proliferation as compared to the unstimulated cells with average SI of 1.58 ± 0.19 (Figure 4.3.5c, page 90).

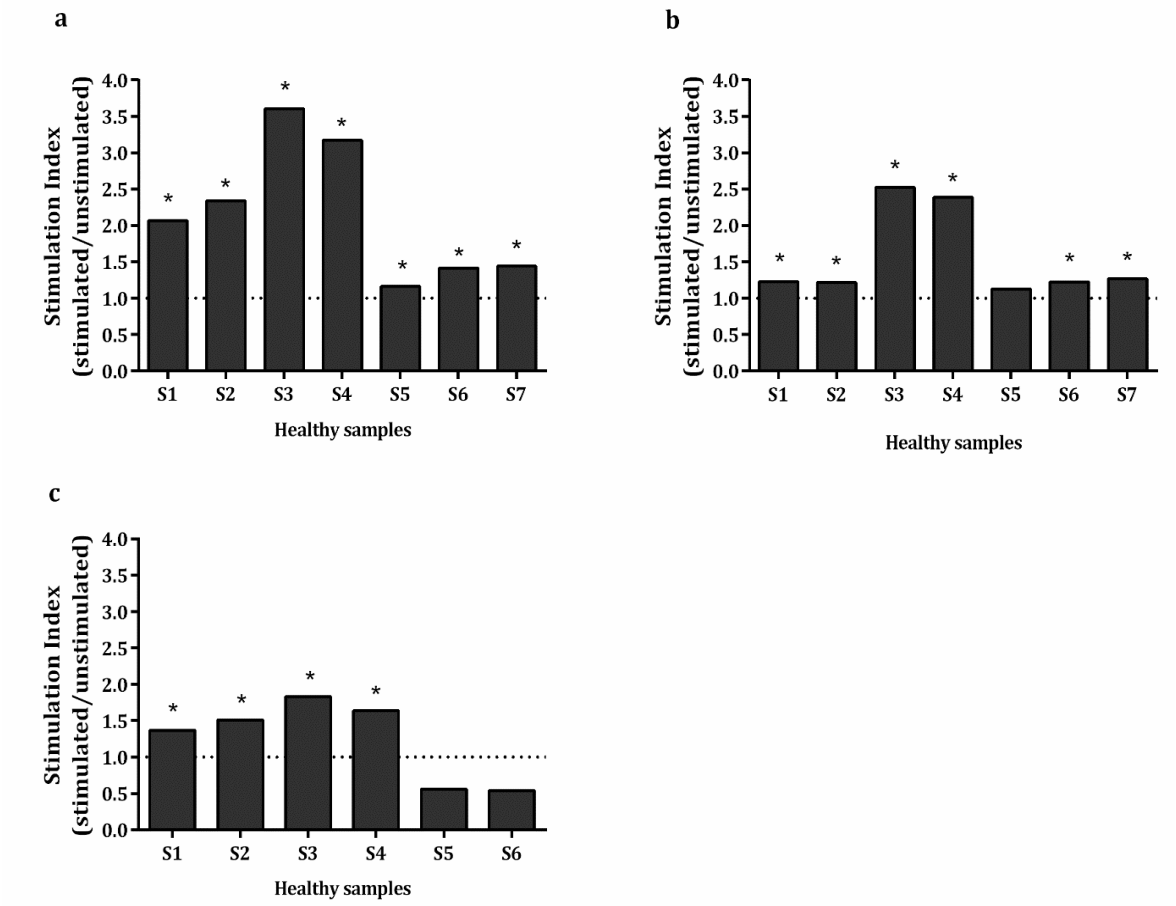

Figure 4.3.5. Matrix 1 peptides induced PBMC proliferation. (a) P_M1 (b) P_M2 and (c) P_M3. 2×10^6 cells/well were stimulated with peptide (25µg/ml) in the presence of rIL-2 (20 ng/mL) and complete RPMI-1640 in a 24 well cell culture plate, along with some wells containing unstimulated cells. The PBMC culture was re-stimulated with peptide and IL-2 by replacing 1 ml of fresh media at days 4 and 7. On 10th day, peptide stimulated and unstimulated cells were harvested, recounted. Unstimulated cells were distributed in two set of triplicates; one set stimulated with 10 µg/mL of con A (positive control), whereas the other set having the unstimulated cells (negative control). Peptide stimulated cells distributed in triplicates were given final stimulus with 25 µg/mL peptide in the presence of IL-2 (20 ng/ml). At the end of 16th

day, proliferation was measured by MTT assay. Stimulation index (SI) is the ratio of average absorbance of the peptide stimulated cells and unstimulated cells measured at 570/630 nm. Statistical significant differences of the mean values between unstimulated vs. peptide stimulated cells were assessed by unpaired Student's t – test, as indicated by * ($P<0.05$).

4.3.2.4. Variable proliferative response was elicited by different peptides of HA, NA and M1 protein

Variable positive responses were observed in different peptides of HA, NA and M1 protein. Matrix 1 peptides manifested the highest proliferative potential among all the peptides considered in this study (Figure 4.3.6, page 91, Table 4.3.1, page 92). Although, HA peptides also elicited good immunogenic response. Two peptides of NA (P_N2 and P_N4) displayed relatively weak proliferative potential as compared to P_N5 and P_N6.

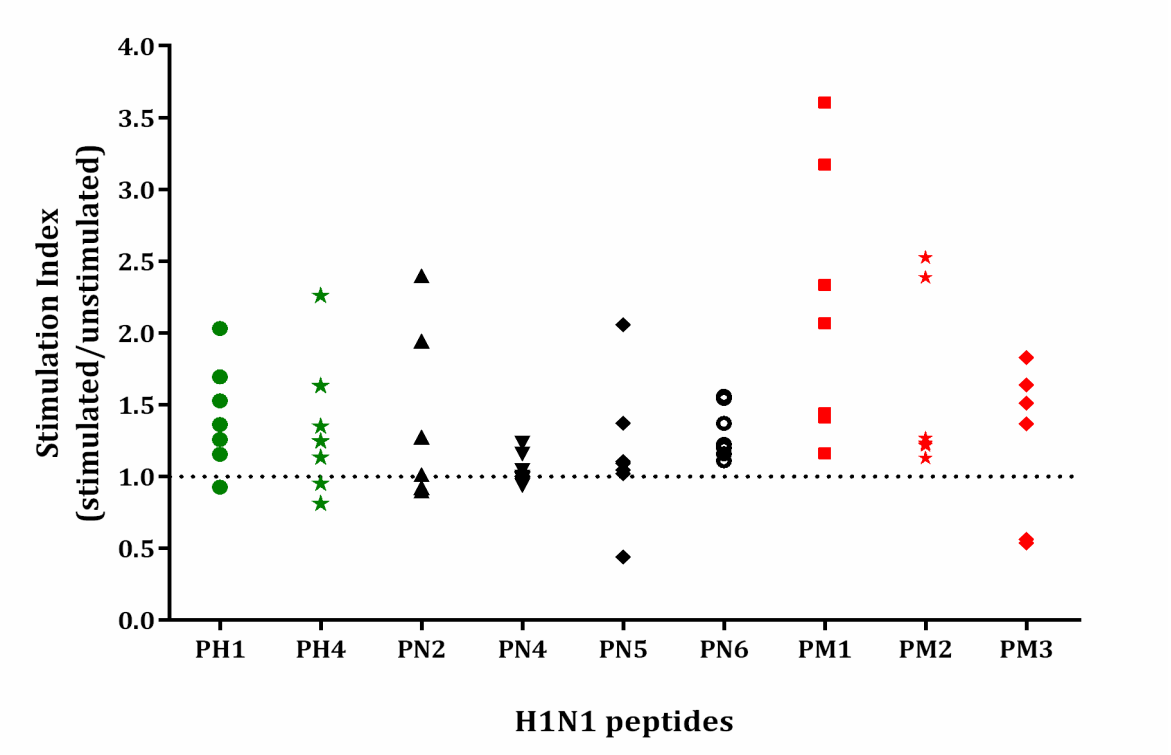

Figure 4.3.6. PBMC proliferation induced by all the nine H1N1 influenza peptides. PBMC were stimulated with peptide on day 1, 4, 7 and 10 in the presence of rIL-2. Unstimulated cells cultured in presence of rIL-2, served as negative control. Proliferation was determined following multiple stimulation at the end of day 16 by MTT assay. Stimulation index (SI) is the ratio of average absorbance of the peptide stimulated cells and unstimulated cells measured at 570/630 nm. Each color represent peptides belonging to a particular protein (hemagglutinin peptides depicted in green; neuraminidase peptides depicted in black; matrix 1 peptides depicted in red), whereas each point represents the healthy PBMC samples screened for proliferation induced by each peptide.

Table 4.3.1. Positive responders of selected nine peptides H1N1 influenza virus along with average stimulation index of responders

Peptide	Sequence	No. of sample	Positive Responders (significant responder*)	Average Stimulation index of the responders (mean± SD)
P_H1	STDTVDTVLEKNVTVTHSVNLL	7	6 ($4^{*)}$	1.50 ± 0.32
P_H4	KVNSVIEKMNTQFTAVGKEF	7	5 (4^{*})	1.52 ± 0.45
P_N2	IRIGSKGDVFVIREPFIS	6	4 (3^{*})	1.65 ± 0.63
P_N4	WHGSNRPWVSF	7	3 (2^{*})	1.14 ± 0.09
P_N5	GSFVQHPELTGL	7	6 (4^{*})	1.28 ± 0.04
P_N6	TIWTSGSSISFCGVNSD	7	7 (6^{*})	1.31 ± 0.18
P_M1	ILGFVFTLTVPSERGLQRRRF	7	7 (7^{*})	2.17 ± 0.86
P_M2	LIRHENRMVLASTTAKA	7	7 (6^{*})	1.56 ± 0.60
P_M3	LQAYQKRMGVQMQR	6	4 (4^{*})	1.58 ± 0.19

* Statistical significant at $p<0.05$

4.4 Determination of immune response of these predicted peptides based on cytokines production/expression in PBMC culture

Among the T cells, $CD8^+$ T cells as well as $CD4^+$ T cells (specifically Th1 cells) produce IFN-γ as a result of infection. An essential attribute of a vaccine development is better immunologic memory which could result in sustained T-cell immunity after healing of live infections. IFN-γ production by Th1 cells is the signature of recruitment of $CD4^+$ cells to impart long term immunity (Agallou et al., 2014). In most of the studies, peptide specific effector T cell responses was measured based on IFN-γ production (Francis et al., 2015; Moutaftsi et al., 2006; Smith et al., 2015). Hence, in the present study, sandwich ELISA was carried to measure the IFN-γ production in culture supernatant. PBMC were stimulated with peptide on day 1, 4, 7 and 10 and at the end of 12^{th} day, culture supernatant was collected and tested for the presence of IFN-γ by ELISA. Concanavalin A

(con A) was used as positive control, whereas unstimulated cells served as negative control.

4.4.1. Optimisation of supernatant collection time to measure IFN-γ by ELISA

After the last peptide stimulation on day 10, culture supernatant of the peptide stimulated cells, con A stimulated cells (positive control) and unstimulated cells (negative control) was collected in triplicates after 24, 48 and 76 h to measure extracellularly secreted IFN-γ level (Figure 4.4.1, page 93). In case of peptide stimulated cells, maximum extracellular IFN-γ secretion was recorded after 48 h. Hence for further experimentation, IFN-γ secretion was measured after 48 h of last peptide stimulation (day 12).

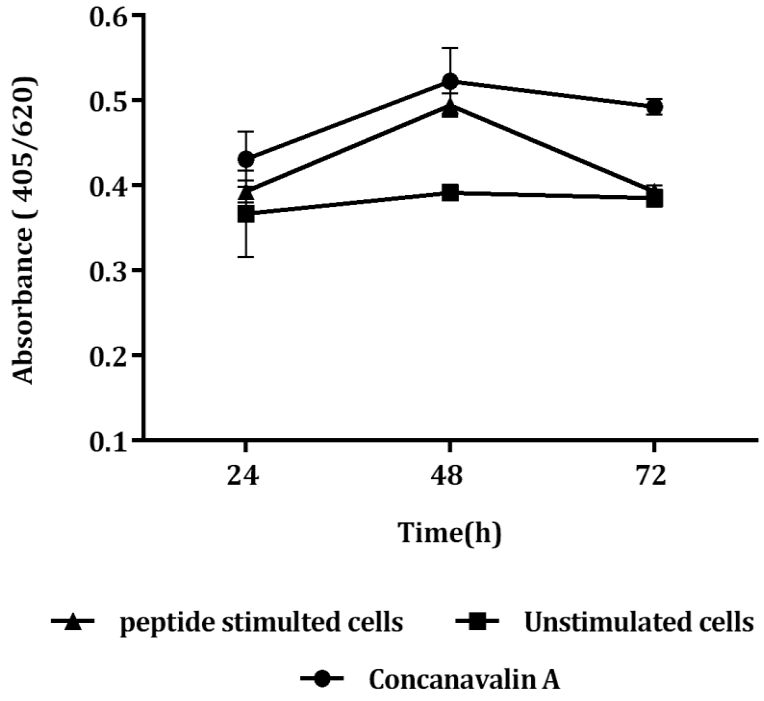

Figure 4.4.1. Con A and peptide induced IFN-γ secretion by PBMC at different time intervals. 2×10^6 cells/well were stimulated with peptide (25µg/ml) in the presence of rIL-2 (20 ng/mL) and complete RPMI-1640 in a 24 well cell culture plate, along with some wells containing unstimulated cells. The PBMC culture was re-stimulated with peptide and IL-2 by replacing 1 ml of fresh media at days 4 and 7. On 10th day, peptide stimulated and unstimulated cells were harvested, recounted. Unstimulated cells were distributed in two set of triplicates; one set stimulated with 10 µg/mL of con A (positive control), whereas the other set having the unstimulated cells (negative control). Peptide stimulated cells distributed in triplicates were given final stimulus with 25 µg/mL peptide in the presence of IL-2 (20 ng/ml). Culture supernatant was collected at the end of 11^{th}, 12^{th} and 13^{th} day (24h, 48h and 72h post final stimulation) for IFN-γ measurement by ELISA.

4.4.2 Peptide induced IFN-γ secretion

IFN-γ measurements were carried with different peptides and con A in few healthy samples to check consistency of results. It was observed that the *in vitro* IFN-γ secretion was substantial as well as consistent with the different PBMC samples (Figure 4.4.2, page 94). Increase in IFN-γ secretion in response to con A and peptide stimulus was expressed as fold increase (ratio of absorbance of peptide stimulated cells and unstimulated cells). Samples displaying fold increase >1 were considered as positive responders. Most of the samples displayed large IFN-γ secretion with con A, although the fold increase in IFN-γ secretion varied from 4 to 9 times. Most of the peptides were screened for seven healthy blood samples, except P_N2 and P_M3 (six samples each).

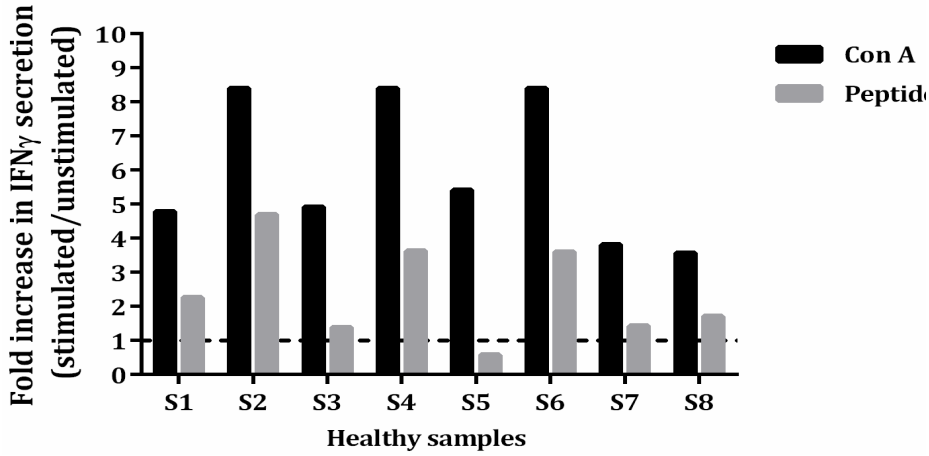

Figure 4.4.2. Con A and peptide induced IFN-γ secretion by PBMC. 2×10^6 cells/well were stimulated with peptide (25μg/ml) in the presence of rIL-2 (20 ng/mL) and complete RPMI-1640 in a 24 well cell culture plate, along with some wells containing unstimulated cells. The PBMC culture was re-stimulated with peptide and IL-2 by replacing 1 ml of fresh media at days 4 and 7. On 10th day, peptide stimulated and unstimulated cells were harvested, recounted. Unstimulated cells were distributed in two set of triplicates; one set stimulated with 10 μg/mL of con A (positive control), whereas the other set having the unstimulated cells (negative control). Peptide stimulated cells distributed in triplicates were given final stimulus with 25 μg/mL peptide in the presence of IL-2 (20 ng/ml). Culture supernatant was collected at the end of 12th day (48h post final stimulation) for IFN-γ measurement by ELISA. Fold change is the ratio of average absorbance of the peptide stimulated cells and unstimulated cells at 405/620 nm.

4.4.2.1 Hemagglutinin peptides induced IFN-γ secretion by PBMC

P_H1 and P_H4 have shown good IFN-γ secretion as compared to the unstimulated cells (Figure 4.4.3, page 94). Average fold increase of 2.20 ± 0.38 and 1.74 ± 1.31 in the level of extracellular IFN-γ was observed respectively for P_H1 and P_H4. All the samples stimulated

with P_H1 have shown significantly high IFN-γ production relative to controls, whereas five samples have shown significant IFN-γ production when stimulated with P_H4 peptide (Figure 4.4.3, page 94). However, it is noteworthy that all seven samples tested for P_H1 and P_H4 induced IFN-γ secretion have shown positive response.

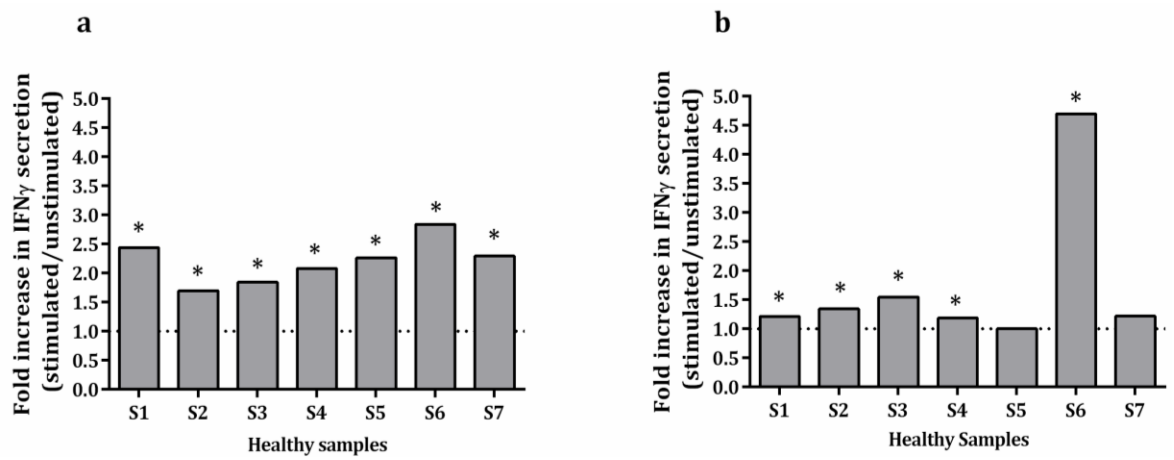

Figure 4.4.3. Hemagglutinin peptide induced IFN-γ production (a) P_H1 and (b) P_H4. 2×10^6 cells/well were stimulated with HA peptides (25µg/ml) in the presence of rIL-2 (20 ng/mL) and complete RPMI-1640 in a 24 well cell culture plate, along with some wells containing unstimulated cells. The PBMC culture was re-stimulated with peptide and rIL-2 by replacing 1 ml of fresh media at days 4 and 7. On 10th day, peptide stimulated and unstimulated cells were harvested, recounted. Unstimulated cells were distributed in two set of triplicates; one set stimulated with 10 µg/mL of con A (positive control), whereas the other set having the unstimulated cells (negative control). Peptide stimulated cells distributed in triplicates were given final stimulus with 25 µg/mL peptide in the presence of rIL-2 (20 ng/ml). Culture supernatant was collected at the end of 12th day (48h post final stimulation) for IFNγ measurement by ELISA. Fold change is the ratio of average absorbance of the peptide stimulated cells and unstimulated cells at 405/620 nm. Statistical significant differences of the mean values between unstimulated vs. peptide stimulated cells were assessed by unpaired Student's t –test, as indicated by * ($P<0.05$).

4.4.2.2. Neuraminidase peptides induced IFN-γ secretion by PBMC

Neuraminidase peptides stimulated samples have responded variedly towards IFN-γ production (Figure 4.4.4, page 95) and it appears that the response is relatively weaker in term of number of positive responders. Peptide P_N2 and P_N5 have shown IFN-γ secretion in average number of samples (3 and 4 samples respectively). Three samples have shown significant increase in IFN-γ level on stimulation with P_N2 and P_N5 (Figure 4.4.4 a, c, page 95). Average fold increase in IFN-γ production observed in case of P_N2 and P_N5 was 1.52 ± 0.58 and 1.45 ± 0.26 respectively. In other two peptides (P_N4 and P_N6),

the number of positive responders were less than 50% of the samples tested. Only one sample has shown significantly high IFN-γ production out of three positive responders after P_N6 stimulation, whereas both the positive responders have shown significant response after P_N4 stimulation (Figure 4.4.4 a, c, page 95). Average fold increase in IFN-γ production was observed in case of P_N4 (2.87 ± 1.06) and P_N6 (2.05 ± 1.34).

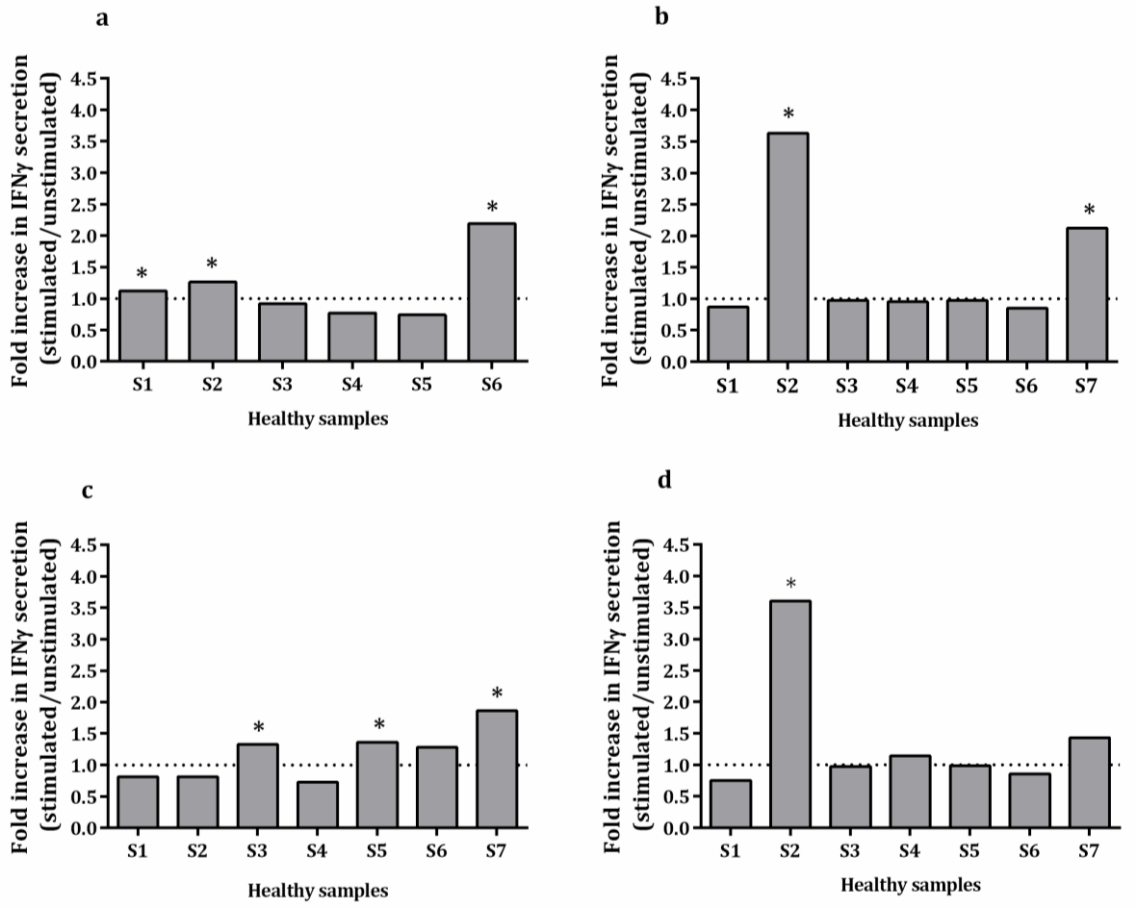

Figure 4.4.4. Neuraminidase peptides induced IFN-γ production (a) P_N2 (b) P_N4 (c) P_N5 and (d) P_N6. 2×10^6 cells/well were stimulated with NA peptides (25μg/ml) in the presence of rIL-2 (20 ng/mL) and complete RPMI-1640 in a 24 well cell culture plate, along with some wells containing unstimulated cells. The PBMC culture was re-stimulated with peptide and rIL-2 by replacing 1 ml of fresh media at days 4 and 7. On 10th day, peptide stimulated and unstimulated cells were harvested, recounted. Unstimulated cells were distributed in two set of triplicates; one set stimulated with 10 μg/mL of con A (positive control), whereas the other set having the unstimulated cells (negative control). Peptide stimulated cells distributed in triplicates were given final stimulus with 25 μg/mL peptide in the presence of IL-2 (20 ng/ml). Culture supernatant was collected at the end of 12th day (48h post final stimulation) for IFNγ measurement by ELISA. Fold change is the ratio of average absorbance of the peptide stimulated cells and unstimulated cells at 405/620 nm. Statistical significant differences of the mean values between unstimulated vs. peptide stimulated cells were assessed by unpaired Student's t –test, as indicated by * ($P<0.05$).

4.4.2.3. Matrix 1 peptides induced IFN-γ secretion by PBMC

Among the matrix 1 peptides, P_M3 has shown IFN-γ production in all the six samples with significantly high production in five samples (Figure 4.4.5c, page 96). Average fold increase in IFNγ production recorded after P_M3 stimulation was 2.46 ± 0.61. P_M1 and P_M2 have shown average fold increase of 1.80 ± 0.37 and 1.44 ± 0.42 respectively. Out of the seven samples screened, three positive responders have shown significant IFN-γ production in case of P_M1 (Figure 4.4.5a, page 96), on the other hand four out five positive responders showed significantly high secretion of the cytokine on stimulation with P_M2 (Figure 4.4.5b, page 96). P_M3 displayed best immunogenicity among the three matrix 1 peptides (Figure 4.4.5c, page 96).

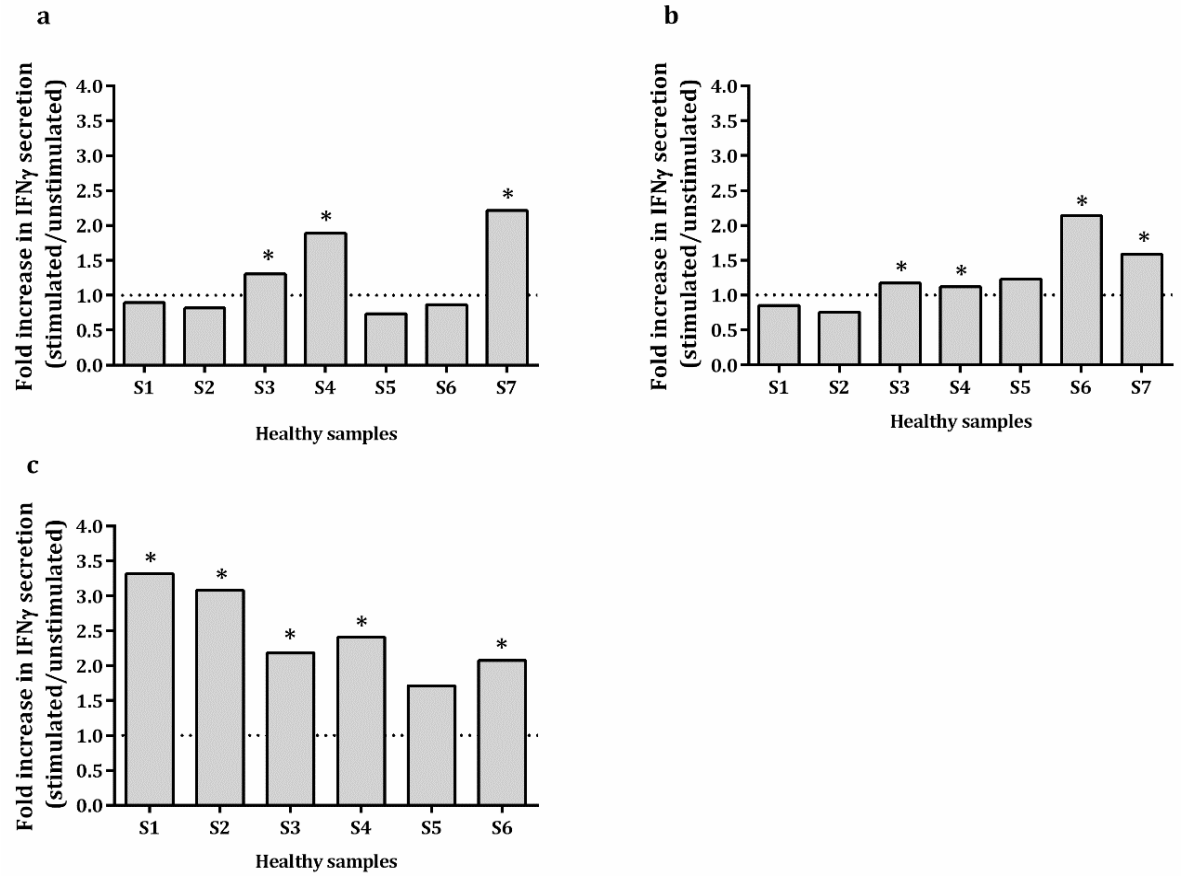

Figure 4.4.5. Matrix 1 peptides induced IFN-γ production. (a) P_M1 (b) P_M2 and (c) P_M3. 2×10^6 cells/well were stimulated with M1 peptides (25μg/ml) in the presence of rIL-2 (20 ng/mL) and complete RPMI-1640 in a 24 well cell culture plate, along with some wells containing unstimulated cells at. The PBMC culture was re-stimulated with peptide and IL-2 by replacing 1 ml of fresh media at days 4 and 7. On 10th day, peptide stimulated and unstimulated cells were harvested, recounted. Unstimulated cells were distributed in two set of triplicates; one set stimulated with 10 μg/mL of con A (positive control), whereas the other set having the unstimulated cells (negative control). Peptide stimulated cells distributed in triplicates were given final stimulus with 25 μg/mL peptide in the presence of IL-2 (20 ng/ml). Culture

supernatant was collected at the end of 12th day (48h post final stimulation) for IFN-γ measurement by ELISA. Fold change is the ratio of average absorbance of the peptide stimulated cells and unstimulated cells at 405/620 nm. Statistical significant differences of the mean values between unstimulated vs. peptide stimulated cells were assessed by unpaired Student's t –test, as indicated by * (P<0.05).

4.4.2.4. Comparison between IFN-γ secretions induced by of HA, NA and M1 peptides

IFN-γ secretions were found to vary in the selected peptides of HA, NA and M1 protein (Figure 4.4.6, page 97). Both peptides of HA have shown high IFN-γ production thus these HA peptides may exhibit strong immunogenicity (Table 4.4.1, page 98). P_M3 peptide of M1 protein acted as strong immunogen by stimulating IFN-γ secretion in all six samples which have shown high IFN-γ secretion. P_M2 showed moderate immunogenic response in five positive responders. NA peptides were found to be the weakest immunogens as number of positive responders observed was small (≤ 3). The same kind of variation was observed in PBMC induced proliferation of these peptides. Variable response was observed for each blood samples (healthy donor) in terms of proliferation and IFN-γ release towards influenza peptides of HA, NA and M1 protein (Appendix A, B and C).

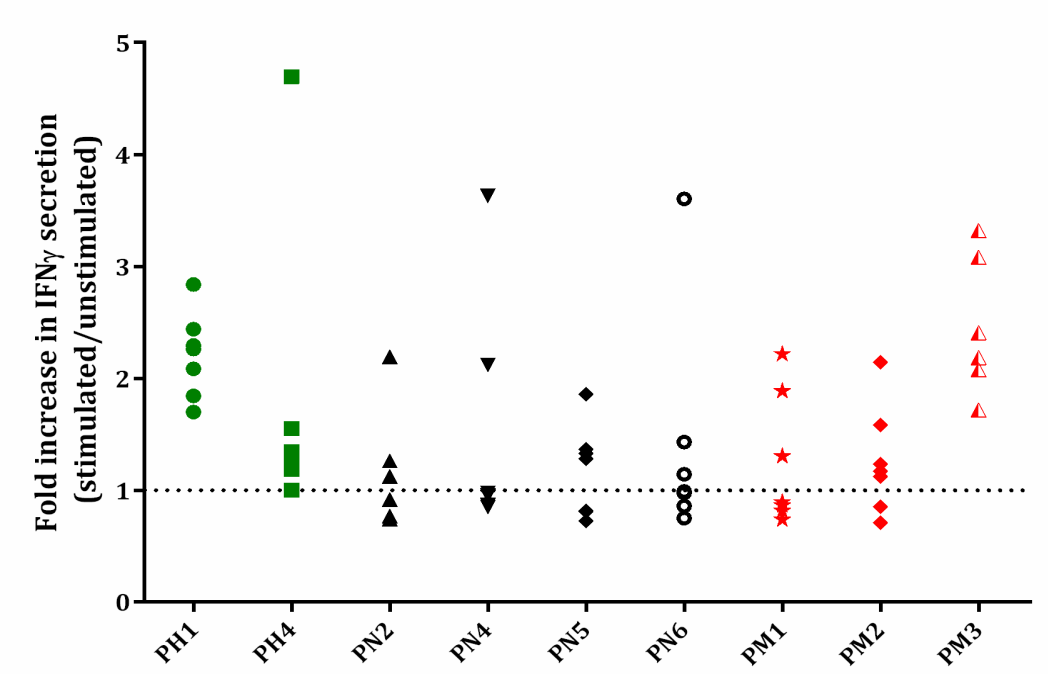

Figure 4.4.6. IFN-γ secretion of all the nine H1N1 influenza peptides. PBMC were stimulated with peptide on day 1, 4, 7 and 10 in the presence of rIL-2. Unstimulated cells cultured in presence of rIL-2, served as negative control. IFN-γ was determined following multiple stimulation at the end of day 12 by ELISA. Fold change is the ratio of average absorbance of the peptide stimulated cells and unstimulated cells measured at 405/620 nm. Each color represent peptides belonging to a particular protein (hemagglutinin peptides depicted in green; neuraminidase peptides

depicted in black; matrix 1 peptides depicted in red), whereas each point represents the healthy PBMC samples screened for peptide induced IFN-γ.

Table 4.4.1. Positive responders of selected nine peptides H1N1 influenza virus along with average fold increase in IFN-γ secretion

Peptide	**Sequence**	**No. of sample**	**Positive responders (significant responder*)**	**Average fold increase in IFN-γ secretion of the positive responders (mean ± SD)**
P_H1	STDTVDTVLEKNVTVTHSVNLL	7	7 (7*)	2.20 ± 0.38
P_H4	KVNSVIEKMNTQFTAVGKEF	7	7 (5*)	1.74 ± 1.31
P_N2	IRIGSKGDVFVIREPFIS	6	3 (3*)	1.52 ± 0.58
P_N4	WHGSNRPWVSF	7	2 (2*)	2.87 ± 1.06
P_N5	GSFVQHPELTGL	7	4(3*)	1.45 ± 0.26
P_N6	TIWTSGSSISFCGVNSD	7	3 (1*)	2.05 ± 1.34
P_M1	ILGFVFTLTVPSERGLQRRRF	7	3(3*)	1.80 ± 0.37
P_M2	LIRHENRMVLASTTAKA	7	5 (4*)	1.44 ± 0.42
P_M3	LQAYQKRMGVQMQR	6	6 (5*)	2.46 ± 0.61

Chapter 5: Discussion

Antigenic variations impede the development of a universal or broadly reactive influenza vaccine. The protection conferred by the current strain-specific influenza vaccines is IgG mediated, which fails to neutralize the mutant or heterosubtypic influenza virus. This drawback of current influenza vaccine strategy has spurred the development of an alternative approach effective in imparting cross protective immunity against range of influenza virus. T cell mediated immune response to counter influenza A virus infection has been well characterized in humans (La Gruta & Turner, 2014; Sun & Braciale, 2013). Substantial evidence from various animal and human studies suggests that T cells, specifically $CD8^+$ T cells (CTL), are positive correlates of cross-subtype immunity during secondary influenza A virus infection (Duan & Thomas, 2016). $CD4^+$ T cells promote B cell response as well as activation and proliferation of $CD8^+$ T cell. In agreement with this, influenza vaccine based on the highly conserved T cell epitopes capable of eliciting cellular immune response will potentially overcome the need of annual vaccine reformulation. Numerous peptides have been identified to elicit T cell mediated immunity (Assarsson et al., 2008; Atsmon et al., 2014; Choo et al., 2014; Duvvuri et al., 2013; Francis et al., 2015). Various studies conducted in the past have indicated that influenza virus peptides identified by different epitope prediction algorithms have proven to be highly immunogenic (Pedersen et al., 2016; Sun et al., 2010). Most remarkable example is that of the peptides of influenza identified by Stoloff and colleagues (2007) using *in silico* approach, which are the constituents of an influenza vaccine currently undergoing phase II clinical trial under the concept name of FluV (Pleguezuelos et al., 2012; Stoloff & Caparros-Wanderley, 2007). Three H1N1 proteins viz. HA, NA and M1 were considered for immunogenic peptide identification in the present study. HA and NA protein are appealing targets for a universal vaccine against H1N1 influenza virus since they play a crucial role in viral pathogenesis. Further, they are large-sized, most abundant and readily accessible. M1 protein is a highly conserved internal influenza protein, thus a suitable target for universal influenza vaccine development. Present study is reporting highly conserved immunogenic peptides of HA, NA and M1 proteins of H1N1 influenza virus containing multiple $CD8^+$ and $CD4^+$ T cell epitopes.

5.1. Immunoinformatics based identification of conserved peptides containing multiple T cell epitopes

The availability of a substantial amount of data relevant to immunology research, particularly clinical and epidemiological data, has pioneered the contemporary domain of immunoinformatics or computational immunology. Immunoinformatics guided T cell epitope prediction is speculated to improve the selection of targets for vaccine design by reducing the time and expenses involved in the traditional technique. An initial *in silico* screening of antigenic proteins paves the way to quick identification of putative epitopes which are then synthesised and tested *in vitro* for their immunogenic potential. Highly conserved peptides containing epitopes provide a smart approach for designing a universal influenza virus vaccine. The current study considered 3661 protein sequences of HA, 2079 sequences of NA and 458 sequences of M1 protein belonging to H1N1 subtype, which is the largest of its kind to the best of our knowledge.

Many influenza epitopes identified by immunoinformatics approach have proven to be immunogenic in *in vitro* and *in vivo* studies (Assarsson et al., 2008; Babon et al., 2009; Duvvuri et al., 2013; Ichihashi et al., 2011; Schanen et al., 2011). Other than influenza, epitopes of *Leishmania infantum*, *Mycobacterium tuberculosis*, *Mycobacterium bovis, Schistosoma mansoni* and epitopes responsible for peanut-allergy have also been identified *in silico* and successfully proven to be immunogenic (Agallou et al., 2014; Chen et al., 2012; Mustafa, 2011; Oliveira et al., 2016; Pascal et al., 2013).

Multiple factors like proteasomal C-terminal cleavage, TAP (transporter associated with antigen processing) transport efficiency, stability of the peptide–HLA complex and peptide-HLA-TCR complex and peptide susceptibility to proteolysis in lysosome determine the immunogenicity of an epitope. Therefore, the use of a single computational algorithm for T cell epitope prediction may lead to a substantial number of false positives and false negatives. Performance of the consensus prediction approach of epitope prediction (using multiple predictions to define an epitope) has been found to be superior to the single predictive strategy (Moutaftsi et al., 2006; Trost et al., 2007). The consensus approach (i.e., combining and comparing the different prediction algorithms to identify epitopes) has been applied in various studies, and its immunogenic potential has been verified *in vitro* and *in vivo* (Chen et al., 2012; Ichihashi

et al., 2011). In the present study, six epitope prediction tools (three tools to predict epitopes for each class of HLA), which are based on different parameters were employed to identify HLA class I and II epitope from H1N1 influenza proteins.

Some cases of Guillain–Barre Syndrome were reported after monovalent inactivated influenza vaccination (Galeotti et al., 2013; Kwong et al., 2013). Molecular mimicry between egg-produced sialylated HA and human proteins was cited as the potential cause of these rare cases (Pleguezuelos et al., 2012). As reported earlier, epitopes derived from H5N1 avian influenza virus proteins have shown partial identity to the human proteome (Gustiananda, 2011). Hence, epitopes predicted by all the three tools for each class of HLA were analysed for similarity with human proteome by BLASTp. In the present study, few predicted epitopes were found similar to some human proteins. One of the predicted Matrix 1 epitope GILGFVFTL is considered to be immunodominant in HLA-A2 individuals, and it also overlaps with nuclear localization signals (Terajima & Ennis, 2012). However, this epitope was homologous to human tetraspanin-33, which is in accordance with an earlier report (Gustiananda, 2011). It is one of the most extensively studied epitope of the M1 protein, nonetheless it was still eliminated from further consideration to avoid any chances of molecular mimicry. Epitopes of H1N1 which were found identical or partially identical to human peptides by BLASTp analysis were removed and overlapping epitopes were merged to generate long peptides containing multiple $CD8^+$ and $CD4^+$ T cell epitopes.

Expanding knowledge about antigen presentation and recognition has facilitated the advancement in vaccine development, especially peptide based vaccine. Peptide as a choice of vaccine candidate offers benefits such as coverage of wide HLA-restrictions, absence of infectious potential, self-reactivity and easy of production but the bottleneck associated with this approach is that they target one or few epitopes thus limiting the immune response generated. Peptides containing multiple epitopes for generating antigen specific cytotoxic T lymphocytes (CTLs) as well as antigen-specific $CD4^+$ helper T cells may serve as a good alternative to overcome this drawback (Guo et al., 2013). The use of larger synthetic peptide fragments containing both HLA class I and II epitopes was shown to elicit T cell response. In a pre-clinical study, long peptides obtained from internal influenza proteins viz. NP, M1 and PB1 containing T cell and B cell epitopes were used to immunize mice and ferrets. Following challenge, reduction in viral titer was observed in the lungs of animal models in response to vaccination

(Rosendahl Huber et al., 2015). In an early phase clinical studies, larger peptide fragments from the internal proteins of influenza were found to induce both, class I and class II T-cell response (Francis et al., 2015). Flu-v is a synthetic peptide based vaccine which is an equimolar mixture of four long peptides of internal influenza proteins and is currently undergoing clinical trials. This vaccine has been reported to be safe and to elicit cellular immunity (Pleguezuelos et al., 2012). Another influenza vaccine, Multimeric-001, is composed of linear epitopes of various influenza proteins expressed as a single recombinant polyepitope peptide and is also undergoing clinical trials (Atsmon et al., 2012; Biondvax, 2016). Hence it is evident that larger synthetic peptides containing multiple T cell epitopes possess greater potential of becoming a better vaccine candidate than conventional 9mer immunogenic epitopes. In agreement with these findings, current study has reported fourteen peptides (Five, six and three for HA, NA and M1 protein respectively) containing multiple T cell epitopes on H1N1 virus.

Some of the peptides of HA, NA and M1 i.e. P_H2, P_H5, P_N1 and P_N3 have already been reported for their immunogenicity in the form of some bigger peptides (Assarsson et al., 2008; Babon et al., 2009; Cusick et al., 2009; Duvvuri et al., 2013; Moise et al., 2013; Richards et al., 2007; Richards et al., 2009; Roti et al., 2008; Sundararajan et al., 2012; Yang et al., 2013). Some longer peptides containing matrix 1 peptides P_M2 and P_M3 have also been reported to elicit immunogenic response by various research groups (Babon et al., 2009; Sundararajan et al., 2012; Yang et al., 2006). However, considering the stronger candidature of M1 peptides relative to HA and NA as influenza vaccine candidates (owing to higher degree of conservation) P_M2 and P_M3 peptides were included, whereas P_H2, P_H6, P_N1, P_N3 were eliminated from further investigations. Thus, the peptides undertaken for further considerations in the current study were P_H1, P_H3, P_H4, P_N2, P_N4, P_N5, P_N6, P_M1, P_M2 and P_M3.

5.2. Analysis of HLA-peptide interaction

The epitopes are presented to T cells as peptide-HLA complex expressed on the surface of any nucleated cell or specialised antigen presenting cell. HLA genes are the most polymorphic loci among the different individuals of the world. Till July of 2015, 13,412 HLA alleles have been recognised by IMGT/HLA Database (Mack, 2015). So, the peptide capable of binding to a large array of HLA molecules is expected to be immunogenic in population distributed worldwide. All the ten peptides selected in the present work

were predicted to bind to large number of HLA molecules. Population coverage analysis performed for these influenza peptides revealed that the probability of induction of immune response by P_H1, P_N2, P_N6, P_M1 and P_M2 peptides is quite high (>90%) in most of the populations, thus making them excellent vaccine candidates. Other peptides viz. P_H3, P_H4, P_N4 and P_N5 also exhibited a good but highly variable (50-90%) demographic coverage among Asia, Europe, Africa, North America, South America and Oceania counties. To further validate promiscuous nature of the identified peptides towards a wide range of HLAs, the predicted $CD8^+$ T cell epitopes/ $CD4^+$ T cell peptides were also analysed for their binding with HLAs on the basis of structure based molecular docking approach.

Molecular docking has been recognized as a valuable technique in computer aided drug designing (Agallou et al., 2014; Mahaddalkar et al., 2015; Singh et al., 2014; Suri et al., 2015; Vijayan et al., 2015). It is an expeditious, reliable and accurate technique for analysing the binding of peptide with HLA class I and II molecules (Patronov et al., 2011). Previous studies have demonstrated the application of molecular docking in identifying and designing novel peptides having binding affinity towards HLA molecules (Agallou et al., 2014; Oliveira et al., 2016). It has been applied in combination with sequence based epitope prediction algorithm and *in vitro* peptide stimulation technique to identify potential peptide vaccine candidates against *Leishmania infantum* and *Schistosoma mansoni* (Agallou et al., 2014; Oliveira et al., 2016). In another study conducted on H5N1 nucleoprotein, epitopes were identified by molecular docking and further tested for their immunogenicity in *in vivo* system by means of IFN-γ ELISA and flow cytometry based cell proliferation assay (Hou et al., 2012).

Conformational flexibility of peptide-HLA interaction poses a challenge in molecular docking studies. Autodock Vina is a new generation software of Autodock family with improved speed and accuracy. Many studies have used Autodock vina to analyze HLA-peptide binding (Alam & Ashraf, 2013; Antunes et al., 2010; Jain et al., 2015; Sakib et al., 2014; Srivastava et al., 2016; Yasmin et al., 2016). Although, Autodock vina is not used widely for HLA-peptide docking but various studies conducted *in vitro* and *in vivo* have demonstrated the immunogenicity of epitopes identified by AutoDock vina (Oliveira et al., 2016).

In light of the demographic presentation of the peptides analysed by population coverage analysis tool, different HLA of class I and II were selected for analysing peptide

HLA interaction by AutoDock vina. Docking of peptides already known to bind to these HLA's (native peptides) and the predicted epitopes/peptides revealed that the binding energy of the native peptides was comparable to that of the epitope/peptides identified *in silico* in the present study. Many of the epitopes/peptides illustrated better binding potential with the HLA than the native peptides. $CD4^+$ peptide WHGSNRPWV (P_N4) has in fact shown significantly higher binding energy than the native peptides of respective HLA. Only three $CD8^+$ T cell epitopes viz. DTVDTVLEK (P_H1), KVNSVIEKM (P_H4) and MVLASTTAK (P_M2), have shown significantly lower binding energy than the native peptides. It is noteworthy that in some cases, experimental epitopes have displayed higher binding energy as compared to the native peptides. Similarly, $CD4^+$ T cell peptides have shown higher binding energy values against few HLA II alleles. Hence, it can be suggested that peptides exhibited overall good structural compatibility and binding affinity with class I and II HLA molecules, confirming the promiscuous immunogenic nature of both the peptides, as predicted earlier by the sequence based prediction tools.

5.3. *In vitro* assessment of peptide immunogenicity

Even though the *in silico* approach of epitope prediction is extensively used to screen the putative epitopes among numerous possible vaccine targets in a given protein, the results obtained via *in silico* approach need to be validated experimentally in *in vitro* and *in vivo* system. The*in silico* approach helps in decreasing *in vitro* experimentation typically by at least 20-fold (Jawa et al., 2013).

As per the IRD (Influenza research database) records available on August 15, 2016, 182 peptides of hemagglutinin, 69 peptides of neuraminidase and 102 peptides of M1 protein belonging to different H1N1 strains have been reported to elicit T cell mediated immune response in humans (Squires et al., 2012). Most of these reported peptides were specific to virus strains, but all the peptides (except P_N6) selected in the present study were identified to be > 90% conserved across different strains of H1N1 virus.

On continuous encounter with the antigen/peptide, first response of the lymphocytes is to undergo proliferation followed by differentiation to generate specialised cells which specifically identify and exterminate the pathogen. Hence, measuring the lymphocyte proliferation is a key step towards identification of immunogenic peptides. Proliferation

can be measured using several techniques. Cell proliferation can be measured based on DNA synthesis, markers associated with cell proliferation, ATP concentration and metabolic activity. Radioactivity based ^{3}H thymidine uptake assay, fluorescence based bromodeoxyuridine (BrdU) assay, carboxyfluorescein succinimidyl ester (CFSE) assay and colorimetry based MTT, XTT, MTS and WST1 assays are employed to measure cell proliferation (Owen et al., 2013). MTT assay has been reported as a sensitive and safe non-radioactive assay for measuring PBMC proliferation by various studies (do Livramento et al., 2013; Weichert et al., 1991; Zhuge et al., 2012). It not only measures the viability of the cells in PBMC culture but also measures their metabolic activity.

The secretion of IFN-γ along with some other cytokines denotes antigen-specific T cell proliferation and differentiation. Therefore, its accurate assessment in peptide stimulated PBMC culture is critical in evaluating the immunogenicity of the peptide. In the current scenario, three techniques that are most widely used for cytokine detection are flow cytometry (intracellular cytokine staining, ICS), ELISpot and ELISA (Coughlan & Lambe, 2015). Flow cytometry and ELISpot measure the number of cytokine-positive/cytokine secreting cells whereas ELISA measures the total amount of cytokine secreted extracellularly. A study done in the recent past reported that there can be a lack of correlation between IFN-γ values measured by these three techniques (Hagen et al., 2015). Higher count of cytokine-positive cells (ICS) does not necessarily indicate higher frequency of spot forming cells (ELISpot). Similarly, high count of spot forming cells (SFCs) doesn't assure secretion of huge amount of cytokine as compared to the sample with lower SFCs (Hagen et al., 2015). ELISA has been used for detection of extracellular IFN-γ released as a result of antigen induced proliferation of T cells (Atsmon et al., 2012; Hou et al., 2012; Ohkuri et al., 2009; Stoloff & Caparros-Wanderley, 2007).

Many research groups have evaluated the immune reactivity of peptides in *in vitro* lymphocyte proliferation assay based on MTT and IFN-γ ELISA (Chakraborty et al., 2008; Pasricha et al., 2006; Rana et al., 2011). Proliferation and IFN-γ secretion pattern obtained for the nine peptides under consideration in the present study was variable in terms of number of positive responders. Proliferation pattern obtained for these peptides under consideration in the present study has shown significant increase in the proliferation as compared to the unstimulated cells in several healthy individuals. However, peptides of HA and M1 protein were found to have large number of positive

responders. In case of NA, P_N5 and P_N6 peptides have also shown good response though the other two peptides of NA (P_N2 and P_N4) appear to have less number of positive responders. Significantly higher secretion of IFN-γ level was observed in most peptide stimulated cells for most of the healthy samples. Similar to proliferation result, HA and M1 peptides were found to have large number healthy samples showing significantly higher IFN-γ level. NA peptides appear to have weak response in terms of proliferation as well as IFN-γ release. Disparity is observed in the immunogenic response of peptides on account of HLA allotype diversity and variation in the PBMC cell subsets among the healthy volunteers. Five or more samples exhibited positive response in PBMC proliferation as well as IFNγ secretion in case P_H1, P_H4 and P_M2 peptides which indicated a positive correlation between the two factors determining the immunogenic potential of peptides. However, in case of other peptides lack of correlation was observed between the two factors considered in the present study to explain the immunogenicity of the peptides. This observation can be attributed to the different experimental setups used to perform these assays, including the time frame.

Four peptides LSSVSSFERFEIF (P_H2), YQILAIYSTVASSLVL (P_H5), LQIGNIISIW (P_N1) and FFLTQGALLN (P_N3), assayed in the present study have been reported to elicit immunogenic response. These peptides have not been a part of some longer peptides which have been reported to elicit $CD4^+$ T-cell responses (Assarsson et al., 2008; Babon et al., 2009; Cusick et al., 2009; Duvvuri et al., 2013; Moise et al., 2013; Richards et al., 2007; Richards et al., 2009; Roti et al., 2008; Sundararajan et al., 2012; Yang et al., 2013). Further, peptides P_H1, P_H3, P_H4, P_N2, P_N6 and P_M1 have not been reported in the earlier studies, but some peptides which share partial identity with these peptides have been reported to elicit immunogenicity (Assarsson et al., 2008; Babon et al., 2009; Duvvuri et al., 2013; Schanen et al., 2011). For instance, peptides VLEKNVTVTHSVNLL (Duvvuri et al., 2013) and STDTVDTVLEKNVTVTHS (Cusick et al., 2009) which are similar to peptide P_H1 have been proven to elicit $CD4^+$ T cell mediated immune response by means of IFNγ release assay and T cell proliferation assays. In another example peptide LGFVFTLTVPSERG (Braendstrup et al., 2013) and ILGFVFTLTVPSERG (Ge et al., 2010) similar to P_M1 have been reported to induce $CD4^+$ T cell proliferation and IFNγ production. Peptides GDVFVIREPFISCSH and NTTIWTSGSSISFCGVN sharing partial identity with P_N2 and P_N6 peptides respectively elicit IFN-γ response (Assarsson et al., 2008; Babon et al., 2009).

A major challenge associated with peptide vaccines is the low immunogenicity of peptides in contrast to whole pathogen vaccines (Gottlieb & Ben-Yedidia, 2014). Various other challenges are linked with peptide based vaccines. Small peptides usually bind to large number of non-professional APCs and thus are presented with sub optimal co-stimulation, which may lead to induction of tolerance. Short peptides often lack secondary or tertiary structures and are thus prone to rapid degradation by tissue and serum peptides (Slingluff, 2011).

Immunogenicity of peptides can be improved in multiple ways viz. addition of CD4 T the cell help, addition of adjuvants, using a mixture of synthetic peptides which may be chemically produced or as recombinant protein containing the poly-epitopes expressed in various expression systems (Rosendahl Huber et al., 2014). CD4 helper peptide (PADRE) binds with high or intermediate affinity to the most common HLA-DR types, and allows it to activate a wide range of $CD4^+$ T cells. Natural tetanus sequences are promiscuous in binding to HLA class II molecules and providing efficient co-stimulus. Another approach is the inclusion of CD40-CD40L as co-stimulatory signals to enhance the activation of $CD4^+$ and $CD8^+$ T cells via DC. CD40L upregulates the expression of ICAM-1, CD80 and CD86 molecules on DC which in turn promotes T cell proliferative responses and IFN-γ production. Coupling the peptide to TLR-activating lipids results in the formation of self adjuvanting lipopeptides. TLRs activation on APCs promotes the internalisation and presentation of peptides on HLAs (Rosendahl Huber et al., 2014).

Adjuvants act as immunostimulants in vaccine formulations to enhance the potency of immune response generated. MF59 and Montanide ISA 51VG are some of the examples of adjuvants being used for the T cell based peptide vaccines which are currently under clinical trials (Soema et al., 2015). Conserved T cell epitopes from various internal proteins (internal as well as surface proteins) or multiple copies of single immunodominant epitope in tandem have also been used to enhance the immunogenicity of peptide immunogens in *in vivo* systems (Rosendahl Huber et al., 2015; Subbarao & Matsuoka, 2013; Wiersma et al., 2015). Different platforms for vaccine delivery that can be used to enhance the efficiency of same epitopesinclude soluble peptides with adjuvant, subunit or domain epitopes fused to a carrier protein, nanoparticles and virus-like particles (VLPs) (Zhang et al., 2014). Further, prime-boost strategy of immunisation has also been used as one of the procedures to enhance memory T cell count (Woodland, 2004).

In light of the above facts this work could be extended to immunophenotyping of the peptide induced PBMC, in order to identify the immune pathway responsible for the immunogenic response observed against each of the peptides. Immunogenicity of these peptides can be analysed in animal models. In addition to that, different formulations like combination with adjuvants, carrier proteins or mixture of synthetic peptides can be used to enhance the immunogenicity of these peptides in *in vivo* models.

To conclude, we present nine highly conserved immunogenic synthetic peptides of H1N1 virus containing multiple overlapping $CD4^+$ and $CD8^+$ T cell epitopes which are restricted by wide range of HLAs. These peptides belong to the most abundantly expressed influenza protein. Further, these peptides were found to elicit immune response in most of the healthy PBMC samples. Hence, these peptides offer a great potential as broadly reactive T cell based vaccine candidates in the fight against epidemic as well as pandemic influenza.

Summary

Influenza poses major health concern worldwide due to unforeseen pandemic threats and seasonal epidemics among humans. Owing to antigenic variation in H1N1 influenza virus, vaccine development persists as a challenge. Vaccine based on conserved immunogenic moiety is one of the viable options. Identification of immunogenic region i.e. epitope is a crucial step in peptide based vaccine design. The conventional approach in defining the epitope experimentally is an exhaustive and expensive process. Immunoinformatics or computational immunology has played an instrumental role in screening the epitopes which reduces the number of peptides needed for experimental validation for vaccine design.

Full length non-redundant protein sequence of hemagglutinin (3661), neuraminidase (2079) and M1 protein (458) sequences were retrieved. Sequences were aligned and conserved sequences were identified. 12, 15 and 10 conserved peptides identified for HA, NA and M1 protein respectively which were used to predict T cell epitope using a consensus approach. Predicted epitopes were analyzed by BLASTp and epitopes sharing identity with human peptides were eliminated from the studies. Epitopes sharing overlaps were merged to generate peptides fragments containing multiple $CD8^+$ and $CD4^+$ T cell epitopes. Five such peptides were identified for HA, six for NA and three for M1 protein. Four peptides out of these fourteen were eliminated from further considerations based on previous literatures which have reported the immunogenicity of these peptides. The ten selected peptides (P_H1, P_H3 and P_H4 of HA, P_N2, P_N4, P_N5 and P_N6 of NA and P_M1, P_M2 and $P_M3$of M1 protein) were found to be conserved in more than 90% of the sequences obtained for the respective proteins except P_N6 which was 80% conserved. Immunogenic response against antigen varies in different population owing to high HLA polymorphism. The selected peptides not only carry several epitopes but were predicted to bind to diverse HLA molecules. In addition, the population coverage analysis in present study unveiled that these peptides has shown significant population coverage in different continents of the world. Hence, these peptide sequences have the potential to induce a potent immunogenic response among individuals belonging to different populations around the world.

The predicted $CD8^+$ T cell epitopes and $CD4^+$ T cell epitopes were docked with the class I and II HLA molecules, using native bound peptides as test peptides. Molecular docking of most of the $CD8^+$ T cell epitopes and $CD4^+$ T cell epitopes containing peptides with HLA class I and II molecules respectively, revealed no significant difference in the binding energy. Moreover, some of the identified peptides had higher binding energy and thus better binding potential than native peptides of various HLA molecules. Docking results confirmed the strong binding potential of each of the predicted epitopes and peptides to various HLAs.

Further these peptides were commercially synthesized and assessed for their immunogenic response by *in vitro* lymphocyte proliferation assay based on MTT and IFN-γ ELISA. Most of the peptides elicited immunogenic response leading to significant proliferation as compared to the unstimulated cells. Proliferative response induced by HA and MI peptides among various PBMC samples was observed to be higher as compared to NA peptides in terms of number of positive responders. Similarly, most of the HA and M1 peptides elicited significantly higher IFN-γ secretion in different blood samples as compared to NA peptides. P_H1, P_H4 and P_M2 peptides have shown proliferation as well as higher secretion of IFN-γ in most of the healthy samples (≥5).

In the present study, we have reported highly conserved immunogenic peptides of HA, NA and M1 protein of H1N1 influenza virus, containing multiple overlapping $CD4^+$ and $CD8^+$ T cell epitopes which are restricted by wide range of HLA molecules. Findings of the *in vitro* assessment of these peptides suggested that most of the peptides were capable of eliciting immunogenicity in terms of proliferation and IFN-γ release. The highly conserved immunogenic peptide of H1N1 identified in the present study may serve as potential candidates for the development of broadly reactive T cell based influenza vaccine.

References

1. Agallou, M., Athanasiou, E., Koutsoni, O., Dotsika, E., Karagouni, E. 2014. Experimental validation of multi-epitope peptides including promising MHC class I- and class II-restricted epitopes of four known Leishmania infantum proteins. *Front Immunol*, 5, 268.
2. Akiyama, Y., Komiyama, M., Nakamura, Y., Iizuka, A., Oshita, C., Kume, A., Nogami, M., Miyata, H., Ashizawa, T., Yoshikawa, S., Kiyohara, Y., Yamaguchi, K. 2012. Identification of novel MAGE-A6- and MAGE-A12-derived HLA-A24-restricted cytotoxic T lymphocyte epitopes using an in silico peptide-docking assay. *Cancer Immunol Immunother*, 61(12), 2311-9.
3. Alam, M.J., Ashraf, K.U.M. 2013. Prediction of an epitope-based computational vaccine strategy for gaining concurrent immunization against the venom proteins of Australian box Jellyfish. *Toxicol Int*, 20(3), 235-253.
4. Alizadeh, Z., Karrow, N., Mallard, B.A. 2003. Biological effect of varying peptide binding affinity to the BoLA-DRB3*2703 allele. *Genet Sel Evol*, 35(1), S51-65.
5. Altschul, S.F., Gish, W., Miller, W., Myers, E.W., Lipman, D.J. 1990. Basic local alignment search tool. *J Mol Biol*, 215(3), 403-10.
6. Andreatta, M., Nielsen, M. 2016. Gapped sequence alignment using artificial neural networks: application to the MHC class I system. *Bioinformatics*, 32(4), 511-7.
7. Antunes, D.A., Vieira, G.F., Rigo, M.M., Cibulski, S.P., Sinigaglia, M., Chies, J.A.B. 2010. Structural allele-specific patterns adopted by epitopes in the MHC-I cleft and reconstruction of MHC:peptide complexes to cross-reactivity assessment. *PLoS ONE*, 5(4), e10353.
8. Arnon, R., Ben-Yedidia, T., Levi, R. 2000. Peptide-based vaccine for influenza, Google Patents.
9. Arranz, R., Coloma, R., Chichón, F.J., Conesa, J.J., Carrascosa, J.L., Valpuesta, J.M., Ortín, J., Martín-Benito, J. 2012. The structure of native influenza virion ribonucleoproteins. *Science*, 338(6114), 1634-1637.
10. Assarsson, E., Bui, H.H., Sidney, J., Zhang, Q., Glenn, J., Oseroff, C., Mbawuike, I.N., Alexander, J., Newman, M.J., Grey, H., Sette, A. 2008. Immunomic analysis of the repertoire of T-cell specificities for influenza A virus in humans. *J Virol*, 82(24), 12241-51.
11. Atsmon, J., Caraco, Y., Ziv-Sefer, S., Shaikevich, D., Abramov, E., Volokhov, I., Bruzil, S., Haima, K.Y., Gottlieb, T., Ben-Yedidia, T. 2014. Priming by a novel universal influenza vaccine (Multimeric-001)-a gateway for improving immune response in the elderly population. *Vaccine*, 32(44), 5816-23.
12. Atsmon, J., Kate-Ilovitz, E., Shaikevich, D., Singer, Y., Volokhov, I., Haim, K.Y., Ben-Yedidia, T. 2012. Safety and immunogenicity of multimeric-001--a novel universal influenza vaccine. *J Clin Immunol*, 32(3), 595-603.

13. Babon, J.A., Cruz, J., Orphin, L., Pazoles, P., Co, M.D., Ennis, F.A., Terajima, M. 2009. Genome-wide screening of human T-cell epitopes in influenza A virus reveals a broad spectrum of CD4(+) T-cell responses to internal proteins, hemagglutinins, and neuraminidases. *Hum Immunol*, 70(9), 711-21.

14. Backert, L., Kohlbacher, O. 2015. Immunoinformatics and epitope prediction in the age of genomic medicine. *Genome Med*, 7(1), 119.

15. Bao, Y., Bolotov, P., Dernovoy, D., Kiryutin, B., Zaslavsky, L., Tatusova, T., Ostell, J., Lipman, D. 2008. The influenza virus resource at the National Center for Biotechnology Information. *J Virol*, 82(2), 596-601.

16. Bekkat-Berkani, R., Ray, R., Jain, V.K., Chandrasekaran, V., Innis, B.L. 2016. Evidence update: GlaxoSmithKline's inactivated quadrivalent influenza vaccines. *Expert Rev Vaccines*, 15(2), 201-14.

17. Ben-Yedidia, T., Arnon, R. 2005. Towards an epitope-based human vaccine for influenza. *Hum Vaccin*, 1(3), 95-101.

18. Berlanda Scorza, F., Tsvetnitsky, V., Donnelly, J.J. 2016. Universal influenza vaccines: Shifting to better vaccines. *Vaccine*. 34(26), 2926-33.

19. Berman, H.M., Westbrook, J., Feng, Z., Gilliland, G., Bhat, T.N., Weissig, H., Shindyalov, I.N., Bourne, P.E. 2000. The protein data bank. *Nucleic Acids Res*, 28(1), 235-42.

20. Bhasin, M., Raghava, G.P. 2004. Prediction of CTL epitopes using QM, SVM and ANN techniques. *Vaccine*, 22(23-24), 3195-204.

21. Bhasin, M., Raghava, G.P. 2005. Pcleavage: an SVM based method for prediction of constitutive proteasome and immunoproteasome cleavage sites in antigenic sequences. *Nucleic Acids Res*, 33(Web Server issue), W202-7.

22. Bianchi, E., Liang, X., Ingallinella, P., Finotto, M., Chastain, M.A., Fan, J., Fu, T.M., Song, H.C., Horton, M.S., Freed, D.C., Manger, W., Wen, E., Shi, L., Ionescu, R., Price, C., Wenger, M., Emini, E.A., Cortese, R., Ciliberto, G., Shiver, J.W., Pessi, A. 2005. Universal influenza B vaccine based on the maturational cleavage site of the hemagglutinin precursor. *J Virol*, 79(12), 7380-8.

23. Bier, K., York, A., Fodor, E. 2011. Cellular cap-binding proteins associate with influenza virus mRNAs. *J Virol*, 92(7), 1627-1634.

24. Binh, N.T., Wakai, C., Kawaguchi, A., Nagata, K. 2013. The N-terminal region of influenza virus polymerase PB1 adjacent to the PA binding site is involved in replication but not transcription of the viral genome. *Front microbiol*, 4, 398.

25. Biondvax. 2016. BiondVax's universal flu vaccine phase 2b clinical trial recruitment complete, Vol. 2016. http://www.biondvax.com/2016/03/biondvaxs-universal-flu-vaccine-phase-2b-clinical-trial-recruitment-complete/

26. Bogner, P., Capua, I., Cox, N.J., Lipman, D.J. 2006. A global initiative on sharing avian flu data. *Nature*, 442(7106), 981-981.

27. Bommakanti, G., Citron, M.P., Hepler, R.W., Callahan, C., Heidecker, G.J., Najar, T.A., Lu, X., Joyce, J.G., Shiver, J.W., Casimiro, D.R., ter Meulen, J., Liang, X., Varadarajan, R. 2010. Design of an HA2-based Escherichia coli expressed influenza immunogen

that protects mice from pathogenic challenge. *Proc Natl Acad Sci U S A*, 107(31), 13701-6.

28. Bouvier, N.M., Palese, P. 2008. The biology of influenza viruses. *Vaccine*, 26(4), D49-D53.
29. Braendstrup, P., Justesen, S., Østerbye, T., Nielsen, L.L.B., Mallone, R., Vindeløv, L., Stryhn, A., Buus, S. 2013. MHC class II tetramers made from isolated recombinant α and β chains refolded with affinity-tagged peptides. *PLoS ONE*, 8(9), e73648.
30. Brincks, E.L., Roberts, A.D., Cookenham, T., Sell, S., Kohlmeier, J.E., Blackman, M.A., Woodland, D.L. 2013. Antigen-specific memory regulatory CD4+Foxp3+ T cells control memory responses to influenza virus infection. *J Immunol*, 190(7), 3438-46.
31. Brown, D.M., Lee, S., Garcia-Hernandez Mde, L., Swain, S.L. 2012. Multifunctional CD4 cells expressing gamma interferon and perforin mediate protection against lethal influenza virus infection. *J Virol*, 86(12), 6792-803.
32. Brusic, V., Petrovsky, N., Zhang, G., Bajic, V.B. 2002. Prediction of promiscuous peptides that bind HLA class I molecules. *Immunol Cell Biol*, 80(3), 280-285.
33. Bui, H.H., Sidney, J., Dinh, K., Southwood, S., Newman, M.J., Sette, A. 2006. Predicting population coverage of T-cell epitope-based diagnostics and vaccines. *BMC Bioinform*, 7(1), 153.
34. Bui, M., Whittaker, G., Helenius, A. 1996. Effect of M1 protein and low pH on nuclear transport of influenza virus ribonucleoproteins. *J virol*, 70(12), 8391-8401.
35. Bullough, P.A., Hughson, F.M., Skehel, J.J., Wiley, D.C. 1994. Structure of influenza haemagglutinin at the pH of membrane fusion. *Nature*, 371(6492), 37-43.
36. Burleigh, L.M., Calder, L.J., Skehel, J.J., Steinhauer, D.A. 2005. Influenza a viruses with mutations in the m1 helix six domain display a wide variety of morphological phenotypes. *J virol*, 79(2), 1262-1270.
37. Carragher, D.M., Kaminski, D.A., Moquin, A., Hartson, L., Randall, T.D. 2008. A novel role for non-neutralizing antibodies against nucleoprotein in facilitating resistance to influenza virus. *J Immunol*, 181(6), 4168-76.
38. CDC USA. 2015. People at high risk of developing flu–related complications, Vol. 2016. http://www.cdc.gov/flu/about/disease/high_risk.htm
39. CDC USA. 2016. Reported infections with variant influenza viruses in the United States since 2005, Vol. 2016. http://www.cdc.gov/flu/swineflu/variant-cases-us.htm
40. Chakraborty, K., Bose, A., Pal, S., Sarkar, K., Goswami, S., Ghosh, D., Laskar, S., Chattopadhyay, U., Baral, R. 2008. Neem leaf glycoprotein restores the impaired chemotactic activity of peripheral blood mononuclear cells from head and neck squamous cell carcinoma patients by maintaining CXCR3/CXCL10 balance. *Int Immunopharmacol*, 8(2), 330-340.
41. Chase, G.P., Rameix-Welti, M.-A., Zvirbliene, A., Zvirblis, G., Götz, V., Wolff, T., Naffakh, N., Schwemmle, M. 2011. Influenza virus ribonucleoprotein complexes

gain preferential access to cellular export machiner y through chromatin targeting. *PLoS Pathog*, 7(9), e1002187.

42. Chauhan, A., Zubair, S., Tufail, S., Sherwani, A., Sajid, M., Raman, S.C., Azam, A. & Owais, M. 2011. Fungus-mediated biological synthesis of gold nanoparticles: potential in detection of liver cancer. Int J Nanomedicine, 6, 2305-19.
43. Cheever, M.A., Higano, C.S. 2011. PROVENGE (Sipuleucel-T) in prostate cancer: the first FDA-approved therapeutic cancer vaccine. *Clin Cancer Res*, 17(11), 3520-26.
44. Chen, F., Zhai, M.X., Zhu, Y.H., Qi, Y.M., Zhai, W.J., Gao, Y.F. 2012. In vitro and in vivo identification of a novel cytotoxic T lymphocyte epitope from Rv3425 of Mycobacterium tuberculosis. *Microbiol Immunol*, 56(8), 548-53.
45. Chen, W., Calvo, P.A., Malide, D., Gibbs, J., Schubert, U., Bacik, I., Basta, S., O'Neill, R., Schickli, J., Palese, P. 2001. A novel influenza A virus mitochondrial protein that induces cell death. *Nat med*, 7(12), 1306-12.
46. Choo, J.A., Liu, J., Toh, X., Grotenbreg, G.M., Ren, E.C. 2014. The immunodominant influenza A virus M158-66 cytotoxic T lymphocyte epitope exhibits degenerate class I major histocompatibility complex restriction in humans. *J Virol*, 88(18), 10613-23.
47. Consortium, T.U. 2015. UniProt: a hub for protein information. *Nucleic Acids Res*, 43(D1), D204-12.
48. Corti, D., Voss, J., Gamblin, S.J., Codoni, G., Macagno, A., Jarrossay, D., Vachieri, S.G., Pinna, D., Minola, A., Vanzetta, F., Silacci, C., Fernandez-Rodriguez, B.M., Agatic, G., Bianchi, S., Giacchetto-Sasselli, I., Calder, L., Sallusto, F., Collins, P., Haire, L.F., Temperton, N., Langedijk, J.P., Skehel, J.J., Lanzavecchia, A. 2011. A neutralizing antibody selected from plasma cells that binds to group 1 and group 2 influenza A hemagglutinins. *Science*, 333(6044), 850-6.
49. Coughlan, L., Lambe, T. 2015. Measuring cellular immunity to influenza: methods of detection, applications and challenges. *Vaccines (Basel)*, 3(2), 293-319.
50. Crotty, S. 2011. Follicular helper CD4 T cells (TFH). *Annu Rev Immunol*, 29, 621-63.
51. Cummings, J.F., Guerrero, M.L., Moon, J.E., Waterman, P., Nielsen, R.K., Jefferson, S., Gross, F.L., Hancock, K., Katz, J.M., Yusibov, V. 2014. Safety and immunogenicity of a plant-produced recombinant monomer hemagglutinin-based influenza vaccine derived from influenza A (H1N1)pdm09 virus: a Phase 1 dose-escalation study in healthy adults. *Vaccine*, 32(19), 2251-9.
52. Cusick, M.F., Wang, S., Eckels, D.D. 2009. In vitro responses to avian influenza H5 by human CD4 T cells. *J Immunol*, 183(10), 6432-41.
53. Dawood, F.S., Iuliano, A.D., Reed, C., Meltzer, M.I., Shay, D.K., Cheng, P.-Y., Bandaranayake, D., Breiman, R.F., Brooks, W.A., Buchy, P., Feikin, D.R., Fowler, K.B., Gordon, A., Hien, N.T., Horby, P., Huang, Q.S., Katz, M.A., Krishnan, A., Lal, R., Montgomery, J.M., Mølbak, K., Pebody, R., Presanis, A.M., Razuri, H., Steens, A., Tinoco, Y.O., Wallinga, J., Yu, H., Vong, S., Bresee, J., Widdowson, M.-A. 2012. Estimated global mortality associated with the first 12 months of 2009 pandemic

influenza A H1N1 virus circulation: a modelling study. *Lancet Infect Dis*, 12(9), 687-95.

54. De Filette, M., Martens, W., Smet, A., Schotsaert, M., Birkett, A., Londono-Arcila, P., Fiers, W., Saelens, X. 2008. Universal influenza A M2e-HBc vaccine protects against disease even in the presence of pre-existing anti-HBc antibodies. *Vaccine*, 26(51), 6503-7.
55. De Groot, A.S., Ardito, M., McClaine, E.M., Moise, L., Martin, W.D. 2009. Immunoinformatic comparison of T-cell epitopes contained in novel swine-origin influenza A (H1N1) virus with epitopes in 2008-2009 conventional influenza vaccine. *Vaccine*, 27(42), 5740-7.
56. Diebold, S.S., Kaisho, T., Hemmi, H., Akira, S. & Reis E Sousa, C. 2004. Innate antiviral responses by means of TLR7-mediated recognition of single-stranded RNA. *Science,* 303(5663), 1529-31.
57. do Livramento, A., Sampaio, J., Schultz, J., Batista, K.Z.S., Treitinger, A., de Cordova, C.M.M., Spada, C. 2013. In vitro lymphocyte stimulation by recombinant hepatitis B surface antigen: A tool to detect the persistence of cellular immunity after vaccination. *J Virol Methods*, 193(2), 572-78.
58. Dolfi, D.V., Duttagupta, P.A., Boesteanu, A.C., Mueller, Y.M., Oliai, C.H., Borowski, A.B., Katsikis, P.D. 2011. Dendritic cells and CD28 costimulation are required to sustain virus-specific CD8+ T cell responses during the effector phase in vivo. *J Immunol*, 186(8), 4599-608.
59. Donnes, P., Kohlbacher, O. 2005. Integrated modeling of the major events in the MHC class I antigen processing pathway. *Protein Sci*, 14(8), 2132-40.
60. Duan, S., Thomas, P.G. 2016. Balancing immune protection and immune pathology by CD8+ T cell responses to influenza infection. *Front Immunol*, 7, 1-16.
61. Dubois, J., Terrier, O., Rosa-Calatrava, M. 2014. Influenza viruses and mRNA splicing: doing more with less. *MBio*, 5(3), e00070-14.
62. Duvvuri, V.R., Duvvuri, B., Alice, C., Wu, G.E., Gubbay, J.B., Wu, J. 2014. Preexisting CD4+ T-cell immunity in human population to avian influenza H7N9 virus: whole proteome-wide immunoinformatics analyses. *PLoS One*, 9(3), e91273.
63. Duvvuri, V.R., Duvvuri, B., Jamnik, V., Gubbay, J.B., Wu, J., Wu, G.E. 2013. T cell memory to evolutionarily conserved and shared hemagglutinin epitopes of H1N1 viruses: a pilot scale study. *BMC Infect Dis*, 13(1), 204.
64. Dynavax. 2010. Dynavax Begins Phase 1b Study for Universal Flu Vaccine, Vol. 2016. http://investors.dynavax.com/releasedetail.cfm?ReleaseID=510260
65. Edgar, R.C. 2004. MUSCLE: a multiple sequence alignment method with reduced time and space complexity. *BMC Bioinformatics*, 5(1), 113.
66. Engelhardt, O.G., Smith, M., Fodor, E. 2005. Association of the influenza A virus RNA-dependent RNA polymerase with cellular RNA polymerase II. *J virol*, 79(9), 5812-18.
67. Fae, K.C., Oshiro, S.E., Toubert, A., Charron, D., Kalil, J., Guilherme, L. 2005. How an autoimmune reaction triggered by molecular mimicry between streptococcal M

protein and cardiac tissue proteins leads to heart lesions in rheumatic heart disease. *J Autoimmun*, 24(2), 101-9.

68. FDA, U. 2015. Influenza (Flu) Antiviral Drugs and Related Information, Vol. 2016. http://www.fda.gov/drugs/drugsafety/informationbydrugclass/ucm100228.htm
69. Fislová, T., Thomas, B., Graef, K.M., Fodor, E. 2010. Association of the influenza virus RNA polymerase subunit PB2 with the host chaperonin CCT. *J virol*, 84(17), 8691-99.
70. Fontana, J., Cardone, G., Heymann, J.B., Winkler, D.C., Steven, A.C. 2012. Structural changes in Influenza virus at low pH characterized by cryo-electron tomography. *J virol*, 86(6), 2919-29.
71. Foo, S.Y., Phipps, S. 2010. Regulation of inducible BALT formation and contribution to immunity and pathology. *Mucosal Immunol*, 3(6), 537-44.
72. Fouchier, R.A.M., Schneeberger, P.M., Rozendaal, F.W., Broekman, J.M., Kemink, S.A.G., Munster, V., Kuiken, T., Rimmelzwaan, G.F., Schutten, M., van Doornum, G.J.J., Koch, G., Bosman, A., Koopmans, M., Osterhaus, A.D.M.E. 2004. Avian influenza A virus (H7N7) associated with human conjunctivitis and a fatal case of acute respiratory distress syndrome. *Proc Natl Acad Sci U S A*, 101(5), 1356-61.
73. Francis, J.N., Bunce, C.J., Horlock, C., Watson, J.M., Warrington, S.J., Georges, B., Brown, C.B. 2015. A novel peptide-based pan-influenza A vaccine: A double blind, randomised clinical trial of immunogenicity and safety. *Vaccine*, 33(2), 396-402.
74. Fujii, K., Fujii, Y., Noda, T., Muramoto, Y., Watanabe, T., Takada, A., Goto, H., Horimoto, T., Kawaoka, Y. 2005. Importance of both the coding and the segment-specific noncoding regions of the influenza A virus NS segment for its efficient incorporation into virions. *J virol*, 79(6), 3766-74.
75. Fujii, Y., Goto, H., Watanabe, T., Yoshida, T., Kawaoka, Y. 2003. Selective incorporation of influenza virus RNA segments into virions. *Proc Natl Acad Sci U S A*, 100(4), 2002-7.
76. Fujiyoshi, Y., Kume, N.P., Sakata, K., Sato, S. 1994. Fine structure of influenza A virus observed by electron cryo-microscopy. *EMBO J,* 13(2), 318.
77. Furuya, Y., Chan, J., Regner, M., Lobigs, M., Koskinen, A., Kok, T., Manavis, J., Li, P., Mullbacher, A., Alsharifi, M. 2010. Cytotoxic T cells are the predominant players providing cross-protective immunity induced by {gamma}-irradiated influenza A viruses. *J Virol*, 84(9), 4212-21.
78. Gack, M.U., Albrecht, R.A., Urano, T., Inn, K.-S., Huang, I.-C., Carnero, E., Farzan, M., Inoue, S., Jung, J.U., García-Sastre, A. 2009. Influenza A virus NS1 targets the ubiquitin ligase TRIM25 to evade recognition by the host viral RNA sensor RIG-I. *Cell host microbe*, 5(5), 439-49.
79. Galeotti, F., Massari, M., D'Alessandro, R., Beghi, E., Chio, A., Logroscino, G., Filippini, G., Benedetti, M.D., Pugliatti, M., Santuccio, C., Raschetti, R. 2013. Risk of Guillain-Barre syndrome after 2010-2011 influenza vaccination. *Eur J Epidemiol*, 28(5), 433-44.
80. Galiano, M., Agapow, P.-M., Thompson, C., Platt, S., Underwood, A., Ellis, J., Myers, R., Green, J., Zambon, M. 2011. Evolutionary pathways of the pandemic influenza A (H1N1) 2009 in the UK. *PloS one*, 6(8), e23779.

81. Ge, X., Tan, V., Bollyky, P.L., Standifer, N.E., James, E.A., Kwok, W.W. 2010. Assessment of seasonal influenza A virus-specific CD4 T-cell responses to 2009 pandemic H1N1 swine-origin influenza A virus. *J Virol*, 84(7), 3312-9.

82. Glaser, L., Stevens, J., Zamarin, D., Wilson, I.A., García-Sastre, A., Tumpey, T.M., Basler, C.F., Taubenberger, J.K., Palese, P. 2005. A single amino acid substitution in 1918 influenza virus hemagglutinin changes receptor binding specificity. *J virol*, 79(17), 11533-36.

83. Gonzalez-Galarza, F.F., Takeshita, L.Y., Santos, E.J., Kempson, F., Maia, M.H., da Silva, A.L., Teles e Silva, A.L., Ghattaoraya, G.S., Alfirevic, A., Jones, A.R., Middleton, D. 2015. Allele frequency net 2015 update: new features for HLA epitopes, KIR and disease and HLA adverse drug reaction associations. *Nucleic Acids Res*, 43(Database issue), D784-8.

84. Gottlieb, T., Ben-Yedidia, T. 2014. Epitope-based approaches to a universal influenza vaccine. *J Autoimmun*, 54, 15-20.

85. Gravel, C., Li, C., Wang, J., Hashem, A.M., Jaentschke, B., Van Domselaar, G., He, R., Li, X. 2011. Quantitative analyses of all influenza type A viral hemagglutinins and neuraminidases using universal antibodies in simple slot blot assays. *J Vis Exp*, 50, 2784-90.

86. Guo, C., Manjili, M.H., Subjeck, J.R., Sarkar, D., Fisher, P.B., Wang, X.Y. 2013. Therapeutic cancer vaccines: past, present, and future. *Adv Cancer Res*, 119, 421-75.

87. Gupta, S.K., Srivastava, M., Akhoon, B.A., Smita, S., Schmitz, U., Wolkenhauer, O., Vera, J., Gupta, S.K. 2011. Identification of immunogenic consensus T-cell epitopes in globally distributed influenza-A H1N1 neuraminidase. *Infect Genet Evol*, 11(2), 308-19.

88. Gustiananda, M. 2011. Immunoinformatics analysis of H5N1 proteome for designing an epitope-derived vaccine and predicting the prevalence of pre-existing cellular-mediated immunity toward bird flu virus in Indonesian population. *Immunome Res*, 7(3), 1-11.

89. Hagen, J., Zimmerman, R., Goetz, C., Bonnevier, J., Houchins, J.P., Reagan, K., Kalyuzhny, A.E. 2015. Comparative multi-donor study of IFNγ secretion and expression by human PBMCs using ELISPOT side-by-side with ELISA and flow cytometry assays. *Cells*, 4(1), 84-95.

90. Hamada, H., Bassity, E., Flies, A., Strutt, T.M., Garcia-Hernandez Mde, L., McKinstry, K.K., Zou, T., Swain, S.L., Dutton, R.W. 2013. Multiple redundant effector mechanisms of CD8+ T cells protect against influenza infection. *J Immunol*, 190(1), 296-306.

91. Harpur, A.G., Zimiecki, A., Wilks, A.F., Falk, K., Rotzschke, O., Rammensee, H.G. 1993. A prominent natural H-2 Kd ligand is derived from protein tyrosine kinase JAK1. *Immunol Lett*, 35(3), 235-7.

92. Hassainya, Y., Garcia-Pons, F., Kratzer, R., Lindo, V., Greer, F., Lemonnier, F.A., Niedermann, G., van Endert, P.M. 2005. Identification of naturally processed HLA-A2--restricted proinsulin epitopes by reverse immunology. *Diabetes*, 54(7), 2053-9.

93. Heer, A.K., Shamshiev, A., Donda, A., Uematsu, S., Akira, S., Kopf, M., Marsland, B.J. 2007. TLR signaling fine-tunes anti-influenza B cell responses without regulating effector T cell responses. *J Immunol*, 178(4), 2182-91.

94. Hoft, D.F., Babusis, E., Worku, S., Spencer, C.T., Lottenbach, K., Truscott, S.M., Abate, G., Sakala, I.G., Edwards, K.M., Creech, C.B., Gerber, M.A., Bernstein, D.I., Newman, F., Graham, I., Anderson, E.L., Belshe, R.B. 2011. Live and inactivated influenza vaccines induce similar humoral responses, but only live vaccines induce diverse T-cell responses in young children. *J Infect Dis*, 204(6), 845-53.

95. Holzhutter, H.G., Frommel, C., Kloetzel, P.M. 1999. A theoretical approach towards the identification of cleavage-determining amino acid motifs of the 20 S proteasome. *J Mol Biol*, 286(4), 1251-65.

96. Hou, Y., Guo, Y., Wu, C., Shen, N., Jiang, Y., Wang, J. 2012. Prediction and identification of T cell epitopes in the H5N1 influenza virus nucleoprotein in chicken. *PLoS One*, 7(6), e39344.

97. Huang, P., Yu, S., Wu, C., Liang, L. 2013. Highly conserved antigenic epitope regions of hemagglutinin and neuraminidase genes between 2009 H1N1 and seasonal H1N1 influenza: vaccine considerations. *J Transl Med*, 11, 47.

98. Ichihashi, T., Yoshida, R., Sugimoto, C., Takada, A., Kajino, K. 2011. Cross-protective peptide vaccine against influenza A viruses developed in HLA-A*2402 human immunity model. *PLoS One*, 6(9), e24626.

99. ICTV. 2014. Virus Taxonomy: 2014 Release, Vol. 2016. http://www.ictvonline.org/virusTaxonomy.asp

100. Inovio. 2010. SynCon® vaccines targeting avian flu and other subtypes with pandemic potential, Vol. 2016. http://www.inovio.com/products/infectious-disease-vaccines/influenza/pandemic/

101. Isin, B., Doruker, P., Bahar, I. 2002. Functional motions of influenza virus hemagglutinin: a structure-based analytical approach. *Biophys J*, 82(2), 569-81.

102. Iwasaki, A., Pillai, P.S. 2014. Innate immunity to influenza virus infection. *Nat Rev Immunol*, 14(5), 315-28.

103. Jacob, L., Vert, J.P. 2008. Efficient peptide-MHC-I binding prediction for alleles with few known binders. *Bioinformatics*, 24(3), 358-66.

104. Jagger, B., Wise, H., Kash, J., Walters, K.-A., Wills, N., Xiao, Y.-L., Dunfee, R., Schwartzman, L., Ozinsky, A., Bell, G. 2012. An overlapping protein-coding region in influenza A virus segment 3 modulates the host response. *Science*, 337(6091), 199-204.

105. Jain, A., Tripathi, P., Shrotriya, A., Chaudhary, R., Singh, A. 2015. In silico analysis and modeling of putative T cell epitopes for vaccine design of Toscana virus. *3 Biotech*, 5(4), 497-503.

106. Jawa, V., Cousens, L.P., Awwad, M., Wakshull, E., Kropshofer, H., De Groot, A.S. 2013. T-cell dependent immunogenicity of protein therapeutics: Preclinical assessment and mitigation. *Clin Immunol*, 149(3, Part B), 534-55.

107. Jayasekera, J.P., Moseman, E.A., Carroll, M.C. 2007. Natural antibody and complement mediate neutralization of influenza virus in the absence of prior immunity. *J Virol*, 81(7), 3487-94.

108. Jegaskanda, S., Weinfurter, J.T., Friedrich, T.C., Kent, S.J. 2013. Antibody-dependent cellular cytotoxicity is associated with control of pandemic H1N1 influenza virus infection of macaques. *J Virol*, 87(10), 5512-22.

109. Jupelli, M., Guentzel, M.N., Meier, P.A., Zhong, G., Murthy, A.K., Arulanandam, B.P. 2008. Endogenous IFN-gamma production is induced and required for protective immunity against pulmonary chlamydial infection in neonatal mice. *J Immunol*, 180(6), 4148-55.

110. Kantoff , P.W., Higano , C.S., Shore , N.D., Berger , E.R., Small , E.J., Penson , D.F., Redfern , C.H., Ferrari , A.C., Dreicer , R., Sims , R.B., Xu , Y., Frohlich , M.W., Schellhammer , P.F. 2010. Sipuleucel-T immunotherapy for castration-resistant prostate cancer. *N Engl J Med*, 363(5), 411-22.

111. Karrow, N.A., Leffel, E.K., Guo, T.L., Zhang, L.X., McCay, J.A., Germolec, D.R., White, K.L., Jr. 2001. Dermal exposure to cinnamaldehyde alters lymphocyte subpopulations, number of interferon-gamma-producing cells, and expression of B7 costimulatory molecules and cytokine messenger RNAs in auricular lymph nodes of B6C3F1 mice. *Am J Contact Dermat*, 12(1), 6-17.

112. Kennell, A.S., Gould, K.G., Salaman, M.R. 2014. Proliferation assay amplification by IL-2 in model primary and recall antigen systems. *BMC Research Notes*, 7(1), 1-4.

113. Kim, J.H., Skountzou, I., Compans, R., Jacob, J. 2009. Original antigenic sin responses to influenza viruses. *J Immunol*, 183(5), 3294-301.

114. Kim, T.S., Braciale, T.J. 2009. Respiratory dendritic cell subsets differ in their capacity to support the induction of virus-specific cytotoxic CD8(+) T cell responses. *PLoS ONE*, 4(1), e4204.

115. Knowlden, Z.A.G., Sant, A.J. 2016. CD4 T cell epitope specificity determines follicular versus non-follicular helper differentiation in the polyclonal response to influenza infection or vaccination. *Scientific Reports*, 6, 28287.

116. Kok, W.L., Denney, L., Benam, K., Cole, S., Clelland, C., McMichael, A.J., Ho, L.-P. 2012. Pivotal Advance: Invariant NKT cells reduce accumulation of inflammatory monocytes in the lungs and decrease immune-pathology during severe influenza A virus infection. *J Leukoc Biol*, 91(3), 357-68.

117. Krammer, F., Palese, P. 2015. Advances in the development of influenza virus vaccines. *Nat Rev Drug Discov*, 14(3), 167-82.

118. Krammer, F., Pica, N., Hai, R., Margine, I., Palese, P. 2013. Chimeric hemagglutinin influenza virus vaccine constructs elicit broadly protective stalk-specific antibodies. *J Virol*, 87(12), 6542-50.

119. Kreijtz, J.H., Fouchier, R.A., Rimmelzwaan, G.F. 2011. Immune responses to influenza virus infection. *Virus Res*, 162(1-2), 19-30.

120. Krol, E., Rychlowska, M., Szewczyk, B. 2014. Antivirals--current trends in fighting influenza. *Acta Biochim Pol*, 61(3), 495-504.

121. Kumar, M., Putzki, N., Limmroth, V., Remus, R., Lindemann, M., Knop, D., Mueller, N., Hardt, C., Kreuzfelder, E., Grosse-Wilde, H. 2006. CD4+CD25+FoxP3+ T lymphocytes fail to suppress myelin basic protein-induced proliferation in patients with multiple sclerosis. *J Neuroimmunol*, 180(1-2), 178-84.

122. Kwong, J.C., Vasa, P.P., Campitelli, M.A., Hawken, S., Wilson, K., Rosella, L.C., Stukel, T.A., Crowcroft, N.S., McGeer, A.J., Zinman, L., Deeks, S.L. 2013. Risk of Guillain-Barre syndrome after seasonal influenza vaccination and influenza health-care encounters: a self-controlled study. *Lancet Infect Dis*, 13(9), 769-76.

123. La Gruta, N.L., Turner, S.J. 2014. T cell mediated immunity to influenza: mechanisms of viral control. *Trends Immunol*, 35(8), 396-402.

124. Lakadamyali, M., Rust, M.J., Zhuang, X. 2004. Endocytosis of influenza viruses. *Microbes and infection*, 6(10), 929-36.

125. Larsen, M.V., Lelic, A., Parsons, R., Nielsen, M., Hoof, I., Lamberth, K., Loeb, M.B., Buus, S., Bramson, J., Lund, O. 2010. Identification of CD8+ T cell epitopes in the West Nile virus polyprotein by reverse-immunology using NetCTL. *PLoS One*, 5(9), e12697.

126. Larsen, M.V., Lundegaard, C., Lamberth, K., Buus, S., Lund, O., Nielsen, M. 2007. Large-scale validation of methods for cytotoxic T-lymphocyte epitope prediction. *BMC Bioinformatics*, 8(1), 424.

127. Lata, S., Bhasin, M., Raghava, G.P. 2009. MHCBN 4.0: A database of MHC/TAP binding peptides and T-cell epitopes. *BMC Res Notes*, 2(1), 61.

128. Lee, Y.T., Kim, K.H., Ko, E.J., Lee, Y.N., Kim, M.C., Kwon, Y.M., Tang, Y., Cho, M.K., Lee, Y.J., Kang, S.M. 2014. New vaccines against influenza virus. *Clin Exp Vaccine Res*, 3(1), 12-28.

129. Lefranc, M.-P., Giudicelli, V., Duroux, P., Jabado-Michaloud, J., Folch, G., Aouinti, S., Carillon, E., Duvergey, H., Houles, A., Paysan-Lafosse, T., Hadi-Saljoqi, S., Sasorith, S., Lefranc, G., Kossida, S. 2015. IMGT®, the international ImMunoGeneTics information system® 25 years on. *Nucleic Acids Res*, 43(D1), D413-22.

130. Li, W., Murthy, A.K., Lanka, G.K., Chetty, S.L., Yu, J.J., Chambers, J.P., Zhong, G., Forsthuber, T.G., Guentzel, M.N., Arulanandam, B.P. 2013. A T cell epitope-based vaccine protects against chlamydial infection in HLA-DR4 transgenic mice. *Vaccine*, 31(48), 5722-8.

131. Liang, Y., Hong, Y., Parslow, T.G. 2005. cis-Acting packaging signals in the influenza virus PB1, PB2, and PA genomic RNA segments. *J virol*, 79(16), 10348-55.

132. Liechti, R., Gleizes, A., Kuznetsov, D., Bougueleret, L., Le Mercier, P., Bairoch, A., Xenarios, I. 2010. OpenFluDB, a database for human and animal influenza virus. *Database (Oxford)*, 2010, baq004.

133. Limberis, M.P., Figueredo, J., Calcedo, R., Wilson, J.M. 2007. Activation of CFTR-specific T Cells in cystic fibrosis mice following gene transfer. *Mol Ther*, 15(9), 1694-700.

134. Liu, C., Yang, X., Duffy, B., Mohanakumar, T., Mitra, R.D., Zody, M.C., Pfeifer, J.D. 2013. ATHLATES: accurate typing of human leukocyte antigen through exome sequencing. *Nucleic Acids Res*, 41(14), e142.

135. Liu, M., Li, X., Yuan, H., Zhou, J., Wu, J., Bo, H., Xia, W., Xiong, Y., Yang, L., Gao, R., Guo, J., Huang, W., Zhang, Y., Zhao, X., Zou, X., Chen, T., Wang, D., Li, Q., Wang, S., Chen, S., Hu, M., Ni, X., Gong, T., Shi, Y., Li, J., Zhou, J., Cai, J., Xiao, Z., Zhang, W., Sun, J., Li, D., Wu, G., Feng, Z., Wang, Y., Chen, H., Shu, Y. 2015. Genetic diversity of avian influenza A (H10N8) virus in live poultry markets and its association with human infections in China. *Sci Rep*, 5, 7632.

136. Liu, Q., Liu, D.Y. & Yang, Z.Q. 2013. Characteristics of human infection with avian influenza viruses and development of new antiviral agents. *Acta Pharmacol Sin*, 34(10), 1257-69.

137. Lowe, D.B., Taylor, J.L., Storkus, W.J. 2014. Monitoring Antigen-Specific T Cell Responses Using Real-Time PCR. *Methods mol biol (Clifton, N.J.)*, 1186, 65-74.

138. Lund, O., Nielsen, M., Kesmir, C., Petersen, A.G., Lundegaard, C., Worning, P., Sylvester-Hvid, C., Lamberth, K., Roder, G., Justesen, S., Buus, S., Brunak, S. 2004. Definition of supertypes for HLA molecules using clustering of specificity matrices. *Immunogenetics*, 55(12), 797-810.

139. Mack, S.J. 2015. A gene feature enumeration approach for describing HLA allele polymorphism. *Hum Immunol*, 76(12), 975-81.

140. Mahaddalkar, T., Suri, C., Naik, P.K., Lopus, M. 2015. Biochemical characterization and molecular dynamic simulation of beta-sitosterol as a tubulin-binding anticancer agent. *Eur J Pharmacol*, 760, 154-62.

141. Mao, L., Yang, Y., Qiu, Y., Yang, Y. 2012. Annual economic impacts of seasonal influenza on US counties: spatial heterogeneity and patterns. *Int J Health Geogr*, 11(1), 16.

142. Mariner, J.C., House, J.A., Mebus, C.A., Sollod, A.E., Chibeu, D., Jones, B.A., Roeder, P.L., Admassu, B., van 't Klooster, G.G. 2012. Rinderpest eradication: appropriate technology and social innovations. *Science*, 337(6100), 1309-12.

143. Matrosovich, M.N., Matrosovich, T.Y., Gray, T., Roberts, N.A., Klenk, H.-D. 2004. Neuraminidase is important for the initiation of influenza virus infection in human airway epithelium. *J virol*, 78(22), 12665-7.

144. Matza, D., Badou, A., Jha, M.K., Willinger, T., Antov, A., Sanjabi, S., Kobayashi, K.S., Marchesi, V.T., Flavell, R.A. 2009. Requirement for AHNAK1-mediated calcium signaling during T lymphocyte cytolysis. *Proc Natl Acad Sci U S A*, 106(24), 9785-90.

145. Mazanec, M.B., Coudret, C.L., Fletcher, D.R. 1995. Intracellular neutralization of influenza virus by immunoglobulin A anti-hemagglutinin monoclonal antibodies. *J Virol*, 69(2), 1339-43.

146. McGill, J., Van Rooijen, N., Legge, K.L. 2010. IL-15 trans-presentation by pulmonary dendritic cells promotes effector CD8 T cell survival during influenza virus infection. *J Exp Med*, 207(3), 521-34.

147. Mesri, Enrique A., Feitelson, M.A., Munger, K. 2014. Human viral oncogenesis: A cancer hallmarks analysis. *Cell Host & Microbe*, 15(3), 266-82.

148. Minu, M., Singh, D., Mahaddalkar, T., Lopus, M., Winter, P., Ayoub, A.T., Missiaen, K., Tilli, T.M., Pasdar, M., Tuszynski, J. 2016. Chemical synthesis, pharmacological evaluation and in silico analysis of new 2,3,3a,4,5,6-

hexahydrocyclopenta[c]pyrazole derivatives as potential anti-mitotic agents. *Bioorg Med Chem Lett,* 26(16), 3855-61.

149. Miotto, O., Heiny, A., Tan, T.W., August, J.T., Brusic, V. 2008. Identification of human-to-human transmissibility factors in PB2 proteins of influenza A by large-scale mutual information analysis. *BMC Bioinformatics*, 9 (1), S18.

150. Mishra, B. 2015. 2015 Resurgence of Influenza A (H1N1) 09: Smoldering Pandemic in India? *J Glob Infect Dis*, 7(2), 56-9.

151. Moise, L., Tassone, R., Latimer, H., Terry, F., Levitz, L., Haran, J.P., Ross, T.M., Boyle, C.M., Martin, W.D., De Groot, A.S. 2013. Immunization with cross-conserved H1N1 influenza CD4+ T-cell epitopes lowers viral burden in HLA DR3 transgenic mice. *Hum Vaccin Immunother*, 9(10), 2060-8.

152. Momose, F., Basler, C.F., O'Neill, R.E., Iwamatsu, A., Palese, P., Nagata, K. 2001. Cellular splicing factor RAF-2p48/NPI-5/BAT1/UAP56 interacts with the influenza virus nucleoprotein and enhances viral RNA synthesis. *J Virol*, 75(4), 1899-1908.

153. Morens, D.M., Taubenberger, J.K., Harvey, H.A., Memoli, M.J. 2010. The 1918 influenza pandemic: lessons for 2009 and the future. *Crit care med*, 38(4), e10.

154. Mosmann, T. 1983. Rapid colorimetric assay for cellular growth and survival: application to proliferation and cytotoxicity assays. *J Immunol Methods*, 65(1-2), 55-63.

155. Moutaftsi, M., Peters, B., Pasquetto, V., Tscharke, D.C., Sidney, J., Bui, H.H., Grey, H., Sette, A. 2006. A consensus epitope prediction approach identifies the breadth of murine T(CD8+)-cell responses to vaccinia virus. *Nat Biotechnol*, 24(7), 817-9.

156. Mozdzanowska, K., Maiese, K., Furchner, M., Gerhard, W. 1999. Treatment of influenza virus-infected SCID mice with nonneutralizing antibodies specific for the transmembrane proteins matrix 2 and neuraminidase reduces the pulmonary virus titer but fails to clear the infection. *Virol*, 254(1), 138-46.

157. Mukherjee, S., Majumdar, S., Vipat, V.C., Mishra, A.C., Chakrabarti, A.K. 2012. Non structural protein of avian influenza A (H11N1) virus is a weaker suppressor of immune responses but capable of inducing apoptosis in host cells. *Virol J*, 9(1), 149.

158. Muramoto, Y., Noda, T., Kawakami, E., Akkina, R., Kawaoka, Y. 2013. Identification of novel influenza A virus proteins translated from PA mRNA. *J virol*, 87(5), 2455-62.

159. Mustafa, A.S. 2011. Comparative evaluation of MPT83 (Rv2873) for T helper-1 cell reactivity and identification of HLA-promiscuous peptides in *Mycobacterium bovis* BCG-vaccinated healthy subjects. *Clin Vaccine Immunol*, 18(10), 1752-9.

160. Naito, T., Kiyasu, Y., Sugiyama, K., Kimura, A., Nakano, R., Matsukage, A., Nagata, K. 2007. An influenza virus replicon system in yeast identified Tat-SF1 as a stimulatory host factor for viral RNA synthesis. *Proc Natl Acad Sci U S A* 104(46), 18235-40.

161. Neirynck, S., Deroo, T., Saelens, X., Vanlandschoot, P., Jou, W.M., Fiers, W. 1999. A universal influenza A vaccine based on the extracellular domain of the M2 protein. *Nat Med*, 5(10), 1157-63.

162. Nelson, M.I., Holmes, E.C. 2007. The evolution of epidemic influenza. *Nat rev genet*, 8(3), 196-205.

163. Neumann, G., Noda, T., Kawaoka, Y. 2009. Emergence and pandemic potential of swine-origin H1N1 influenza virus. *Nature*, 459(7249), 931-39.

164. Nguyen-Van-Tam, J.S., Nair, P., Acheson, P., Baker, A., Barker, M., Bracebridge, S., Croft, J., Ellis, J., Gelletlie, R., Gent, N., Ibbotson, S., Joseph, C., Mahgoub, H., Monk, P., Reghitt, T.W., Sundkvist, T., Sellwood, C., Simpson, J., Smith, J., Watson, J.M., Zambon, M., Lightfoot, N. 2006. Outbreak of low pathogenicity H7N3 avian influenza in UK, including associated case of human conjunctivitis. *Euro Surveill*, 11(5), E060504.2.

165. Nielsen, M., Lund, O. 2009. NN-align. An artificial neural network-based alignment algorithm for MHC class II peptide binding prediction. *BMC Bioinformatics*, 10, 296.

166. Nielsen, M., Lundegaard, C., Lund, O. 2007. Prediction of MHC class II binding affinity using SMM-align, a novel stabilization matrix alignment method. *BMC Bioinformatics*, 8, 238.

167. Nielsen, M., Lundegaard, C., Lund, O., Kesmir, C. 2005. The role of the proteasome in generating cytotoxic T-cell epitopes: insights obtained from improved predictions of proteasomal cleavage. *Immunogenetics*, 57(1-2), 33-41.

168. O'Brien, C., Flower, D.R., Feighery, C. 2008. Peptide length significantly influences in vitro affinity for MHC class II molecules. *Immunome Res*, 4, 6-6.

169. Ohkuri, T., Wakita, D., Chamoto, K., Togashi, Y., Kitamura, H., Nishimura, T. 2009. Identification of novel helper epitopes of MAGE-A4 tumour antigen: useful tool for the propagation of Th1 cells. *Br J Cancer*, 100(7), 1135-43.

170. Oliveira, F.M., Coelho, I.E.V., Lopes, M.D., Taranto, A.G., Junior, M.C., Santos, L.L.D., Villar, J.A.P.F., Fonseca, C.T., Lopes, D.D.O. 2016. The Use of Reverse Vaccinology and Molecular Modeling Associated with Cell Proliferation Stimulation Approach to Select Promiscuous Epitopes from Schistosoma mansoni. *Appl Biochem Biotechnol*, 179(6), 1023-40.

171. O'Neill, R.E., Jaskunas, R., Blobel, G., Palese, P., Moroianu, J. 1995. Nuclear import of influenza virus RNA can be mediated by viral nucleoprotein and transport factors required for protein import. *J Bioll Chem*, 270(39), 22701-4.

172. O'Neill, R.E., Talon, J., Palese, P. 1998. The influenza virus NEP (NS2 protein) mediates the nuclear export of viral ribonucleoproteins. *EMBO J*, 17(1), 288-96.

173. Owen, J.A., Punt, J., Kuby, J., Stranford, S.A. 2013. *Kuby Immunology*. W.H. Freeman.

174. Paget, C., Ivanov, S., Fontaine, J., Renneson, J., Blanc, F., Pichavant, M., Dumoutier, L., Ryffel, B., Renauld, J.C., Gosset, P., Gosset, P., Si-Tahar, M., Faveeuw, C., Trottein, F. 2012. Interleukin-22 is produced by invariant natural killer t lymphocytes during influenza a virus infection: potential role in protection against lung epithelial damages. *Journal of Biological Chemistry*, 287(12), 8816-29.

175. Palese, P., Shaw, M. 2007. Fields virology. *Orthomyxoviridae: The Viruses and Their Replication, 5th edn, Philadelphia, PA: Lippincott Williams & Wilkins, Wolters Kluwer Business*, 1647-89.

176. Palese, P., Young, J.F. 1982. Variation of influenza A, B, and C viruses. *Science*, 215(4539), 1468-74.

177. Parida, R., Shaila, M.S., Mukherjee, S., Chandra, N.R., Nayak, R. 2007. Computational analysis of proteome of H5N1 avian influenza virus to define T cell epitopes with vaccine potential. *Vaccine*, 25(43), 7530-9.

178. Parker, K.C., Bednarek, M.A., Coligan, J.E. 1994. Scheme for ranking potential HLA-A2 binding peptides based on independent binding of individual peptide side-chains. *J Immunol*, 152(1), 163-75.

179. Pascal, M., Konstantinou, G.N., Masilamani, M., Lieberman, J., Sampson, H.A. 2013. In silico prediction of Ara h 2 T cell epitopes in peanut-allergic children. *Clin Exp Allergy*, 43(1), 116-27.

180. Pasricha, N., Datta, U., Chawla, Y., Singh, S., Arora, S.K., Sud, A., Minz, R.W., Saikia, B., Singh, H., James, I., Sehgal, S. 2006. Immune responses in patients with HIV infection after vaccination with recombinant Hepatitis B virus vaccine. *BMC Infect Dis*, 6(1), 65.

181. Paterson, D., Fodor, E. 2012. Emerging roles for the influenza A virus nuclear export protein (NEP). 8(12), e1003019.

182. Patronov, A., Dimitrov, I., Flower, D.R., Doytchinova, I. 2011. Peptide binding prediction for the human class II MHC allele HLA-DP2: a molecular docking approach. *BMC Structural Biology*, 11(1), 1-10.

183. Patronov, A., Doytchinova, I. 2013. T-cell epitope vaccine design by immunoinformatics. *Open Biol*, 3(1), 120139.

184. Pedersen, G.K., Sjursen, H., Nostbakken, J.K., Jul-Larsen, A., Hoschler, K., Cox, R.J. 2014. Matrix M(TM) adjuvanted virosomal H5N1 vaccine induces balanced Th1/Th2 CD4(+) T cell responses in man. *Hum Vaccin Immunother*, 10(8), 2408-16.

185. Pedersen, S.R., Christensen, J.P., Buus, S., Rasmussen, M., Korsholm, K.S., Nielsen, M., Claesson, M.H. 2016. Immunogenicity of HLA class I and II double restricted influenza a-derived peptides. *PLoS One*, 11(1), e0145629.

186. Perez, J.T., Zlatev, I., Aggarwal, S., Subramanian, S., Sachidanandam, R., Kim, B., Manoharan, M. 2012. A small-RNA enhancer of viral polymerase activity. *J virol*, 86(24), 13475-85.

187. Pleguezuelos, O., Robinson, S., Stoloff, G.A., Caparros-Wanderley, W. 2012. Synthetic Influenza vaccine (FLU-v) stimulates cell mediated immunity in a double-blind, randomised, placebo-controlled Phase I trial. *Vaccine*, 30(31), 4655-60.

188. Plotkin, J.B., Dushoff, J., Levin, S.A. 2002. Hemagglutinin sequence clusters and the antigenic evolution of influenza A virus. *Proc Natl Acad Sci U S A*, 99(9), 6263-8.

189. Pollard, R.B., Rockstroh, J.K., Pantaleo, G., Asmuth, D.M., Peters, B., Lazzarin, A., Garcia, F., Ellefsen, K., Podzamczer, D., van Lunzen, J., Arasteh, K., Schurmann, D., Clotet, B., Hardy, W.D., Mitsuyasu, R., Moyle, G., Plettenberg, A., Fisher, M., Fatkenheuer, G., Fischl, M., Taiwo, B., Baksaas, I., Jolliffe, D., Persson, S., Jelmert, O., Hovden, A.O., Sommerfelt, M.A., Wendel-Hansen, V., Sorensen, B. 2014. Safety and efficacy of the peptide-based therapeutic vaccine for HIV-1, Vacc-4x: a phase

2 randomised, double-blind, placebo-controlled trial. *Lancet Infect Dis*, 14(4), 291-300.

190. Potter, C.W. 2001. A history of influenza. *J Appl Microbiol*, 91(4), 572-9.

191. Pujari, R., Kumar, N., Ballal, S., Eligar, S.M., Anupama, S., Bhat, G., Swamy, B.M., Inamdar, S.R., Shastry, P. 2015. Rhizoctonia bataticola lectin (RBL) induces phenotypic and functional characteristics of macrophages in THP-1 cells and human monocytes. *Immunol Lett*, 163(2), 163-72.

192. Pujari, R., Nagre, N.N., Chachadi, V.B., Inamdar, S.R., Swamy, B.M., Shastry, P. 2010. Rhizoctonia bataticola lectin (RBL) induces mitogenesis and cytokine production in human PBMC via p38 MAPK and STAT-5 signaling pathways. *Biochim Biophys Acta*, 1800(12), 1268-75.

193. Purcell, A.W., McCluskey, J., Rossjohn, J. 2007. More than one reason to rethink the use of peptides in vaccine design. *Nat Rev Drug Discov*, 6(5), 404-14.

194. Puzelli, S., Rossini, G., Facchini, M., Vaccari, G., Di Trani, L., Di Martino, A., Gaibani, P., Vocale, C., Cattoli, G., Bennett, M., McCauley, J.W., Rezza, G., Moro, M.L., Rangoni, R., Finarelli, A.C., Landini, M.P., Castrucci, M.R., Donatelli, I. 2014. Human infection with highly pathogenic A(H7N7) avian influenza virus, Italy, 2013. *Emerg Infect Dis*, 20(10), 1745-9.

195. Quah, B.J.C., Parish, C.R. 2010. The use of carboxyfluorescein diacetate succinimidyl ester (cfse) to monitor lymphocyte proliferation. *J Vis Exp,* (44), 2259.

196. Rammensee, H., Bachmann, J., Emmerich, N.P., Bachor, O.A., Stevanovic, S. 1999. SYFPEITHI: database for MHC ligands and peptide motifs. *Immunogenetics*, 50(3-4), 213-9.

197. Rana, D., Menachery, J., Chawla, Y., Duseja, A., Dhiman, R., Arora, S. 2011. HBV specific T-cell responses in hepatitis B. *Trop Gastroenterol*, 32(4), 273-8.

198. Reche, P.A., Glutting, J.P., Reinherz, E.L. 2002. Prediction of MHC class I binding peptides using profile motifs. *Hum Immunol*, 63(9), 701-9.

199. Renegar, K.B., Small, P.A., Jr., Boykins, L.G., Wright, P.F. 2004. Role of IgA versus IgG in the control of influenza viral infection in the murine respiratory tract. J Immunol, 173(3), 1978-86.

200. Richards, K.A., Chaves, F.A., Krafcik, F.R., Topham, D.J., Lazarski, C.A., Sant, A.J. 2007. Direct ex vivo analyses of HLA-DR1 transgenic mice reveal an exceptionally broad pattern of immunodominance in the primary HLA-DR1-restricted CD4 T-cell response to influenza virus hemagglutinin. *J Virol*, 81(14), 7608-19.

201. Richards, K.A., Chaves, F.A., Sant, A.J. 2009. Infection of HLA-DR1 transgenic mice with a human isolate of influenza a virus (H1N1) primes a diverse CD4 T-cell repertoire that includes CD4 T cells with heterosubtypic cross-reactivity to avian (H5N1) influenza virus. *J Virol*, 83(13), 6566-77.

202. Robb, N.C., Fodor, E. 2012. The accumulation of influenza A virus segment 7 spliced mRNAs is regulated by the NS1 protein. *J Gen Virol*, 93(1), 113-18.

203. Robb, N.C., Smith, M., Vreede, F.T., Fodor, E. 2009. NS2/NEP protein regulates transcription and replication of the influenza virus RNA genome. *Journal of general virology*, 90(6), 1398-407.

204. Robinson, J., Halliwell, J.A., Hayhurst, J.D., Flicek, P., Parham, P., Marsh, S.G. 2015. The IPD and IMGT/HLA database: allele variant databases. *Nucleic Acids Res*, 43(Database issue), D423-31.

205. Rosendahl Huber, S., van Beek, J., de Jonge, J., Luytjes, W., van Baarle, D. 2014. T cell responses to viral infections - opportunities for peptide vaccination. *Front Immunol*, 5, 171.

206. Rosendahl Huber, S.K., Camps, M.G.M., Jacobi, R.H.J., Mouthaan, J., van Dijken, H., van Beek, J., Ossendorp, F., de Jonge, J. 2015. Synthetic long peptide influenza vaccine containing conserved t and b cell epitopes reduces viral load in lungs of mice and ferrets. *PLoS ONE*, 10(6), e0127969.

207. Rossman, J.S., Jing, X., Leser, G.P., Lamb, R.A. 2010. Influenza virus M2 protein mediates ESCRT-independent membrane scission. *Cell*, 142(6), 902-13.

208. Rossman, J.S., Lamb, R.A. 2011. Influenza virus assembly and budding. *Virol*, 411(2), 229-36.

209. Rothbarth, P.H., Groen, J., Bohnen, A.M., de Groot, R., Osterhaus, A.D. 1999. Influenza virus serology--a comparative study. *J Virol Methods*, 78(1-2), 163-9.

210. Roti, M., Yang, J., Berger, D., Huston, L., James, E.A., Kwok, W.W. 2008. Healthy human subjects have CD4+ T cells directed against H5N1 influenza virus. *J Immunol*, 180(3), 1758-68.

211. Roy, S., Barik, S., Banerjee, S., Bhuniya, A., Pal, S., Basu, P., Biswas, J., Goswami, S., Chakraborty, T., Bose, A., Baral, R. 2013. Neem leaf glycoprotein overcomes indoleamine 2,3 dioxygenase mediated tolerance in dendritic cells by attenuating hyperactive regulatory T cells in cervical cancer stage IIIB patients. *Hum Immunol*, 74(8), 1015-23.

212. Ruigrok, R.W., Barge, A., Durrer, P., Brunner, J., Ma, K., Whittaker, G.R. 2000. Membrane interaction of influenza virus M1 protein. *Virol*, 267(2), 289-98.

213. Sakib, M.S., Islam, M.R., Hasan, A.K.M.M., Nabi, A.H.M.N. 2014. Prediction of epitope-based peptides for the utility of vaccine development from fusion and glycoprotein of nipah virus using in silico approach. *Adv Bioinformatics*, 2014, 402492.

214. Samson, M., Pizzorno, A., Abed, Y., Boivin, G. 2013. Influenza virus resistance to neuraminidase inhibitors. *Antiviral Res*, 98(2), 174-85.

215. Schanen, B.C., De Groot, A.S., Moise, L., Ardito, M., McClaine, E., Martin, W., Wittman, V., Warren, W.L., Drake, D.R., 3rd. 2011. Coupling sensitive in vitro and in silico techniques to assess cross-reactive CD4(+) T cells against the swine-origin H1N1 influenza virus. *Vaccine*, 29(17), 3299-309.

216. Schnell, J.R., Chou, J.J. 2008. Structure and mechanism of the M2 proton channel of influenza A virus. *Nature*, 451(7178), 591-95.

217. Schrauwen, E.J., Fouchier, R.A. 2014. Host adaptation and transmission of influenza A viruses in mammals. *Emerg Microbes Infect*, 3(2), e9.

218. Selman, M., Dankar, S.K., Forbes, N.E., Jia, J.-J., Brown, E.G. 2012. Adaptive mutation in influenza A virus non-structural gene is linked to host switching and induces a novel protein by alternative splicing. *Emerg Microbes Infect*, 1(11), e42.

219. Sha, B., Luo, M. 1997. Structure of a bifunctional membrane-RNA binding protein, influenza virus matrix protein M1. *Nat Struct Mol Biol*, 4(3), 239-44.

220. Shen, Y., Maupetit, J., Derreumaux, P., Tuffery, P. 2014. Improved PEP-FOLD approach for peptide and miniprotein structure prediction. *J Chem Theory Comput*, 10(10), 4745-58.

221. Shimizu, T., Takizawa, N., Watanabe, K., Nagata, K., Kobayashi, N. 2011. Crucial role of the influenza virus NS2 (NEP) C-terminal domain in M1 binding and nuclear export of vRNP. *FEBS letters*, 585(1), 41-46.

222. Shtyrya, Y., Mochalova, L., Bovin, N. 2009. Influenza virus neuraminidase: structure and function. *Acta naturae*, 1(2), 26.

223. Shukla, S.A., Rooney, M.S., Rajasagi, M., Tiao, G., Dixon, P.M., Lawrence, M.S., Stevens, J., Lane, W.J., Dellagatta, J.L., Steelman, S., Sougnez, C., Cibulskis, K., Kiezun, A., Hacohen, N., Brusic, V., Wu, C.J., Getz, G. 2015. Comprehensive analysis of cancer-associated somatic mutations in class I HLA genes. *Nat Biotech*, 33(11), 1152-8.

224. Singh, B. 2004. PepBuild: a web server for building structure data of peptides/proteins. *Nucleic acids res.* 32, W559-61.

225. Singh, H., Raghava, G.P. 2001. ProPred: prediction of HLA-DR binding sites. *Bioinformatics*, 17(12), 1236-7.

226. Singh, S., Bajpai, U., Lynn, A.M. 2014. Structure based virtual screening to identify inhibitors against MurE enzyme of *Mycobacterium tuberculosis* using AutoDock Vina. *Bioinformation*, 10(11), 697-702.

227. Singh, S., Singh, H., Tuknait, A., Chaudhary, K., Singh, B., Kumaran, S. & Raghava, G.P.S. 2015. PEPstrMOD: structure prediction of peptides containing natural, non-natural and modified residues. *Biol Direct,* 10(1), 1-19.

228. Skehel, J., Bayley, P., Brown, E., Martin, S., Waterfield, M., White, J., Wilson, I., Wiley, D. 1982. Changes in the conformation of influenza virus hemagglutinin at the pH optimum of virus-mediated membrane fusion. *Proc Natl Acad Sci U S A,* 79(4), 968-72.

229. Skehel, J.J., Wiley, D.C. 2000. Receptor binding and membrane fusion in virus entry: the influenza hemagglutinin. *Annu rev biochem*, 69(1), 531-69.

230. Slingluff, C.L. 2011. The present and future of peptide vaccines for cancer: single or multiple, long or short, alone or in combination? *Cancer J (Sudbury, Mass.)*, 17(5), 343-50.

231. Smith, C., Okern, G., Rehan, S., Beagley, L., Lee, S.K., Aarvak, T., Schjetne, K.W., Khanna, R. 2015. Ex vivo expansion of human T cells for adoptive immunotherapy using the novel Xeno-free CTS Immune Cell Serum Replacement. *Clin Trans Immunol*, 4(1), e31.

232. Soema, P.C., van Riet, E., Kersten, G., Amorij, J.P. 2015. Development of cross-protective influenza a vaccines based on cellular responses. *Front Immunol*, 6, 237.

233. Soghoian, D.Z., Streeck, H. 2010. Cytolytic CD4(+) T cells in viral immunity. *Expert Rev Vaccines*, 9(12), 1453-63.

234. Somvanshi, P., Singh, V., Seth, P.K. 2008. Prediction of epitopes in hemagglutinin and neuraminidase proteins of influenza A virus H5N1 strain: a clue for diagnostic and vaccine development. *Omics*, 12(1), 61-9.

235. Song, J.M., Van Rooijen, N., Bozja, J., Compans, R.W., Kang, S.M. 2011. Vaccination inducing broad and improved cross protection against multiple subtypes of influenza A virus. *Proc Natl Acad Sci U S A*, 108(2), 757-61.

236. Squires, R.B., Noronha, J., Hunt, V., Garcia-Sastre, A., Macken, C., Baumgarth, N., Suarez, D., Pickett, B.E., Zhang, Y., Larsen, C.N., Ramsey, A., Zhou, L., Zaremba, S., Kumar, S., Deitrich, J., Klem, E., Scheuermann, R.H. 2012. Influenza research database: an integrated bioinformatics resource for influenza research and surveillance. *Influenza Other Respir Viruses*, 6(6), 404-16.

237. Srivastava, P.N., Jain, R., Dubey, S.D., Bhatnagar, S., Ahmad, N. 2016. Prediction of epitope-based peptides for vaccine development from coat proteins GP2 and VP24 of ebola virus using immunoinformatics. *International Journal of Peptide Research and Therapeutics*, 22(1), 119-33.

238. Steel, J., Lowen, A.C., Wang, T.T., Yondola, M., Gao, Q., Haye, K., Garcia-Sastre, A., Palese, P. 2010. Influenza virus vaccine based on the conserved hemagglutinin stalk domain. *MBio*, 1(1), e00018-10.

239. Stoloff, G.A., Caparros-Wanderley, W. 2007. Synthetic multi-epitope peptides identified in silico induce protective immunity against multiple influenza serotypes. *Eur J Immunol*, 37(9), 2441-9.

240. Strober, W. 2001. *Trypan blue exclusion test of cell viability*. *2008/04/25 ed*.

241. Sturniolo, T., Bono, E., Ding, J., Raddrizzani, L., Tuereci, O., Sahin, U., Braxenthaler, M., Gallazzi, F., Protti, M.P., Sinigaglia, F., Hammer, J. 1999. Generation of tissue-specific and promiscuous HLA ligand databases using DNA microarrays and virtual HLA class II matrices. *Nat Biotechnol*, 17(6), 555-61.

242. Subbarao, K., Matsuoka, Y. 2013. The prospects and challenges of universal vaccines for influenza. *Trends Microbiol*, 21(7), 350-8.

243. Sugrue, R., Bahadur, G., Zambon, M., Hall-Smith, M., Douglas, A., Hay, A. 1990. Specific structural alteration of the influenza haemagglutinin by amantadine. *The EMBO journal*, 9(11), 3469.

244. Sun, J., Braciale, T.J. 2013. Role of T cell immunity in recovery from influenza virus infection. *Curr Opin Virol*, 3(4), 425-9.

245. Sun, J., Madan, R., Karp, C.L., Braciale, T.J. 2009. Effector T cells control lung inflammation during acute influenza virus infection by producing IL-10. *Nat Med*, 15(3), 277-84.

246. Sun, Y., Liu, J., Yang, M., Gao, F., Zhou, J., Kitamura, Y., Gao, B., Tien, P., Shu, Y., Iwamoto, A., Chen, Z., Gao, G.F. 2010. Identification and structural definition of

H5-specific CTL epitopes restricted by HLA-A*0201 derived from the H5N1 subtype of influenza A viruses. *J Gen Virol*, 91(Pt 4), 919-30.

247. Sundar, K., Boesen, A., Coico, R. 2007. Computational prediction and identification of HLA-A2.1-specific Ebola virus CTL epitopes. *Virology*, 360(2), 257-63.

248. Sundararajan, A., Huan, L., Richards, K.A., Marcelin, G., Alam, S., Joo, H., Yang, H., Webby, R.J., Topham, D.J., Sant, A.J., Sangster, M.Y. 2012. Host differences in influenza-specific CD4 T cell and B cell responses are modulated by viral strain and route of immunization. *PLoS One*, 7(3), e34377.

249. Suri, C., Joshi, H.C., Naik, P.K. 2015. Molecular modeling reveals binding interface of gamma-tubulin with GCP4 and interactions with noscapinoids. *Proteins*, 83(5), 827-43.

250. Tao, W., Ziemer, K.S., Gill, H.S. 2014. Gold nanoparticle-M2e conjugate coformulated with CpG induces protective immunity against influenza A virus. *Nanomedicine (Lond)*, 9(2), 237-51.

251. Terajima, M., Ennis, F.A. 2012. Nuclear export signal and immunodominant CD8+ T cell epitope in influenza A virus matrix protein 1. *J Virol*, 86(18), 10258.

252. Tong, S., Zhu, X., Li, Y., Shi, M., Zhang, J., Bourgeois, M., Yang, H., Chen, X., Recuenco, S., Gomez, J. 2013. New world bats harbor diverse influenza A viruses. *PLoS Pathog*, 9(10), e1003657.

253. Toseland, C.P., Clayton, D.J., McSparron, H., Hemsley, S.L., Blythe, M.J., Paine, K., Doytchinova, I.A., Guan, P., Hattotuwagama, C.K., Flower, D.R. 2005. AntiJen: a quantitative immunology database integrating functional, thermodynamic, kinetic, biophysical, and cellular data. *Immunome Res*, 1(1), 4.

254. Trost, B., Bickis, M., Kusalik, A. 2007. Strength in numbers: achieving greater accuracy in MHC-I binding prediction by combining the results from multiple prediction tools. *Immunome Res*, 3, 5.

255. Trott, O., Olson, A.J. 2010. AutoDock Vina: improving the speed and accuracy of docking with a new scoring function, efficient optimization, and multithreading. *J Comput Chem*, 31(2), 455-61.

256. Tung, C.W., Ho, S.Y. 2007. POPI: predicting immunogenicity of MHC class I binding peptides by mining informative physicochemical properties. *Bioinformatics*, 23(8), 942-9.

257. Tung, C.W., Ziehm, M., Kamper, A., Kohlbacher, O., Ho, S.Y. 2011. POPISK: T-cell reactivity prediction using support vector machines and string kernels. *BMC Bioinformatics*, 12(1), 446.

258. Turley, C.B., Rupp, R.E., Johnson, C., Taylor, D.N., Wolfson, J., Tussey, L., Kavita, U., Stanberry, L., Shaw, A. 2011. Safety and immunogenicity of a recombinant M2e-flagellin influenza vaccine (STF2.4xM2e) in healthy adults. *Vaccine*, 29(32), 5145-52.

259. Tweed, S.A., Skowronski, D.M., David, S.T., Larder, A., Petric, M., Lees, W., Li, Y., Katz, J., Krajden, M., Tellier, R., Halpert, C., Hirst, M., Astell, C., Lawrence, D., Mak, A. 2004. Human illness from avian influenza H7N3, British Columbia. *Emerg Infect Dis*, 10(12), 2196-99.

260. Ungchusak, K., Auewarakul, P., Dowell, S.F., Kitphati, R., Auwanit, W., Puthavathana, P., Uiprasertkul, M., Boonnak, K., Pittayawonganon, C., Cox, N.J., Zaki, S.R., Thawatsupha, P., Chittaganpitch, M., Khontong, R., Simmerman, J.M., Chunsutthiwat, S. 2005. Probable person-to-person transmission of avian influenza A (H5N1). *N Engl J Med*, 352(4), 333-40.

261. Vijayan, R., Subbarao, N., Manoharan, N. 2015. *In silico* analysis of conformational changes induced by normal and mutation of macrophage infectivity potentiator catalytic residues and its interactions with rapamycin. *Interdiscip Sci*, 7(3), 326-33.

262. Vita, R., Overton, J.A., Greenbaum, J.A., Ponomarenko, J., Clark, J.D., Cantrell, J.R., Wheeler, D.K., Gabbard, J.L., Hix, D., Sette, A., Peters, B. 2015. The immune epitope database (IEDB) 3.0. *Nucleic Acids Res*, 43(Database issue), D405-12.

263. Wang, B.Z., Gill, H.S., He, C., Ou, C., Wang, L., Wang, Y.C., Feng, H., Zhang, H., Prausnitz, M.R., Compans, R.W. 2014. Microneedle delivery of an M2e-TLR5 ligand fusion protein to skin confers broadly cross-protective influenza immunity. *J Control Release*, 178, 1-7.

264. Wang, W., Li, R., Deng, Y., Lu, N., Chen, H., Meng, X., Wang, W., Wang, X., Yan, K., Qi, X., Zhang, X., Xin, W., Lu, Z., Li, X., Bian, T., Gao, Y., Tan, W., Ruan, L. 2015. Protective efficacy of the conserved NP, PB1, and M1 proteins as immunogens in DNA- and vaccinia virus-based universal influenza A virus vaccines in Mice. *Clin Vaccine Immunol*, 22(6), 618-30.

265. Wang, Y., Zhou, L., Shi, H., Xu, H., Yao, H., Xi, X.G., Toyoda, T., Wang, X., Wang, T. 2009. Monoclonal antibody recognizing SLLTEVET epitope of M2 protein potently inhibited the replication of influenza A viruses in MDCK cells. *Biochem Biophys Res Commun*, 385(1), 118-22.

266. Watanabe, T., Watanabe, S., Noda, T., Fujii, Y., Kawaoka, Y. 2003. Exploitation of nucleic acid packaging signals to generate a novel influenza virus-based vector stably expressing two foreign genes. *J Virol*, 77(19), 10575-83.

267. Webby, R.J., Webster, R.G. 2001. Emergence of influenza A viruses. *Philos Trans R Soc Lond B Biol Sci*, 356(1416), 1817-28.

268. Weichert, H., Blechschmidt, I., Schroder, S., Ambrosius, H. 1991. The MTT-assay as a rapid test for cell proliferation and cell killing: application to human peripheral blood lymphocytes (PBL). *Allerg Immunol (Leipz)*, 37(3-4), 139-44.

269. Weis, W.I., Brünger, A.T., Skehel, J.J., Wiley, D.C. 1990. Refinement of the influenza virus hemagglutinin by simulated annealing. *J mol biol*, 212(4), 737-61.

270. WHO. 1980. A revision of the system of nomenclature for influenza viruses: a WHO memorandum. *Bull World Health Organ*, 58(4), 585-91.

271. WHO. 2003. Avian influenza in the Netherlands, Vol. 2016. http://www.who.int/csr/don/2003_04_24/en/#

272. WHO. 2005. Ten things you need to know about pandemic influenza, Vol. 2016. 2005.

273. WHO. 2010. Pandemic (H1N1) 2009 - update 112, Vol. 2016. http://www.who.int/csr/don/2010_08_06/en/#

274. WHO. 2013. Influenza at the human animal interface, Vol. 2016. http://www.who.int/influenza/human_animal_interface/Influenza_Summary_IRA_HA_interface_20December13.pdf

275. WHO. 2014. Influenza (Seasonal) Fact sheet N°211, Vol. 2016. http://www.who.int/mediacentre/factsheets/fs211/en/

276. WHO. 2014a. Status of Vaccine Research and Development of Universal Influenza Vacci http://who.int/immunization/research/meetings_workshops/Universal_Influenza_VaccineRD_Sept2014.pdf

277. WHO. 2015. Human infection with avian influenza A(H5N6) virus – China, Vol. 2016. http://www.who.int/csr/don/12-february-2015-avian-influenza/en/#

278. WHO. 2015a. Influenza at the human-animal interface, Vol. 2015. http://www.who.int/influenza/human_animal_interface/Influenza_Summary_IRA_HA_interface_15October_2015.pdf

279. WHO. 2016. Human infection with avian influenza A(H7N9) virus – China, Vol. 2016. http://www.who.int/csr/don/10-february-2016-avian-influenza-china/en/#

280. WHO. 2016a. Archives of the smallpox eradication programme, Vol. 2016. http://www.who.int/archives/fonds_collections/bytitle/fonds_6/en/#

281. WHO. 2016b. Influenza at the human animal interface, Vol. 2016. http://www.who.int/influenza/human_animal_interface/Influenza_Summary_IRA_HA_interface_25_02_2016.pdf?ua=1

282. WHO. 2016c. Poliomyelitis Fact sheet, Vol. 2016. http://www.who.int/mediacentre/factsheets/fs114/en/#

283. Wiersma, L., Rimmelzwaan, G.F., de Vries, R.D. 2015. Developing Universal Influenza Vaccines: Hitting the Nail, Not Just on the Head. *Vaccines*, 3(2), 239-62.

284. Wise, H.M., Foeglein, A., Sun, J., Dalton, R.M., Patel, S., Howard, W., Anderson, E.C., Barclay, W.S., Digard, P. 2009. A complicated message: Identification of a novel PB1-related protein translated from influenza A virus segment 2 mRNA. *J Virol*, 83(16), 8021-31.

285. Wise, H.M., Hutchinson, E.C., Jagger, B.W., Stuart, A.D., Kang, Z.H., Robb, N., Schwartzman, L.M., Kash, J.C., Fodor, E., Firth, A.E. 2012. Identification of a novel splice variant form of the influenza A virus M2 ion channel with an antigenically distinct ectodomain. *PLoS pathogens*, 8(11), e1002998.

286. Wohlbold, T.J., Nachbagauer, R., Xu, H., Tan, G.S., Hirsh, A., Brokstad, K.A., Cox, R.J., Palese, P., Krammer, F. 2015. Vaccination with adjuvanted recombinant neuraminidase induces broad heterologous, but not heterosubtypic, cross-protection against influenza virus infection in mice. *MBio*, 6(2), e02556.

287. Woodland, D.L. 2004. Jump-starting the immune system: prime-boosting comes of age. *Trends Immunol*, 25(2), 98-104.

288. Woodland, D.L. 2016. Influenza Vaccines. *Viral Immunol*, 29(4), 197.

289. Wullner, D., Zhou, L., Bramhall, E., Kuck, A., Goletz, T.J., Swanson, S., Chirmule, N., Jawa, V. 2010. Considerations for optimization and validation of an in vitro PBMC

derived T cell assay for immunogenicity prediction of biotherapeutics. *Clin Immunol*, 137(1), 5-14.

290. Yang, I.S., Lee, J.Y., Lee, J.S., Mitchell, W.P., Oh, H.B., Kang, C., Kim, K.H. 2009. Influenza sequence and epitope database. *Nucleic Acids Res*, 37(Database issue), D423-30.

291. Yang, J., James, E., Gates, T.J., DeLong, J.H., LaFond, R.E., Malhotra, U., Kwok, W.W. 2013. CD4+ T cells recognize unique and conserved 2009 H1N1 influenza hemagglutinin epitopes after natural infection and vaccination. *Int Immunol*, 25(8), 447-57.

292. Yang, J., James, E.A., Huston, L., Danke, N.A., Liu, A.W., Kwok, W.W. 2006. Multiplex mapping of CD4 T cell epitopes using class II tetramers. *Clin Immunol*, 120(1), 21-32.

293. Yasmin, T., Akter, S., Debnath, M., Ebihara, A., Nakagawa, T., Nabi, A.H.M.N. 2016. In silico proposition to predict cluster of B- and T-cell epitopes for the usefulness of vaccine design from invasive, virulent and membrane associated proteins of C. jejuni. *In Silico Pharmacology*, 4(1), 1-10.

294. Ye, Q., Krug, R.M., Tao, Y.J. 2006. The mechanism by which influenza A virus nucleoprotein forms oligomers and binds RNA. *Nature*, 444(7122), 1078-82.

295. Zambon, M.C. 1999. Epidemiology and pathogenesis of influenza. *J Antimicrob Chemother*, 44 (B), 3-9.

296. Zhang, G.L., Petrovsky, N., Kwoh, C.K., August, J.T., Brusic, V. 2006. PRED(TAP): a system for prediction of peptide binding to the human transporter associated with antigen processing. *Immunome Res*, 2(1), 1.

297. Zhang, H., Lund, O., Nielsen, M. 2009. The PickPocket method for predicting binding specificities for receptors based on receptor pocket similarities: application to MHC-peptide binding. *Bioinformatics*, 25(10), 1293-9.

298. Zhang, H., Wang, L., Compans, R.W., Wang, B.Z. 2014. Universal influenza vaccines, a dream to be realized soon. *Viruses*, 6(5), 1974-91.

299. Zhang, X.W. 2013. A combination of epitope prediction and molecular docking allows for good identification of MHC class I restricted T-cell epitopes. *Comput Biol Chem*, 45, 30-5.

300. Zhuge, Z.-Y., Zhu, Y.-H., Liu, P.-Q., Yan, X.-D., Yue, Y., Weng, X.-G., Zhang, R., Wang, J.-F. 2012. Effects of Astragalus polysaccharide on immune responses of porcine PBMC stimulated with PRRSV or CSFV. *PLoS ONE*, 7(1), e29320.

301. Zürcher, T., Marión, R.M., Ortín, J. 2000. Protein synthesis shut-off induced by influenza virus infection is independent of PKR activity. *J Virol*, 74(18), 8781-4.

Appendix A

A comparison table of hemagglutinin peptides induced PBMC proliferation and Interferon (IFN)-γ secretion in each sample

	P_H1		P_H2	
	SI* of PBMC	FI# in IFN-γ	SI of PBMC	FI in IFN-γ
Sample 1	1.36	2.26	1.25	1.21
Sample 2	2.03	2.29	2.26	1.35
Sample 3	1.70	2.84	0.95	1.55
Sample 4	1.26	2.44	1.13	1.19
Sample 5	0.93	1.70	1.35	1.00
Sample 6	1.16	2.09	1.63	4.70
Sample 7	1.06	1.84	0.81	1.22

* SI: Stimulation index (SI) is the ratio of average absorbance of the peptide stimulated cells and unstimulated cells measured at 570/630 nm.

FI: Fold change: Fold change is the ratio of average absorbance of the peptide stimulated cells and unstimulated cells at 405/620 nm.

Appendix B

A comparison table of neuraminidase peptides induced PBMC proliferation and Interferon (IFN)-γ secretion in each sample

	P_N2		P_N4		P_N5		P_N6	
	SI* of PBMC	FI# in Interferon-γ	SI of PBMC	FI in Interferon-γ	SI of PBMC	FI in Interferon-γ	SI of PBMC	FI in Interferon-γ
Sample 1	2.40	1.12	1.23	0.87	0.44	0.81	1.37	0.75
Sample 2	1.94	1.26	0.94	3.63	1.09	0.81	1.16	3.60
Sample 3	1.02	0.92	0.99	0.97	1.10	1.33	1.20	0.97
Sample 4	0.92	0.77	1.04	0.95	1.02	0.73	1.22	1.14
Sample 5	0.90	0.74	1.00	0.98	2.06	1.36	1.54	0.99
Sample 6	1.28	2.19	0.98	0.85	1.05	1.29	1.11	0.86
Sample 7			1.16	2.12	1.37	1.86	1.56	1.43

* SI: Stimulation index (SI) is the ratio of average absorbance of the peptide stimulated cells and unstimulated cells measured at 570/630 nm.

FI: Fold change: Fold change is the ratio of average absorbance of the peptide stimulated cells and unstimulated cells at 405/620 nm.

Appendix C

A comparison table of matrix 1 peptides induced PBMC proliferation and Interferon (IFN)-γ secretion in each sample

	P_M1		P_M2		P_M3	
	SI* of PBMC	FI# in Interferon-γ	SI of PBMC	FI in Interferon-γ	SI of PBMC	FI in Interferon-γ
Sample 1	2.07	0.89	1.23	0.85	1.37	3.32
Sample 2	2.34	0.82	1.22	0.76	1.51	3.08
Sample 3	3.61	1.30	2.52	1.17	1.83	2.19
Sample 4	3.17	1.89	2.39	1.12	1.64	2.41
Sample 5	1.16	0.74	1.13	1.23	0.56	1.72
Sample 6	1.41	0.86	1.23	2.14	0.54	2.08
Sample 7	1.44	2.22	1.27	1.58		

* SI: Stimulation index (SI) is the ratio of average absorbance of the peptide stimulated cells and unstimulated cells measured at 570/630 nm.

FI: Fold change: Fold change is the ratio of average absorbance of the peptide stimulated cells and unstimulated cells at 405/620 nm.

VIRAL IMMUNOLOGY
Volume 27, Number 5, 2014

Pp. 225–234
DOI: 10.1089/vim.2013.0135

Conserved Peptides Containing Overlapping CD4+ and CD8+ T-Cell Epitopes in the H1N1 Influenza Virus: An Immunoinformatics Approach

Neha Lohia and Manoj Baranwal

Abstract

Pandemic threats of the H1N1 influenza virus have drawn attention to developing a universal vaccine against circulating and future strains of this virus. An immunoinformatics study was conducted to identify conserved peptides containing CD4+ and CD8+ T-cell epitopes from all the hemagglutinin (HA) and neuraminidase (NA) protein sequences available until February 2013 to cover the seasonal as well as the pandemic strains of the H1N1 virus. In the present study, six different immunoinformatics prediction programs were used in order to define the epitopes. Five conserved peptides of HA and six of NA protein were obtained that contained overlapping CD4+ and CD8+ T-cell epitopes. These identified peptides have a binding affinity for a large number of major histocompatibility complex (MHC) alleles. WHGSNRPWVSF of NA protein is a new peptide whose T-cell response has not been previously reported. Population coverage studies have shown that these peptide fragments have the capacity to induce a potent immune response among individuals from different populations around the world. Hence, these HA and NA peptides may be considered as interesting candidates for vaccine design.

Introduction

Influenza A virus belongs to the orthomyxovirdae family of viruses associated with acute respiratory illness in a wide range of avian and mammalian species. Their classification depends upon the serologic reactivity of surface glycoprotein hemagglutinin (HA) and neuraminidase (NA). Seventeen serotypes of HA (49) and 10 serotypes of NA are currently in circulation in avian and mammalian hosts (25).

The evolution of new escape variants of influenza A virus has given rise to influenza epidemics and periodic pandemics worldwide. Variability is introduced by point mutations within HA and NA by virtue of error-prone replication cycles of the virus inside the host, resulting in antigenic drift and therefore the rise of epidemic strains every 1–2 years. Additionally, because of the segmented nature of the genome (eight single-stranded negative sense RNA segments), genetic reassortment occurs during co-circulation of various influenza A virus subtypes, resulting in the replacement of HA or NA subtypes with novel ones and giving rise to new virus subtypes that have never been in human circulation. This antigenic shift results in global pandemics if the new virus easily sustains person-to-person transmission. Genetic diversity also bestows these viruses with a dynamic adjustability to their habitats, leading to quick selection of genomic variants that combat the immune responses of infected hosts.

Envelope glycoproteins HA and NA are primarily associated with the pathogenesis of the influenza virus. HA is a homotrimeric molecule in which each protomer is composed of a HA1 and HA2 subunit linked by a disulfide bond and is attached to the virion membrane via carboxy-terminal of the HA2 subunit. HA aids the entry of the viral genome into the infected cells by binding to sialic acid-containing receptors via the HA1 subunit on the surface of the host cells, thus causing the fusion of the viral envelope with the host endosomal membrane via N-terminal fusion peptide of the HA2 subunit (8,44). NA is a mushroom-shaped homotetrameric protein on the surface of the influenza virus, which catalyzes the cleavage of terminal sialic acid linked α-ketosidically to an array of surface biomolecule-like glycoproteins and glycolipids. The removal of sialic acid from the surface of the infected cell as well as new virions is considered essential for the release of viral progeny from the host cell (42). Also, sialic acid removal from mucins, glycocalix, and cilia of the respiratory tract restricts virus access to the membrane receptors of the target cells (26).

The H1N1 subtype of the influenza A virus has been responsible for two disastrous pandemics in the last 100 years: Spanish flu in 1918–1919, which was responsible for the global mortality of 50 million people (22), and Swine flu in 2009–2010, which caused 18,449 deaths worldwide (52). Emergence of novel strains or subtypes of H1N1 often lead to

Department of Biotechnology, Thapar University, Patiala, India.

seasonal and pandemic outbreaks. Monitoring antigenic drift and shift in the H1N1 virus is critical, not only to anticipate changes in virulence but also to reformulate vaccines against the circulating strains from time to time. The long detention time from pandemic strain isolation to wide-scale generation of a vaccine can prove highly detrimental in a pandemic situation. One way to overcome the need to update the vaccine each time is to design a universal vaccine that will provide protection against any H1N1 strain. Such a vaccine would be effective against all current and future strains of H1N1 virus, as opposed to the current vaccines, which are effective only against the known circulating virus strains (20).

The significant role of T-cell responses in handling viral infections underscores the importance of T-cell epitope identification. T-cell responses have been associated with a reduction in pathology and recovery in *in vivo* models (38) and *ex vivo* studies carried out in immunized humans (27). Swain *et al.* have suggested that both CD4+ and CD8+ T-cells participate in primary viral clearance, as well as contributing toward an anamnestic response during influenza virus infection (47). CD8+ T-cells eliminate infected cells via contact-dependent lysis and perforin-mediated cytotoxicity (10), whereas CD4+ T-cells exert their antiviral activity via lymphokine production and CD4+-driven B-cell responses, boosting the production of influenza virus-specific antibodies (5). Hence, a T-cell epitope-based vaccine that is directed against the conserved regions of viral proteins should be developed. By employing the conventional approach, some of the transiently expressed proteins may be overlooked for their candidature as an antigenic epitope. Moreover, abundantly expressed proteins are not necessarily strong candidates for vaccine (13). Immunoinformatics-driven T-cell epitope mapping and prediction algorithms appear to be leading the charge in identifying novel epitopes, which can be used as vaccines against hypervariable viruses such as H1N1 as well as various other diseases.

Acknowledging the critical role of HA and NA in the pathogenesis of influenza, the focus of the present study is to identify conserved immunogenic peptides from HA and NA that can provide coverage against globally distributed strains of H1N1 by applying an *in silico* approach. A combination of various immunoinformatics prediction tools was exercised separately for CD4+ and CD8+ T-cell epitopes to obtain a set of probable candidates for a peptide-based universal influenza vaccine.

Materials and Methods

Conserved peptides identification

Full-length hemagglutinin (HA) and neuraminidase (NA) protein sequences of H1N1, infecting humans all over the world from January 1918 to February 2013, were retrieved from the National Center for Biotechnology Information (NCBI) influenza virus resource database. The protein sequences were aligned using Multiple Sequence Comparison by Log-Expectation (MUSCLE) (12). The Antigen Variability ANAlyzer (AVANA) tool was used to find the conserved peptide stretch ($\geq$9 amino acids) of aligned sequences that showed at least 80% conservancy of the reported H1N1 HA and NA peptide sequences (28). In this study, ''conservation'' means identical peptide sequences that are present in at least 80% of total HA and NA protein sequences.

CD8+ T-cell binding peptide prediction

Three different immunoinformatics tools—NetCTL v1.2 (24), BIMAS (34), and SYFPEITHI (39)—were employed to predict nonamers that have the ability to bind class I MHC (HLA) molecules.

NetCTL v1.2 predicts CD8+ T-cell epitopes for 12 supertypes of class I major histocompatibility complex (MHC) taking into account TAP transport efficiency, C terminal cleavage, and MHC class I binding peptide. BIMAS identifies epitopes that contain allele-specific binding motifs for 33 HLA class I alleles (9 HLA-A, 20 HLA-B, and 4 HLA-C) based on measurement of the dissociation half-life of ($t_{1/2}$) of β_2 microglobulin (34). The algorithm generates and scans all possible overlapping nonamers against each one of the 33 HLA alleles. The SYFPEITHI database is a collection of class I and class II MHC ligands and peptide motifs of human and other species, which are continuously updated. The prediction is based on reported motifs and takes into account the amino acids in the anchor and auxiliary anchor locus, as well as other frequently appearing amino acids. The scoring system assesses every amino acid within a given peptide, and allocates a score based on the frequency of the respective amino acids in natural ligands, T-cell epitopes, or binding peptides. Different threshold scores were considered for each tool in the initial prediction of CD8+ T-cell epitopes. In NetCTL and SYPFEITHI, threshold scores were 0.75 and 13 respectively. Further predicted epitopes from each tool were compared to find the common epitopes. Peptides were only defined as epitopes and selected for further analysis when they were commonly predicted by all three tools.

CD4+ T-cell binding peptide prediction

The MHC class II complex presents peptides to CD4+ T-helper lymphocytes that evoke cellular and antibody mediated immunity against the foreign antigen. Three different tools were used to predict class II MHC restricted epitopes: SMM align (31), NetMHC II (30), and ProPred (43). SMM align attempts to recognize MHC class II binding motifs by generating a position-specific weight matrix that ideally reproduces the IC_{50} affinity values for each peptide (31). NetMHC II v2.2 predicts epitope binding to 14 HLA-DR, 6 HLA-DQ, and 6 HLA-DP alleles using artificial neural networks. Results are expressed in terms of IC_{50} and percentage rank to a set of 1,000,000 random natural peptides. ProPred is a matrix-based prediction algorithm for class II MHC prediction, which employs a literature-based amino-acid/position coefficient table (43). In SMM align and NetMHC II, the threshold for IC_{50} was taken as 500 nM for the prediction of CD4+ epitopes. Peptides were considered as epitopes only when they were commonly predicted by each tool, as discussed for the prediction of CD8+ epitopes.

BLAST screening

The similarity of the host self protein may lead to an immunogenic response against the self antigen, which may lead to autoimmunity. Hence, in order to obtain nonself and novel epitopes, peptides predicted for class I and II MHC molecules were analyzed for their homology with annotated human proteome using BLAST (1). Nonamers sharing a minimum of seven out of nine identical amino acid sequences with the human peptides, without gaps or mismatches, were eliminated

from further consideration (48). The final conserved epitopes showing an overlap were merged into a single peptide fragment.

Mapping of conserved regions and peptide fragments

The Discovery Studio v3.5 visualizer tool was used to locate the conserved regions and predicted peptide fragments of HA and NA identified on the three-dimensional structure of the respective protein. The protein structure available in the PDB data for HA (A/California/04/2009 [H1N1]; PDB id; 3LZG) and NA (A/California/04/2009 [H1N1]; PDB id 3TI3) was used as the base structure to visualize the conserved regions, as well as the predicted peptide fragments of HA and NA proteins respectively.

HLA distribution analysis

Because of the extremely polymorphic nature of HLA alleles and their variation among populations from different geographical areas, population coverage analysis becomes important. The population coverage tool by IEDB (7) calculates the proportion of individuals responding to a given set of epitopes with known HLA restriction using the peptide-MHC data and HLA genotypic frequency. Analysis of the peptides was carried out for 78 populations across 11 geographical zones and in Indian populations. HLA allele frequency data for the Indian population (North India and Delhi) were obtained from the Allele Frequency Net Database (16).

Results

Conserved peptides of HA and NA protein of the H1N1 virus

In order to cover the majority of genetic variants of H1N1 isolates around the world, 3,661 HA and 2,079 NA protein sequences were obtained after removing the redundant sequences. Because of the frequent antigenic variations in H1N1, previously identified epitopes may lose their potency to generate an immune response against all the variants. Hence, it is important to find those peptides of HA and NA proteins that are conserved across the various strains of the H1N1 virus. The MUSCLE tool was used in the present study to align the protein sequences, and then conservation of the sequences was estimated using the AVANA tool. In the HA protein of the H1N1 virus, 12 peptide regions (CS_H1–CS_H12), ranging from 11 to 43 amino acids, were found to be conserved, out of which the first three were confined to HA1 and remaining nine were located in the HA2 subunit of HA (Table 1). Fifteen conserved regions were identified in the NA protein (CS_N1–CS_N15) ranging in size from 9 to 28 amino acids (Table 2). Two conserved sequences of HA (CS_H11 and CS_H12) and NA (CS_N1 and CS_N2) were found to be located in the transmembrane and cytoplasmic domains of the respective protein. These 12 (for

Table 1. Conserved Peptide Fragments of H1N1 Virus Hemagglutinin Protein

	Conserved peptide sequence	*Length*
CS_H1	CIGYHANNSTDTVDTVLEKNVTV THSVNLLE	31
CS_H2	AGWILGNPECE	11
CS_H3	YEELREQLSSVSSFERFEIFPK	22
CS_H4	PSIQSRGLFGAIAGFIEGGWTGMVDG WYGYHHQNEQGSGYAAD	43
CS_H5	ITNKVNSVIEKMNTQFTAVGKEFN	24
CS_H6	ENLNKKVDDGF	11
CS_H7	DIWTYNAELLVLLENERTLD	20
CS_H8	HDSNVKNLYEKV	12
CS_H9	QLKNNAKEIGNGCFEFYHKC	20
CS_H10	CMESVKNGTYDYPKYSEE	18
CS_H11	YQILAIYSTVASSLVL	16
CS_H12	VSLGAISFWMCS	12

Table 2. Conserved Peptide Fragments of H1N1 Virus Neuraminidase Protein

	Conserved peptide sequence	*Length*
CS_N1	MNPNQKIITIGS	12
CS_N2	LQIGNIISIW	10
CS_N3	KDNSIRIGSKGDVFVIREPFISCS	24
CS_N4	LECRTFFLTQGALLNDKHSNGT	22
CS_N5	FESVAWSASACHDG	14
CS_N6	WLTIGISGPDNGAVAVLKYNGIIT	24
CS_N7	ILRTQESEC	9
CS_N8	YEECSCYPD	9
CS_N9	CVCRDNWHGSNRPWVSFNQNL	21
CS_N10	YQIGYICSG	9
CS_N11	YGNGVWIGRTKS	12
CS_N12	GFEMIWDPNGWT	12
CS_N13	WSGYSGSFVQHPELTGLDCIRPC FWVEL	28
CS_N14	TIWTSGSSISFCGVNSDT	18
CS_N15	WSWPDGAELPFTIDK	15

Table 3. Predicted CD4+ and CD8+ T-Cell Epitopes of H1N1 Virus Hemagglutinin Protein

Conserved sequence	*$CD8^+$ T-cell epitopes*	*$CD4^+$ T-cell epitopes*
CS_H1	DTVDTVLEK STDTVDTVL TVLEKNVTV TVTHSVNLL	LEKNVTVTH VTVTHSVNL
CS_{H3}	VSSFERFEI SSFERFEIF	LSSVSSFER
CS_H4	GLFGAIAGF GMVDGWYGY IAGFIEGGW WTGMVDGWY HQNEQGSGY	FGAIAGFIE
CS_H5	KMNTQFTAV KVNSVIEKM QFTAVGKEF	IEKMNTQFT MNTQFTAVG
CS_H7		LVLLENERT
CS_H8	HDSNVKNLY	
CS_H9	EIGNGCFEF	
CS_H10	MESVKNGTY SVKNGTYDY	
CS_H11	IYSTVASSL QILAIYSTV STVASSLVL YQILAIYST	ILAIYSTVA IYSTVASSL LAIYSTVAS YQILAIYST
CS_H12	SLGAISFWM VSLGAISFW	

Table 4. H1N1 Hemagglutinin Peptides Containing Overlapping $CD4^+$ and $CD8^+$ T-Cell Epitopes

	Peptides enriched $CD8^+$ T-cell epitope	*No. of epitopes*	*Peptides enriched $CD4^+$ T-cell epitopes*	*No. of epitopes*	*Fragments containing $CD4^+$ and $CD8^+$ T-cell epitopes*
CS_H1	STDTVDTVLEKNVTVTHSVNLL	4	LEKNVTVTHSVNL	2	STDTVDTVLEKNVTVTHSVNLL
CS_H3	VSSFERFEIF	2	LSSVSSFER	1	LSSVSSFERFEIF
CS_H4	GLFGAIAGFIEGGWTGMVDGWYGY	4	FGAIAGFIE	1	GLFGAIAGFIEGGWTGMVDGWYGY
	HQNEQGSGY	1			
CS_H5	KVNSVIEKMNTQFTAVGKEF	3	IEKMNTQFTAVG	2	KVNSVIEKMNTQFTAVGKEF
CS_H7			LVLLENERT	1	
CS_H8	HDSNVKNLY	1			
CS_H9	EIGNGCFEF	1			
CS_H10	MESVKNGTYDY	2			
CS_H11	YQILAIYSTVASSLVL	4	YQILAIYSTVASSL	4	YQILAIYSTVASSLVL
CS_H12	VSLGAISFWM	2			

HA) and 15 (for NA) conserved peptides were selected for epitope prediction.

Identification of CD4+ and CD8+ T-cell epitopes for HA protein

HA is an antigenic glycoprotein that is present on the surface of the H1N1 virus and is associated with membrane fusion and pathogenesis. Since different tools use different parameters to assess the MHC binding epitope, it is interesting to look for those epitopes that are predicted by more than one tool. Different immunoinformatics tools were used for CD8+ T-cell epitopes (NetCTL, BIMAS, and Syfpeithi) and CD4+ T-cell epitopes prediction (NetMHCII, ProPred, and IEDB SMM align). All the predicted epitopes were compared, and then a set of epitopes was obtained that was predicted by all the tools. Initially, 32 putative CD8+ T-cell epitopes (MHC class I binding epitopes) and 12 CD4+ T-cell epitopes (MHC class II binding epitopes) were identified for the HA protein. After BLAST analysis, eight of the predicted CD8+ T-cell epitopes and one of predicted CD4+ T-cell epitopes were found to be homologous to a few human proteins (data not shown), and so these epitopes were eliminated from further consideration. Twenty-four CD8+ and and 11 CD4+ T-cell epitopes were selected that are nonself in humans (Table 3).

Among the CD8+ T-cell epitopes, six were confined to the HA1 subunit, and 18 were confined to the HA2 subunit of the HA protein. In the case of the CD4+ T-cell epitopes, three were located in the HA1 subunit and the remaining eight were in the HA2 subunit of the HA protein. Six and four epitopes binding to class I and II MHC respectively were located in the transmembrane/cytoplasmic domain of H1N1 HA.

As per our epitope selection criteria, none of the CD8+ T-cell epitopes was found in the three conserved regions (CS_H2, CS_H6, and CS_H7). Also, in six conserved regions (CS_H2, CS_H6, CS_H8, CS_H9, CS_H10, and CS_H12), no CD4+ T-cell epitopes could be found.

The epitopes that had overlapping amino acid sequences were merged to generate a single peptide fragment. Hence, 10 MHC class I binding peptides (each containing single or multiple epitopes) ranging in length from 9 to 24 amino acids were obtained after merging. Similarly, six MHC class II binding peptides of 9 to 14 amino acids were also obtained. Finally, we obtained five peptides (two peptides in the HA1 subunit and three peptides in the HA2 subunit) that contained both CD4+ and CD8+ T-cell epitopes (Table 4). MHC is highly polymorphic. Hence, it is better if the peptide is predicted for a large number of alleles. All five selected peptides were predicted for a large group of alleles and have more than 90% conservancy (Table 5).

Identification of CD4+ and CD8+ T-cell epitopes for NA protein

NA is another surface glycoprotein involved in viral budding and the release of viral progeny. Conserved peptides of NA protein were considered to predict the CD4+ and CD8+ T-cell epitopes. Epitope prediction for each class was done in the same way as for the HA protein. Thirteen MHC I binding epitopes located in eight conserved regions and nine MHC class II epitopes in six conserved regions were selected based on the criteria that they should be predicted by each tool (Table 6). BLAST analysis of NA revealed that none of the predicted CD4+ and CD8+ T-cell epitopes of NA was homologous to the human proteome.

Table 5. Final Set of Peptides of H1N1 Hemagglutinin Containing Both CD4+ and CD8+ T-Cell Epitopes in Different Subunits of Hemagglutinin Protein Predicted to Bind Large Numbers of Major Histocompatibility Complex Alleles

	Peptide	*Subunit*	*No. of class I MHC alleles*	*No. of class II MHC alleles*	*Conservation (%)*
P_H1	STDTVDTVLEKNVTVTHSVNLL	HA1	26	12	90.4
P_H2	LSSVSSFERFEIF	HA1	20	17	95.7
P_H3	GLFGAIAGFIEGGWTGMVDGWYGY	HA2	17	7	91.5
P_H4	KVNSVIEKMNTQFTAVGKEF	HA2	13	15	95.5
P_H5	YQILAIYSTVASSLVL	HA2	23	49	96.6

MHC, major histocompatibility complex.

Table 6. Predicted CD4+ and CD8+ T-Cell Epitopes of H1N1 Virus Neuraminidase Protein

Conserved sequence	*CD8+ T-cell epitopes*	*CD4+ T-cell epitopes*
CS_N2	LQIGNIISI QIGNIISIW	LQIGNIISI
CS_N3	DVFVIREPF VFVIREPFI	FVIREPFIS IRIGSKGDV
CS_N4	FFLTQGALL	FFLTQGALL FLTQGALLN
CS_N6	GPDNGAVAV	
CS_N9	GSNRPWVSF	WHGSNRPWV
CS_N13	GSFVQHPEL IRPCFWVEL VQHPELTGL	FVQHPELTG
CS_N14	TIWTSGSSI WTSGSSISF	ISFCGVNSD WTSGSSISF
CS_N15	WPDGAELPF	

Two epitopes binding to class I and one to class II MHC were confined to the transmembrane/cytoplasmic domain of the protein. We also observed that seven (CS_N1 CS_N5, CS_N7, CS_N8, CS_N10, CS_N11, and CS_N12) conserved regions failed to predict common CD4+ and CD8+ T-cell epitopes.

After considering the overlapping epitopes, nine MHC class I binding peptides (length 9–12 amino acids) and six MHC class II binding peptides (length 9–18 amino acids) were obtained. Finally, six conserved peptides sequences were generated that contained overlapping CD4+ and CD8+ T-cell epitopes (Table 7). All six selected peptides were predicted for a large group of alleles and have more than 90% conservancy, except for one peptide, which has 80% conservancy (Table 8).

Mapping of conserved and selected peptide fragments on the three-dimensional structure of HA and NA

The three-dimensional structures of HA (PDB id 3LZG) and NA (PDB id 3TI3) were taken as the base structures to map the conserved regions. Since both the proteins are multimeric structures (HA homotrimeric, NA homotetrameric), only monomers were selected and opened in the Discovery Studio v3.5 visualizer, and then conserved regions and final selected peptide fragments enriched in CD4+ and CD8+ T-cell epitopes were mapped (Fig. 1). A few conserved sequences (CS_H11, CS_H12, CS_N1, and CS_N2) and their predicted peptides are located in the transmembrane/cytoplasmic domains of HA and NA and could not be mapped, as these domains were not present in the PDB structure of these proteins.

Population coverage analysis

Population coverage analysis is very important for the calculation of the expected response of predicted peptides in populations from different geographical areas. Peptides containing CD4+ and CD8+ T-cell epitopes for HA and NA, as shown in Tables 4 and 7 respectively, were taken into consideration for population coverage analysis by IEDB. These peptides fragments along with the predicted MHC binding data obtained by virtue of the epitope prediction servers were used as input in the IEDB population coverage tool. Based on these input data, the tool calculated the expected fraction of individuals from different populations that were going to respond to the peptide fragments. Putative class I and II MHC binding peptide fragments of HA have shown an average population coverage of 97.61% and 79.15% respectively (Fig. 2). The tool predicted an average population coverage of 96.63% and 90.82% for MHC class I and II binding peptide fragments of NA respectively. Population coverage analysis of MHC class II binding peptide fragments of HA and NA revealed 100% population coverage for European and North American populations.

Discussion

Immunoinformatics-driven prediction of peptides containing T-cell epitopes can significantly improve the selection of targets for vaccine design. The traditional technique of investigating immunogenic peptides experimentally for their potential as a vaccine target is a laborious and exorbitant process. Hence, an initial *in silico* screening of immunogenic peptides is the method of choice in the current scenario. Earlier studies by Torjan *et al.* (50), Assarsson *et al.* (2), and Gurung *et al.* (18) indicated that epitopes predicted by various bioinformatics tools have proven to be immunogenic in *in vitro* and *in vivo* experiments. Frequent mutations of HA and NA proteins because of the antigenic drift rules out the potency of predefined epitopes against all the variants. Hence, we focused on conserved peptide sequences to predict the epitopes. Highly conserved peptides containing epitopes provide an alternative approach for designing a universal influenza virus vaccine. The current study considered 3,661 protein sequences of H1N1 HA and 2,079 sequences of H1N1 NA, which is the largest of its kind to the best of our knowledge. While most earlier

Table 7. H1N1 Neuraminidase Peptides Containing Overlapping CD4+ and CD8+ T-Cell Epitopes

	Peptide enriched CD8+ T-cell epitope	*No. of epitopes*	*Peptide enriched CD4+ T-cell epitope*	*No. of epitopes*	*Fragments containing CD4+ and CD8+ T-cell epitopes*
CS_N2	LQIGNIISIW	2	LQIGNIISI	1	LQIGNIISIW
CS_N3	DVFVIREPFI	2	IRIGSKGDVFVIREPFIS	2	IRIGSKGDVFVIREPFIS
CS_N4	FFLTQGALL	1	FFLTQGALLN	2	FFLTQGALLN
CS_N6	GPDNGAVAV	1			
CS_N9	GSNRPWVSF	1	WHGSNRPWV	1	WHGSNRPWVSF
CS_N13	GSFVQHPELTGL	2	FVQHPELTG	1	GSFVQHPELTGL
	IRPCFWVEL	1			
CS_N14	TIWTSGSSISF	2	WTSGSSISFCGVNSD	2	TIWTSGSSISFCGVNSD
CS_N15	WPDGAELPF	1			

Table 8. Final Set of Peptides of H1N1 Neuraminidase Containing Both CD4+ and CD8+ T-Cell Epitopes Predicted to Bind a Large Number of Major Histocompatibility Complex Alleles

	Peptide	*No. of class I MHC alleles*	*No. of class II MHC alleles*	*Conservation (%)*
P_N1	LQIGNIISIW	17	21	93.6
P_N2	IRIGSKGDVFVIREPFIS	16	43	90.9
P_N3	FFLTQGALLN	12	39	97.8
P_N4	WHGSNRPWVSF	9	4	97.3
P_N5	GSFVQHPELTGL	21	8	97.7
P_N6	TIWTSGSSISFCGVNSD	18	10	80.0

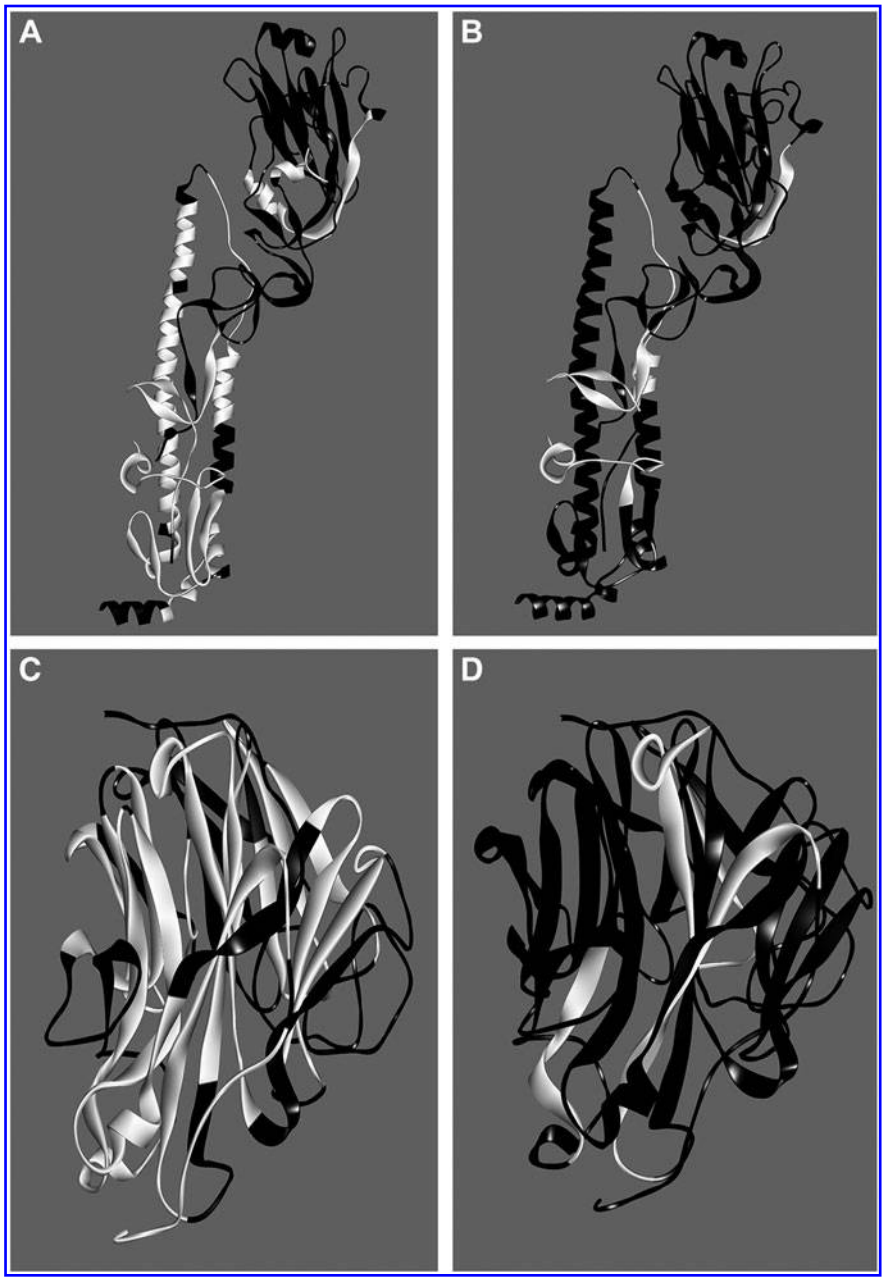

FIG. 1. Mapping of conserved regions and predicted peptide fragments containing CD4+ and CD8+ T-cell epitopes onto the crystal structures of hemagglutinin (pdb id: 3LZG) and neuraminidase (pdb id: 3TI3). **(A)** Conserved regions of hemagglutinin (white). **(B)** Predicted peptide fragments of hemagglutinin P_H1, P_H2, P_H3, and P_H4 are depicted in white. **(C)** Conserved regions of neuraminidase (white). **(D)** Predicted peptide fragments of neuraminidase P_N2, P_N3, P_N4, P_N5, and P_N6 are depicted in white.

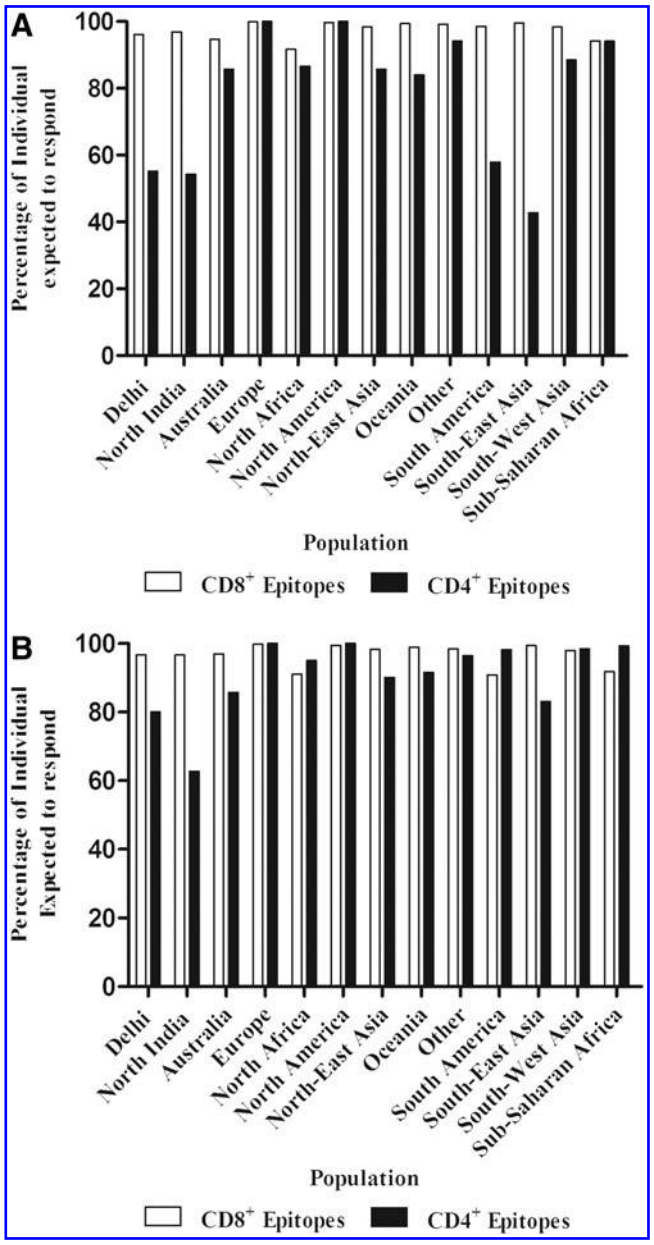

FIG. 2. Population coverage for predicted peptides containing CD4+ and CD8+ T-cell epitopes in 11 geographical zones predefined in the IEDB server database and Indian population. **(A)** H1N1 virus hemagglutinin protein. **(B)** H1N1 virus neuraminidase protein.

studies targeted selected strains of H1N1 (11,17), we considered all the HA and NA sequences in circulation from January 1918 to February 2013, which covers all the seasonal as well as the pandemic strains of H1N1.

There have only been a few studies undertaken on epitope prediction in the H1N1 virus based on the *in silico* approach. Moreover, in these studies, only one or two epitope prediction programs were used (11,21,45). In contrast to previous studies, we used six different prediction programs based on different approaches in order to define the epitopes. Normally, prediction tools are based on the probability of binding peptides with respective MHC. MHC–peptide interaction is one of the major factors for evoking an immune response, but there are some other factors that may also be of influence. These factors could be proteasomal C-terminal cleavage, TAP (transporter associated with antigen processing) transport efficiency, and stability of the peptide–MHC complex (35). NetCTL uses TAP transport efficiency and C terminal cleavage in addition to MHC class I peptides binding for epitope prediction (22), while BIMAS epitope prediction is based on the dissociation half-life of the MHC–peptide complexes (34). Thus, our prediction is based on multiple factors while defining the peptides as epitopes.

It has been reported that the predicted epitopes in the H5N1 avian influenza virus has shown partial identity to the human proteome (33). Hence, there is the possibility of an autoimmune response due to any kind of molecular mimicry between the conserved epitope and the human proteome. Guillain–Barré Syndrome reported after monovalent inactivated influenza vaccination might be due to vaccine peptides sharing homology to the human proteome (14,23). Nine predicted epitopes of HA protein were found to be homologous to a few human proteins using BLAST analysis, so these epitopes were eliminated from further consideration. Homologous epitopes were found to be absent in the case of NA peptides.

Peptide-based vaccines have certain advantages, including safety, specificity, ease of cGMP production, and absence of infectious potential, but there are some limitations too (29,34). MHC restriction, lack of helper activity, and weak presentation of antigen by APC due to exchange into the MHC as compared to cross-presentation processing are some limitations associated with small peptide vaccines. These limitations may be overcome by using multiple peptide vaccines, which include both CD4+ and CD8+ T-cell epitopes or longer peptides with CD4+ and CD8+ T-cell epitopes (29). The current study reports peptides that were generated based on overlapping CD4+ and CD8+ T-cell epitopes. Ten and six peptides of HA (each containing single or multiple epitopes) having binding affinity to class I and II MHC respectively were obtained. Finally, five peptides of HA ranging from 13–24 amino acids, which contain both $CD4^+$ and CD8+ T-cell epitopes, were obtained (Table 5). Similarly, we report six peptides containing overlapping CD4+ and CD8+ T-cell epitopes in the NA protein (Table 8). Interestingly, these predicted peptides of HA and NA were found to be more than 90% conserved, except one peptide, which had 80% conservation.

MHC polymorphism is complicated by the fact that MHC distribution varies among different ethnic groups around the world. Genetic polymorphisms of MHC significantly influence the variation in viral vaccine response in the human population (6,32). Hence, it is important to consider peptide-enriched epitopes, which could be effective in evoking an immune response in large populations. The present results show that most of our peptides have binding affinity with a large number of MHC alleles. Peptide YQILAIYSTVASSLVL of HA and peptide IRIGSKGDVFVIREPFIS of the NA protein are predicted for binding to 72 and 59 MHC alleles respectively. Further, the population coverage analysis tool available in IEDB was also used to address this issue. It was found that most of these predicted peptides showing an average population coverage of more than 90%. Interestingly, peptide fragments containing CD4+ T-cell epitopes of HA and NA revealed 100% population coverage in case of European and North American populations. Population

coverage studies suggest that these peptide fragments are capable of inducing a potent immune response among individuals belonging to different populations around the world.

Epitopes were examined for their uniqueness from the Influenza Research Database (46). In agreement with previous findings, peptides YQILAIYSTVASSLVL and LSSVSSFERFEIF of the HA protein and LQIGNIISIW and FFLTQGALLN of the NA protein have been reported for CD4+ T-cell responses (3,9,41). GSFVQHPELTGL of the NA protein is very similar to an already reported CD4+ T-cell epitope SGSFVQHPELTGL of influenza virus A/Puerto Rico/8/34 (H1N1) (19). As per the current studies, these peptides also contain CD8+ T-cell epitopes, but those peptides showing CD8+ T-cell responses have not been reported. Partial sequences of some of these peptides of HA and NA proteins were reported to induce T-cell responses (15,53). These reported peptides were either strain-specific or recent strains of the H1N1 influenza virus and specific for a few MHC alleles. In contrast to these studies, we have generated our peptides of HA and NA proteins from all reported strains of H1N1 until February 2013. These peptides also covered a large number of alleles. WHGSNRPWVSF of the NA protein is a new peptide whose T-cell response has not previously been reported. T-cells play an important role in the protection of influenza infection. T-helper cells regulate the production of high affinity antibodies (36). Hence, these predicted peptides may also evoke the B-cell response for the production of antibodies. Previous studies have shown that some of the partial sequences of these predicted peptides evoke the B-cell response as well (54). The immunoinformatics approach reduces the time and money required to identify peptides as vaccine candidates, and reduces the number of peptides needed to synthesize for experimental validation. The application of different immunoinformatics tools to find the conserved peptides containing epitopes is only a screening step, and peptides obtained by this approach need to be validated experimentally.

Currently available vaccines are trivalent and quadrivalent influenza vaccines, which are a live-attenuated influenza vaccine and an inactivated influenza vaccine. The trivalent influenza vaccine contains two influenza A subtypes (H1N1 and H3N2) and an influenza B variant, while in the quadrivalent vaccine, one more influenza B variant is included (37,40,51). These vaccines are reformulated annually based on the strains of virus that are expected to circulate in humans. The efficacy of inactivated or attenuated influenza vaccines is limited due to the antigenic drift and occasional antigenic shift of the HA and NA proteins. Hence, there is need of a universal vaccine to provide prevention against seasonal as well as pandemic influenza strains. Conserved peptides containing epitopes would be the ideal candidate for such a vaccine. Recently, BiondVax's Multimeric-001 vaccine candidate based on conserved epitopes of HA, nucleoprotein, and matrix protein has shown encouraging results in early clinical trials (4). In the present study, conserved peptides containing overlapping CD4+ and CD8+ T-cell epitopes in HA and NA proteins were obtained, which may be considered for the design of a universal vaccine against the H1N1 influenza virus.

Acknowledgments

We gratefully acknowledge AICTE, India, and DST, India, for their financial support.

Author Disclosure Statement

No competing financial interests exist.

References

1. Altschul SF, Gish W, Miller W, Myers EW, and Lipman D. Basic local alignment search tool. J Mol Biol 1990;215: 403–410.
2. Assarsson E, Bui HH, Sidney J, *et al.* Immunomic analysis of the repertoire of T-cell specificities for influenza A virus in humans. J Virol 2008;82:12241–12251.
3. Babon JA, Cruz J, Orphin L, *et al.* Genome-wide screening of human T-cell epitopes in influenza A virus reveals a broad spectrum of CD4(+) T-cell responses to internal proteins, hemagglutinins, and neuraminidases. Hum Immunol 2009;70:711–721.
4. Ben-Yedidia T. Multimeric-001: BiondVax's universal flu vaccine. Interview by Duc Le. Expert Rev Vaccines 2010; 9:241–242.
5. Brown DM, Román E, and Swain SL. CD4 T cell responses to influenza infection. Semin Immunol 2004;16:171–177.
6. Brusic V, and August JT. The changing field of vaccine development in the genomics era. Pharmacogenomics 2004; 5:597–600.
7. Bui HH, Sidney J, Dinh K, Southwood S, Newman MJ, and Sette A. Predicting population coverage of T-cell epitope-based diagnostics and vaccines. BMC Bioinformatics 2006; 7:153.
8. Bullough PA, Hughson FM, Skehel JJ, and Wiley DC. Structure of influenza haemagglutinin at the pH of membrane fusion. Nature 1994;371:37–43.
9. Cusick MF, Wang S, and Eckels DD. *In vitro* responses to avian influenza H5 by human CD4 T cells. J Immunol 2009; 183:6432–6441.
10. Doherty PC, Topham DJ, Tripp RA, Cardin RD, Brooks JW, and Stevenson PG. Effector CD4+ and CD8+ T-cell mechanisms in the control of respiratory virus infections. Immunol Rev 1997;159:105–117.
11. Duvvuri VR, Marchand-Austin A, Eshaghi A, Patel SN, Low DE, and Gubbay JB. Potential T cell epitopes within swine-origin triple reassortant influenza A (H3N2) variant virus which emerged in 2011: an immunoinformatics study. Vaccine 2012;30:6054–6063.
12. Edgar RC. MUSCLE: a multiple sequence alignment method with reduced time and space complexity. BMC Bioinformatics 2004;5:113.
13. Flower DR. 2009. Vaccines: data driven prediction of binders, epitopes and immunogenicity: 167–215. Bioinformatics for Vaccinology, John Wiley & Sons, Ltd, Chichester, United Kingdom.
14. Galeotti F, Massari M, D'Alessandro R, *et al*. Risk of Guillain–Barré syndrome after 2010–2011 influenza vaccination. Eur J Epidemiol 2013;28:433–344.
15. Ge X, Gebe JA, Bollyky PL, *et al*. Peptide–MHC cellular microarray with innovative data analysis system for simultaneously detecting multiple CD4 T-cell responses. PLoS One 2010;5:e11355.
16. Gonzalez-Galarza FF, Christmas S, Middleton D, and Jones AR. Allele frequency net: a database and online repository

for immune gene frequencies in worldwide populations. Nucleic Acid Research 2011;39:D913–D919.
17. Gupta SK, Srivastava M, Akhoon BA, *et al*. Identification of immunogenic consensus T-cell epitopes in globally distributed influenza-A H1N1 neuraminidase. Infect Genet Evol 2011;11:308–319.
18. Gurung RB, Purdie AC, Begg DJ, and Whittington RJ. *In silico* screened Mycobacterium avium subsp. paratuberculosis (MAP) recombinant proteins upregulated under stress conditions are immunogenic in sheep. Vet Immunol Immunopathol 2012;149:186–196.
19. Hackett CJ, Horowitz D, Wysocka M, and Eisenlohr LC. Immunogenic peptides of influenza virus subtype N1 neuraminidase identify a T-cell determinant used in class II major histocompatibility complex-restricted responses to infectious virus. J Virol 1991;65:672–676.
20. Heiny AT, Miotto O, Srinivasan KN, *et al*. Evolutionarily conserved protein sequences of influenza a viruses, avian and human, as vaccine targets. PLoS One 2007;2: e1190.
21. Huang P, Yu S, Wu C, and Liang L. Highly conserved antigenic epitope regions of hemagglutinin and neuraminidase genes between 2009 H1N1 and seasonal H1N1 influenza: vaccine considerations. J Transl Med 2013; 11:47.
22. Johnson NP, and Mueller J. Updating the accounts: global mortality of the 1918–1920 ''Spanish'' influenza pandemic. Bull Hist Med 2002;76:105–115.
23. Kwong JC, Vasa PP, Campitelli MA, *et al*. Risk of Guillain–Barré syndrome after seasonal influenza vaccination and influenza health-care encounters: a self-controlled study. Lancet Infect Dis 2013;13:769–776.
24. Larsen MV, Lundegaard C, Lamberth K, Buus S, Lund O, and Nielsen M. Large-scale validation of methods for cytotoxic T-lymphocyte epitope prediction. BMC Bioinformatics 2007;8:424.
25. Li Q, Sun X, Li Z, *et al*. Structural and functional characterization of neuraminidase-like molecule N10 derived from bat influenza A virus. Proc Natl Acad Sci U S A 2012;109:18897–18902.
26. Matrosovich MN, Matrosovich TY, Gray T, Roberts NA, and Klenk HD. Neuraminidase is important for the initiation of influenza virus infection in human airway epithelium. J Virol 2004;78:12665–12667.
27. McElhaney JE, Xie D, Hager WD, *et al*. T cell responses are better correlates of vaccine protection in the elderly. J Immunol 2006;176:6333–6339.
28. Miotto O, Heiny A, Tan TW, August JT, and Brusic V. Identification of human-to-human transmissibility factors in PB2 proteins of influenza A by large-scale mutual information analysis. BMC Bioinformatics 2008;9 Suppl 1:S18.
29. Naylor PH, Egan JE, and Berinstein NL. Peptide based vaccine approaches for cancer—a novel approach using a WT-1 synthetic long peptide and the IRX-2 immunomodulatory regimen. Cancers (Basel) 2011;3:3991–4009.
30. Nielsen M, and Lund O. NN-align. An artificial neural network-based alignment algorithm for MHC class II peptide binding prediction. BMC Bioinformatics 2009; 10:296.
31. Nielsen M, Lundegaard C, and Lund O. Prediction of MHC class II binding affinity using SMM-align, a novel stabilization matrix alignment method. BMC Bioinformatics 2007;8:238.
32. Ovsyannikova IG, Jacobson RM, and Poland GA. Variation in vaccine response in normal populations. Pharmacogenomics 2004;5:417–427.
33. Parida R, Shaila MS, Mukherjee S, Chandra NR, and Nayak R. Computational analysis of proteome of H5N1 avian influenza virus to define T cell epitopes with vaccine potential. Vaccine 2007;25:7530–7539.
34. Parker KC, Bednarek MA, and Coligan JE. Scheme for ranking potential HLA-A2 binding peptides based on independent binding of individual peptide side-chains. J Immunol 1994;152:163–175.
35. Patronov A, and Doytchinova I. T-cell epitope vaccine design by immunoinformatics. Open Biol 2013;3:120139.
36. Paul WE, and Benacerraf B. Functional specificity of thymus-dependent lymphocytes. Science 1977;195:1293–1300.
37. Pica N, and Palese P. Toward a universal influenza virus vaccine: prospects and challenges. Annu Rev Med 2013;64: 189–202.
38. Powell TJ, Strutt T, Reome J, *et al*. Priming with cold-adapted influenza A does not prevent infection but elicits long-lived protection against supralethal challenge with heterosubtypic virus. J Immunol 2007;178: 1030–1038.
39. Rammensee H, Bachmann J, Emmerich NP, Bachor OA, and Stevanović S. SYFPEITHI: database for MHC ligands and peptide motifs. Immunogenetics 1999;50: 213–219.
40. Rudolph W, and Ben Yedidia T. A universal influenza vaccine: where are we in the pursuit of this ''Holy Grail''? Hum Vaccin 2011;7:10–11.
41. Schanen BC, De Groot AS, Moise L, *et al*. Coupling sensitive *in vitro* and *in silico* techniques to assess cross-reactive CD4(+) T cells against the swine-origin H1N1 influenza virus. Vaccine 2011;29:3299–3309.
42. Shtyrya YA, Mochalova LV, and Bovin NV. Influenza virus neuraminidase: structure and function. Acta Naturae 2009;1:26–32.
43. Singh H, and Raghava GP. ProPred: prediction of HLA-DR binding sites. Bioinformatics 2001;17:1236–1237.
44. Skehel JJ, Bayley PM, Brown EB, *et al*. Changes in the conformation of influenza virus hemagglutinin at the pH optimum of virus-mediated membrane fusion. Proc Natl Acad Sci U S A 1982;79:968–972.
45. Somvanshi P, Singh V, and Seth PK. Prediction of epitopes in hemagglutinin and neuraminidase proteins of influenza A virus H5N1 strain: a clue for diagnostic and vaccine development. OMICS 2008;12:61–69.
46. Squires RB, Noronha J, Hunt V, *et al.* Influenza research database: an integrated bioinformatics resource for influenza research and surveillance. Influenza Other Respi Viruses 2012;6:404–416.
47. Swain SL, Dutton RW, and Woodland DL. T cell responses to influenza virus infection: effector and memory cells. Viral Immunol 2004;17:197–209.
48. Tan PT, Heiny AT, Miotto O, *et al*. Conservation and diversity of influenza A H1N1 HLA-restricted T cell epitope candidates for epitope-based vaccines. PLoS One 2010;5: e8754.
49. Tong S, Li Y, Rivailler P, *et al*. A distinct lineage of influenza A virus from bats. Proc Natl Acad Sci U S A 2012;109:4269–4274.
50. Trojan A, Urosevic M, Hummerjohann J, Giger R, Schanz U, and Stahel RA. Immune reactivity against a novel HLA-

A3-restricted influenza virus peptide identified by predictive algorithms and interferon-gamma quantitative PCR. J Immunother 2003;26:41–46.
51. Wang L, Zhang H, Compans RW, and Wang BZ. Universal influenza vaccines—a short review. J Immunol Clin Res 2013;1:1003–1009.
52. World Health Organization global alert response update 112. 2010. Available at www.who.int/csr/don/2010_08_06/en/index.html. (accessed April, 2014).
53. Yang J, James EA, Huston L, Danke NA, Liu AW, and Kwok WW. Multiplex mapping of CD4 T cell epitopes using class II tetramers. Clin Immunol 2006;120:21–32.
54. Zhao K, Shi X, Zhao Y, *et al*. Preparation and immunological effectiveness of a swine influenza DNA vaccine encapsulated in chitosan nanoparticles. Vaccine 2011;29:8549–8556.

Address correspondence to:
Dr. Manoj Baranwal
Thapar University
Patiala 147004
India

E-mail: manoj.baranwal@thapar.edu

This article has been cited by:

1. Lohia Neha, Baranwal Manoj. 2015. Identification of Conserved Peptides Comprising Multiple T Cell Epitopes of Matrix 1 Protein in H1N1 Influenza Virus. *Viral Immunology* **28**:10, 570-579. [Abstract] [Full Text HTML] [Full Text PDF] [Full Text PDF with Links] [Supplemental Material]
2. Satarudra Prakash Singh, Bhartendu Nath Mishra. 2015. Major histocompatibility complex linked databases and prediction tools for designing vaccines. *Human Immunology* . [CrossRef]

VIRAL IMMUNOLOGY
Volume 28, Number 10, 2015

Pp. 1–10
DOI: 10.1089/vim.2015.0060

Research Article

Identification of Conserved Peptides Comprising Multiple T Cell Epitopes of Matrix 1 Protein in H1N1 Influenza Virus

Neha Lohia and Manoj Baranwal

Abstract

Cell mediated immune response plays a key role in combating viral infection and thus identification of new vaccine targets manifesting T cell mediated response may serve as an ideal approach for influenza vaccine. The present study involves the application of an immunoinformatics-based consensus approach for epitope prediction (three epitope prediction tools each for CD4+ and CD8+ T cell epitopes) and molecular docking to identify peptide sequences containing T cell epitopes using the conserved sequences from all the Matrix 1 protein sequences of H1N1 virus available until April 2015. Three peptides comprising CD4+ and CD8+ T cell epitopes were obtained, which were not exactly reported in earlier studies. Population coverage study of these multi-epitope peptides revealed that they are capable of inducing a potent immune response belonging to individuals from different populations and ethnicity distributed around the globe. Conservation study with other subtypes of influenza virus infecting humans (H2N2, H5N1, H7N9, and H3N2) revealed that these three peptides were conserved (>90%), with 100% identity in most of these strains. Hence, these peptides can impart immunity against H1N1 as well as other subtypes of influenza virus. A molecular docking study of the predicted peptides with class I and II human leukocyte antigen (HLA) molecules has shown that the majority of them have comparable binding energies to that of native peptides. Hence, these peptides from Matrix 1 protein of H1N1 appear to be promising candidates for universal vaccine design.

Introduction

The emanation of new strains and subtypes of influenza A virus due to frequent antigenic drifts and occasional shifts can be attributed to the fact that negative-sense single-stranded RNA containing influenza virus has error-prone replication and a segmented genome. Thus, influenza virus is capable of expressing serologically distinct surface glycoproteins, rendering humoral immune response ineffective against heterologous virus strains (55). This results in seasonal and pandemic outbreaks leading to fatalities worldwide. Thus, influenza vaccines have to be reformulated with the ever-changing influenza strains. Internal viral proteins often display a low rate of mutation compared with surface proteins (51). Thus, internal influenza proteins such as the Matrix 1 (M1) protein appear to be a propitious candidate for a universal peptide-based vaccine, which may be capable of imparting heterosubtypic immunity and thus averting the need to monitor antigenic drifts and shifts constantly.

As an internal protein, M1 appears to be less immunogenic, especially in the production of antibodies, compared with surface hemagglutinin (HA) and neuraminidase (NA) proteins. But in recent years, this protein has been targeted to develop a universal influenza vaccine (3,12,38). In a recent study conducted by Wang *et al*. (50), mice vaccinated with DNA plasmids and recombinant vaccinia virus expressing the M1 protein in combination with other conserved proteins (nucleoprotein and polymerase basic protein 1) were completely or partially protected after challenge with a lethal dose of influenza A virus (strain A/Puerto Rico/8/1934 H1N1). In another study, HA and M1 proteins (H5N1) expressed in *Pichia pastoris* were purified and used to immunize mice. A higher antibody mediated immune response was observed in mice against rHA and rM1 than mice immunized with either HA or M1 antigens (44).

The M1 protein is transcribed and further translated as one of the proteins coded by segment seven of the influenza A genome, along with other two splice variant: M2 ion channel and M42 (53). The M1 monomer (252 amino acid) is 60 Å long (40), carrying two globular regions—the N-terminal (1–164) and C-terminal (165–252)—linked by a protease-sensitive loop. Crystallographic studies have revealed that the

Department of Biotechnology, Thapar University, Patiala, India.

M1 protein is composed of nine α-helices (H1–H9). These α-helices are organized into two four-helix bundles: N-terminal domain (H1–H4) and C terminal domain (H6–H9) connected via another helix linker (H5). The M1 protein lies beneath the viral envelope and plays diverse roles in the life cycle of the influenza A virus. It binds simultaneously to the viral envelope and RNA. It encapsulates the ribonucleoprotein (RNP) complex of influenza virus in the membrane envelope, thus stabilizing the membrane architecture. The M1 protein is also assumed to form cross-links with the cytoplasmic tail of HA and NA proteins, and commences viral budding from the host cell. During the virus entry, low pH induces a structural transition in the M1 protein inside the endosomal compartment, leading to the formation of unstable M1 monomers. This dislodging of the M1 protein shell expedites the release of vRNPs into the cytoplasm. Viral RNPs thus enter the nucleus and initiate the transcription and replication of the viral genome. The M1 protein in association with nuclear export protein (NEP) also facilitates the nucleocytoplasmic transport of newly formed vRNPs. Influenza virus exists in two different morphological forms: spherical (~ 100 nm diameter) and filamentous ($\sim 100\,\text{nm} \times 2\text{–}20\,\mu\text{m}$) virions (18). The filamentous trait of influenza virus has been traced to helix 6 domains of the M1 protein (8). The helix 6 domain (91–105 amino acids) of the M1 protein has been recognized as the multifunctional domain acting as a nuclear localization signal (NLS) for the translocation of the M1 protein in the nucleus and transcription inhibition motifs. Thus, the M1 protein plays multiple roles in influenza virus replication, from virus entry, uncoating, assembly, and budding of the virus particle.

Adaptive immune response plays a vital role in viral clearance, and thus highlights the importance of T cell epitope identification among various influenza virus proteins. Humoral immune response helps in influenza virus clearance mainly via complement dependent lytic antibodies (54). Cell mediated immune response targeted toward viral peptides, which are likely to be shared between different virus strains, may offer large dimensions to the immunity imparted against various strains and subtypes of influenza virus. Considering this fact, the current study is focused on identification of conserved immunogenic peptides comprising multiple T cell epitopes from the M1 protein of H1N1 influenza virus by applying a combination of various immunoinformatics tools that may be interesting candidates for a peptide-based universal influenza vaccine. Further, molecular docking was performed with the identified immunogenic peptide to calculate the binding affinity with different human leukocyte antigen class I and II molecules.

Materials and Methods

Sequence retrieval and conservation analysis

In the current study, full-length M1 protein sequences of H1N1, infecting humans all over the world, were retrieved until April 2015 from the Influenza Research Database (IRD; NIH/DHHS). MUSCLE and AVANA tools were used to obtain the conserved peptide stretches (≥90%) (17,27,28). Conservation refers to identical peptide sequences that are present in at least 90% of total M1 protein sequences, and these conserved peptide sequences were used for further epitope prediction. Full-length M1 protein sequences identified from human isolates of H5N1, H3N2, H7N9, and H2N2 were also retrieved from the IRD for conservancy analysis.

Identification of T cell epitopes

Performance of the consensus prediction approach of epitope prediction was found to be superior to the single predictive strategy (29). In our earlier report, the consensus approach has been used for epitope prediction of H1N1 HA and NA proteins (28). The current study also employed different prediction tools: NetCTL 1.2, SYFPEITHI, and BIMAS (26,34,39) for class I binding (CD8+ T cell) epitopes and Immune Epitope Database (IEDB)–based SMM align, ProPred and NetMHC II for class II binding (CD4+ T cell) epitopes (32,33,43). Threshold scores taken for the class I epitope prediction tool, SYPFEITHI, Net-CTL, and BIMAS were 20, 0.75, and 20, whereas for class II HLA prediction tools, SMM align, and NetMHC II, it was $IC_{50} \leq 500$ nM. All the HLA alleles/supertypes provided in each prediction tool were considered for epitope prediction (Table 1). NetCTL predicts epitopes for HLA supertypes in place of alleles. Each supertype represents a set of HLA alleles that share largely overlapping peptide-binding specificity. Class I HLA has been classified into 12 different supertypes. As per the criteria defined in a previous report (27), peptides were defined as epitopes, and further epitopes showing identity to the human proteome based on pBLAST (2) were eliminated from further studies. The final conserved epitopes showing an overlap were merged into a single peptide.

HLA distribution analysis

An epitope can elicit an immune response in individuals expressing the HLA capable of binding that epitope. HLA polymorphism exists among different geographical areas and ethnicities. Thus, selecting epitopes with binding

Table 1. Human Leukocyte Antigen Alleles Provided in Different Epitope Prediction Tools

CD8+ T cell epitope		*CD4+ T cell epitope*	
Prediction tools	*HLA alleles/supertypes*[a]	*Prediction tools*	*HLA alleles*
NetCTL v1.2	5[b] HLA-A and 7 HLA-B	IEDB-SMM	5 HLA-DP, 6 HLA-DQ, and 15 HLA-DR
BIMAS	9 HLA-A, 20 HLA-B, and 4 HLA-C	NetMHC II v2.2	14 HLA-DR, 6 HLA-DQ, and 6 HLA-DP
SYFPEITHI	7 HLA-A and 26 HLA-B	ProPred	51 HLA-DR

[a]NetCTL predicts epitopes for HLA supertypes in place of alleles. Each HLA supertype represents a set of HLA alleles that share largely overlapping peptide binding specificity.
[b]Number signifies the number of HLA alleles/supertypes.
HLA, human leukocyte antigen.

affinity with multiple HLA alleles increases the coverage of the population targeted by peptide-based vaccines. The IEDB population coverage analysis tool is based on an allele frequency database that provides allele frequencies for 115 countries and 20 different ethnicities grouped into 16 different geographical areas (7). Analysis of the peptides was carried out for the populations distributed in 16 geographical zones, as well as 20 ethnic groups all over the world.

Molecular docking of peptides comprising epitopes

High-resolution crystallographic structures of 10 class I HLA and five class II HLA molecules were fetched from the protein data bank. These HLA molecules represented various supertypes of class I and II HLA (13,42). The naturally bound peptides (native peptides) of the HLA molecules were cut apart using the Discovery studio visualizer (v4.1) and docked again using the AutoDock Vina tool as the test set (49). The grid for each of the HLA molecules was defined based on native peptides. The structure of the peptides comprising epitopes was generated using the PEP-FOLD server (48). These generated structures were used for docking with class I and II HLA molecules.

Results

Conserved peptides of the M1 protein in H1N1 virus

To cover all the genetic variants of H1N1 isolates around the world, 458 sequences of the M1 protein (human host) were obtained after removing the duplicate ones. Frequent mutations in influenza virus render previously identified epitopes non-immunogenic. Thus, peptides of the M1 protein conserved among all the strains of H1N1 can prove to be more effective candidates of immunogenicity. Ten conserved peptide sequences of the M1 protein (M1.1–M1.10) were identified using AVANA, and ranged in size from 12 to 49 amino acids (Table 2). The first seven (M1.1–M1.7) conserved peptides are confined to the membrane-binding domain of the M1, whereas the last three (M1.8–M1.10) conserved peptides are located in the RNP-binding domain.

Identification of peptides comprising CD4+ and CD8+ T cell epitopes

Cell mediated immunity plays an important role in controlling influenza infection. Hence, the T cell epitope prediction was carried out based on different immunoinformatics tools for CD8+ T cell epitopes (NetCTL, BIMAS, and Syfpeithi) and CD4+ T cell epitopes prediction (NetMHC II, ProPred, and IEDB-based SMM align). After comparing the predicted epitopes with the respective HLA restriction, a set of epitopes was obtained that was predicted by all the tools separately for class I and II HLA. BLAST analysis revealed no specific homology of the human proteome with any of the predicted CD4+ T cell epitopes, but among CD8+ T cell epitopes of the M1 protein, one epitope was found to be homologous as per the set criterion, so it was eliminated from further studies (data not shown). Finally, 10 CD8+ T cell epitopes (class I HLA binding epitopes) and nine CD4+ T cell epitopes (HLA class II binding epitopes) of the M1 protein were considered for further analysis (Table 3). In Net MHCII 2.2 and IEDB-based SMM align, the binding affinity of the CD4+ T epitope to HLA is given as IC_{50}. For each predicted epitope, the IC_{50} value varies with various combinations of HLA alleles and tools used. The range of IC_{50} values for predicted CD4+ T cell epitopes is given in Table 3 to show their binding affinity with HLA. Epitopes MVLASTTAK and IRHENRMVL of the M1.8 conserved sequence were predicted to bind to both class I and II HLA molecules. Epitopes having overlapping amino acid sequences in the respective conserved regions were merged to generate a longer peptide having multiple epitopes. In this way, six peptides of CD8+ T cell epitopes (length 9–15 amino acids) and three peptides containing CD4+ T epitopes (length 12–17 amino acids) were obtained (Table 4). The overlapping epitopes in these peptides belong to either the same or different alleles/supertypes (Table 4). The epitopes belonging to same versus different alleles/supertypes are represented as common versus unique alleles/supertypes, respectively (Table 4). Further, these putative immunogenic peptides were merged to generate a single peptide containing multiple CD4+ and CD8+ T cell epitopes, confined to a particular conserved region. Finally, three peptides (one peptide in the membrane binding domain and two peptides in the RNP binding domain) were obtained that contained both CD4+ and CD8+ T cell epitopes (Table 5).

Table 2. Conserved Peptide Sequences of H1N1 Virus Matrix 1 Protein

	Conserved sequence	*Length*
M1.1	MSLLTEVETYVLSI	14
M1.2	PSGPLKAEIAQRLE	14
M1.3	VFAGKNTDLEALMEWLKTRPILSPL TKGILGFVFTLTVPSERGLQRRRF	49
M1.4	QNALNGNGDPNNMDRAV	17
M1.5	KLKREITFHGAKE	13
M1.6	GALASCMGLIYNRMG	15
M1.7	CATCEQIADSQH	12
M1.8	TTTNPLIRHENRMVLASTTAKAMEQ	25
M1.9	AGSSEQAAEAMEV	13
M1.10	NLQAYQKRMGVQMQRFK	17

Table 3. Predicted CD4+ and CD8+ T Cell Epitopes of H1N1 Virus Matrix 1 Protein

Conserved sequence	*CD8+ T cell epitope*	*CD4+ T cell epitope*	*IC50 value[a] (range) for CD4+ T cell epitope*
M1.1	SLLTEVETY		
	LLTEVETYV		
M1.2	LKAEIAQRL		
M1.3	ERGLQRRRF	FVFTLTVPS	6.7–449
	KTRPILSPL	FTLTVPSER	10.3–495
	RPILSPLTK	ILGFVFTLT	54.9–481
M1.8	IRHENRMVL	IRHENRMVL	59.1–437.4
	MVLASTTAK	MVLASTTAK	53.4–461
		VLASTTAKA	10.5–498.6
		LIRHENRMV	31–496
M1.9	QAYQKRMGV	LQAYQKRMG	43.8–359
	KRMGVQMQR	YQKRMGVQM	37.8–447.9

[a]Range of IC_{50} value for predicted epitopes with different HLA alleles using NetMHCII 2.2 and IEDB-SMM align.

Table 4. H1N1 Matrix 1 Peptides Containing Overlapping CD4+ or CD8+ T Cell Epitopes Along with Their Number of HLA Alleles

Peptide-enriched CD8+ T cell epitope	*Epitope*	*Unique HLA supertypes/ alleles*	*Common HLA supertypes/ alleles*	*Peptide-enriched CD4+ T cell epitope*	*Epitope*	*Unique HLA alleles*	*Common alleles*
SLLTEVETYV	SLLTEVETY	4	1				
	LLTEVETYV	1					
LKAEIAQRL	LKAEIAQRL	1					
ERGLQRRRF	ERGLQRRRF	1		ILGFVFTLTVPSER	FVFTLTVPS	47	4
KTRPILSPLTK	KTRPILSPL	5	2		FTLTVPSER	5	
	RPILSPLTK	2			ILGFVFTLT	8	
IRHENRMVLASTTAK	IRHENRMVL	6	Nil	LIRHENRMVLASTTAKA	IRHENRMVL	17	3
	MVLASTTAK	3			MVLASTTAK	33	
					VLASTTAKA	18	
					LIRHENRMV	19	
QAYQKRMGVQMQR	QAYQKRMGV	4	Nil	LQAYQKRMGVQM	LQAYQKRMG	13	6
	KRMGVQMQR	1			YQKRMGVQM	3	

The epitopes belonging to the same versus different alleles/supertypes are represented as common versus unique alleles/supertypes, respectively.
"Nil" specifies that none of the HLAs was predicted to be common to any of the epitopes belonging to the overlapping fragment.

Table 5. H1N1 Matrix 1 Peptides Containing Overlapping CD4+ and CD8+ T Cell Epitopes

Conserved sequence	*Peptide-enriched CD8+ T cell epitope*	*No. of epitopes*	*Peptide-enriched CD4+ T cell epitope*	*No. of epitopes*	*Final peptides containing CD4+ and CD8+ T cell epitopes*
M1.1	SLLTEVETYV	2			
M1.2	LKAEIAQRL	1			
M1.3	ERGLQRRRF	1	ILGFVFTLTVPSER	3	ILGFVFTLTVPSERGLQRRRF
M1.3	KTRPILSPLTK	2			
M1.8	IRHENRMVLASTTAK	2	LIRHENRMVLASTTAKA	4	LIRHENRMVLASTTAKA
M1.9	QAYQKRMGVQMQR	2	LQAYQKRMGVQM	2	LQAYQKRMGVQMQR

Conservation of peptides containing multiple epitopes among other subtypes of influenza A virus

Three final selected peptides containing multiple CD4+ and CD8+ T cell epitopes were searched for 100% identity as a measure of conservation in seasonal H1N1, pandemic H1N1, H5N1, H3N2, H2N2, and H7N9 M1 protein sequences. The first peptide (ILGFVFTLTVPSERGLQRRRF) is conserved (≥90.9%) among all the subtypes of the influenza A virus (Table 6). The second (LIRHENRMVLASTTAKA) and third (LQAYQKRMGVQMQR) peptides were also found be conserved (≥90%) in most of these subtypes (Table 6). High conservation was not observed for the second and third peptides in H3N2. Hence, identity consideration was relaxed to ≥90%, and it was then found be conserved (≥97%). In H7N9, the third peptide (LQAYQKRMGVQMQR) was replaced by LQAYQNRMGVQLQR with mutation at the sixth and twelfth position in all the sequences. Additional data containing multiple sequence alignment showing sequence identity of the three final selected peptides in seasonal H1N1, pandemic H1N1, H5N1, H3N2, H2N2, and H7N9 are given in Supplementary Tables S1–S6 (Supplementary Data are available online at www.liebertpub.com/vim).

Population coverage of HLA predicted to bind M1 peptides

HLA polymorphism among populations from different geographical areas and ethnicities results in a variation of the peptide's immunogenic response. Hence, population coverage analysis becomes important. Population coverage analysis of the three M1 peptides was carried out for populations distributed in 16 geographical zones and 20 ethnicities (Fig. 1). The average population coverage was observed to be 98.13% jointly for class I and II HLA binding peptides of M1. Among the different geographical zones, 100% of populations of South Asian, European, North American, and East, West, and Central African populations are expected to respond to these predicted epitopes. Further, HLA distribution analysis was also carried out among the different ethnicities distributed worldwide, which resulted in an average of 98.61% coverage of HLA (Fig. 1B). Among various races, Asians, blacks, Caucasians, Melanesians, and Siberians showed 100% coverage.

Peptide docking with class I and II HLA molecules

The first and most important step toward the generation of an efficient adaptive immune response is the binding of the immunogenic peptide to the peptide-binding groove of the HLA molecule inside the host cell. The AutoDock Vina tool was employed to calculate the binding affinity of the peptide-containing epitope with class I and II HLA molecules. The crystallographic structures of peptide bound ten HLA class I (resolution 1.3–2 Å) and five HLA class II molecules (resolution 1.7–2.75 Å) were taken from protein data bank (PDB id mentioned in Tables 7 and 8) for docking. Each of the HLA molecules represents different HLA supertype (13, 42). Native peptides were separated from the respective HLA molecule and docked to obtain the binding energy that was used as a test set for comparison. Since class I HLA is known to bind short peptides (length 9 amino acids), the predicted five class I HLA peptides (part of three final peptides containing multiple epitopes) were used for docking with the class I HLA molecules. Considering that class II HLA can accommodate bigger peptides, three peptides containing multiple epitopes (part of three final peptides) were docked with the class II HLA molecules. The PEP-FOLD generated structures of these peptides containing epitopes were docked with different HLA I and II molecules. It was observed that most of the peptides showed comparable binding energy to that of the native peptides with respective HLA molecules (Tables 7 and 8). However, some of the

Table 6. Conservation of Final Peptides of Matrix 1 Protein Among Other Subtypes of Influenza Virus A Infecting Humans

Peptide sequence	*H1N1 seasonal (153[a])*	*H1N1 pandemic (307)*	*H3N2 (344)*	*H5N1 (33)*	*H7N9 (6)*	*H2N2 (26)*
ILGFVFTLTVPSERGLQRRRF	93.46%	94.46%	95.06%	90.91%	100.00%	96.15%
LIRHENRMVLASTTAKA	92.81%	95.44%	97.09%[b]	100.00%	100.00%	100.00%
LQAYQKRMGVQMQR	91.50%	94.46%	96.80%[b]	75.76%	—	100.00%

Conservations were recorded at 100% sequence identity.
[a]Number of full-length, nonredundant sequences of the M1 protein available in the database until April 2015.
[b]Conservation at identity ≥90%.

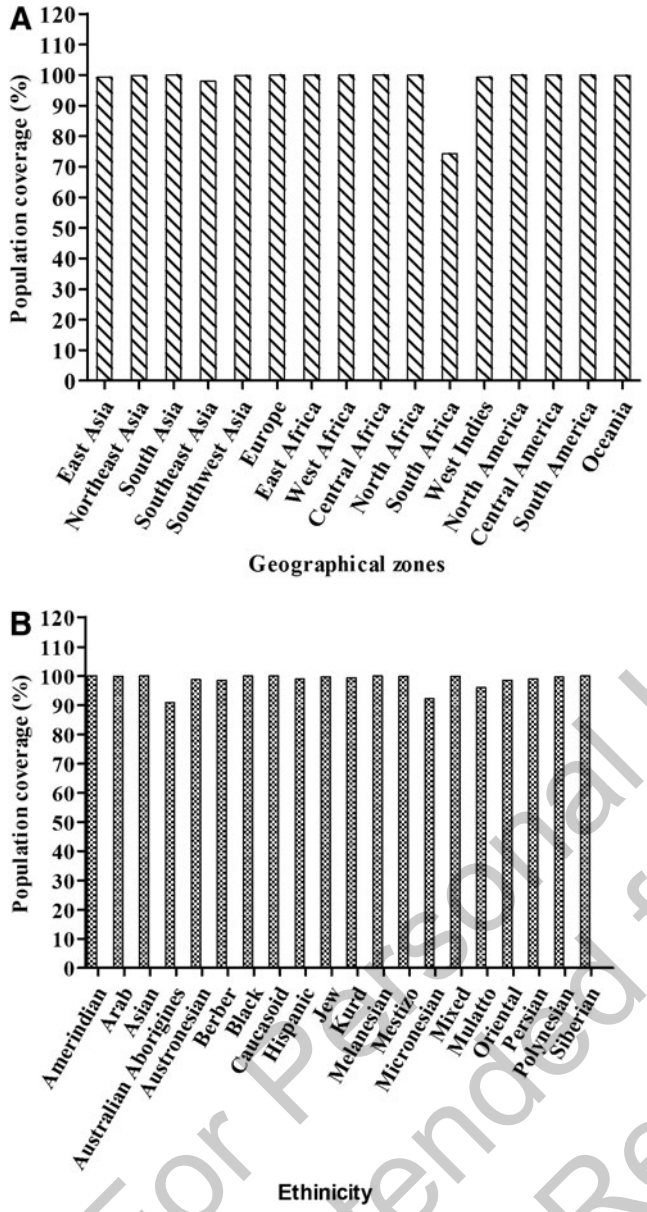

FIG. 1. Population coverage analysis of predicted Matrix 1 (M1) peptides showing the expected response. (**A**) Population distributed in 16 different geographical zones. (**B**) Twenty different ethnic groups of the world.

peptides were found to bind outside the peptide-binding groove of HLA, which were designated as nonbinders (NBs; Tables 7 and 8). The binding energy of these peptides was spotted within the range of native peptides for both class I and II HLA molecules (Fig. 2A and B). Dunnett's multiple comparison test was carried out to compare the binding energy between these peptides and native peptides as the control peptide. Binding energies of three out of five peptides for class I HLA and all three peptides for class II HLA were not found to be significantly different from respective control peptides. Binding energies of the MVLASTTAK and KRMGVQMQR peptides appear to be significantly less compared with the control peptide. Furthermore, analysis of these results showed that the MVLASTTAK and KRMGVQMQR peptides were not binding in the peptide-binding groove of five and two HLA class I molecules. The peptide containing the MVLASTTAK epitope also did not fit in the binding groove of three class II HLA molecules. Hence, this peptide may be not a good binder for either class I or II HLA.

Discussion

The availability of a substantial amount of data of relevance to immunology research, particularly clinical and epidemiologic data, has pioneered the contemporary domain of immunoinformatics or computational immunology. Immunoinformatics-guided epitope prediction (T and B cell) is speculated to improve the selection of targets for vaccine design by reducing the time and cost of laboratory identification of epitopes. Studies undertaken against *Mycobacterium tuberculosis* (24) and *Leishmania amazonensis* (36) have demonstrated the efficiency of computationally predicted epitopes to evoke an immune response both *in vitro* and *in vivo*. Furthermore, studies conducted against influenza virus proteins by Duvvuri *et al*. (15) and Sun *et al.* (46) established the success of computational approaches in predicting epitopes. In these studies, the predicted influenza epitopes prove to be immunogenic in the case of healthy human peripheral blood mononuclear cells and murine models.

Genome- or proteome-wide *in silico* screening of severe and ever-changing entities such as the influenza virus for putative immunogenic peptides can accelerate the global pursuit of universal influenza vaccine development. Incessant mutations (antigenic shift and drift) in influenza forfend the immunogenic potency of predefined epitopes against all the variants of a particular subtype of influenza

Table 7. Binding Energies (kCal/mol) Obtained from Docking of CD8+ T Cell Peptides and Native Peptides Against Different Class I HLA Alleles

PDB id	*HLA alleles*	*Native peptide*	*ERGLQRRRF*	*IRHENRMVL*	*MVLASTTAK*	*QAYQKRMGV*	*KRMGVQMQR*
1M6O	HLA-B44	−9.10	−7.40	NB	NB	−6.30	NB
2A83	HLA-B27	−7.60	−7.90	−7.90	−5.50	−7.60	−6.60
2BVP	HLA-B57	−9.30	−8.50	NB	NB	NB	−7.00
3BO8	HLA-A1	−7.60	−6.80	−7.2	−6.00	−7.30	−6.20
3C9N	HLA-B62	−8.10	−6.70	−7.5	NB	−7.80	−6.80
3MRK	HLA-A2	−7.30	−6.50	−6.5	NB	−6.90	−6.80
3RL1	HLA-A3	−6.60	−7.60	−6.9	NB	−6.80	NB
3SPV	HLA-B8	−11.40	−9.60	−9.2	−7.60	−8.20	−8.50
3VCL	HLA-B7	−9.10	−8.10	−7.7	−7.80	−8.00	−7.00
3WL9	HLA-A24	−7.80	−8.40	−6.1	−5.30	−6.10	−6.70

Table 8. Binding Energies (kCal/mol) Obtained from Docking of CD4+ T Cell Peptides and Native Peptides Against Different Class II HLA Alleles

PDB id	*HLA allele*	*Native peptide*	*ILGFVFTLTVPSER*	*LIRHERMVLASTTAKA*	*LQAYQKRMGVQM*
1A6A	HLA-DR3	−5.3	−7.8	−6.7	−6.8
1D5M	HLA-DR4	−7	−6.4	−5.1	−5.8
1KLU	HLA-DR1	−5.7	−7.3	NB	−7.3
1S9V	HLA-DQ2	−8.7	−7.1	NB	−7.5
3PL6	HLA-DQ1	−6.9	−6.1	NB	−7.2

virus, as well as other subtypes in case of cross-reactive epitopes. Hence, targeting conserved peptide sequences to identify the epitopes appears to be an elite approach for vaccine design. The current study involved 458 unique protein sequences of H1N1 M1 (including seasonal as well pandemic strains of H1N1) deposited worldwide until April 2015, which is the largest as far as it is possible to tell from the literature for the identification of T cell epitopes from the M1 protein (H1N1). This is in contrast to earlier studies undertaken to predict T cell epitopes of the M1 protein in H7N9 and H3N2 (14,16,21), which considered reference strains for epitope prediction.

The current study was undertaken using a consensus approach of epitope prediction, which employs different prediction programs in order to define the epitopes (27). Use of a single computational algorithm for T cell epitope prediction may lead to a substantial number of false positives and false negatives. Taking this into consideration, the consensus approach (i.e., combining and comparing the different prediction algorithms to identify epitopes) has been applied in various studies, and its immunogenic potential has been verified *in vitro* and *in vivo* (11,41). The immunogenicity of peptides depends on multiple factors mediating peptide immune response, such as HLA-peptide binding, TAP transport efficiency, C-terminal cleavage, and binding stability of the peptide–HLA complex. Considering this, multiple prediction tools for CD8+ T cell epitopes (NetCTL, BIMAS, and SYFPEITHI) and CD4+ T cell epitopes (ProPred, SMM align, and NetMHC II v2.2) were employed, which are based on different immunogenic factors and algorithms. NetCTL v1.2 is an Artificial Neural Network (ANN)–based tool that predicts CD8+ T cell epitopes taking into account TAP transport efficiency and C terminal cleavage, while BIMAS identifies epitopes based on the measurement of the dissociation half-life of ($t_{1/2}$) of β_2 microglobulin. The SYFPEITHI is a continuously updated database of MHC ligands and peptide motifs of human and other species, which predicts epitopes based on reported motifs. ProPred employs a literature-based amino acid/position coefficient table, and presents the HLA-DR binding propensity of given protein sequence (43). SMM align and NetMHC II v2.2 employs a position-specific weight matrix and ANN, respectively, for binding affinity to different HLA-DR, and their binding affinity is given as IC_{50} values. These T cell epitope prediction tools have been extensively used and their efficacy has been verified experimentally by various studies (9,11,20,41). In addition to the multi-immunogenic factor and different prediction algorithms, the consensus approach also offers advantages with regard to predicting large numbers of different HLA alleles.

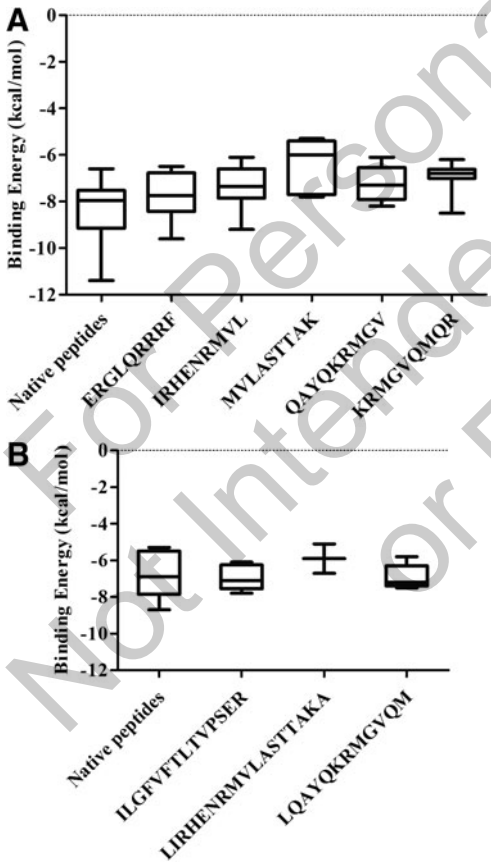

FIG. 2. Binding energy of the predicted peptides and native peptides after docking with (**A**) class I HLA and (**B**) class II HLA. The bars extend from the 25th percentile to the 75th percentile with a horizontal line at the median. Whiskers extend to the smallest value up to the largest. HLA, human leukocyte antigen.

Earlier studies have reported partially identical stretches of peptides between human and influenza proteins (21). Any kind of molecular mimicry between the predicted epitopes and host protein (human) may lead to cross-reactivity and, further, autoimmune response. One predicted epitope of the M1 protein, GILGFVFTL, was found to be homologous to human tetraspanin-33 during BLAST analysis, which is accordance with an earlier report (21). It is considered to be immunodominant in HLA-A2 individuals, and it also overlaps with NLS (47). Although, it is one of the most extensively studied epitopes of the M1 protein, in this study it was still eliminated from further consideration to avoid any chances of molecular mimicry.

Vaccines induce virus-specific antibodies that bind specifically to the pathogen and mediate effector functions, thus

limiting the infection. Normally, the surface proteins of the virus are the prime targets of antibodies secreted by B cells. However, frequent mutations in influenza A virus strains render these pre-existing antibodies ineffective over time. Prototypically, the virus has been known to be eliminated by T cell mediated immune response. CD8+ T cells employ perforin, Fas/Fas-Ligand, and tumor necrosis factor-related apoptosis-inducing ligand (TRAIL) mediated mechanisms to kill virus-infected cells and thus clear viral infection (22). CD4+ T cells, however, contribute toward antiviral immune response primarily by assisting CD8+ T cells and B cells by releasing antiviral cytokines (1). Thus, a T cell epitope-based vaccination approach appears to activate both humoral and cell mediated arms of adaptive immunity to eliminate viral infection jointly.

Expanding knowledge about antigen presentation and recognition has facilitated the advancement in vaccine development, especially peptide-based vaccines. Peptide-based vaccines are favored because they lack the risk of reversion to virulent and genetic integration or recombination. Additionally, they are relatively easy to produce and can be modified to enhance their immunogenicity, stability, and solubility (37). Furthermore, T cell epitopes (peptides) are expressed on the surface of antigens, presenting as a peptide–HLA complex. Because of the high polymorphism in HLA among different populations and ethnic groups, a variable immunogenic response of some epitopes is expected. Thus, peptides capable of multiple HLA restriction or peptides bearing multiple epitopes are preferred as vaccine targets for extensive and impartial population coverage required for a vaccine. Peptides containing both CD4+ and CD8+ T cell epitopes may improve the immunogenicity and clinical outcomes of peptide-based vaccines (31). *In silico* epitopes prediction tools enable multi-epitope peptides to be selected in a prompt and cost-effective way, with vast coverage among the world's population. With this in mind, the current study reported three M1 peptides that were generated after merging the CD4+ and CD8+ T cell epitopes predicted by the immunoinformatics approach.

Certain groups of individuals are highly vulnerable to influenza infection and related complications, including children (<5 years), the elderly (>65 years), pregnant women, and people with special medical conditions such as asthma, AIDS, cancer, chronic lung disease, and so on. Furthermore, Blumenshine *et al*. (7) suggested that various factors determine the severity of pandemic influenza, including differential exposure to influenza due to income or ethnicity, unequal levels of susceptibility, differential access to prophylaxis, and treatment after disease develops. A study in the United States reported higher rate of hospitalization among Asian/Pacific Islanders, non-Hispanic blacks, and Hispanics compared with non-Hispanic whites during the 2009 pandemic (30). Another study showed a relatively high rate of pandemic (H1N1) fatality in Southeast Asians and Americans compared with Europeans and Africans (10). Globally, as reported by the World Health Organization (52), influenza activity has been higher in the southern hemisphere compared with the northern hemisphere. Moreover, the circulating strains of influenza keep mutating, thereby changing the susceptibility of a specific ethnic group toward influenza. Thus, there is an alarming need to view influenza from a global prospective. Interestingly, the population coverage analysis in the present study unveiled that predicted peptides showed an average population coverage of >98%, combining class I and II HLA epitopes among various geographical areas as well as ethnicities. Hence, these peptide sequences not only contain multiple T cell epitopes but also have the potential to induce a potent immunogenic response among individuals belonging to different populations around the world.

It was interesting to find a vaccine candidate that may be effective not only in one type of influenza virus but also in other subtypes. Hence, these identified peptides were studied for their conservation in other subtypes of influenza virus infecting humans (H2N2, H5N1, H7N9, and H3N2). This conservation study revealed that these three peptides were found to be >90% conserved, with 100% identity in most of the strains. These data suggest that these peptides can impart immunity against H1N1 as well as other subtypes of influenza virus (heterosubtypic immunity).

Molecular docking is employed not only for computer-aided drug designing, but also for peptide–HLA interactions. The docking approach was found to be reliable and accurate for evaluating peptide binding to HLAs (5,35). Peptides binding to class I HLA are normally nonamer, while for class II HLA they vary in length from 12 to 25 amino acids. Hence, peptides containing nonamer epitopes were docked with class I HLA, whereas longer sequences containing multiple epitopes were considered for docking with class II HLA. These peptide sequences were found to have comparable binding energy with that of natural bound peptides (test peptides) for both class I and II HLA, except that two class I HLA restricted MVLASTTAK and KRMGVQMQR. This could be because these epitopes failed to bind HLA molecules in the designated space, and thus were assumed to be NBs. Hence, the peptide containing this epitope may not have good affinity with either of the HLA molecules. This observation can be explained by the fact that the epitopes were not predicted to bind to all HLA molecules. However, most the peptides showed a good binding affinity with class I and II HLA molecules. A similar study was conducted, taking into account class I HLA alleles, in which nucleoprotein epitopes were identified and docked with four HLA-B molecules (23). In contrast, the present study included docking studies for both class I (10 molecules) and class II (five molecules) HLA molecules.

Databases such as the IEDB and the IRD provide complete information regarding experimentally determined epitopes via means of submission as well as available literature. Comparing conserved predicted CD4+ and CD8+ T cell epitopes with the experimentally determined epitopes from the data sets (IEDB) enabled the current study to assess the novelty of identified multi-epitope peptides. It provides an account of experimental data pertaining to antibody and T cell epitopes studied in humans, nonhuman primates, and other species. As of March 7, 2015, the IEDB reported 167 T cell epitopes and four linear B cell epitopes of the M1 protein in the human host. Previous findings suggest that the three peptides identified in the present study have not been reported, although some substrings of peptide fragments have been reported to induce a CD4+ and CD8+ T cell response (4,19,56). The literature reports that the substrings of these peptides bind specifically to only one or two HLA alleles, whereas the current study reports that these peptides are capable of binding to a large number of class I and II

HLA alleles. Thus, this can be considered for experimental validation *in vitro*.

CD4+ T cells are considered to be an important factor in B cell activation and further antibody production. Hence, these peptides may also evoke a B cell response against the influenza virus. This is in accordance with an earlier study in which one of our identified peptides (LQAYQKRMGVQMQR) forms part of the B cell epitope, reported to induce IgG production in patients who have just recovered from H5N1 infection (25).

Internal proteins are more conserved than surface proteins. Hence, internal proteins such as the M1 protein and nucleoprotein are now being considered as an excellent target for a universal influenza vaccine. The M1 protein in various forms is being considered as a candidate for the generation of an adaptive T cell mediated immune response against influenza. In order to improve the immunogenic potential of an M1-based vaccine, several strategies have been suggested, including the administration of high-dose formulations of the vaccine, combination of modified vectored vaccine backbones, and adjuvants (3). In 2010, a study reported that the M1 protein expressed in *Escherichia coli* when used to immunize BALB/c mice by intranasal drip using chitosan adjuvant could protect 70% and 30% of the mice challenged with PR8 (H1N1) virus and A/Chicken/Henan/12/2004 (H5N1) virus, respectively (45). A novel influenza virus MVA-NP+M1 (modified vaccinia virus Ankara expressing conserved influenza internal nucleoprotein and M1 protein) targeting the M1 protein is under clinical trial (3). Although 167 linear M1 T cell epitopes have been reported in the human host, there is still a need for some probable peptide candidates in order to design a universal vaccine. The present study has identified three peptide sequences that contain these reported T cell epitopes based on immunoinformatics and molecular docking. These approaches serve as an initial screening and filtering step toward shortlisting potential immunogenic epitopes to synthesize for experimental validation, thus saving time, effort, and resources.

Acknowledgments

We gratefully acknowledge financial support from the DST, New Delhi, India (SERB/F/5066/2012-13).

Author Disclosure Statement

No competing financial interests exist.

References

1. Alberts B, Johnson A, Lewis J, *et al*. Molecular Biology of the Cell. 4th ed. New York: Garland Science, 2002.
2. Altschul SF, Gish W, Miller W, *et al.* Basic local alignment search tool. J Mol Biol 1990;215:403–410.
3. Antrobus RD, Berthoud TK, Mullarkey CE, *et al.* Coadministration of seasonal influenza vaccine and MVA-NP+M1 simultaneously achieves potent humoral and cell-mediated responses. Mol Ther 2014;22:233–238.
4. Assarsson E, Bui HH, Sidney J, *et al*. Immunomic analysis of the repertoire of T-cell specificities for influenza A virus in humans. J Virol 2008;82:12241–12251.
5. Atanasova M, Dimitrov I, Flower DR, *et al*. HLA class II binding prediction by molecular docking. Mol Inf 2011;30: 368–375.
6. Bui HH, Sidney J, Dinh K, *et al*. Predicting population coverage of T-cell epitope-based diagnostics and vaccines. BMC Bioinformatics 2006;7:153.
7. Blumenshine P, Reingold A, Egerter S, *et al*. Pandemic influenza planning in the United States from a health disparities perspective. Emerg Infect Dis 2008;14:709–715.
8. Burleigh LM, Calder LJ, Skehel JJ, *et al*. Influenza a viruses with mutations in the M1 helix six domain display a wide variety of morphological phenotypes. J Virol 2005;79: 1262–1270.
9. Chaves FA1, Lee AH, Nayak JL, *et al*. The utility and limitations of current Web-available algorithms to predict peptides recognized by CD4 T cells in response to pathogen infection. J Immunol 2012;188:4235–4248.
10. Chen CL, Xiao L, Zhou YP, *et al*. Ethnic differences in susceptibilities to A(H1N1) flu: an epidemic parameter indicating a weak viral virulence. Afr J Biotechnol 2009;8: 7379–7382.
11. Chen F, Zhai MX, Zhu YH, *et al*. *In vitro* and *in vivo* identification of a novel cytotoxic T lymphocyte epitope from Rv3425 of *Mycobacterium tuberculosis*. Microbiol Immunol 2012;56:548–553.
12. Choi JG, Kim MC, Kang HM, *et al*. Protective efficacy of baculovirus-derived influenza virus-like particles bearing H5 HA alone or in combination with M1 in chickens. Vet Microbiol 2013;162:623–630.
13. Doytchinova IA, and Flower DR. *In silico* identification of supertypes for class II HLAs. J Immunol 2005;174:7085–7095.
14. Duvvuri VR, Duvvuri B, Alice C, *et al*. Preexisting CD4+ T-cell immunity in human population to avian influenza H7N9 virus: whole proteome-wide immunoinformatics analyses. PLoS One 2014;9:e91273.
15. Duvvuri VR, Duvvuri B, Jamnik V, *et al.* T cell memory to evolutionarily conserved and shared hemagglutinin epitopes of H1N1 viruses: a pilot scale study. BMC Infect Dis 2013;13:204–215.
16. Duvvuri VR, Marchand-Austin A, Eshaghi A, *et al*. Potential T cell epitopes within swine-origin triple reassortant influenza A (H3N2) variant virus which emerged in 2011: an immunoinformatics study. Vaccine 2012;30:6054–6063.
17. Edgar RC. MUSCLE: a multiple sequence alignment method with reduced time and space complexity. BMC Bioinformatics 2004;5:113–131.
18. Fujiyoshi Y, Kume NP, Sakata K, *et al.* Fine structure of influenza A virus observed by electron cryo-microscopy. EMBO J 1994;13:318–326.
19. Gianfrani C, Oseroff C, Sidney J, *et al*. Human memory CTL response specific for influenza A virus is broad and multispecific. Hum Immunol 2000;61:438–452.
20. Gideon HP, Wilkinson KA, Rustad TR, *et al.* Bioinformatic and empirical analysis of novel hypoxia-inducible targets of the human antituberculosis T cell response. J Immunol 2012;189:5867–5876.
21. Gustiananda M. Immunoinformatics analysis of H5N1 proteome for designing an epitope-derived vaccine and predicting the prevalence of pre-existing cellular-mediated immunity toward bird flu virus in Indonesian population. Immunome Res 2011;7:1–11.
22. Hamada H, Bassity E, Flies A, *et al.* Multiple redundant effector mechanisms of CD8+ T cells protect against influenza infection. J Immunol 2013;190:296–306.
23. Hou Y, Guo Y, Wu C, *et al.* Prediction and identification of T cell epitopes in the H5N1 influenza virus nucleoprotein in chicken. PLoS One 2012;7:e39344.

24. Khan MK, Zaman S, Chakraborty S, *et al. In silico* predicted mycobacterial epitope elicits *in vitro* T-cell responses. Mol Immunol 2014;61:16–22.
25. Khurana S, Suguitan AL Jr, Rivera Y, *et al*. Antigenic fingerprinting of H5N1 avian influenza using convalescent sera and monoclonal antibodies reveals potential vaccine and diagnostic targets. PLoS Med 2009;6:e1000049.
26. Larsen MV, Lundegaard C, Lamberth K, *et al*. Large-scale validation of methods for cytotoxic T-lymphocyte epitope prediction. BMC Bioinformatics 2007;8:424–435.
27. Lohia N, and Baranwal M. Conserved peptides containing overlapping CD4+ and CD8+ T-cell epitopes in the H1N1 influenza virus: an immunoinformatics approach. Viral Immunol 2014;27:225–234.
28. Miotto O, Heiny A, Tan TW, *et al*. Identification of human-to-human transmissibility factors in PB2 proteins of influenza A by large-scale mutual information analysis. BMC Bioinformatics 2008;9:S18.
29. Moutaftsi M, Peters B, Pasquetto V, *et al.* A consensus epitope prediction approach identifies the breadth of murine T (CD8+)-cell responses to vaccinia virus. Nat Biotechnol 2006;24:817–819.
30. Navaranjan D, Rosella LC, Kwong JC, *et al*. Ethnic disparities in acquiring 2009 pandemic H1N1 influenza: a case-control study. BMC Public Health 2014;14:214–223.
31. Naylor PH, Egan JE, and Berinstein NL. Peptide based vaccine approaches for cancer-a novel approach using a WT-1 synthetic long peptide and the IRX-2 immunomodulatory regimen. Cancers (Basel) 2011;3:3991–4009.
32. Nielsen M, and Lund O. NN-align. An artificial neural network-based alignment algorithm for HLA class II peptide binding prediction. BMC Bioinformatics 2009;10:296–305.
33. Nielsen M, Lundegaard C, and Lund O. Prediction of HLA class II binding affinity using SMM-align, a novel stabilization matrix alignment method. BMC Bioinformatics 2007;8:238–249.
34. Parker KC, Bednarek MA, and Coligan JE. Scheme for ranking potential HLA-A2 binding peptides based on independent binding of individual peptide side-chains. J Immunol 1994;152:163–175.
35. Patronov A, Dimitrov I, Flower DR, *et al*. Peptide binding prediction for the human class II HLA allele HLA-DP2: a molecular docking approach. BMC Str Biol 2011;11:32–41.
36. Pereira BA, Silva FS, Rebello KM, *et al. In silico* predicted epitopes from the COOH-terminal extension of cysteine proteinase B inducing distinct immune responses during Leishmania (Leishmania) amazonensis experimental murine infection. BMC Immunol 2011;12:44–55.
37. Purcell AW, McCluskey J, and Rossjohn J. More than one reason to rethink the use of peptides in vaccine design. Nat Rev Drug Discov 2007;6:404–414.
38. Quan, FS, Kim MC, Lee BJ, *et al.* Influenza M1 VLPs containing neuraminidase induce heterosubtypic cross-protection. Virology 2012;430:127–135.
39. Rammensee H, Bachmann J, Emmerich NP, *et al.* SYFPEITHI: database for HLA ligands and peptide motifs. Immunogenetics 1999;50:213–209.
40. Safo MK, Musayev FN, Mosier PD, *et al*. Crystal structures of influenza A virus matrix protein M1: variations on a theme. PLoS One 2014;9:e109510.
41. Seyed N, Zahedifard F, Safaiyan S, *et al. In silico* analysis of six Leishmania major antigens and *in vitro* evaluation of specific epitopes eliciting HLA-A2 restricted CD8 T cell response. PLoS Negl Trop Dis 2011;5:e1295.
42. Sidney J, Peters B, Frahm N, *et al*. HLA class I supertypes: a revised and updated classification. BMC Immunol 2008;9:1–15.
43. Singh H, and Raghava GP. ProPred: prediction of HLA-DR binding sites. Bioinformatics 2001;17:1236–1237.
44. Subathra M, Santhakumar P, Satyam Naidu S, *et al.* Expression of avian influenza virus (H5N1) hemagglutinin and matrix protein 1 in Pichia pastoris and evaluation of their immunogenicity in mice. Appl Biochem Biotechnol 2014;172:3635–3645.
45. Sui Z, Chen Q, Fang F, *et al*. Cross-protection against influenza virus infection by intranasal administration of M1-based vaccine with chitosan as an adjuvant. Vaccine 2010;28:7690–7698.
46. Sun Y, Liu J, Yang M, *et al.* Identification and structural definition of H5-specific CTL epitopes restricted by HLA-A*0201 derived from the H5N1 subtype of influenza A viruses. J Gen Virol 2010;91:919–930.
47. Terajima M, and Ennis FA. Nuclear export signal and immunodominant CD8+ T cell epitope in influenza A virus matrix protein 1. J Virol 2012;86:10258.
48. Thevenet P, Shen Y, Maupetit J, *et al.* PEP-FOLD: an updated de novo structure prediction server for both linear and disulfide bonded cyclic peptides. Nucleic Acids Res 2012;40:W288–293.
49. Trott O, and Olson AJ. AutoDock Vina: improving the speed and accuracy of docking with a new scoring function, efficient optimization and multithreading. J Comput Chem 2010;31:455–461.
50. Wang W, Li R, Deng Y, *et al.* Protective Efficacy of the Conserved NP, PB1, and M1 Proteins as Immunogens in DNA- and Vaccinia Virus-Based Universal Influenza A Virus Vaccines in Mice. Clin Vaccine Immunol 2015;22:618–630.
51. Wei K, Chen Y, Lin Y, *et al*. Genetic dynamic analysis of the influenza A H5N1 NS1 gene in China. PLoS One 2014;9:e101384.
52. WHO. Influenza update 2015. www.who.int/influenza/surveillance_monitoring/updates/latest_update_GIP_surveillance/en/ (accessed August 1, 2015).
53. Wise HM, Hutchinson EC, Jagger BW, *et al*. Identification of a novel splice variant form of the influenza A virus M2 ion channel with an antigenically distinct ectodomain. PLoS Pathog 2012;8:e1002998.
54. Woodland DL. Antibody responses to influenza a virus infection. Viral Immunol 2014;27:367.
55. Woodland DL, Hogan RJ, and Zhong W. Cellular immunity and memory to respiratory virus infections. Immunol Res 2001;24:53–67.
56. Yang P, Wang W, Gu H, *et al*. Protection against influenza H7N9 virus challenge with a recombinant NP-M1-HSP60 protein vaccine construct in BALB/c mice. Antiviral Res 2014;111:1–7.

Address correspondence to:
Dr. Manoj Baranwal
Department of Biotechnology
Thapar University
Patiala 147004
India

E-mail: manoj.baranwal@thapar.edu